Phenolics and phenolic-polysaccharide linkages in Chinese water chestnut (*Eleocharis dulcis*) cell walls.

Terri Grassby
BSc Chemistry with Industrial Experience

Submitted for the degree of
Doctor of Philosophy
University of East Anglia
Institute of Food Research

March 2008

Abstract:

The main aim was to investigate the cell-wall cross-links in Chinese water chestnut (CWC), in particular ferulic-acid-containing phenolic-polysaccharide cross-links. The secondary aims were: to understand the gross composition of CWC cell walls from the parenchyma, epidermis and sub-epidermis tissues of the corm and the role of cell-wall composition in the plant's physiology, and to determine whether CWC contained higher oligomers of ferulic acid. Cell-wall composition was investigated using a range of chemical analyses including alkali phenolic extraction and methylation analysis. Chemical and biochemical methods were evaluated for their ability to produce oligosaccharide fragments attached to ferulic acid species. Mild acid hydrolysis followed by column chromatography using Biogel P-2 was the method chosen. LC-MS was used to identify compounds of interest.

The compositions of the epidermal tissues differed particularly in the proportions of lignin and cellulose present. The relative amounts and proportions of the phenolics varied considerably, possibly indicating their functions in the different tissues. A multitude of phenolics were detected, a number of which now have detailed UV information recorded about them. The LC-MS results indicate that trimers and tetramers of ferulic acid are present, and provide some degree of structural information for the trimers. A reasonable level of solubilisation was achieved with mild acid hydrolysis, releasing ~70% of the arabinose, xylose and galactose present into the supernatant. LC-MS indicated that multiple species containing ferulic acid or diferulic acids linked to one or more pentose sugars are present in the TFA hydrolysate and Biogel P-2 fractions, indicating that ferulic acid and diferulic acid are linked to cell-wall sugars in CWC as in many other monocots. Trimers and tetramers of ferulic acid were detected in a non-maize substrate for the first time, implying the possibility of higher oligomers of ferulic acid being present naturally in a wide range of cell walls.

Contents:

Figures:

Acknowledgements:

The project and my living expenses were funded by a BBSRC (Biotechnology and Biological Sciences Research Council) Committee grant. I would like to thank Keith Waldron and Craig Faulds for the help and training they have given me since the start of my PhD, and Adrian Parr for his advice as part of my supervisory committee and help with the MS data interpretation.

Mary Parker used her considerable microscopy expertise to produce the micrographs of autofluorescence in Chinese water chestnut cell walls as well as training me to use the optical microscope. Fred Mellon ran my phenolic extraction samples on the HPLC-MS machines and helped me to interpret the data produced. Zara Merali did Klason lignin on my samples. Andrew Jay trained me in the methylation methods and prepared the first batch of lithium dimsyl reagent, as well as helping to carry out the methods on my samples. John Eagles ran and patiently printed out the GC-MS data from all the methylation linkage analyses. Katerina Kolenova shared with me her TLC method for detection of sugars. Ian Colquhoun, Mark Philo and Laetitia Shintu assisted me with the LC-SPE-NMR and associated data interpretation.

The numerous people who came and/or went in the lab in the last three years; Andrew, Peter, Zara, Sam, Fiona, Graham and Giusy made the time fly by with their gossip and jokes and Giovanna, who kept us all on our toes with her little disasters.

Finally, I thank Mark for putting up with and encouraging me every step of the way, even while writing his own thesis. I also thank my (soon to be) extended family for not quite understanding what I've been doing for three years, but supporting me every step of the way anyway.

1 Introduction:

Cells are the basic building blocks of all multicellular organisms. They can differentiate themselves to produce a vast array of specialised cells capable of forming the tissues required for all the organs found in plants and animals.

1.1 Plant cells

The main differences between plant and animal cells are: plant cells have a defined cell wall, primarily made up of cellulose; plant cells contain a vacuole in addition to the cytoplasm; plant cells, that are capable of photosynthesis, contain chloroplasts which contain the photosynthetic pigment chlorophyll (Figure 1).

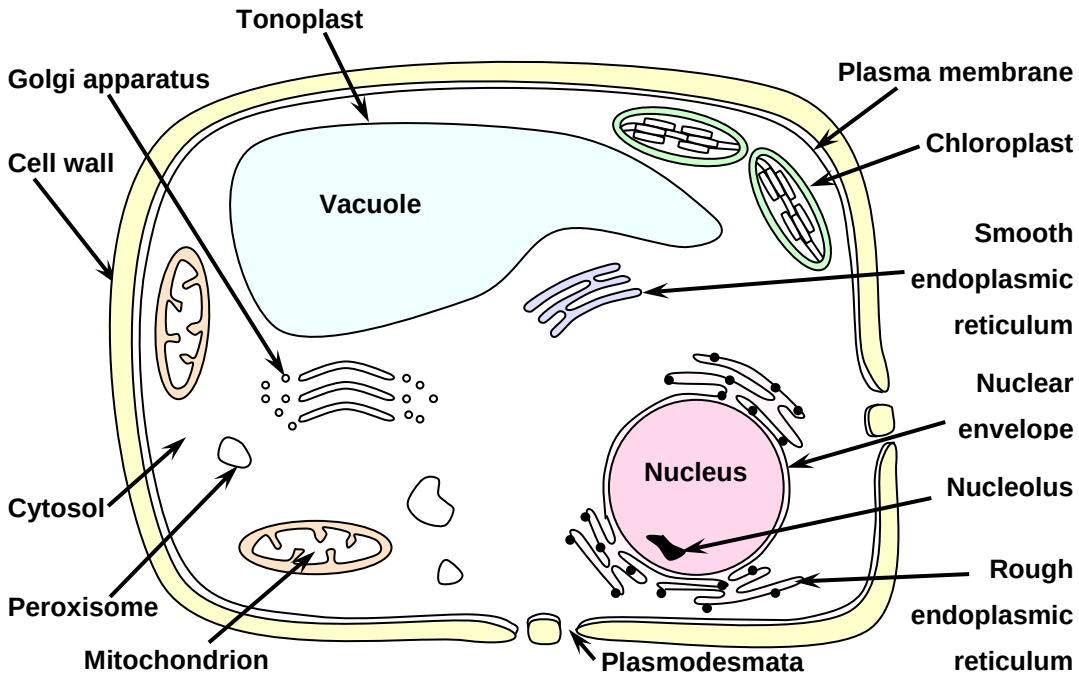

Figure 1: Features of a typical plant cell, based on Lack and Evans (2001).

1.1.1 Structures in plant cells

The plasma membrane surrounds the cytoplasm, an aqueous fluid called cytosol in which the organelles are situated. A matrix of actin microfibrils and

tubulin microtubules facilitates the support and movement of the organelles within the cell. The nucleus contains most of the cell's genetic information in the form of DNA and is surrounded by the nuclear envelope. The mitochondria and chloroplasts also contain some genetic information. The vacuole is a storage organelle that is also involved in osmotic regulation, particularly maintaining cell turgor. It may occupy up to 90% of the cell volume, it contains solutes dissolved in water, and is bounded by a membrane called the tonoplast. The system of membranes found within the cell is termed the endomembrane system, and this includes the nuclear envelope, the endoplasmic reticulum and the Golgi apparatus. The endomembrane system is involved with the synthesis and transport of materials within the cell. The chloroplasts (often found in the leaves and stems only) contain the chlorophyll necessary for photosynthesis. The mitochondria generate adenosine triphosphate (ATP) from stored food reserves, which is then used in many of the metabolic processes of the cell (Lack and Evans, 2001). The peroxisomes are small organelles that break down organic molecules by oxidation, producing hydrogen peroxide in the process. The hydrogen peroxide is then converted to water and oxygen. Plant cell walls are described in depth in Section §1.2.

Plant tissues are made up from cells with a common function, either one type of cell (simple tissues) or a collection of different cell types (complex tissues). The three main types of plant tissue are: ground, dermal and vascular; and they contain cells that may differ from the idealised version shown in Figure 1 to a greater or lesser extent. The ground tissues contribute to the structural strength and function of the plant. Parenchyma tissue is the most abundant type of ground tissue in the plant, forming the bulk of the leaves, roots and stems. The cells in parenchyma have thin flexible walls and large vacuoles, which often act as storage for food reserves or water. Sclerenchyma tissue is made up of dead cells, with lignified secondary walls, in organs that have completed their lateral growth. These cells are either very long, thin fibres which occur singly or in strands and bundles; or are irregularly shaped, often branched sclereids, which also appear singly or in groups. It is small groups of sclereids scattered throughout the parenchyma of pears (*Pyrus*) that gives pears their characteristic gritty texture. The cells that make up the protective outer covering of an organ

form a dermal tissue known as the epidermis. These cells are usually parenchyma or parenchyma-like cells that form a complete covering to protect the organ from pathogens and mechanical damage. There are two types of vascular tissue, xylem and phloem. Xylem generally carries water and water-soluble minerals from the plant roots to the growing shoots. Phloem carries sugars and amino acids from sites of synthesis or storage, to sites of storage or use as required (Lack and Evans, 2001).

1.2 Plant cell walls

Plant cell walls are deposited in a series of layers. The earliest layers are deposited during cell division, so the layer formed first adjoins the cell wall of the neighbouring cell and further layers are then deposited between this first layer and the plasma membrane. The first layer is the middle lamella, which is found in the middle of the double wall formed by two adjacent cells. The middle lamella is the remains of the cell plate that was laid down during cell division; because the cell plate is stretched during cell growth the middle lamella is extremely thin and is thicker at the cell corners. The second layer deposited is the primary cell wall. The primary cell wall is synthesised continuously while the cell is still growing, so it generally maintains a constant thickness in the range 0.1 - 1.0 µm (Cosgrove, 2005). Most cells only have these first two layers; however, some go on to develop a secondary cell wall when they begin to differentiate. This secondary wall is generally thicker than the primary cell wall and can vary considerably between different cell types. All the wall layers are made up of two phases: a microfibrillar phase and a matrix phase. Plasmodesmata penetrate the cell wall, through which the cytoplasmic matrices of adjacent cells are connected.

The microfibrillar phase is relatively homogeneous in composition, being mainly cellulose with a high degree of crystallinity. This phase can be seen under an electron microscope (Carpita and Gibeaut, 1993). The matrix phase is non-crystalline, extremely chemically complex, and appears to be featureless under an electron microscope. The main constituents of the matrix phase are:

pectins, hemicelluloses, proteins and phenolics (Figure 2). The relative amounts of these constituents vary depending on the part of the wall, the type of cell, the species and possibly even the stage in the cell cycle.

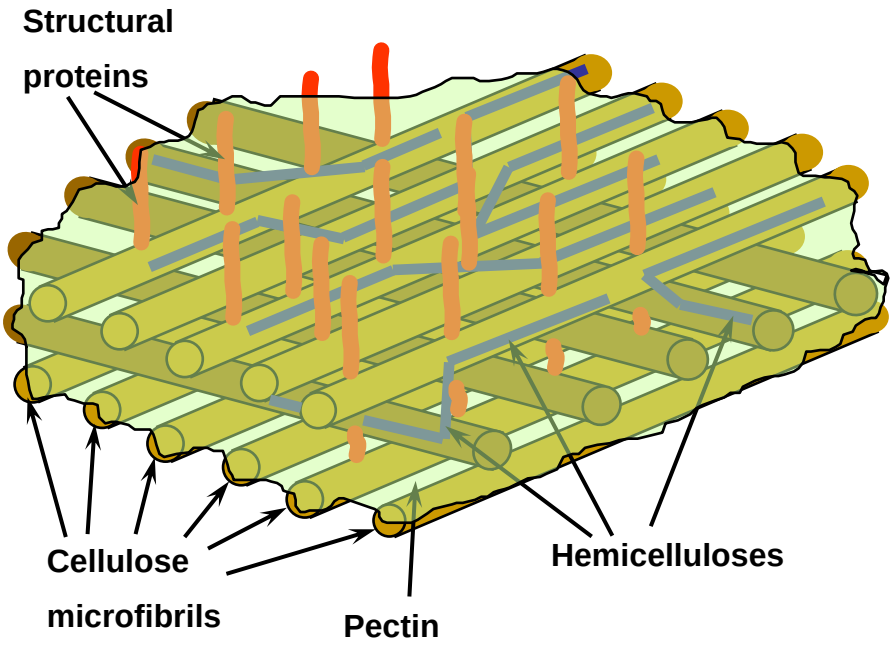

Figure 2: Simplified cell-wall structure diagram, from Waldron and Faulds (2007).

In general dicots have about equal proportions of cellulose, hemicellulose and pectin, but in monocots, pectin is normally present in significantly lower amounts (Ishii, 1997). As well as the variations in the polysaccharide composition of cell walls between species, there are also variations in the detailed structure of the polymers themselves.

1.2.1 Cellulose microfibrils

Cellulose microfibrils are extremely long, thin structures made of ~36 β-1,4-glucan chains, aligned along the length of the microfibril (Weber *et al.*, 1995). They are synthesised from uridine diphosphoglucose (UDPG) and guanosine diphosphoglucose (GDPG) by UDPG- and GDPG-utilising cellulose synthases (EC 2.4.1.12 and 2.4.1.29). Each cellulose synthase molecule aggregates with five others to form a complex, and then the complexes form a rosette with six-fold symmetry. The rosettes bridge the plasma membrane and are positioned

to align with the underlying pattern of microtubules (Burk and Ye, 2002). The cellulose synthase rosettes create a number of cellulose chains at the same time, which then form the microfibrils (Lack and Evans, 2001). The cellulose molecules form a (para) crystalline lattice held together with intramolecular and intermolecular hydrogen bonds. The microfibrils of hydrated cell walls have been imaged using Atomic Force Microscopy (AFM) by Kirby *et al* (1996), see Figure 3. The AFM image shows the microfibrils in a laminated structure where the different layers appear to have a "crossed" orientation (Emons and Mulder, 2000), similar to that shown in Figure 2. The microfibrils are separated from and connected to each other by the matrix phase, predominantly the pectin and hemicellulose components.

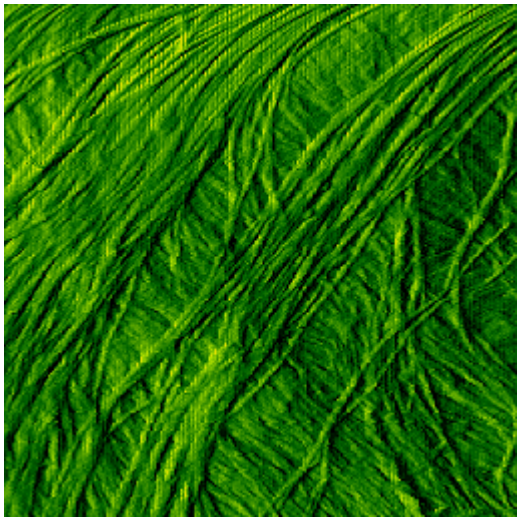

Figure 3: AFM error-signal-mode image of hydrated Chinese water chestnut cell wall (false colour), from Kirby* et al *(1996).

1.2.2 Pectin

Wall polysaccharides other than cellulose are synthesised in the Golgi and delivered to the wall via secretory vesicles (Weber *et al.*, 1995).

Pectins are traditionally classified as the fraction removed from the cell wall by a hot, aqueous solution of a chelating agent or hot, dilute acid (Brett and Waldron, 1996). Pectins contain polysaccharides made up of predominantly galacturonic acid, rhamnose, arabinose and galactose. They are generally found in the

middle lamella and primary walls of dicotyledonous plants and in smaller amounts in some monocotyledonous plants. Commonly identified pectins include:

Homogalacturonans (HG) - α1,4-linked galacturonic acid backbone, which may be partially esterified.

$$[\rightarrow 4)\text{-}\alpha\text{-GalA-}(1]_n$$

Rhamnogalacturonan I (RG I) – α1,4-linked galacturonic acid and α1,2-linked rhamnose backbone with long chains of 1,5-linked arabinose and 1,4-linked galactose as side chains.

$$[\rightarrow 4)\text{-}\alpha\text{-GalA-}(1\rightarrow 2)\text{-}\alpha\text{-Rha-}(1]_n$$
$$4$$
$$\downarrow$$

Rhamnogalacturonan II (RG II) – a complex structure of galacturonic acid, rhamnose, arabinose and galactose in the ratio 10:7:5:5, with small amounts of the rare sugars, such as aceric acid, apiose and 3-deoxy-manno-octulosonic acid (KDO).

Arabinan – α1,5-linked arabinose backbone with single arabinose residues attached at C2 or C3 as side chains.

$$[\rightarrow 5)\text{-}\alpha\text{-Ara-}(1\rightarrow 5)\text{-}\alpha\text{-Ara-}(1]_n$$
$$\begin{array}{cc} 2 & 3 \\ \downarrow & \downarrow \\ 1 & 1 \\ \alpha\text{-Ara} & \alpha\text{-Ara} \end{array}$$

Galactan – β1,4-linked galactose backbone.

$$[\rightarrow 4)\text{-}\beta\text{-Gal-}(1]_n$$

Arabinogalactan I (AG I) – β1,4-linked galactose backbone with short α1,5-linked arabinose side chains.

$$[\rightarrow 4)\text{-}\beta\text{-Gal-}(1]_n$$

3

↓

1

α-Ara

Arabinogalactan II (AG II) – β1,3-linked and β1,6-linked galactose backbone with multiple branches, β1,3-linked arabinose is present on the outer chains.

Rhamnogalacturonan II was first isolated and characterised from suspension-cultured sycamore cell walls (Darvill *et al.*, 1978) and subsequently identified in onion (Ishii, 1982).

Sugar beet pectins are primarily RG I and arabinan (Bonnin *et al.*, 2002; Levigne *et al.*, 2002; Levigne *et al.*, 2004a). Japanese quince pectins consist of arabinans, highly methylated HG and rhamnogalacturonans (Thomas *et al.*, 2003).

Under certain conditions, pectins form gels. The naturally-occurring pectins in fruit cell walls cause jams and jellies to thicken (May, 2000; Voragen *et al.*, 1995), but they are also used for textural control in fruit products, dairy products, desserts, soft drinks and pharmaceuticals (May, 1990).

1.2.3 Hemicelluloses

Hemicelluloses are usually strongly bound to the cellulose microfibrils by hydrogen bonds, so generally they can only be removed by relatively concentrated alkali solutions after the removal of pectin. The type of hemicellulose present varies greatly between different cell types and species (Brett and Waldron, 1996). Commonly identified hemicelluloses include:

Mannans – β1,4-linked mannose backbone.

$$[\rightarrow 4)\text{-}\beta\text{-Man-}(1]_n$$

(Gluco)mannans – β1,4-linked glucose and mannose backbone (with single galactose residues as side chains in gymnosperms).

$$[\rightarrow 4)\text{-}\beta\text{-Man-}(1\rightarrow 4)\text{-}\beta\text{-Man-}(1\rightarrow 4)\text{-}\beta\text{-Glc-}(1]_n$$

(Galactogluco)mannans – β1,4-linked glucose and mannose backbone with galactose attached by α(1-6) bonds as side chains. Galactoglucomannans containing very little glucose act as storage polysaccharides in the cell walls of some seeds (e.g. lupin) (Brett and Waldron, 1996).

$$[\rightarrow 4)\text{-}\beta\text{-Man-}(1\rightarrow 4)\text{-}\beta\text{-Man-}(1]_n$$
$$6$$
$$\downarrow$$
$$1$$
$$\alpha\text{-Gal}$$

(Glucurono)mannans – α1,4-linked mannose and β1,2-linked glucuronic acid backbone with galactose or arabinose attached to C6 or C3 of mannose respectively.

$$[\rightarrow 4)\text{-}\beta\text{-Man-}(1\rightarrow 2)\text{-}\beta\text{-GlcA-}(1]_n$$
$$3 \qquad 6$$
$$\downarrow \qquad \downarrow$$

(Arabino)xylans (AX) – β1,4-linked xylose backbone with acetyl esters and arabinose attached at C2 or C3 of xylose, and 4-*O*-methylglucuronic acid attached at C2 of xylose.

$$\left[\rightarrow 4)\text{-}\beta\text{-Xyl-}(1\rightarrow 4)\text{-}\beta\text{-Xyl-}(1\right]_n$$

2 3

↓ ↓

1 1

4-O-Me-β-GlcA α-Ara

Mixed-linkage glucans – β1,3-linked and β1,4-linked glucose backbone.

$$\left[\rightarrow 3)\text{-}\beta\text{-Glc-}(1\rightarrow 4)\text{-}\beta\text{-Glc-}(1\rightarrow 4)\text{-}\beta\text{-Glc-}(1\right]_n$$

Callose – β1,3-linked glucose backbone.

$$\left[\rightarrow 3)\text{-}\beta\text{-Glc-}(1\right]_n$$

Xyloglucan (XG) – β1,4-linked glucose backbone with xylose attached at C6, sometimes further substituted by Fuc α(1-2) Gal β(1-2) or Ara (1-2).

$$\left[\rightarrow 4)\text{-}\beta\text{-Glc-}(1\rightarrow 4)\text{-}\beta\text{-Glc-}(1\rightarrow 4)\text{-}\beta\text{-Glc-}(1\rightarrow 4)\text{-}\beta\text{-Glc-}(1\right]_n$$

6 6

↓ ↓

1 1

α-Xyl α-Xyl

2

↓

1

β-Gal

2

↓

1

α-Fuc

Xyloglucan is the major hemicellulose of dicot primary walls, at ~20% of the primary cell wall, whereas in monocots it is a relatively minor component at ~1-5% (Fry, 1988). Redgwell and Selvendran (1986) found xyloglucan in onion, which showed structural features in common with the xyloglucans of dicotyledonous plants. Carrot cell wall hemicelluloses consist of xylan, mannan and xyloglucan (Massiot *et al.*, 1988). Maize cell wall hemicelluloses consist of glucuronoarabinoxylan, mixed-linkage glucan, xyloglucan and glucomannan (Carpita *et al.*, 2001).

1.2.4 Phenolic compounds

Phenolics are a group of compounds which have one or more hydroxyl groups directly attached to a benzene ring (Shahidi and Naczk, 2004). They can be divided into different categories dependent on the number of phenol subunits they contain (Robbins, 2003) and further separated according to their structure (Liu, 2004):

- Simple phenolics – one phenol subunit
    - Hydroxybenzoic acids and aldehydes (Gallic acid, vanillin etc)
    - Hydroxycinnamic acids (Ferulic, caffeic, sinapic and *p*-coumaric acid)
- Polyphenols – at least two phenol subunits, which are further split into:
    - Flavonoids (Figure 4) – two phenol subunits
        - Flavonols (Quercetin, Kaempferol etc)
        - Flavones (Apigenin, Chrysin, Luteolin)
        - Flavanols (Catechin, Epicatechin etc)
        - Flavanones (Eriodictyol, Hesperitin, Naringenin)
        - Anthocyanidins (Cyanidin, Pelargonidin, Delphinidin etc)
        - Isoflavonoids (Genistein, Daidzein etc)
    - Stilbenes (Resveratrol etc)
    - Coumarins (Umbelliferone etc)
    - Tannins – three or more phenol subunits

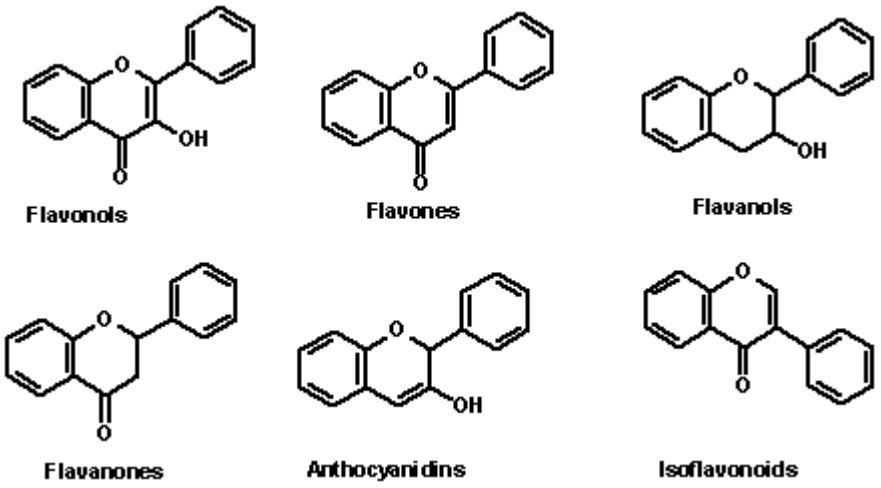

Figure 4: General structures of flavonoids.

Only the simple phenols, particularly the hydroxycinnamic acids, and lignin will be discussed here.

Ferulic acid is often esterified to arabinose and galactose in pectins (Fry, 1983; Ralet *et al.*, 2005). In species with low levels of pectin, ferulic acid may be linked to the arabinose in arabinoxylans (Ishii, 1997) or the xylose in xyloglucans (Ishii *et al.*, 1990). In arabinoxylans, *p*-Coumaric acid is also esterified to arabinose. Further discussion on the exact positions at which polysaccharides are feruloylated and coumaroylated can be found in Chapter 6. The feruloylation of polysaccharides occurs by feruloylation of UDP-arabinose immediately before polysaccharide synthesis or by feruloylation of the newly synthesised chain in the Golgi (Fry, 1987; Myton and Fry, 1994; Obel *et al.*, 2003).

There are two mechanisms by which ferulic acids can be dimerised, photochemical and radical dimerisation. Photochemical dimerisation of *p*-coumaric acid and/or ferulic acid under UV light forms cyclobutane derivatives (Hanley *et al.*, 1993), which are present in secondary rather than primary cell walls (Hartley and Morrison, 1991). The radical mechanism forms dehydrodimers of ferulic acid. The radical mechanism is the predominant one (Bunzel *et al.*, 2004), and it is therefore the dehydrodimers that are focussed on in this study.

The simple phenolics and precursors for lignin are produced via the phenylpropanoid pathway from phenylalanine and tyrosine. Ferulic acid is generally the most abundant simple phenolic in cell walls.

Geissmann and Neukom (1971) showed that, in the presence of peroxidase activity and hydrogen peroxide, two ferulic acid units (esterified to polysaccharides) form a covalent cross-link.

Initially the 5,5'-DiFA was the only ferulic acid dimer found (Hartley and Jones, 1976), but subsequent studies suggested that the radical coupling of ferulic acid should produce a whole range of diferulic acids, with the 8,5'-DiFA (BF) predominating (Ralph *et al.*, 1992), and this was shown to be the case by Ralph *et al* (1994). The 8-*O*-4'-DiFA tends to predominate in grasses (Ralph *et al.*, 1994), but the predominant dimer is 5,5'-DiFA in barley bran (Renger and Steinhart, 2000), 8-*O*-4'-DiFA in chufa (Parker *et al.*, 2000) and 8,5'-DiFA (BF) in sugar beet (Micard *et al.*, 1997a). The diferulic acids found in plant cell walls, including the less frequently reported 4-*O*-5'-DiFA (Bunzel *et al.*, 2000), 8,5'-DiFA (decarboxylated) and 8,8'-DiFA (tetrahydrofuran) (Grabber *et al.*, 2000), are shown in Figure 5. The 8,5'-DiFA (DC) has probably been overlooked in MS-based studies as it is not a true dimer, having lost CO_2, and hence has a molecular weight 44 units lower than the usual 386 at 342. The 8,8'-DiFA (THF) may also have been missed as it incorporates an additional water molecule after radical coupling (Bunzel *et al.*, 2004), and hence has a molecular weight of 404.

Dimerisation of ferulic acid esterified to polysaccharides occurs mostly in the protoplasm of suspension-cultured maize cells, but may occur in the cell wall when H_2O_2 levels increase due to pathogenesis (Fry *et al.*, 2000). In wheat cell suspension cultures it appears that only the 8,5'-DiFA is formed intraprotoplasmically with the other dimers being formed in the cell wall (Obel *et al.*, 2003).

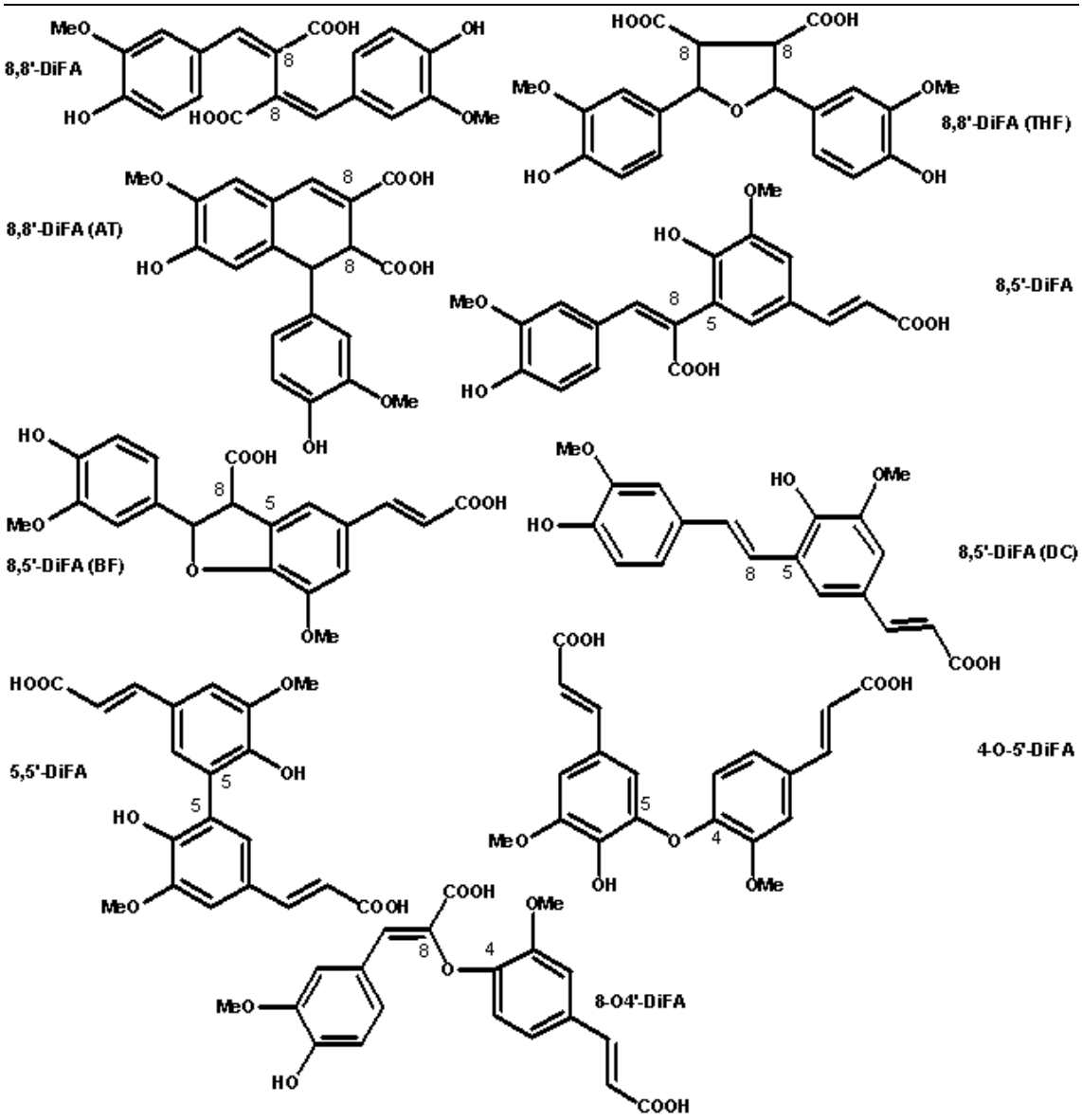

Figure 5: Chemical structures of diferulic acids identified in plant-cell walls.

As there appeared to be no reason why the dimers could not undergo radical coupling themselves, higher oligomers of ferulic acid were hypothesised to be possible. Ward *et al* (2001) generated trimers of ferulic acid (TriFA) enzymically *in vitro* and trimers and higher oligomers of ferulic acid were implied by radiolabelling studies carried out *in planta* by Fry *et al* (2003).

The first trimer to be identified was extracted from maize bran and was the 5,5'/8-*O*-4'-TriFA, published almost simultaneously by Bunzel *et al* (2003a) and Rouau *et al* (2003). Subsequently more trimers were discovered in maize bran (Figure 6):

- 8-*O*-4'/8,5'-TriFA (Bunzel *et al.*, 2005)
- 8-*O*-4'/8-*O*-4'-TriFA and 8-*O*-4'/8,8'(AT)-TriFA (Funk *et al.*, 2005),
- 8,8'(THF)/5,5'-TriFA and 8,5'/5,5'-TriFA (Bunzel *et al.*, 2006)

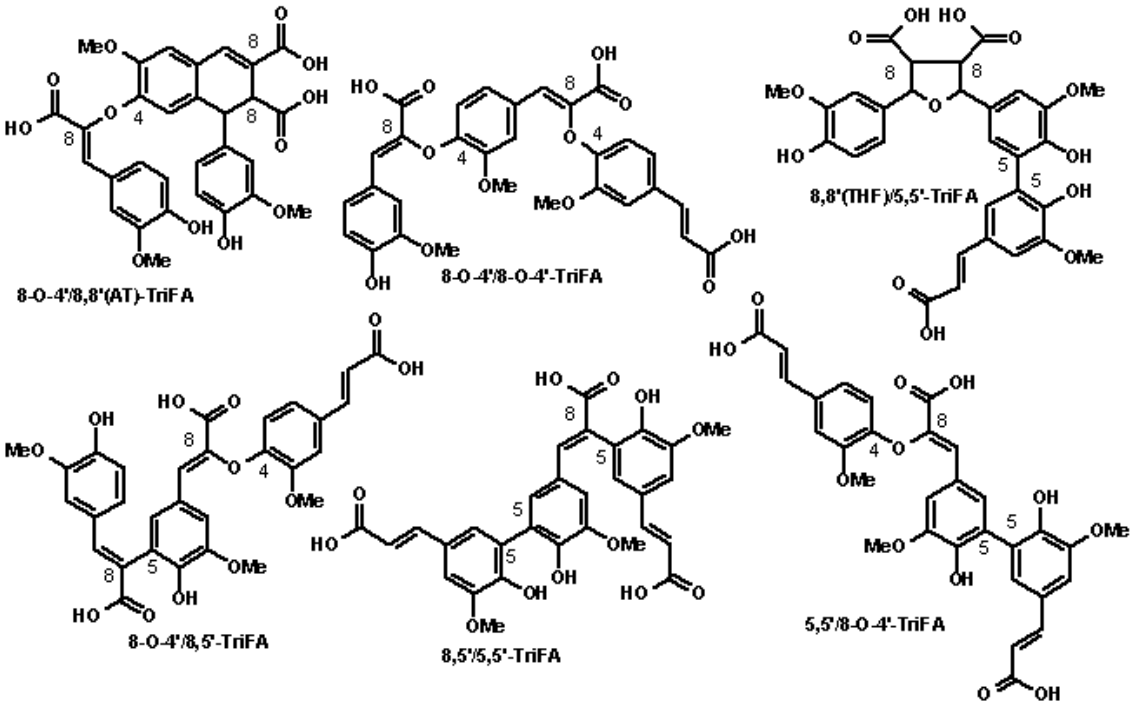

Figure 6: Chemical structures of triferulic acids discovered in maize-cell walls.

Theoretically there are at least 19 possible TriFAs, so there are more to be discovered (Ralph *et al.*, 2004).

Recently, two tetramers of ferulic acid (TetraFA) have been isolated from maize bran by Bunzel *et al* (2006): 4-*O*-8'/5,5'/8-*O*-4'-TetraFA and 4-*O*-8'/5,5'/8,5'-TetraFA (Figure 7).

Other phenolic compounds of interest when discussing plant cell walls are: *p*-coumaric acid, sinapic acid and lignins. *p*-Coumaric acid is generally abundant in the cell walls of cereal stems (Faulds and Williamson, 1999). *p*-Coumaric acid is esterified at the *O*-5 position of arabinose in arabinoxylans of barley straw (Mueller-Harvey *et al.*, 1986), coastal Bermuda grass (Borneman *et al.*, 1990), bamboo shoots (Ishii *et al.*, 1990) and maize bran (Allerdings *et al.*, 2006). There is no evidence that *p*-coumaric acid undergoes radical coupling

reactions itself (Iiyama *et al.*, 1994), but it may take part in radical transfer to sinapyl alcohol, allowing the incorporation of sinapyl alcohol into lignin, even though sinapyl alcohol is a poor substrate for cell-wall peroxidases (Ralph *et al.*, 2004).

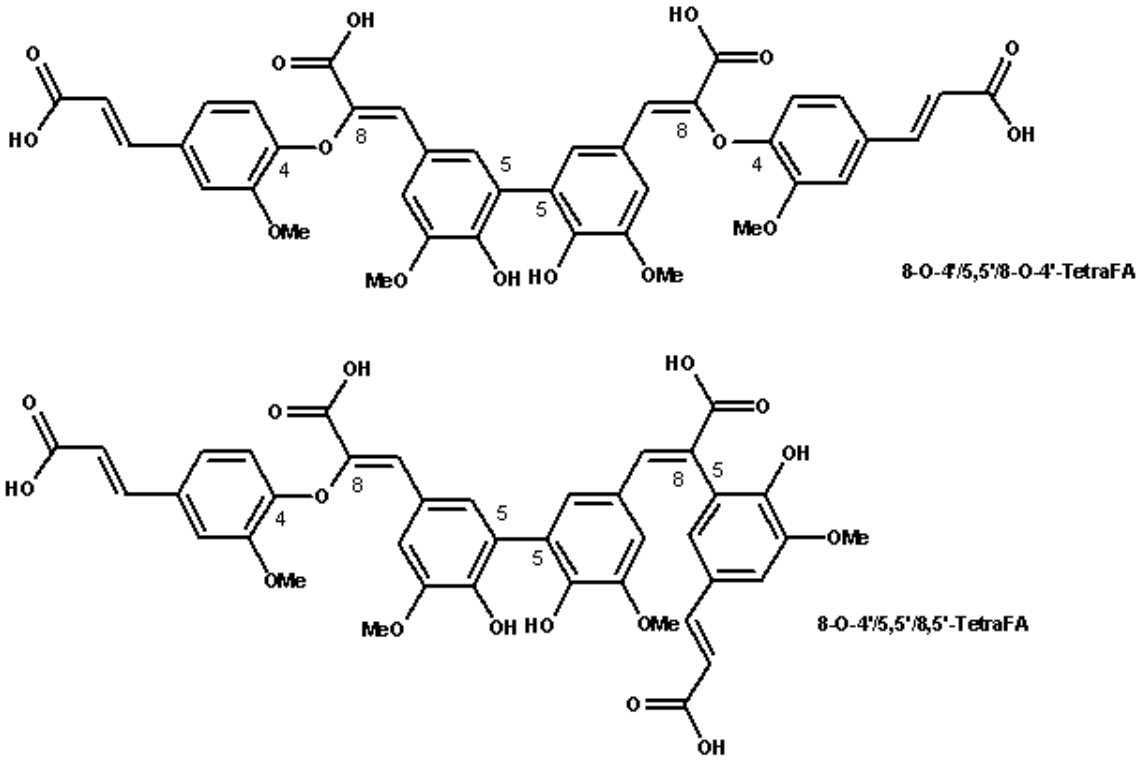

Figure 7: Chemical structures of tetraferulic acids discovered in maize-cell walls.

Sinapic acid has also been found to form dimers with itself (8,8) and ferulic acid (8,8, 8,5 and 8-*O*-4) in cereals and therefore may have a similar influence on cell-wall structure to that of the DiFAs (Bunzel *et al.*, 2003b), although no evidence of sinapic acid being esterified to polysaccharides has been found (Bunzel *et al.*, 2004).

Lignin is a phenolic polymer laid down after cell elongation has ceased. The precursors are *p*-coumaryl, coniferyl and sinapyl alcohols, which become *p*-hydroxyphenyl (H), guaiacyl propane (G) and syringyl (S) subunits linked by a variety of bonds in the polymer. The type of lignin produced depends on the ratio of precursors, for instance: in gymnosperms, lignin contains mainly guaiacyl propane or syringyl subunits; in dicotyledonous angiosperms it

contains guaiacyl propane and syringyl subunits; and in monocotyledonous angiosperms, all three subunits are present (Seigler, 1998). The polymerisation of lignin is a radical-coupling process mediated by peroxidases; as this is a purely chemical process which proteins or enzymes are not controlling, there is no defined primary structure to lignin (Ralph *et al.*, 2004). Growth ceases in fully lignified cells, and as the lignin forms an effective barrier to nutrients and pathogens, lignified cells soon die, but they provide good protection to the rest of the plant and provide structural support. Primary cell walls do not contain lignin, but secondary cell walls contain 5–25% lignin (Bidlack *et al.*, 1992).

Monomeric ferulic acid etherified to lignin is also esterified to arabinoxylans in wheat internodes, thus proving that ferulates cross-link lignin and polysaccharides (Iiyama *et al.*, 1990). In contrast, *p*-coumaric acid does not cross-link lignin and polysaccharides (Iiyama *et al.*, 1994). The interactions between ferulic, diferulic and *p*-coumaric acids and lignin were thought to prevent cell-wall elongation (Fry, 1979), but cessation of growth in tall fescue leaf blades and maize internodes occurs before the maximum accumulation of ferulic and *p*-coumaric acid. In fact, the accretion of ferulate, diferulates and *p*-coumarate continued after growth ended, continuing into secondary wall formation in tall fescue leaf blades and maize internodes (Iiyama *et al.*, 1994; MacAdam and Grabber, 2002). Esters of ferulic acid are etherified to lignin after wall growth ceases and therefore this process does not affect cell-wall elongation (Iiyama *et al.*, 1994).

1.2.5 Proteins

The cell walls of *Arabidopsis* are believed to contain at least 500 proteins, with the possibility that there are up to 2000 (Jamet *et al.*, 2006). Most of the cell wall proteins are glycosylated (Brett and Waldron, 1996). The majority also contain an unusual amino acid, hydroxyproline, which is not found in most protoplasmic proteins. The role of proteins in the cell wall is difficult to study due to problems in extracting them. The two main groups are structural proteins and cell-wall enzymes (Jamet *et al.*, 2006), the latter of which will be

discussed in Section §1.2.6. Type I walls contain between 1 and 20% protein, dependent on the specific tissue, whereas Type II walls contain ~0.5% (Fry, 1988).

Structural proteins:

- Arabinogalactan proteins (AGP) – 90-98% sugar
- Extensin – ~50% sugar
- Glycine-rich proteins – ~70% glycine in a repetitive primary structure; important in plant vascular systems and wound healing
- Proline-rich proteins – 0-20% sugar; contain proline-proline amino acid repeats; involved in plant development and nodule formation
- Proline-rich AGP-like protein

The backbone of extensin is a highly basic polypeptide of M_r ~40000, consisting of mainly hydroxyproline, with significant amounts of serine, lysine, tyrosine and sometimes histidine. The hydroxyprolyl residues are glycosylated by arabinotriose or arabinotetraose and the seryl residues by galactose. Extensin is insoluble in conventional protein solvents, including salt solutions, detergents, phenol/acetic acid/water and cold aqueous acids and alkalis.

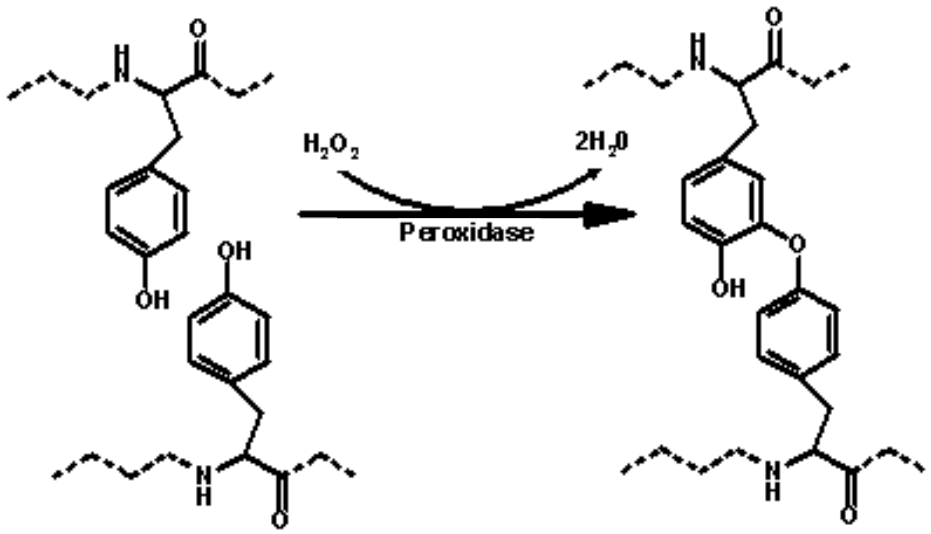

Figure 8: Formation of isodityrosine, based on McNeil* et al *(1984).

The extensin units covalently attach to the protein backbones of other proteins/extensins to form an interlocking network, as shown by Mort and Lamport (1977) who used hydrogen fluoride to remove all the cell wall carbohydrate, including that covalently attached to extensin, and still did not release extensin. The linkage proposed for the covalent linkage between extensin molecules is isodityrosine (Figure 8), as mildly acidified $NaClO_2$ solubilises extensin by breaking phenolic linkages, but not peptide bonds (McNeil *et al.*, 1984).

Arabinogalactan proteins are 2-10% protein; the protein is acidic and contains hydroxyproline, serine, alanine and glycine amino acids. The carbohydrate chains contain galactose, arabinose, rhamnose, mannose, galacturonic and/or glucuronic acids, and have a relatively high degree of polymerization (McNeil *et al.*, 1984). They are involved in cell-cell interactions and plant defence.

Expansins are pH-dependent wall-loosening proteins; they are activated as the wall becomes more acidic. Expansins are capable of wall loosening without the assistance of other enzymes or proteins and the addition of exogenous expansin rapidly stimulates cell growth. Expansin treatment does not reduce the strength of the cell wall, even while it is expanding. No enzymic activity that can account for its action on the wall has been found in expansins, so it is believed to act by disrupting the non-covalent bonds between wall polysaccharides. Expansin action enhances cellulose degradation by cellulases (Cosgrove, 2005).

1.2.6 Enzymes

There are a wide range of enzymes in the cell wall; however, their function in the wall is still to be elucidated in some cases:

- Glycoside hydrolases (EC category 3.2.1)
    - Cellulase (EC 3.2.1.4)
    - Polygalacturonase (EC 3.2.1.15)

    - β-glucosidase (EC 3.2.1.21)
    - β-galactosidase (EC 3.2.1.23)
    - β-xylosidase (EC 3.2.1.37 or 3.2.1.32)
    - α-galactosidase (EC 3.2.1.22)
    - xylanase (EC 3.2.1.8)
- Esterases and lyases (EC categories 3.1 and 4)
    - Pectin methylesterase (EC 3.1.1.11)
    - Acid phosphatase (EC 3.1.3.2)
    - Feruloyl esterase (EC 3.1.1.73)
    - Acetyl esterase (EC 3.1.1.72)
- Transglycosylases
    - Xyloglucan:xyloglucosyl transferase (EC 2.4.1.207)
- Peroxidases (EC 1.11.1.7)
- Malate dehydrogenase (1.1.1.37)
- Proteases (EC category 3.4)

Xyloglucan:xyloglucosyl transferase, otherwise known as xyloglucan endotransglycosylase (XET) or xyloglucan endotransglucosylase/hydrolase (XTH), has some transglycosylase activity in addition to hydrolase activity, allowing it to sever the xyloglucan backbone and connect it to either another xyloglucan chain or water (Cosgrove, 1999; Takeda *et al.*, 2002).

Cellulase may cause wall loosening by releasing xyloglucans trapped in the non-crystalline regions of cellulose microfibrils (Cosgrove, 2005)

Peroxidases produce the H_2O_2 required for the oxidative coupling of cell wall components. They produce the H_2O_2 required to dimerise ferulic acid (linking polysaccharide chains), and tyrosine (linking extensins). They require Ca^{2+} and are inhibited by low pH (Fry, 1986). Peroxidase extracted from horseradish is commonly used in experiments when the formation of ferulic acid dimers (and higher oligomers) is desired (Oudgenoeg *et al.*, 2002).

1.2.7 Structural relationships between polysaccharides in primary cell walls

There are a number of different theories about the precise interplay between the microfibrillar and matrix phases in primary cell walls; these are discussed in detail below and also in the review by Cosgrove (2001). Some of the models specify axes along which the components lie (Figure 9).

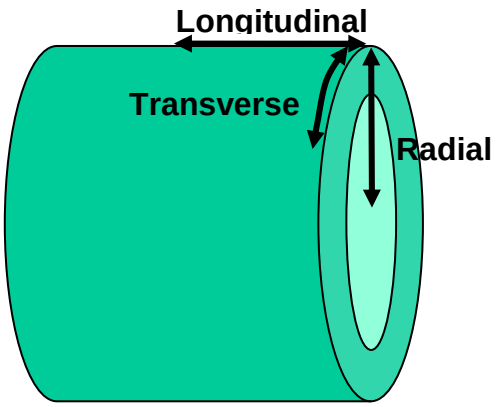

Figure 9: Definition of axes used in cell-wall models.

The "Keegstra and Albersheim" model (Keegstra *et al.*, 1973) is based on suspension-cultured sycamore cell walls. It has xyloglucan tightly bound to cellulose by hydrogen bonds and the reducing ends of xyloglucan are covalently attached to the galactan side chains of rhamnogalacturonan (which could form a stable network between microfibrils directly). A covalent linkage between pectic polysaccharides and the arabinogalactans of AGPs was also included due to the experimental evidence. Cell wall extension is proposed to be possible by creep of the xyloglucan chains along the cellulose microfibrils. This model went out of favour as the linkage between pectin and xyloglucan could not be confirmed (Darvill *et al.*, 1980). It has been revived since, as small amounts of xyloglucan-pectin complexes have been found in suspension-cultured rose cells (Thompson and Fry, 2000), as well as xylan-pectin complexes in asparagus (Waldron and Selvendran, 1992), pectin-xylan-xyloglucan complexes in cauliflower (Femenia *et al.*, 1999a) and xylan-xyloglucan in olive pulp (Coimbra *et al.*, 1995).

The “Fry” model proposes that xyloglucans and arabinoxylans are hydrogen-bonded to cellulose and RG I is esterified to cellulose. The arabinoxylans are linked, through diferulic acid, to each other, as are the RG I polymers. Arabinogalactan is covalently linked to RG I, with calcium bridges forming between stretches of homogalacturonan. Other ionic bonds between acidic homogalacturonan and basic extensin were proposed, primarily that homogalacturonan stretches of RG I are enclosed in loops of extensin (Fry, 1986).

McCann and Roberts proposed a three-dimensional model (McCann *et al.*, 1992), based on onion cell walls, which considered scale as well as bonding (the “improved tethered network” model). The primary cell wall was ~75 nm thick, the middle lamella ~20 nm thick and the microfibrils ~10 nm in diameter, allowing only four layers of parallel microfibrils. Microfibrils are cross-linked and separated by hemicellulose (xyloglucan) chains ~10-20 nm in length. Ester-linked pectins are embedded within the cellulose-xyloglucan framework, but are independent of it, and extend into the middle lamella. The middle lamella pectins are less esterified than those in the rest of the wall, so they are able to form Ca^{2+} cross-links. The pectins can be removed without affecting the structural integrity of the cellulose/hemicellulose network, although some galactan is associated with the microfibrils even after extraction in 4 M KOH. The pectins seem to regulate cell wall porosity and adopt a precise conformation in the cell wall (McCann *et al.*, 1992). The work of McCann (1990) and Whitney *et al* (1995) provided evidence for xyloglucan spanning the distance between microfibrils.

The “multicoat” model of Talbott and Ray (1982) involves the microfibrils being successively coated with hemicellulose and pectin, which connect the microfibrils by virtue of their non-covalent attractions. The symmetry of xyloglucan and cellulose is such that they both have an extended two-fold helix conformation in their crystalline forms and so can associate non-covalently (Gardner and Blackwel, 1974; Ogawa *et al.*, 1990). However, the arabinoxylans have an extended three-fold helix conformation, so there is not a favourable association between them and cellulose, at least not for the highly substituted

arabinoxylans (Yui *et al.*, 1995). Xylans and less highly substituted arabinoxylans may be capable of associating with cellulose (McNeil *et al.*, 1975; Saulnier *et al.*, 2007).

The “warp-weft” model of Lamport and Epstein (1983) includes the xyloglucan linking the microfibrils, but gives a central role to protein cross-links. The cellulose microfibrils (warp) are enclosed by isodityrosine-coupled extensin molecules (weft). The “warp-weft” model is inappropriate for onion cell walls due to the low proportion of cell wall protein (McCann *et al.*, 1990) and this may be true of other similar species.

The “Carpita and Gibeaut” model (Carpita and Gibeaut, 1993) is actually two slightly different models that account for the differences between species; they defined Type I cell walls to be those of dicots and most non-graminaceous monocots and Type II cell walls to be those of the *Gramineae*. The Type I model has xyloglucan chains hydrogen-bonded to the surface of the cellulose microfibrils and woven together by their hydrogen bonds with each other, cross-linking the microfibrils. The cellulose/xyloglucan layer is then sandwiched between layers of covalently linked polygalacturonan (PGA) and rhamnogalacturonan I. The PGA is condensed by Ca^{2+} cross-linking, or in some species by formation of diferulic acid linkages between ferulic acid monomers ester-linked to separate polysaccharide chains In the Type II model, a small amount of xyloglucan binds to the cellulose microfibrils, but was thought to not connect the microfibrils as they do in the Type I model. Type II walls also tend to have low levels of pectin, although RG I and PGA were still envisaged to form a longitudinal layer. The main connection between microfibrils is achieved by glucuronoarabinoxylans, which hydrogen bond to the microfibrils and to each other where there is little substitution of the polysaccharide. As a substantial amount of the non-cellulosic polymers are not removed by treatment with alkali the phenolic cross-linkages are thought to wrap around the cellulose-xyloglucan-GAX interaction sites, preventing their removal. They also considered how cell wall growth and growth cessation might be achieved in the two models. In the Type I model xyloglucans are severed allowing microfibrils to separate; expansion is halted by incorporation of

extensin radially. In the Type II model, mixed-linkage glucans are synthesised during expansion and take on a similar role to the xyloglucans of the Type I wall; expansion is halted somewhat by threonine-rich proteins and more significantly by esterified and etherified phenolic acids, at which point the mixed-linkage glucans are no longer load-bearing.

Unlignified Type II cell walls have glucuronoarabinoxylans and mixed-linkage glucans as their main non-cellulosic cell-wall polysaccharides, with pectic polysaccharides and xyloglucans in smaller amounts. Unlignified Type I cell walls have large amounts of pectic polysaccharides, with smaller amounts of xyloglucans. Some monocots have cell wall compositions that are intermediate between these two extremes; they tend to be the species that have ferulic acid esters in their cell walls, for instance, pineapple (Smith and Harris, 1995).

Although xyloglucan binds strongly to cellulose *in vitro* (Valent and Albersheim, 1974), the models that suggest that the only interaction between cellulose and xyloglucan is hydrogen-bonding probably need to be amended, as there is now evidence that xyloglucan is partly interwoven in the amorphous regions of cellulose, rather than just bound to the surface (Baba *et al.*, 1994). The evidence for this is that concentrated alkali (that makes the microfibrils swell) is required to release xyloglucan, whereas mild alkali that prevents the hydrogen-bonding of xyloglucan to cellulose does not release xyloglucan. In addition, when treatment with concentrated alkali or an endoglucanase is used, virtually no xyloglucan can be detected by an antibody designed for the purpose, but there are still small lengths (M_r 9200, 15 nm) of xyloglucan that can be released (Baba *et al.*, 1994). This means a modification to this model is required as the proposed method for expansion is unlikely to be possible.

Extracellular cross-linking of xylan and xyloglucan chains, by oxidative coupling of phenolics, has been demonstrated in maize cell-suspension cultures (Kerr and Fry, 2004). Modelling the feasibility of intramolecular diferulate formation in grass walls indicated that linkages between ferulates on the same arabinoxylan chain were only possible if the arabinoxylan relaxes its conformation (Hatfield and Ralph, 1999), implying that linkages are formed intermolecularly.

Sugar beet pectins are feruloylated and can be caused to gel by oxidative cross-linking (Iiyama *et al.*, 1994). Sugar beet contains diferulic acids and therefore it is assumed that cross-linking of pectins occurs *in vivo* (Wende *et al.*, 1999).

1.2.8 Cell walls and growth regulation

Although many have tried to determine the mechanism by which cell elongation is made possible by alterations to the cell wall, it has proven extremely difficult. Cell wall elongation is pH-dependent, and decreasing pH increases the growth rate. There is some degree of control over the pH of the cell wall and many of the tropisms, such as phototropism, are produced in this way. The following are interesting results related to cell wall growth.

- Xyloglucan oligosaccharides show inhibitory effects on auxin-stimulated growth of pea (McDougall and Fry, 1988).
- Feruloyl oligosaccharides inhibited auxin-stimulated growth of rice (Ishii, 1997).

1.2.9 Cell walls and defence

Plant cell walls offer two types of defence for the plant as a whole: a passive mechanism and an active defence mechanism.

As a passive defence mechanism, cell walls provide a physical barrier between pathogens and the plant cell contents. The walls of surface cells may be strengthened by the deposition of lignin or silica, which will not only make it more difficult for pathogenic organisms to access the cell contents, but will deter foraging animals, by making digestion more difficult. The outer cell wall of endodermal cells may contain suberin, a layer of fatty acids ester-linked to dicarboxylic acids and phenolics. Epidermal cells may have a layer of cutin, a polymer of long-chain fatty acids held together by ester linkages, above the

primary wall layer. Cutin and suberin are both hydrophobic, allowing the plant to shed water and any associated microbes.

Pathogens attempting to penetrate the walls of their host must secrete a range of cell-wall degrading enzymes. As part of the plant's active defence mechanism, the cell walls are capable of reacting to the attack. The enzymes used by pathogens to break down the polysaccharides in the cell wall produce oligosaccharides that can act as signalling molecules. The cell wall can respond to these signalling molecules in a range of ways: by depositing more lignin and/or cellulose in the cell wall around the attack site (making the wall more difficult to penetrate) (Iiyama *et al.*, 1994), releasing proteins to inhibit the action of the pathogenic enzymes (Albersheim and Anderson, 1971; Juge, 2006) or using enzymes as a counter-attack against the pathogen (Cline and Albersheim, 1981). The oligosaccharide signals may also induce the neighbouring cells to defend themselves.

Phenolic acids have a range of properties that may help the plant defend itself:

- They are astringent, especially in combination (Shahidi and Naczk, 2004), and therefore would deter foraging herbivores
- Sinapic, *p*-coumaric and ferulic acids can inhibit mycelium growth of *Fusarium oxysporum*, and they also inhibit the various cell-wall degrading enzymes secreted by *F. oxysporum* when it attacks date palm (El Modafar and El Boustani, 2001)
- During a pathogen-induced oxidative burst, which may involve extracellular H_2O_2 production, increased coupling of ferulic acid would occur in the cell walls (Fry *et al.*, 2000), increasing the degree of cross-linking and reducing degradability
- Synthesis of feruloyltyramine in response to wounding restricts the enzymic dissolution of cell-wall polymers (Pearce *et al.*, 1998)
- Inactivation of plant viruses (Sridhar *et al.*, 1979)

Presumably a combination of these factors makes ferulic acid a significant factor in the resistance of wheat against wheat midge (Abdel-Aal *et al.*, 2001).

The defence mechanisms of plants exert their influence in agriculture, biodiversity and food production. For instance, increasing the level of polysaccharide cross-linking reduces the digestibility of plant cells in the ruminant gut – a major factor in the economically important production of milk and beef. It reduces further if the cross-linking is between lignin and polysaccharides (Grabber *et al.*, 1996; Ralph *et al.*, 1996).

1.2.10 Cell walls and health

Cell walls are the main source of fibre in the human diet. Dietary fibre is defined as "all the polysaccharides and lignin in the diet that are not digested by the endogenous secretions of the human digestive tract" (Selvendran, 1991). Low intake of foods containing dietary fibre, such as fruit, vegetables and cereals, can contribute to constipation, diverticular disease, colorectal cancer, coronary heart disease, diabetes and obesity (Selvendran, 1991). These negative effects may also be due to a lack of other compounds, such as antioxidants, that are also present in these foods.

Primary wall polysaccharides have been shown to bind heavy metals (Tahiri *et al.*, 2000; 2002), regulate serum cholesterol (Terpstra *et al.*, 2002) and stimulate the immune system (Yu *et al.*, 2001). Also, many phenolics are known to have one or more of the following beneficial activities: antioxidant, antimicrobial, antimutagenic (Ferguson *et al.*, 2003), anti-inflammatory, anticarcinogenic, cholesterol-lowering and prevention of thrombosis and atherosclerosis (Ou and Kwok, 2004).

Hydroxycinnamic acids, and an extract containing hydroxycinnamic acids obtained by the saponification of the cell walls of wheat coleoptiles, have been shown to have antimutagenic properties in a simple bacterial model (Ferguson *et al.*, 2003). Assuming this can be applied to humans, this may provide an explanation as to why diets high in fibre, and hence hydroxycinnamic acids, tend to protect people from cancer of the bowel and digestive tract. Ferulic acid

forms a resonance-stabilized phenoxy radical, which scavenges a range of free radicals. It also increases the activity of enzymes responsible for scavenging free radicals and inhibits enzymes that catalyse the production of free radicals (Kayahara 2000). Ferulic acid (and other phenolic acids) esterified to cell-wall polymers cannot be absorbed in the human gut in this form, but there are microbial esterases present in the intestine that can release them (Andreasen *et al.*, 2001a; Kroon *et al.*, 1997) in a form which can then be absorbed (Andreasen *et al.*, 2001b). Ferulic acid is subsequently excreted as the free form or conjugated to glucuronide in the urine (Chesson *et al.*, 1999; Choudhury *et al.*, 1999).

Diferulic acids are more effective inhibitors of lipid peroxidation and better scavengers of free radicals than ferulic acid on a molar basis (Garcia-Conesa *et al.*, 1997). As with ferulic acid, diferulic acids bound to cell walls are not absorbed directly by humans; however it has been shown in rats that free diferulic acids are absorbed in the intestine (Andreasen *et al.*, 2001b). Caco-2 cells (a cancer cell line that differentiates into enterocyte-like cells similar to those in the small intestine) have the ability to de-esterify model DiFA-diester substrates, particularly the 8-*O*-4'-DiFA diester (Kern *et al.*, 2003). Increasing the concentration of ferulic acid and diferulic acid does not affect the degradation of nonlignified cell wall by human intestinal microbes (Funk *et al.*, 2007).

1.3 Studying the cell-wall matrix

There are many approaches taken for studying the wall matrix and they generally utilise whole tissue or purified cell-wall material. The different approaches are described below.

1.3.1 Microscope-based investigations

The distribution of phenolics in whole tissue can be visualised using UV microscopy (ferulic acid fluoresces blue); and simple chemical treatments, such

as dilute ammonium hydroxide, can induce more intense pH dependent autofluorescence (ferulic acid autofluoresces green). Studies on monocots show that some subclasses and families are more likely to contain high levels of phenolics than others. For instance, the subclass *Commelinales* and the families *Philydraceae*, *Pontederiaceae* and *Haemodoraceae* have relatively high levels (Harris and Hartley, 1980). Even very low levels of ferulic acid (>88 µg/mg) can be detected by pH-dependent autofluorescence (Carnachan and Harris, 2000). Other histochemical stains can be used:

- Alcian blue stains pectin blue
- Ruthenium red stains pectin red
- Sudan 7B stains suberin pink/red
- Fluorol yellow 088 gives a yellow fluorescence with suberin under UV light
- Dimethoxybenzaldehyde stains condensed tannins red
- Naturestoffreagenz A gives a yellow fluorescence with flavonoids under UV light
- Reactive oxygen species give a deep-brown reaction product with H_2O_2 (Gunawardena *et al.*, 2007)
- Phloroglucinol-HCl stains lignin red (Carnachan and Harris, 2000)
- Toluidine blue O stains polychromatically; lignin stains green or blue-green and rhamnogalacturonans stain pink or purple (Carnachan and Harris, 2000)
- Sirofluor, a chemical found in aniline blue, gives a yellow fluorescence with callose (Stone *et al.*, 1984)
- Calcofluor stains cellulose blue (Roberts, 2001)

The distribution of matrix polymers has been investigated using electron microscopy and immunocytochemistry in potatoes (Parker *et al.*, 2001) and peas (*Pisum sativum* L. cv Avola) (McCartney and Knox, 2002). There are a number of monoclonal (mAb) and polyclonal (pAb) antibodies that have been used for this purpose; most of them are specific for a particular polysaccharide or protein epitope; and these are listed in Figure 10:

Probe	Type	Recognised epitope	References
LM1	Mab	Extensin	(Smallwood *et al.*, 1995)
LM2	Mab	AGP	(Smallwood *et al.*, 1996)
LM5	Mab	(1→4)-β-D-galactan	(Jones *et al.*, 1997)
LM6	Mab	(1→5)-α-L-arabinan	(Willats *et al.*, 1998)
LM7	Mab	Randomly methylated HG	(Clausen *et al.*, 2003)
LM8	Mab	Xylogalacturonan	(Willats *et al.*, 2004)
LM9	Mab	Feruloylated (1→4)-β-D-galactan	(Clausen *et al.*, 2004)
LM10	Mab	Unsubstituted or low-substituted xylans	(McCartney *et al.*, 2005)
LM11	Mab	Wheat arabinoxylans and LM10 epitope	(McCartney *et al.*, 2005)
CCRC-M1	Mab	α-(1→2)-Fuc residue on XG	(Kremer *et al.*, 2004)
CCRC-M7	Mab	Arabinosylated (1→6)-β-galactan	(Steffan *et al.*, 1995)
JIM4	Mab	β-D-GlcA-(1,3)-α-D-GalA-(1,2)-α-L-Rha of AGP	(Stacey *et al.*, 1990) (Yates *et al.*, 1996)
JIM5	Mab	Low-methylated HG	(Willats *et al.*, 2000)
JIM7	Mab	Highly methylated HG	(Willats *et al.*, 2000)
JIM8	Mab	Carbohydrate portion of AGP	(Samaj *et al.*, 1998)
JIM11	Mab	Extensin	(Smallwood *et al.*, 1994)
JIM12	Mab	Extensin	(Smallwood *et al.*, 1994)
JIM13	Mab	β-D-GlcA-(1,3)-α-D-GalA-(1,2)-α-L-Rha of AGP	(Knox *et al.*, 1991) (Yates *et al.*, 1996)
Anti X1	Pab	(1→4)-β-linked Xyl regions and Ara substituted regions of AX	(Guillon *et al.*, 2004)
Anti X3	Pab	(1→4)-β-linked Xyl regions of AX	(Guillon *et al.*, 2004)
PAM1	Phage display mAb	De-esterified and unsubstituted GalA of HG	(Willats *et al.*, 1999)
5-*O*-Fer-Ara	Pab	5-*O*-(*trans*-feruloyl)-L-Ara	(Phillipe *et al.*, 2007)

Figure 10: Antibodies used in microscope investigations of plant-cell walls, and the epitopes they bind to.

1.3.2 Chemical investigations

The cell contents can interfere with chemical investigations, so they are usually removed to give relatively pure samples of cell wall. The cell walls of monocotyledonous green asparagus (*Asparagus officinalis* L. cv. Franklin) (Rodríguez-Arcos *et al.*, 2004), Chinese water chestnut (*Eleocharis dulcis*)

parenchyma (Parr *et al.*, 1996), carrot (*Daucus carota* cv. Amstrong) (Ng *et al.*, 1998), potato (*Solanum tuberosum* cv. Cara) (Parker *et al.*, 2001) and chufa (*Cyperus esculentus* L.) (Parker *et al.*, 2000) have been studied in this way. There are a number of methods for extracting specific components of the cell wall and these are normally analysed in a quantitative manner. For sugars, the main method involves analysis of hydrolysed carbohydrates, which can be augmented by analysis of their linkages. Analysis of phenolics is usually carried out after extraction in alkali. Lignin can be quantified using the Klason lignin method. More complex analytical methods, such as thioacidolysis cleavage and nitrobenzene oxidative cleavage, allow the different subunits of lignin to be identified.

1.3.3 Enzyme-based investigations

Much of the work on the linkages between ferulic acid and cell-wall polysaccharides has been done using a sub-class of the carboxylic acid esterases called feruloyl esterases (FAE) (E.C. 3.1.1.73) (Crepin *et al.*, 2004). They were first detected by Deobald and Crawford (1987) in extracellular enzyme preparations from *Streptomyces viridosporus*. As more FAEs were discovered, Crepin *et al* separated them into four distinct classes (A, B, C and D) based on substrate utilisation and primary sequence identities (Crepin *et al.*, 2004). Depending on the substrate, enzymes have variable success rates at degrading plant cell walls. In monocots, such as wheat bran, the FAE needs to be combined with a xylanase to facilitate release of ferulic acid from the arabinoxylan (Faulds and Williamson, 1995). Often in dicots containing ferulic acid, such as sugar beet, a combination of FAE and α-L-arabinofuranosidase is required to get a reasonable release of sugars and/or phenolics when compared to an alkali extraction, where the ferulic acid-pectin ester link is saponified relatively easily. The presence of a xylanase/pectinase enhances the degradation of the polysaccharide matrix by giving FAEs access to their substrate. The FAE classes A and D release DiFAs linked to polysaccharides (Crepin *et al.*, 2004).

Enzymic release of ferulic acid is the preferred method of extraction as it can then be used as a feedstock for other biocatalytic conversions, the results of which can be defined as “natural” products. Ferulic acid can be used to produce vanillin, an economically important chemical in the food, pharmaceutical and cosmetic industries (Topakas *et al.*, 2007).

1.3.4 Mechanical analysis

Cell walls are important in the perception of food when it is consumed, as the strength of the cell walls and the adhesion of adjacent cell walls to one another influences the toughness of food. The tendency of the cells to either rupture or detach from each other when stress is applied will affect the juiciness and texture of the food in the mouth (Figure 11).

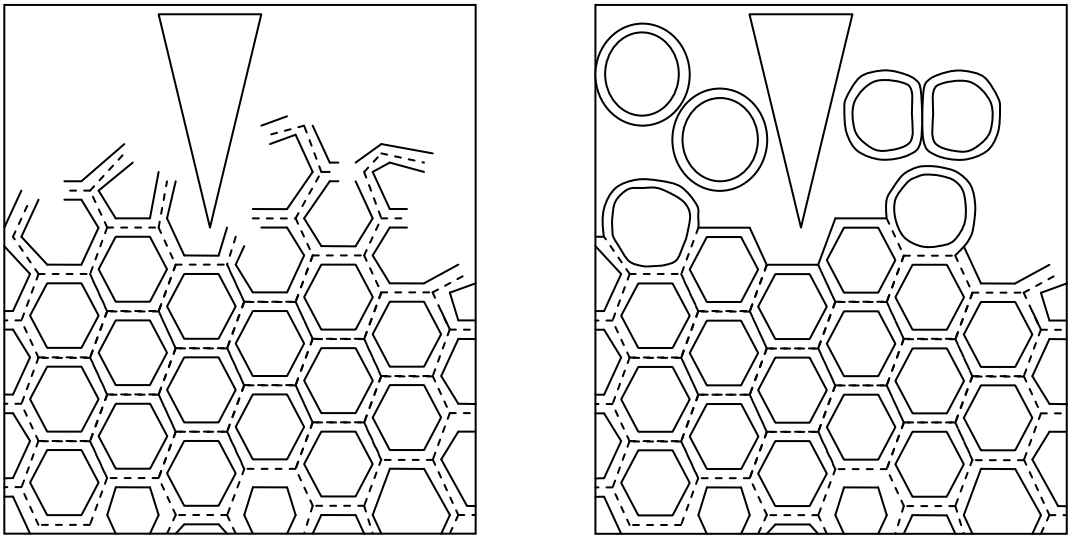

Figure 11: Cell rupture (left) and cell separation (right), based on Brett and Waldron (1996).

Studies on the effects of heating, storage and phenolic extraction on the strength of plant tissues have been done. For most plants, heating and storage decrease the cell adhesion and weaken the tissues, for example potato (Waldron *et al.*, 1997). Chinese water chestnut tensile strength is increased

slightly by heating (Waldron *et al.*, 1997), but is decreased by alkali extraction of phenolics, in particular in 1 M NaOH, when 8,8'-DiFA (AT) is removed, indicating this may form part of a key phenolic-polysaccharide linkage (Parker *et al.*, 2003).

1.4 Chinese water chestnut

Chinese water chestnut (*Eleocharis dulcis* (Burman f.) Trin ex Henschel) is a plant in the family *Cyperaceae*. It grows naturally, and by cultivation, in many parts of Asia, and recently small-scale cultivation has started in Australia and the USA. The inedible leaves grow to between 1 and 1.5 metres high and are used in some countries to produce mats (Klok *et al.*, 2002). The Chinese water chestnut (CWC) corms are oblate spheres, of diameter 3-4 cm, with a dark brown skin and a ring of leaf-bases around the apex (Figure 12).

Figure 12: Chinese water-chestnut corms (left) and a sprouting corm (right).

The edible part of the corm consists of thin-walled parenchyma cells containing starch granules, interspersed with vascular strands (Parker and Waldron, 1995). CWC is widely known to retain a crisp texture when cooked and this has been shown mechanically by three separate groups (Loh and Breene, 1981; Mudahar and Jen, 1991; Parker *et al.*, 2003). They grow in paddy-like ponds, and are therefore beset by a wide range of pathogenic organisms, protection from which

is provided by the outer epidermis. Apart from damage due to animal feeding, growing CWC appears to be susceptible to only a few pathogens such as rust (*Uromyces* sp.), stem blight (*Cylindrosporium eleocharidis*) and water-chestnut wilt caused by a specific *Fusarium oxysporum* (Midmore, 1997). They are easily damaged during harvest, however, giving saprophytic fungi and bacteria access to the inner tissue.

CWC leaves have transverse septa 2-3 mm apart, but only every third/fourth one is usually complete. All plants require oxygen for efficient cellular respiration, and the water-saturated soils in which CWC grow force the plants to cope with anoxic conditions around the underground organs. Oxygen diffuses 10 000 times slower through liquid water than through air, so cellular respiration quickly depletes the available oxygen, leading to anoxia and a large decrease in plant nutrient availability. It also allows the build-up of anaerobic soil microbes. Plants deal with anoxic conditions by facilitating transport of oxygen from the atmosphere to underground or underwater organs. Aerenchyma cells provide pathways for oxygen and carbon dioxide throughout the plant. Movement through aerenchyma may be through diffusion and/or pressurised convection. These mechanisms are important for growth and productivity in plants such as rice (and presumably CWC).

1.4.1 Studies of CWC cell walls

The microscopic investigation of CWC (*Eleocharis dulcis*) parenchyma has included light, UV and electron microscopy (Parker and Waldron, 1995); these included studies that used 50 mM KOH at 100°C for 30 min to separate CWC cells, but allowed the predominance of phenolics at the perimeters of the cell faces to be visualised (Figure 13). Atomic force microscopy studies have shown the lamellar structure of microfibrils in the cell walls of CWC (Figure 3, §1.2.1).

Chemical analyses have generally been restricted to the phenolic acid (alkali-releasable), neutral sugar and uronic acid content of CWC parenchyma cell

walls (Parker and Waldron, 1995; Parr *et al.*, 1996). The neutral sugars were mainly glucose, indicating the presence of cellulose, and arabinose and xylose, implying the presence of arabinoxylan (Parker and Waldron, 1995). The alkali-releasable phenolics were mainly ferulic and coumaric acid, plus six of the nine known diferulic acids (Figure 5, §1.2.4) (Parr *et al.*, 1996).

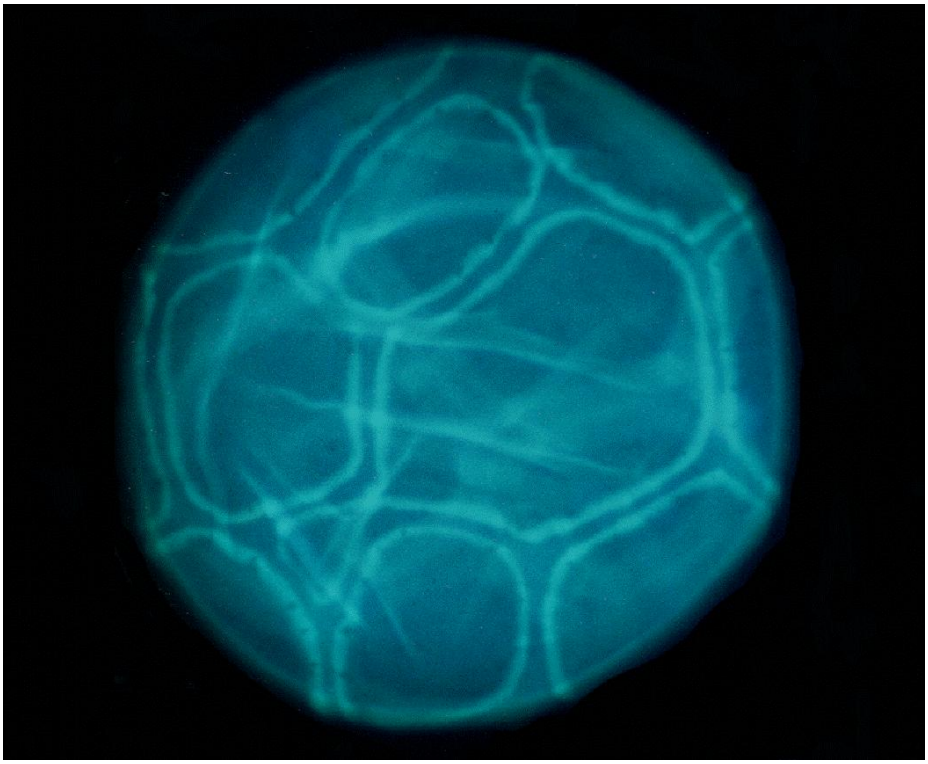

Figure 13: CWC cell in alkali, showing concentration of phenolics at the edges of the cell faces, visualised by UV microscopy, from Parker and Waldron (1995).

Mechanical testing has shown that CWC does not lose mechanical strength when thermally treated. The changes to the carbohydrate structure during thermal treatment do not result in cell separation, even though the pectins in CWC are degraded in the same way as those in potato, which does undergo cell separation under the same conditions (Brett and Waldron, 1996). The phenolic composition may explain the thermal properties of CWC, as treating CWC with increasing concentrations of alkali does induce cell separation of CWC parenchyma (Parker *et al.*, 2003). Parker *et al* (2003) also tested various chemical and enzymic treatments for their ability to cause cell separation.

- Concentrated hot acid induces cell separation and reduces pH-dependent autofluorescence (PDA)
- Weak hot acid also induces cell separation after a longer reaction time, but retains PDA.
- Chelating agents (hot or cold) did not induce cell separation.
- Concentrated alkali (hot or cold) induced cell separation and removed PDA.
- Treatment with endoxylanase induced cell separation and PDA was retained.

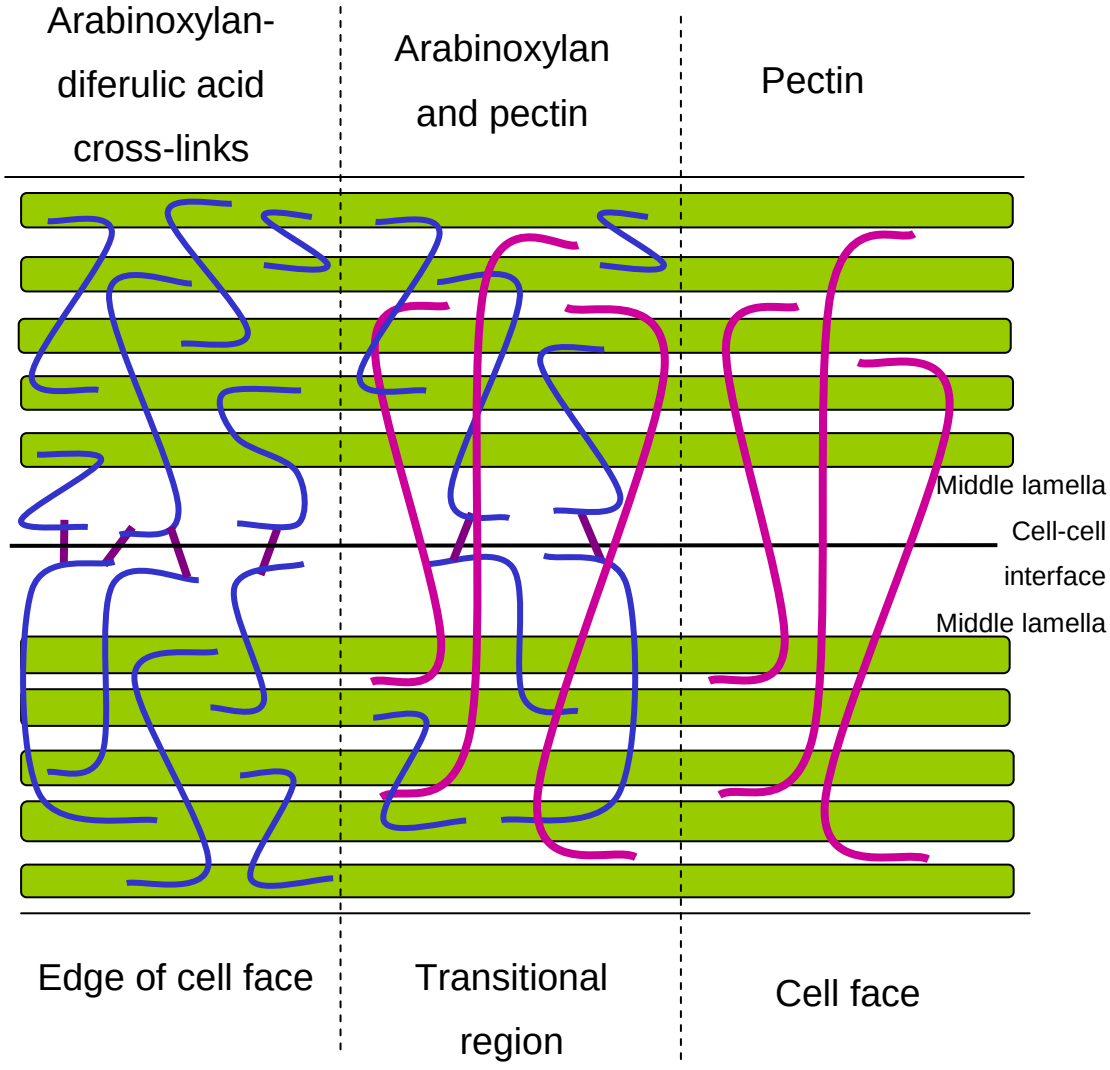

Figure 14: Provisional cell-wall model of CWC parenchyma at the interface of two cells (Cellulose is green, AX is blue, pectin is pink, diferulic acid cross-links are purple).

From these results, it can be assumed that xylans are a key component of CWC cell-cell adhesion, as apparently are diferulic acids, but not calcium-containing pectins. If the cell walls of CWC are consistent with the Type II cell wall then the xylans are arabinoxylans, and they are hydrogen-bonded to the cellulose microfibrils. The high concentration of ferulic and diferulic acids implies that these may cross-link the arabinoxylans, therefore breaking the arabinoxylan backbone, or de-esterifying (di)ferulic acids with alkali will cause cell separation. These results have been incorporated into a provisional cell-wall diagram (Figure 14).

To incorporate the heterogeneity of the cell wall with regards to the distribution of phenolics on the cell surface, the provisional wall model is presented in three sections, one rich in arabinoxylan and ferulic acid (load-bearing edges of cell faces), one rich in pectin (non-load-bearing cell faces), and one where the two are superimposed as they might be in a transitional region. The arabinoxylans are hydrogen-bonded to the surface of the cellulose microfibrils. The pectins form a separate network not connected to the microfibrils or arabinoxylans.

1.5 Analytical theory

1.5.1 Gas-chromatography (GC) theory

Gas chromatography is used to quantify cell wall sugars, as the derivatisation required to make them volatile is relatively quick and simple and gives quantitative results.

A schematic of a gas chromatograph is shown in Figure 15. Gas chromatography involves injection of a vaporised sample onto the head of a chromatographic column. Elution of the sample is achieved due to the flow of an inert gaseous mobile phase such as nitrogen or helium. As the mobile phase is inert it does not interact with the molecules of the analyte; it only transports the analyte through the column. The choice of mobile phase depends to an extent on the detector used and upon economics. Nitrogen is

cheaper than helium, but tends to give slower analyses, as the separating efficiency of nitrogen is worse than helium at high flow rates (Sheffield Hallam University, 2004).

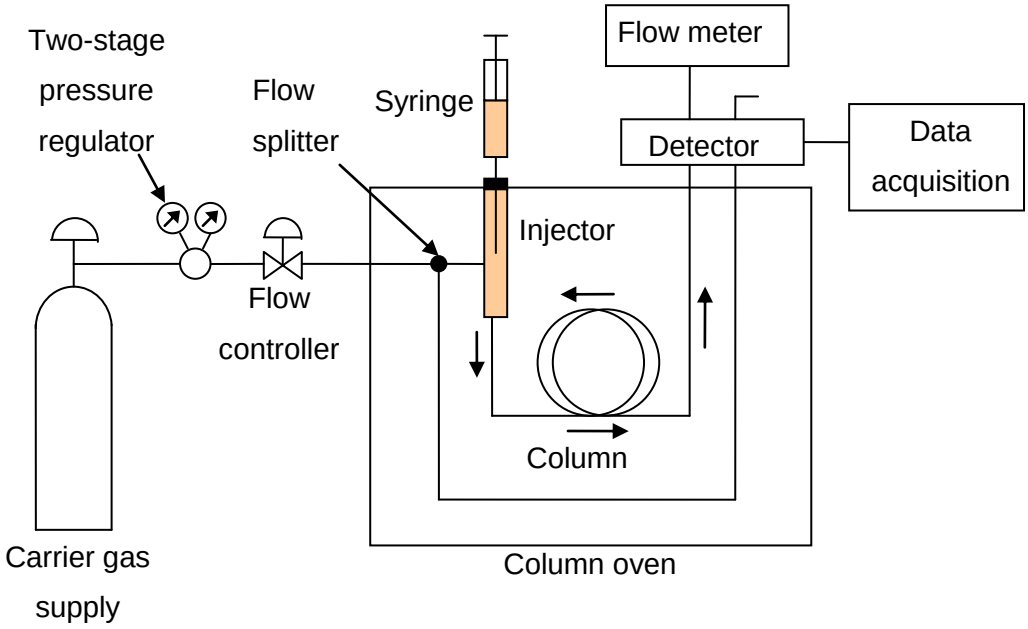

Figure 15: Schematic of a gas chromatograph, based on Skoog* et al *(1996).

Gas chromatography is based upon the partition of the analyte between a gaseous mobile phase and a liquid phase immobilised on the surface of an inert solid. Samples need to be introduced to the column as quickly as possible to maintain good resolution.

A common detector used in gas chromatography is the flame ionisation detector (FID). It pyrolyses the molecules in a hydrogen/air flame, releasing ions and electrons that conduct electricity through the flame. A potential of a few hundred volts is applied between the point of ignition and a collector electrode, the resulting current is amplified and measured. The FID responds to the number of carbon atoms entering the detector per unit time so it is a mass flow detector. It is popular because it has a linear response range of 10^7 and detects most organic compounds. One drawback of the FID is that the sample is destroyed in the process.

Gas chromatography can also be used to analyse phenolics, but this requires silylation to make them volatile; HPLC, which is preferred (described in Section §1.5.2), allows for identification by their UV spectra.

1.5.2 High performance liquid chromatography (HPLC) theory

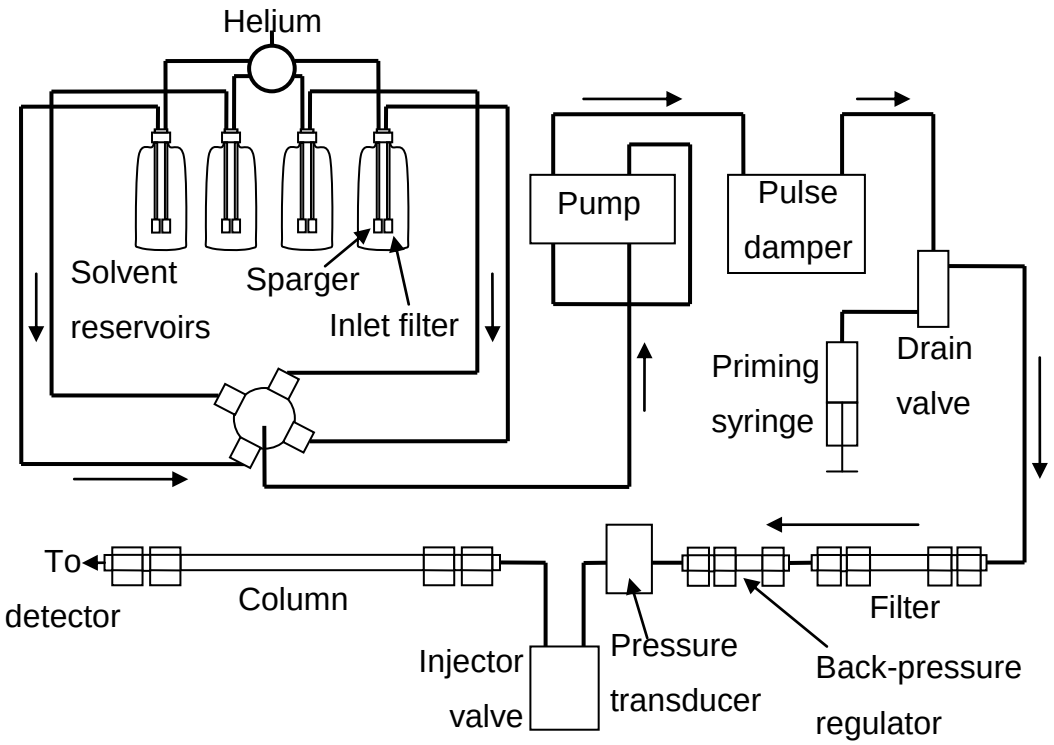

Figure 16: Schematic of a high-performance liquid chromatograph, based on Skoog* et al *(1996).

The vast majority of the research community use reverse-phase HPLC to analyse phenolics (Robbins, 2003). A schematic of a HPLC system is shown in Figure 16. In reverse-phase HPLC, the stationary phase consists of silica with *n*-alkyl chains (normally C_{18} or C_8) covalently bound to their surface, and the mobile phase is an aqueous/water-miscible elution mixture e.g. water and methanol, water and acetonitrile; this results in the most hydrophilic compounds eluting first. Much of the HPLC system is required for the correct regulation of the solvent composition and flow rate.

Three detectors commonly used with HPLC Detectors are UV diode-array detectors (DAD), refractive-index detectors (RI) and mass-spectrometer detectors (MS). Diode-array detectors require light from a broad-spectrum light source to be shone through the sample. The light that is not absorbed by the sample is detected by an array of photosensitive diodes that detect the intensity of a particular wavelength of light, which is then recorded by a computer. The spectra produced are often characteristic of the compound that produced them, aiding identification. Refractive-index detectors detect the change in refractive index between the sample and a suitable reference material; they are sensitive to external environment changes, but are useful for detecting non-ionic and non-light absorbing/fluorescing compounds. Mass spectrometry is described in detail in Section §1.5.3.

1.5.3 Mass spectrometry (MS) theory

A mass spectrometer produces ions from a sample and separates them according to their mass-to-charge ratio. The process of ionisation usually produces molecular and fragment ions giving an indication of molecular weight and structural information that may help with identification. There are a number of methods for ionisation, and the method used depends on the type of compound being analysed.

- Electron impact (EI) – volatile samples
- Chemical ionisation (CI) – volatile samples
- Fast atom bombardment (FAB) – involatile or high molecular weight samples
- Electrospray ionisation (ESI) – involatile or high molecular weight samples
- Matrix-assisted laser desorption ionisation (MALDI) – involatile or high molecular weight samples

The ions are accelerated by applying a voltage to them, and then passed into a mass analyser. There are a number of mass analysers available, although they generally work by exploiting the properties of ion behaviour in magnetic and/or electric fields (a magnetic-sector mass analyser is shown in Figure 17. As the ions have different mass-to-charge ratios (m/z), they will be deflected by different amounts in a magnetic/electric field. With the field at a specific strength, only ions with suitable m/z will reach the detector. If the magnetic field is increased, ions with higher m/z will reach the detector. The detector monitors the ion current, which it magnifies and transmits to the data analysis software. The data is presented as intensity against m/z.

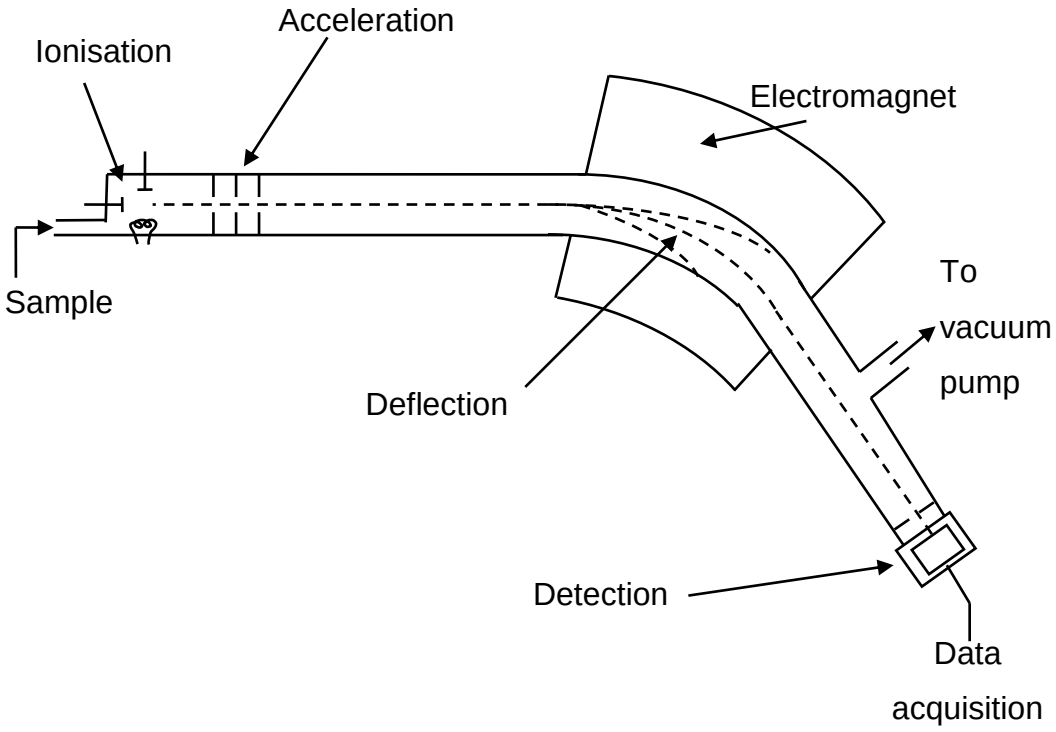

Figure 17: Schematic of a magnetic-sector mass spectrometer.

The ionisation method commonly used to analyse the phenolics as they come off the HPLC column is electrospray ionisation (ESI). ESI is regarded as a "soft" ionisation method as it does not fragment the analyte significantly. A solution of the analyte (10^{-4}-10^{-5} molar) is sprayed through a capillary needle held at a potential of 2-3.5 kV at 10-1000 µl/min, producing a spray of charged droplets at atmospheric pressure. The spray passes through a staged pumping

system during which the droplets shrink due to solvent evaporation, releasing charged molecules. These charged molecules are then mass-analysed by the mass spectrometer. ESI is particularly useful for large molecules, as with this method they acquire multiple charges, bringing them within the mass/charge ratio range of conventional mass spectrometers. ESI is also useful for smaller, highly charged, thermally labile compounds (Mellon, 2000). ESI can be used to produce positive or negative ions. The positive ions are normally adducts of the analyte with hydrogen, sodium or potassium. Instead of a magnetic-sector mass analyser, the mass spectrometers used had a triple quadrupole or time-of-flight (ToF) mass analyser. The quadrupole mass analyser is more complicated than the magnetic-sector mass analyser, but it works along similar principles. The ToF mass analyser uses the principle that each ion is imparted with the same amount of energy, so heavier ions travel more slowly than lighter ions, and therefore measuring the time taken to travel a certain distance can provide the m/z of an ion.

1.6 Aims of investigation

The aims of this investigation were as follows:

1.6.1 Cell walls in different tissues of CWC

Renard *et al* (1999) found different ratios of ferulic acid to dimers in different tissues of quinoa and suggested this may be due to their different roles. There have also been differences in the proportions of diferulic acid isomers present in the tissues of sugar beet (Wende 2000). Parker *et al* (2000) found that the parenchyma cell wall of chufa, another *Cyperaceae*, had ferulic acid as the predominant phenolic, whereas in the epidermis *p*-coumaric acid was predominant. The sugar content also differed considerably. The differences in gross composition of CWC cell walls from three different tissues of the corm: the white, edible parenchyma; the brown outermost layer of epidermis; and the sub-epidermal layer of vascular tissue, were investigated and their likely roles in the plant's physiology put forward.

1.6.2 Cell wall cross-links

The cell wall cross-links in CWC have been inferred, but not properly elucidated; therefore, this investigation focussed on extracting phenolic-polysaccharide fragments and characterising them to see if they were similar to those already seen in the *Amaranthaceae* (feruloylation at the *O*-2 position of Ara residues in arabinans and/or *O*-5 position of Gal residues in galactans) or the *Poaceae* (feruloylation at the *O*-5 position of Ara residues in arabinoxylans) (Ishii, 1997). In particular, the 8,8'-DiFA (AT) was of interest as previous research had implicated it in the thermal stability of CWC mechanical properties (Parker *et al.*, 2003).

1.6.3 Higher oligomers of ferulic acid

As other investigators had shown at the beginning of this investigation (Bunzel *et al.*, 2003a; Rouau *et al.*, 2003), that higher oligomers of ferulic acid were present *in vivo*, the presence of trimers and tetramers was anticipated. Finding higher oligomers of ferulic acid in CWC would show that they are not restricted to maize or even the *Poaceae*. Assuming trimers were found, it was hoped that their molecular structures could be elucidated by NMR.

2 General Materials and Methods:

All reagents, unless otherwise stated, were of analytical grade.

2.1 Source of materials

Fresh CWC (*Eleocharis dulcis* var. unknown) were obtained from local suppliers. The fresh CWC are generally vacuum-packed at source and refrigerated at 4°C during transport and presale storage. The CWC were peeled and chopped into cubes, roughly 1 cm to a side, removing any diseased areas as they were encountered. The pieces of peel, including tops and bottoms, were kept separate from the parenchyma pieces. The peel and parenchyma were frozen in separate vacuum flasks using liquid nitrogen; they were then stored at -20°C until needed.

All the methods presented in this chapter were based on standard methods developed and validated over a period of ten years on a number of different plant species.

2.2 Preparation of cell-wall material (CWM)

There are many ways of preparing cell-wall material, which have been compared in a paper by Renard (2005), but none of the methods described was exactly the same as that described below. Based on the findings of Parr *et al* (1997) that the sodium dodecyl sulfate (SDS) method gave more reproducible results, the following method was adapted from the methods described by Fry (1988) and Brett and Waldron (1996).

Two batches of cell wall material were prepared from CWC parenchyma using the method given below for the following amounts of material: Batch 1 ~400 g frozen fresh weight (4 preparations); Batch 2 ~3,100 g frozen fresh weight (29

preparations). The fresh corms were purchased separately from different suppliers.

2.2.1 Preparation of parenchyma-cell-wall material

Approximately 100 g of CWC parenchyma was blended using a Waring blender (330 W, Fisher) in 200 ml of 1.5% SDS containing 5 mM $Na_2S_2O_5$ (Appendix A) in 2-5 bursts of 30 s until all large lumps had been broken down. Further homogenization was carried out using an Ystral Homogenizer (Ystral GmbH) on power level 3 (500 W, 16000 rpm) for 6 minutes. Drops of octanol were added as required to reduce foaming. The homogenate was filtered through a 100-µm nylon mesh (VWR) and washed with 100 ml 0.5% SDS solution containing 3 mM $Na_2S_2O_5$. The excess liquid was squeezed from the residue, which was transferred to a beaker. Any remaining residue was washed off the mesh using 200 ml 0.5% SDS solution (as before) into the beaker. The suspension was filtered through the mesh again, washing with 100 ml 0.5% SDS solution. Excess liquid was squeezed out of the residue, which was transferred to a 1 L ceramic ball mill. The residue was washed into the ball mill with ~180 ml 0.5% SDS solution, so the tops of the ceramic balls were just showing above the surface. The ball mill was run at 60 rpm for 1 hr at 4°C. The contents of the ball mill were sieved and washed with deionised water into a metal beaker. Unwanted particles of epidermis were decanted off. The cell-wall mixture was filtered through a 100-µm mesh, washing with 1 L of deionised water. A small sample of cell-wall mixture was tested for starch by staining with I_2/KI solution (see Appendix A) and examining it under a microscope, at which point there were usually still some starch granules trapped in cells that had been ruptured. The mesh was washed with ~1 L of deionised water into a metal beaker then homogenised with an Ystral Homogenizer on power level 2 (500 W, 13000 rpm) for 3 minutes to release the starch granules. The mixture was filtered again through the 100-µm mesh and washed with deionised water (~6 L) until no starch was visible under the microscope. The majority of the excess liquid was squeezed out of the residue, which then stuck together in clumps. The residue

was transferred to a plastic bottle with ~70 ml deionised water and frozen (-20°C).

2.2.2 Preparation of epidermis-cell-wall materials

The CWC peel from Batch 1 (3 preparations) was used to produce CWM using the above method, although they were blended using a Waring blender for 4 bursts of 30 s. Once the samples had been ball milled, they were carefully decanted to separate the dark brown outer layer of skin (the epidermis), from the light brown inner layer of epidermis (sub-epidermis), which were called the ECWM and SECWM samples respectively, and the residual parenchyma (not used). The samples of epidermis and sub-epidermis were frozen (-20°C) in deionised water. The frozen samples of epidermis were defrosted and combined, as were the sub-epidermis samples. They were homogenised with an Ystral Homogenizer on power level 2 for 3 minutes to release the starch granules. They were then filtered through a 70-µm nylon mesh and washed with deionised water (2-8 litres) until no starch granules were observed under the microscope. The CWM was redispersed in deionised water and frozen (-20°C).

To obtain dry CWM, the suspensions (Batch 1/Batch 2) were defrosted and filtered through a 70-µm nylon mesh (different mesh used for each tissue to prevent cross contamination) and washed with 250/2000 ml ethanol (BDH). The solid was redispersed in 300/500 ml of ethanol and filtered again through the 70-µm mesh. It was then washed with 400/500 ml ethanol and 150/500 ml of acetone (Fisher). The filter was then turned out onto a suitable dish and left to dry overnight in a fume cupboard, lightly covered with a piece of perforated aluminium foil to prevent contamination. The dry CWM tended to form loosely-associated clumps. During the alcohol washing, the epidermis and sub-epidermis samples released a yellow-coloured compound, which was probably chlorogenic acid. Dry CWMs were stored in sealed jars at room temperature.

2.3 Total phenolic extraction

Triplicate samples of CWM (4.8-5.2 mg) from each of the three tissues were accurately weighed into screw-cap glass culture tubes. 1 ml of de-oxygenated, nitrogen-flushed 4 M sodium hydroxide solution was added to each tube; these were then over-flushed with nitrogen (to prevent oxidation) and mixed. The tubes were wrapped in foil to exclude light, reducing *cis/trans* isomerisation (Hartley and Jones, 1975; Kahnt, 1967), and agitated for 24 hr on a rotary tube mixer. The samples were centrifuged (Mistral 2000 centrifuge) three times at 1000 rpm for 5 min to sediment out the solids and 0.6 ml of the supernatant was pipetted into clean culture tubes. The supernatant was quite brightly coloured, as shown in Figure 18, so to ensure there was sufficient solvent for the phenolics the volume of NaOH was increased to 4 ml in later CWM analyses.

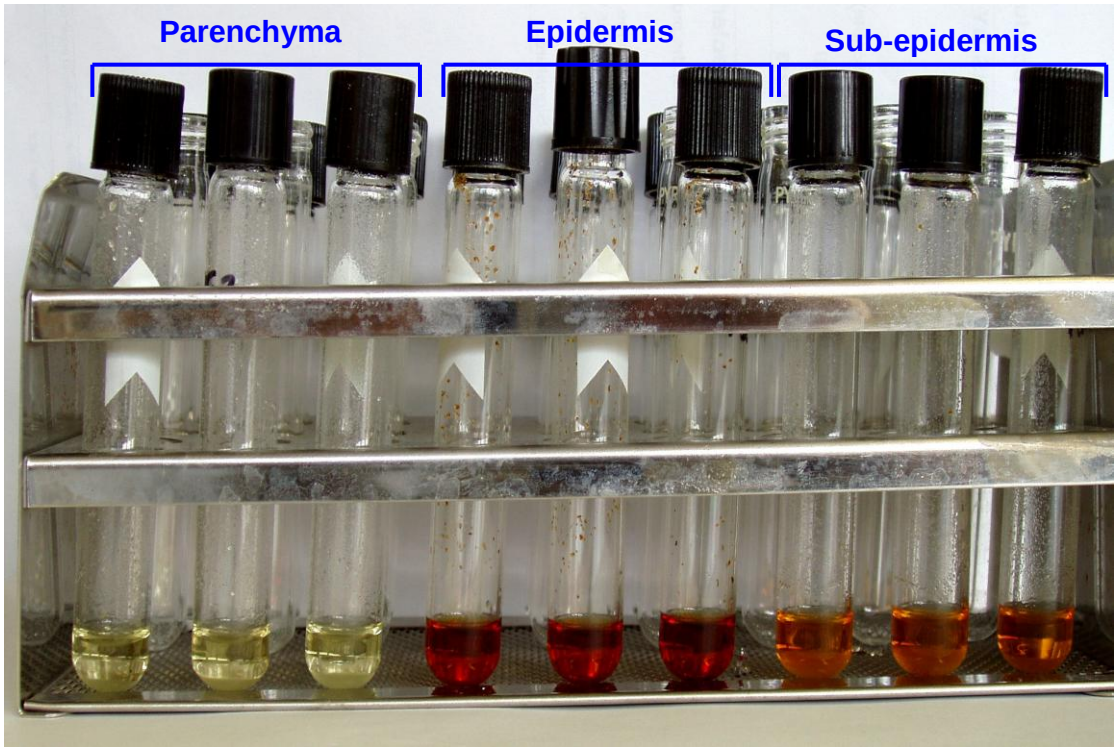

Figure 18: Phenolic extract colours before acidifying; parenchyma (left), epidermis (centre), sub-epidermis (right).

To these tubes 50 µl of *trans*-cinnamic acid solution was added as an internal standard. The solutions were then acidified by dropwise addition of conc. hydrochloric acid (37%, Riedel de Haën) until the pH fell to 2, tested by taking

very small aliquots and spotting them onto pH paper. The tubes were mixed well to make sure the neutralisation was complete. The aqueous phase was then extracted three times with ethyl acetate (Riedel de Haën, HPLC grade), 3 ml, centrifuging for three minutes at 200 rpm to separate the layers. The ethyl acetate extracts were combined in a clean culture tube. The ethyl acetate was evaporated to dryness using a sample concentrator (Techne) set at 40°C, under a flow of N_2. The dry samples were redissolved in 1 ml methanol:water (50:50 v:v). 200 µl of the samples were filtered through a 0.2 µm PVDF filter into a "yellow" Chromacol vial.

The samples were analysed on the HPLC using the method set up for simple phenolics, the main parameters of which are described in Appendix B. Solvent A was acetonitrile:methanol:water (40:40:20 v:v:v) and Solvent B was 10% (v/v) acetonitrile in water, both containing 70 µl/L TFA. The solvent flow was set to 1 ml/min, and the initial solvent composition of 10% A and 90% B was held for 0.5 min, over 25 min the composition was changed linearly to 75% A and 25% B, the composition was further changed to 100% A linearly over 5 min, finally an exponential gradient of -3 returned the solvent composition to 10% A, 90% B over 10 min and this composition was held for 2 min.

2.4 Sequential phenolic extraction

The sequential phenolic extraction was carried out in much the same way as the total phenolic extraction, but with the following differences. Larger samples of 10-12 mg CWM (Batch 1) were used. Four different concentrations of sodium hydroxide solution were used for the extractions, 0.1 M, 1 M, 2 M and 4 M. The extractions were carried out in order, on Batch 1 CWM samples, under the following conditions: (i) 4 ml, 0.1 M NaOH, 1 hr; (ii) 4 ml, 0.1M NaOH, 24 hr; (iii) 4 ml, 1 M NaOH, 24 hr; (iv) 4 ml, 2 M NaOH, 24 hr and (v) 4 ml, 4 M NaOH, 24 hr. All NaOH solutions were made with de-oxygenated deionised water. Between each extraction the samples were centrifuged at 1000-2500 rpm for 5-20 min until the solids sedimented sufficiently to remove the majority of the supernatant, which was pipetted into clean culture tubes. To these tubes

50 µl of *trans*-cinnamic acid solution was added as an internal standard. The solutions were then treated in the same way as the total phenolic extraction samples. Occasionally, the ethyl acetate extractions produced a stable layer of foam above the water/ethyl acetate interface; this was reduced in volume by gentle swirling, which allowed most of the ethyl acetate fraction to be removed.

The experiment was also carried out on ~10 mg of PCWM (Batch 2) under the following conditions: (i) 4 ml, 0.1 M NaOH, 1 hr; (ii) 4 ml, 0.1M NaOH, 24 hr; (iii) 4 ml, 1 M NaOH, 24 hr and (iv) 4 ml, 2 M NaOH, 24 hr, (v) 4 ml, 4M NaOH, 24 hr. For comparison, separate total phenolic extractions over 24 hr or 4 days were also carried out. The extracts were treated as above.

HPLC was carried out on the sequentially extracted samples in the same way as on the total phenolic extracts.

2.5 HPLC-MS analysis

Reverse-phase HPLC followed by positive-ESI MS (and negative ESI MS in some cases) was performed on samples of CWM (~20 mg) extracted in 0.1 M NaOH (8 ml) for 24 hr. The samples were analysed on a Jasco 1500 series HPLC system with a Micromass Quattro II detector operated by Fred Mellon. The HPLC column and method were the same as that used in the phenolic extractions.

2.6 Klason lignin

Lignin analysis was carried out by Zara Merali using the method adapted from Theander and Westerlund (1986) described in Merali *et al* (2007). Duplicate samples of CWM (~50 mg) were dispersed in 0.75 ml of 72% (w/w) H_2SO_4 for 3 hr at room temperature. The samples were diluted with 9.0 ml deionised water and incubated for 2.5 hr in an oven at 100°C. The samples were filtered through pre-weighed sintered glass funnels (10 mm diameter, Fisher Scientific)

under vacuum to recover the insoluble residue. The residue was washed three times with water (<40°C) until it was free of acid. The glass funnels (with residues) were dried at 50°C in an oven until a constant weight was obtained. Klason lignin was calculated gravimetrically as follows:

Lignin (%) = $((W_1-W_2) \times 100)/S$

where:
W_1 = weight of glass filter + dried residue
W_2 = weight of glass filter
S = weight of initial sample

2.7 Neutral sugars

Triplicate samples (2-4 mg) of CWM (Batch 1) from the three tissue types were weighed into clean screw cap culture tubes. To each tube was added 200 µl of 72% (w/w) H_2SO_4, in which the samples were left to stand at room temperature for 3 hours, with occasional mixing. The samples were then put on ice while 2.2 ml of deionised water was added to each tube to dilute the acid to 1 M concentration. Each tube was shaken thoroughly and put in a hotblock (Griffin) at 100-110°C for one hour. From each sample, 0.5 ml was removed to a microtube tube and frozen at -20°C for later use in determining the uronic acid composition. The remaining samples were put back into the hotblock at 100-110°C for a further 1.5 hr. The samples were allowed to cool, and then 200 µl of 1 mg/ml 2-deoxyglucose solution (2-DOG) was added to each tube to act as an internal standard. From these samples 1 ml was transferred to clean culture tubes, which had 300 µl of 25% (w/w) NH_3 solution added. The tubes were mixed and small aliquots of the solutions were tested to check they were alkali, typically pH 8-9. The samples were incubated with 100 µl of 5% (w/w) NH_3 containing 150 mg/ml of $NaBH_4$ for 1 hr at 30°C in a water bath. The samples were put on ice and 200 µl of glacial acetic acid (Riedel de Haën) was added and mixed in. 300 µl of the resulting solution was transferred to a clean culture tube and cooled on ice while 450 µl of 1-methylimidazole (Sigma) and 3 ml of

acetic anhydride were added. The samples were mixed and incubated at 30°C for 30 min in a water bath, before cooling on ice again. Each tube had 3.5 ml of deionised water and 3 ml of dichloromethane (Fluka) added before shaking vigorously and leaving to separate. The lower organic layer was removed by teat pipette to a clean culture tube. The aqueous layer was extracted with a further 2 ml of dichloromethane and the organic layer combined with the previous extract. The dichloromethane extract was extracted twice with 3 ml of deionised water, keeping and combining the dichloromethane layer from each. The dichloromethane was evaporated until only a viscous film of alditol acetates remained, using a sample concentrator (Techne) set at 40°C, under N_2. The samples were then redissolved in 1 ml of acetone (Fisher), 0.1 ml of these solutions were transferred to "yellow" Chromacol vials ready for analysis.

Stock solutions of the following sugars were made up in 25 ml volumetric flasks to a concentration of 1 mg/ml with deionised water: rhamnose, fucose, arabinose, xylose, mannose, galactose and glucose. The standard solutions were made up by combining 0, 100, 200, 300 or 400 µl of each of these stock solutions. Deionised water and 72% (w/w) H_2SO_4 were added to the stock solution mixtures to give a final H_2SO_4 concentration of 1 M.

To each sugar standard, 200 µl of 1 mg/ml 2-deoxyglucose solution (2-DOG) was added as an internal standard. Samples of these sugar standards, 1 ml, were treated the same way as the CWM samples from and including the point at which 300 µl of 25% (w/w) NH_3 was added, to provide a standard curve for the GC, and give response factors for each sugar.

A further hydrolysis of the CWM sugars was carried out using 1 M H_2SO_4 to determine the amount of non-cellulosic sugars. Triplicate samples (2-3 mg) of CWM from the three tissue types were weighed into clean screw-cap culture tubes. Deionised water (2.2 ml) was added to each tube before 200 µl of 72% (w/w) H_2SO_4 was also added, to give a final H_2SO_4 concentration of 1 M. The samples were then incubated at 100-110°C for 2.5 hr and the experiment continued from the equivalent point in the 72% (w/w) H_2SO_4 hydrolysis.

All the alditol acetates produced were run on the GC using the method for sugars analysis set out in Appendix C. The quantification used the calculations from Sawardeker *et al* (1965).

2.8 Uronic acids

The uronic acid samples kept back from the neutral sugars analysis were diluted with 2 ml of deionised water, to give a total volume of 2.5 ml. Standard solutions (5, 15, 25 and 35 µg/ml) of glucuronic acid were made up. Four screw-cap culture tubes per sample/standard were acid-washed, rinsed and dried. The tubes were cooled in ice and cold water. To each tube, 1.2 ml of sulfuric acid reagent (Appendix A) and 0.2 ml of sample/standard were added before being vortexed and placed back in ice and cold water. The tubes were sealed and heated in a hotblock (Techne) at 100-110°C for 10 min. The tubes were cooled in ice and cold water, checking that they were completely cold before proceeding. To three tubes of each set of four was added 20 µl of 0.15% *m*-phenyl phenol in 0.5% NaOH to 3 of 4 replicates. The last tube of each set had 20 µl of 0.5% NaOH added as a control. The tubes were vortexed for a count of ten, and then put in a light-proof box to exclude light from the tubes. After 40 min (parenchyma and epidermis samples) or 55 min (sub-epidermis samples) in the dark, 0.2 ml of each sample/standard was transferred to the wells in a plate for the plate reader. Standards had been out of the dark for approximately two hours by the time the absorbance was measured. Standards were used on both plates used. The plate reader measured the absorbance at 490 nm.

2.9 Methylation analysis of carbohydrate linkages

Three variations on the methylation method were used: the NaOH method, the lithium dimsyl method, and the lithium dimsyl method with a carboxyl reduction step. This analysis was done three separate times either personally or with the help of Andrew Jay and not all methods were carried out on all occasions.

2.9.1 NaOH-catalysed methylation analysis

The method of Nunes and Coimbra (2001) was modified for this part of the methylation analysis. Triplicate samples (3.5-5 mg) of PCWM and SECWM were weighed accurately into small screw cap vials (ECWM was not finely divided enough to be worth attempting). A starch control (0.9 mg) and a blank were also run to identify any contaminants. 1 ml of anhydrous dimethyl sulfoxide (DMSO), which had been stored over activated molecular sieve particles and tested for water using calcium hydride, was added to each vial. The vials were sealed with a PTFE-lined septum. The septa were pierced using short needles, and then the vials were put into a vacuum manifold. The samples were twice degassed for about 5 minutes and then flushed with N_2. The needles were removed and the vials heated for 40 min at 90°C by standing them on a hotblock at 90°C. The samples were sonicated for 1 hr at room temperature. The samples were stored overnight at room temperature, and then sonicated at room temperature for a further 1 hr 35 min. Sodium hydroxide pellets were ground to a powder using a cleaned and dried Janke & Kunkel A10 mill (180 W, 20000rpm). As much sodium hydroxide as possible was collected into a sealed vial before it started to absorb water. Approximately 0.25 g of sodium hydroxide powder was added to each vial. The vials were sealed and degassed for 1 hr (short needles through septa to vent gas), and then flushed with N_2. The samples were sonicated at room temperature for 1 hr and then stored at 4°C for 30 min until they froze solid. 1 ml of methyl iodide was added to each sample using a “bent” needle, while the vials were vented as before. The samples were shaken until they had melted and mixed thoroughly with the methyl iodide, and then stored overnight (~20 hr) at 4°C. To each sample 2 ml of deionised water and 200 µl of glacial acetic acid were added. The vials were shaken until well mixed. The methyl iodide was removed by bubbling N_2 through the solution while the vials were standing on a hotblock at 40°C. Sep Pak tC18 mini columns were preconditioned by sucking through 5 ml acetonitrile and 5 ml deionised water under vacuum (Figure 19). Deionised water (5 ml) was added to each sample, and then the samples were transferred

to the syringe barrels and sucked through. Deionised water (2 x 5 ml) was added to the syringe barrels and sucked through; the contents of the tubes below were discarded, removing excess reagents and unwanted products, such as DMSO, NaI, NaOAc and MeOH (Mort *et al.*, 1983). 5 ml of methanol and 5 ml of methanol:acetonitrile (50:50 v:v) were sucked through the columns to elute the methylated polysaccharides.

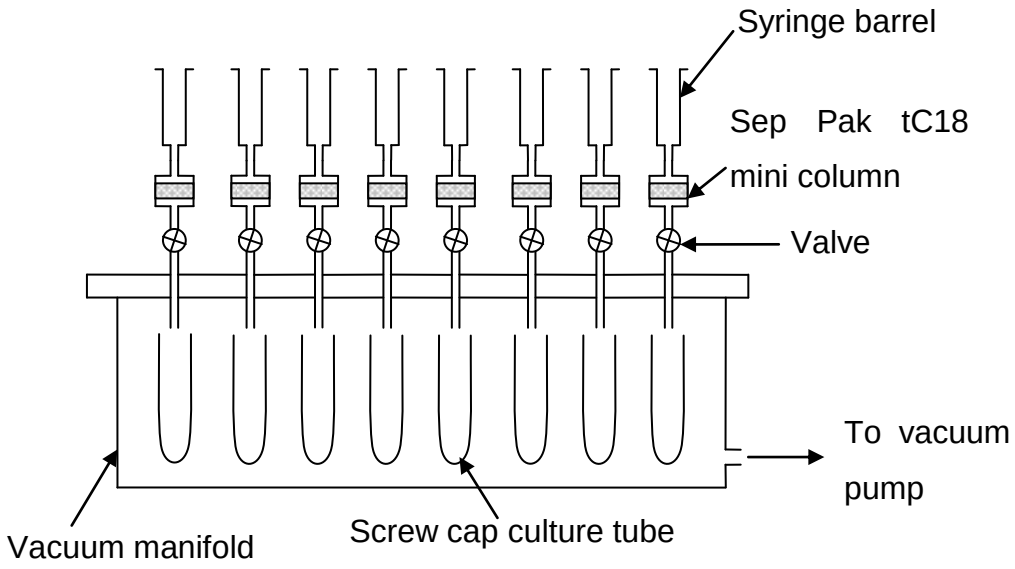

Figure 19: Configuration for separation of methylated polysaccharides during linkage analysis by methylation.

The tubes were then sealed and stored for 4 days at 4°C. The samples were transferred to 50 ml round-bottomed flasks. Sets of five flasks were evaporated at the same time using a five-way connector and a rotary evaporator, at a temperature of 50°C. The dry samples were redissolved in chloroform:methanol (50:50 v:v), and transferred to screw-cap culture tubes, rinsing the flask once with chloroform:methanol. The samples were partly dried down in a sample concentrator at 40°C with N_2 before being stored at 4°C overnight. The remainder of the samples were dried down as before. The hydrolysis and acetylation were as described in Section §2.9.6.

2.9.2 Production of lithium dimsyl catalyst

The following method was used to produce the lithium dimsyl reagent to be used as the catalyst for the methylation. The method was that of Blakeney and Stone (1985). All the glassware was dried at high temperature in an oven and flushed with argon once assembled, to ensure it was free of water. Using a glass syringe, 80 ml of DMSO (stored over activated molecular sieves) was transferred to a 3-necked, 500 ml RBF (with magnetic stirrer bar) under an argon atmosphere. A 150 ml pressure-compensating dropping funnel was fitted to the flask, and the whole system purged with argon three times. Cold butyl lithium (1.6 M in hexane, 100 ml) was transferred by reagent transfer tube to the dropping funnel (Figure 20) and added to the DMSO solution, with stirring, over 10 min.

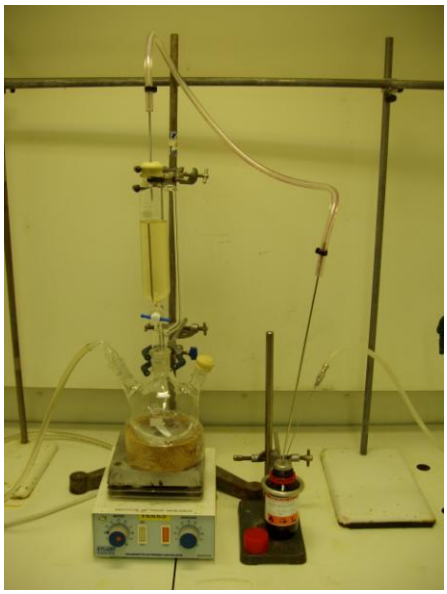

Figure 20: Transferring butyl lithium to dropping funnel.

The reaction warmed the solution to 40°C. The solution became cloudy, and then cleared to give a pale-yellow solution. The solution was stirred for a total of 30 min, and continuous purging with argon removed the evolved butane and hexane. A brown glass bottle (sure-seal type) was oven-dried and purged with argon. Once the upper layer of hexane was gone, the dimsyl solution was transferred (using the glass syringe previously used for the DMSO) to the bottle,

which was sealed with a rubber septum; this was covered in foil and double contained for storage in the freezer.

2.9.3 Samples and initial preparation for lithium dimsyl-catalysed methylation

A blank tube and an acetan polysaccharide were used as controls. The acetan had been produced in-house from *Acetobacter xylinium* (potassium salt, freeze-dried) and had a defined structure (MacCormick *et al.*, 1993; Ojinnaka *et al.*, 1996). The controls and samples, one each of PCWM Batches 1 and 2, were dispersed in dry DMSO (1 ml) under argon by heating at 90°C for 1 hr, then sonicating at 20°C for 2 hr. They were methylated using lithium dimsyl catalyst as described below (§2.9.4); then the methylated samples were divided into two, one portion to be carboxyl-reduced (§2.9.5), the other not, before being hydrolysed and acetylated (§2.9.6).

2.9.4 Lithium dimsyl-catalysed methylation reaction

Lithium dimsyl catalyst (200 µl) was added to the samples using a 1 ml syringe (with Teflon plunger) and then they were left to stand for 10 minutes. The samples were stored in the freezer overnight, before adding 1 ml of methyl iodide to the frozen samples, using a 1 ml syringe. The samples were mixed until homogeneous and all frozen material had melted, before being stored over 4 nights at 4°C. Deionised water (2 ml) and acetic acid (200 µl) were added, and then argon was bubbled gently through the solution to remove excess methyl iodide at 42°C. Deionised water was added (3 ml), and then the solution was washed into prepared dialysis tubing (MWCO 12-14000 Da) using more water. Samples were dialysed against 5 litres of deionised water overnight, with one change of water after 1-2 hr. The contents of each dialysis tube were transferred to 50 ml round-bottomed flasks and evaporated to dryness before being redissolved in 2 ml of chloroform:methanol (1:1 v:v) and filtered through a plug of GF paper in a glass pipette into a sovirel tube. The RBF was rinsed with

2 ml more of chloroform:methanol (1:1 v:v), which was also filtered. The sample was split between two tubes, and was then dried down under N_2 at 40°C. One from each set was dried in an evacuated desiccator over CaO to be used in the carboxyl reduction.

2.9.5 Carboxyl reduction

The carboxyl reduction allows the detection of uronic acids, separate from their neutral equivalents, hence providing more structural information about the polysaccharides. The carboxyl reduction step needs to be done after the methylation of the polysaccharide and before the acid hydrolysis. Lithium triethylborodeuteride ($LiBD(C_2H_5)_3$) is used as a molar solution in tetrahydrofuran to reduce the methyl esters of the carboxyl groups on uronic acids in methylated polysaccharides. They are reduced to di-deuterio-labelled alcohols (unmethylated) at the C-6 of the sugar residues.

The samples that had been dried in a desiccator had 8 ml of $LiBD(C_2H_5)_3$ solution added, using a clean, dry gas-tight syringe with Teflon barrel and "Luer-lok" fitting with needle. The air space above the samples was quickly flushed with argon and the tubes sealed before incubating at 64°C for 4-6 hours. Having cooled overnight, ethanol was added dropwise with cautious mixing, and then the samples were left overnight, unsealed to evolve hydrogen. Each sample was poured into a 25 ml beaker, and 8 ml ethanol, 3 ml water and 2 ml of 20% phosphoric acid (H_3PO_4) were added. Back neutralisation required the addition of ~1 g of Na_2CO_3 and 2 ml water. The supernatant was decanted into a 3 cm sintered glass funnel (no. 3) under suction to a 100 ml Buchner flask. The beaker was rinsed with a further 10 ml of ethanol and 3 x 10 ml of chloroform:methanol (1:1 v:v). The filtrate was transferred to a round-bottomed flask and evaporated to dryness at 50°C, then redissolved in 2 x 2 ml chloroform:methanol (1:1 v:v). The solution was filtered through a plug of GF paper in a glass pipette, into a Sovirel tube, in which it was dried down under N_2 at 40°C (Redgewell and Selvendran, 1986).

2.9.6 Hydrolysis and acetylation

The method of Nunes and Coimbra (2001) was modified for this part of the methylation analysis. The carboxyl-reduced and unreduced samples had 1 ml of 2 M trifluoroacetic acid (TFA) added, the tubes were sealed, gently mixed and heated at 121°C for 1 hr in order for the hydrolysis to occur. The samples were evaporated until dry (~1 hr) at 40°C under N_2. Two drops of 35% ammonia was added to each tube, followed by 100 µl of 5% (w/w) NH_3 containing 150 mg/ml of $NaBD_4$, before heating for 1 hr at 30°C. The samples were put on ice and 200 µl of glacial acetic acid (Riedel de Haën) was added to neutralise the alkali. The samples were acetylated by adding 450 µl of 1-methylimidazole (Sigma) and 3 ml of acetic anhydride and incubating at 30°C for 30 min, before cooling on ice. Each tube had 3-4 ml of deionised water and 3 ml of dichloromethane (Fluka) added before shaking vigorously and leaving to separate. The tubes were centrifuged at 100 rpm for 1 min to separate the layers. The lower organic layer, containing the partially methylated alditol acetates, was removed by Pasteur pipette to a clean tube. The aqueous layer was extracted with a further 2 ml of dichloromethane. The combined organic layers were evaporated at 40°C, under a flow of N_2, until only a viscous film remained. The samples were then redissolved in 0.5 ml of acetone (Fisher). The samples were transferred to two “yellow” Chromacol vials (0.15 ml per sample), ready for analysis by GC and GC-MS. Standards were prepared by purposely undermethylating monosaccharides by the NaOH method, without the sonication steps. The GC and GC-MS (Agilent 5973 Mass Selective Detector) were set up to run the same GC method, which is given in Appendix D, where the mass spectrometry parameters are also listed. The GC-MS was operated by John Eagles.

2.10 Microscopy

Mary Parker carried out light microscopy of the CWC parenchyma, epidermis and sub-epidermis. Transverse sections of the epidermis of CWC were cut by hand and photographed unstained under visible light, and under UV light at pH

9.6 (20 mM NH_4OH) using a Leitz Ortholux II fluorescence microscope. The microscope was fitted with an HBO 50W mercury arc lamp and an exciter and barrier filter combination with transmissions of 340-380 nm and >430 nm, respectively.

2.11 Vortex-induced cell separation (VICS)

Samples of fresh parenchyma (5 mm cubes) and epidermis (7 mm diameter circles, with or without the sub-epidermal layer) were tested in 3 ml of the following solutions: i) Water, ii) 0.5 M H_2SO_4, iii) 0.05 M TFA, iv) 1 M TFA, v) 1 M NaOH, vi) 4 M NaOH; for either 3 hr at 100°C, 24 hr at room temperature or 72 hr at room temperature. Each tube contained two pieces of material. The tubes were vortexed for 30 s and shaken vigorously for a count of 10. Observations were taken of the state of the plant material and scored as shown below.

VICS Scores:

0 No apparent change
1 Original pieces still apparently whole, tiny pieces floating in solution
2 Original pieces substantially whole, small pieces floating in solution
3 Original pieces broken into a number of pieces
4 Original pieces completely broken up, but not into individual cells
5 Most cells separated from others

The colour, opacity and physical properties of the surrounding liquor were observed.

2.12 Sequential extraction

The sequential extraction was different to the sequential phenolic extraction, and had three main stages, as outlined below.

2.12.1 CDTA extraction

The CDTA solution was prepared by mixing 0.48 g of $Na_2S_2O_5$ and 9.1 g of CDTA (Na^+ salt, Sigma) in 400 ml deionised water (to give final concentrations of 5 and 50 mM respectively). NaOH solution (2 M) was added dropwise, bringing the pH back up to 7. As the pH increased the CDTA dissolved. The solution was then made up to 500 ml with deionised water. PCWM (2 g, Batch 2) was extracted with 250 ml of 50mM CDTA at room temperature (~20°C) for 6 hr. The suspension was filtered through GF/C under vacuum and the residue washed with additional deionised water. The filtrate was frozen at -20°C. The residue was treated further with 250 ml of 50 mM CDTA for 2 hr, the residue and filtrate separated as above and the filtrate frozen.

2.12.2 Na_2CO_3 extraction

The residue was sequentially extracted with 250 ml of 50 mM Na_2CO_3 (containing 20 mM $NaBH_4$) at 4°C for 18 hr, then at room temperature (~20°C) for 2 hr. The suspensions were filtered as above and the filtrates neutralised with 4 M acetic acid to prevent further reaction. The filtrates were frozen and the residue extracted further as described below.

2.12.3 KOH extraction

The residue was extracted in 250 ml of degassed 0.5 M, 1 M and 4 M KOH containing 20 mM $NaBH_4$ at room temperature for 2 hr. The KOH suspensions were centrifuged at 15000g for 10 min at 18°C in a Beckmann Avanti J-20 centrifuge using polypropylene copolymer (PPCO) centrifuge bottles. The supernatants were filtered as above and neutralised before being frozen. The KOH supernatants were concentrated by rotary evaporation at 50°C, and then dialysed against deionised water. The dialysed supernatants were frozen, and then the supernatants and final residue were freeze-dried.

3 Characterisation of Cell Walls of Chinese Water Chestnut:

Phenolics of CWC parenchyma-cell walls have been studied previously by Parr *et al* (1996), but not the epidermal tissues, which one would expect to contain greater quantities of phenolics because they are coloured and in closer contact with the waterlogged environment of a paddy field.

Cell-wall polysaccharides were investigated for the three tissues of CWC; parenchyma (PCWM), epidermis (ECWM) and sub-epidermis (SECWM), in order to verify the previous work done on CWC parenchyma by Parr *et al* (1996) and extend this to the other tissues. The neutral sugars and total uronic acid contents were quantified and their linkage patterns investigated to determine the types of polysaccharide present. As CWC is a monocotyledon, one might expect it to have a similar polysaccharide composition to that of other monocotyledons.

3.1 Methods

Neutral sugars, uronic acids, phenolics and Klason lignin were quantified as described in Chapter 2. Linkage analysis was also carried out as described in Chapter 2. All analyses were carried out on Batch 1 CWM unless otherwise stated.

3.2 Results

The yields of purified cell-wall material from the frozen parenchyma, epidermis and sub-epidermis tissues were 5.7, 8.3 and 17.3 g/kg frozen tissue respectively. This is a little low in respect to the parenchyma, but probably just reflects inexperience with the method, as the yield for Batch 2 of parenchyma was 9.6 g/kg frozen tissue.

3.2.1 Phenolic composition

Total phenolic extraction

The HPLC showed that the three tissue types had distinct differences in composition; this can be seen in the raw chromatograms shown in Figures 21-23.

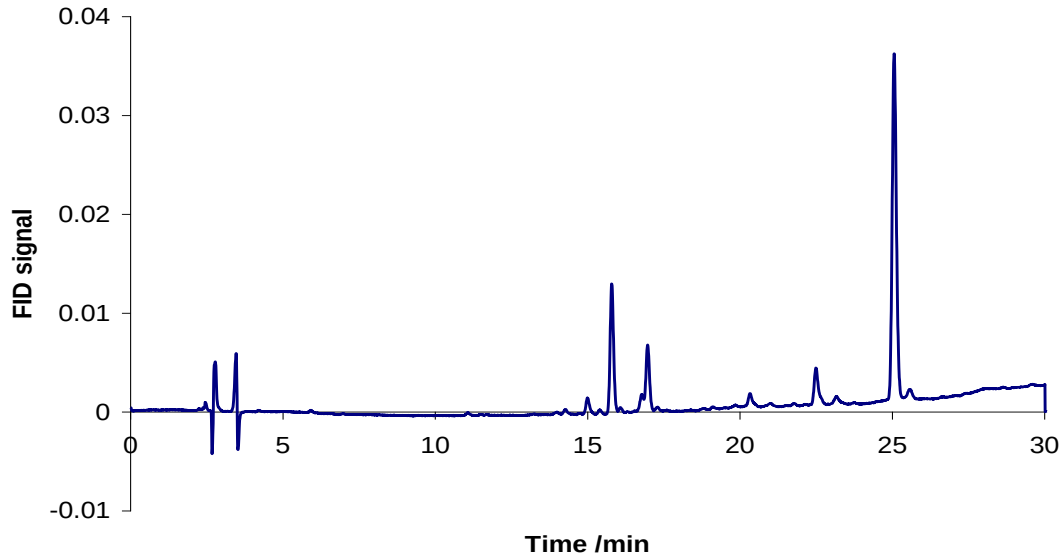

Figure 21: Raw chromatogram for total phenolic extraction of PCWM.

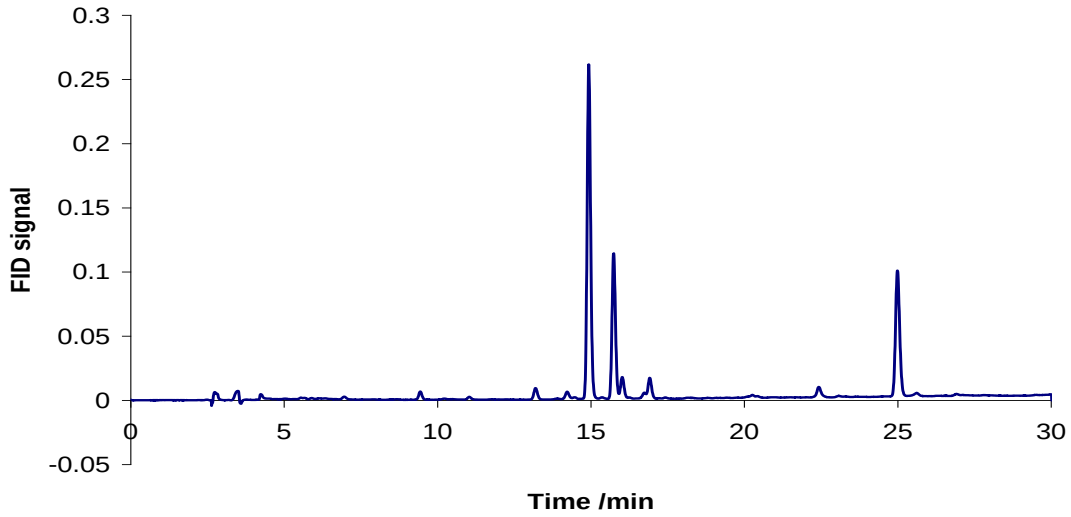

Figure 22: Raw chromatogram for total phenolic extraction of ECWM.

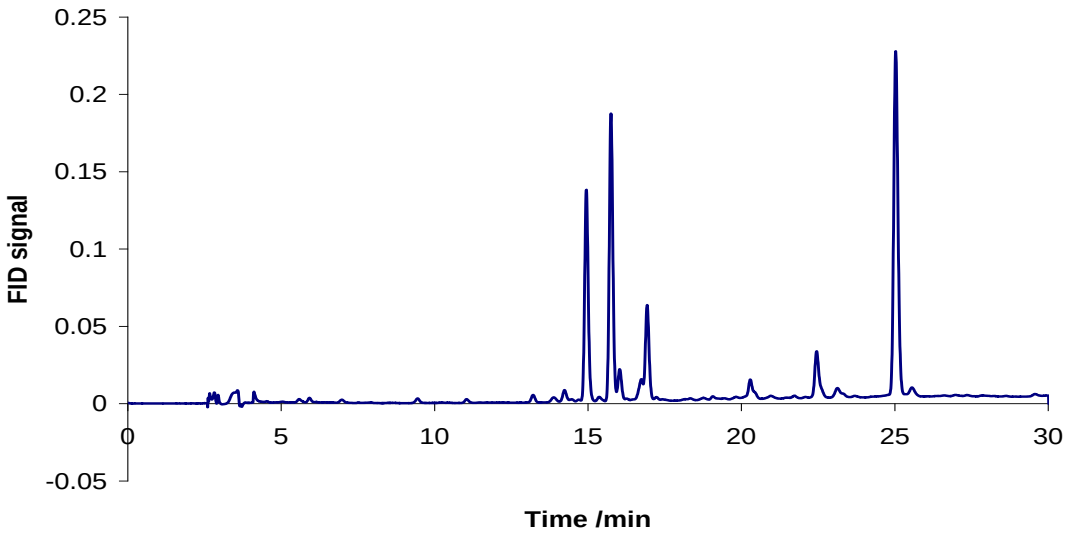

Figure 23: Raw chromatogram for total phenolic extraction of SECWM.

The peak at retention time (R_t) ~25 min is the internal standard, *trans*-cinnamic acid. The peaks at R_t = 15.0, 15.8, 16.1, 16.8, 17.0, 20.3 and 22.5 min are *trans*-*p*-coumaric acid, *trans*-ferulic acid, *cis*-*p*-coumaric acid, 8,5'-DiFA, *cis*-ferulic acid, 5,5'-DiFA and 8-*O*-4'-DiFA respectively. When quantified using the response factors from Waldron *et al* (1996), the PCWM, ECWM and SECWM yielded 12.3, 32.4 and 21.7 µg/mg respectively. The phenolic compositions of the three tissues are shown in Figure 24.

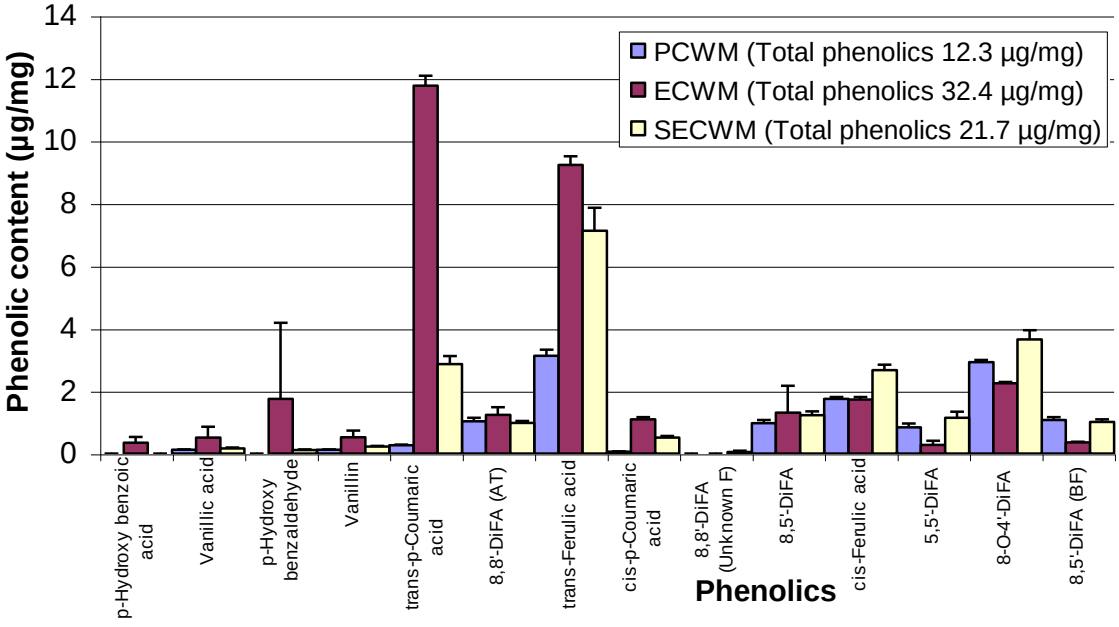

Figure 24: Calculated yields of the phenolic components extracted from the CWM of the three CWC tissues (errors are standard deviations of three determinations).

The epidermis contains by far the most phenolics and the parenchyma contains the least. In PCWM, the yield of phenolics is virtually the same as that found previously by Parr *et al* (1996), with relatively low levels of *p*-coumaric acid; but the percentage of ferulic acid as *cis*-ferulic acid (~36%) is much higher, and the absolute amount of ferulic acid is slightly lower here than previously reported. Other monomeric phenolics were also released in small amounts. The diferulic acids represented the greatest proportion of the phenolics present in PCWM indicating that diferulic acid cross-links may be particularly important in CWC parenchyma, but perhaps less so in the epidermis and sub-epidermis (Figure 25).

	PCWM		ECWM		SECWM	
	µg/mg	Wt%	µg/mg	Wt%	µg/mg	Wt%
Ferulic acids	4.87	39.63	10.96	33.85	9.79	45.05
Diferulic acids	6.84	55.68	5.44	16.81	8.06	37.11
***p*-Coumaric acids**	0.33	2.67	12.85	39.71	3.38	15.54
Other phenolics	0.25	2.02	3.12	9.63	0.50	2.31
Total known phenolics	12.29		32.37		21.73	
Total unknown phenolics	0.48	3.94	2.17	6.69	0.94	4.34

Figure 25: Table showing varying proportions of phenolics in different tissues.

In ECWM, *trans*-*p*-coumaric acid is the predominant phenolic and is present in greater amounts than any other phenolic in any of the tissues. In general SECWM was intermediate between the two tissues, both in yield of total phenolics and the proportions of ferulic acids, diferulic acids and *p*-coumaric acids. Such a marked compositional difference presumably has a significant effect on the cell wall, although as *p*-coumaric acid usually does not form dehydrodimers, it is possible it is attached to lignin, as the vascular SECWM also had elevated levels. Of the ferulic acids, approximately 57%, 30% and 44% were diferulic acids in the PCWM, ECWM and SECWM respectively. The 8-*O*-4'-DiFA was the predominant diferulic acid in all the tissues, which agrees with data from chufa, the other *Cyperaceae* that has been analysed for

phenolics (Parker *et al.*, 2000). The 8,8'-DiFA was detected in SECWM only, and then only in very small amounts (Figure 26). The ECWM had the highest amount of 8,8'-DiFA (AT) of the three tissues, and also significantly lower levels of 5,5'-DiFA and 8,5'-DiFA (BF).

	PCWM		ECWM		SECWM	
	µg/mg	Wt%	µg/mg	Wt%	µg/mg	Wt%
8,8'-DiFA (AT)	1.03	15.01	1.28	23.58	0.98	12.21
8,8'-DiFA	0.00	0.00	0.00	0.00	0.05	0.62
8,5'-DiFA	0.97	14.22	0.82	15.05	1.23	15.25
5,5'-DiFA	0.84	12.31	0.35	6.47	1.15	14.22
8-*O*-4'-DiFA	2.92	42.72	2.23	41.03	3.64	45.20
8,5'-DiFA (BF)	1.08	15.73	0.36	6.54	1.01	12.50

Figure 26: Comparison of the diferulic acid composition in CWC tissues.

Sequential phenolic extraction

The sequential phenolic extraction produced a range of coloured supernatants (Figure 27), most of which became colourless on addition of acid:

	0.1 M 1 hr	0.1 M 24 hr	1 M 24 hr	2 M 24 hr	4 M 24 hr
PCWM	Colourless	Very pale green	Very pale green	Very pale green	Colourless
ECWM	Mid orange	Mid brown	Mid brown	Pale orange	Pale orange
SECWM	Pale yellow	Pale brown	Pale brown	Pale yellow	Pale yellow

Figure 27: Observations of supernatants from CWC tissues during sequential phenolic extraction.

The sequential phenolic extraction results show there are significant differences between the three tissues (Figure 28). The ECWM released 28.5 µg/mg, compared to the SECWM (21.4 µg/mg) and the PCWM (13.7 µg/mg), which were broadly similar to the total phenolic extraction values.

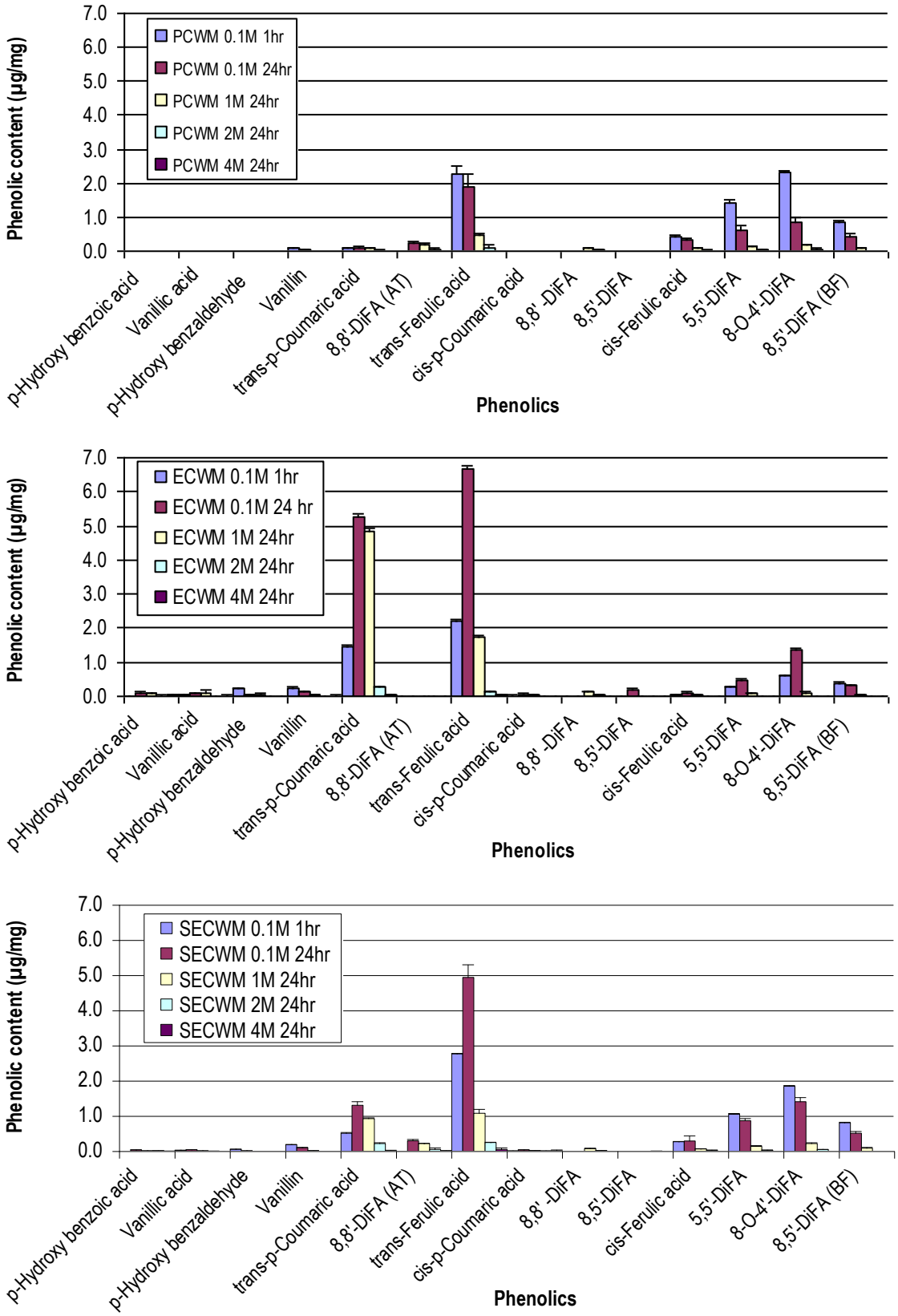

Figure 28: Calculated yields of the phenolic components sequentially extracted from PCWM (top), ECWM (middle) and SECWM (bottom) (errors are standard deviations of three determinations).

The sequential phenolic extractions showed a greater variety of unknown phenolics than the total phenolic extraction, probably due to the larger samples used; generally these unknown phenolics are at low concentrations and they are further described in Chapter 4.

The largest portion of *trans*-ferulic acid in PCWM was released in the 0.1 M 1 hr treatment; however in the ECWM and SECWM, the largest portion was released in the 0.1 M 24 hr treatment. The amount of *trans*-ferulic acid released in the 0.1 M 1 hr treatment seemed to be fairly stable between tissues. These results may indicate the differences in structure of the cell walls themselves or perhaps the ester linkage of the ferulic acid to polysaccharide chains. A comparable pattern could be observed for 5,5'-DiFA, 8-*O*-4'-DiFA and 8,5'-DiFA (BF), where they were extracted from the PCWM and SECWM in the greatest proportion in the 0.1 M 1 hr extraction, whereas in ECWM, it was in the 0.1 M 24 hr extraction. The proportion of *trans*-*p*-coumaric acid released was similar in the 0.1 M 24 hr and 1 M 24 hr extractions, indicating that the bonds holding *p*-coumaric acids in the wall are more alkali-stable than for ferulic acid. The small amounts of 8,8'-DiFA were not released until the 1 M 24 hr extraction and therefore may indicate a minor role for 8,8'-DiFA in cell adhesion.

Other monomeric phenolics were also released, particularly from ECWM. As some were released by the higher concentrations of alkali, they are presumably esterified into the cell wall. Presumably this esterification is via their alcohol groups to carboxylic acids in the cell wall as suggested by Weber *et al* (1995).

While the overall amounts of phenolics released by the total and sequential phenolic extraction methods were broadly similar, the degree of extraction is not consistent across all the components (Figure 29). In PCWM, vanillic acid, 8,8'-DiFA (AT), *cis*-*p*-coumaric acid, 8,5'-DiFA and *cis*-ferulic acid were not extracted as well by the sequential phenolic extraction as by the total phenolic extraction, whereas for *trans*-ferulic acid and 5,5'-DiFA the opposite was true.

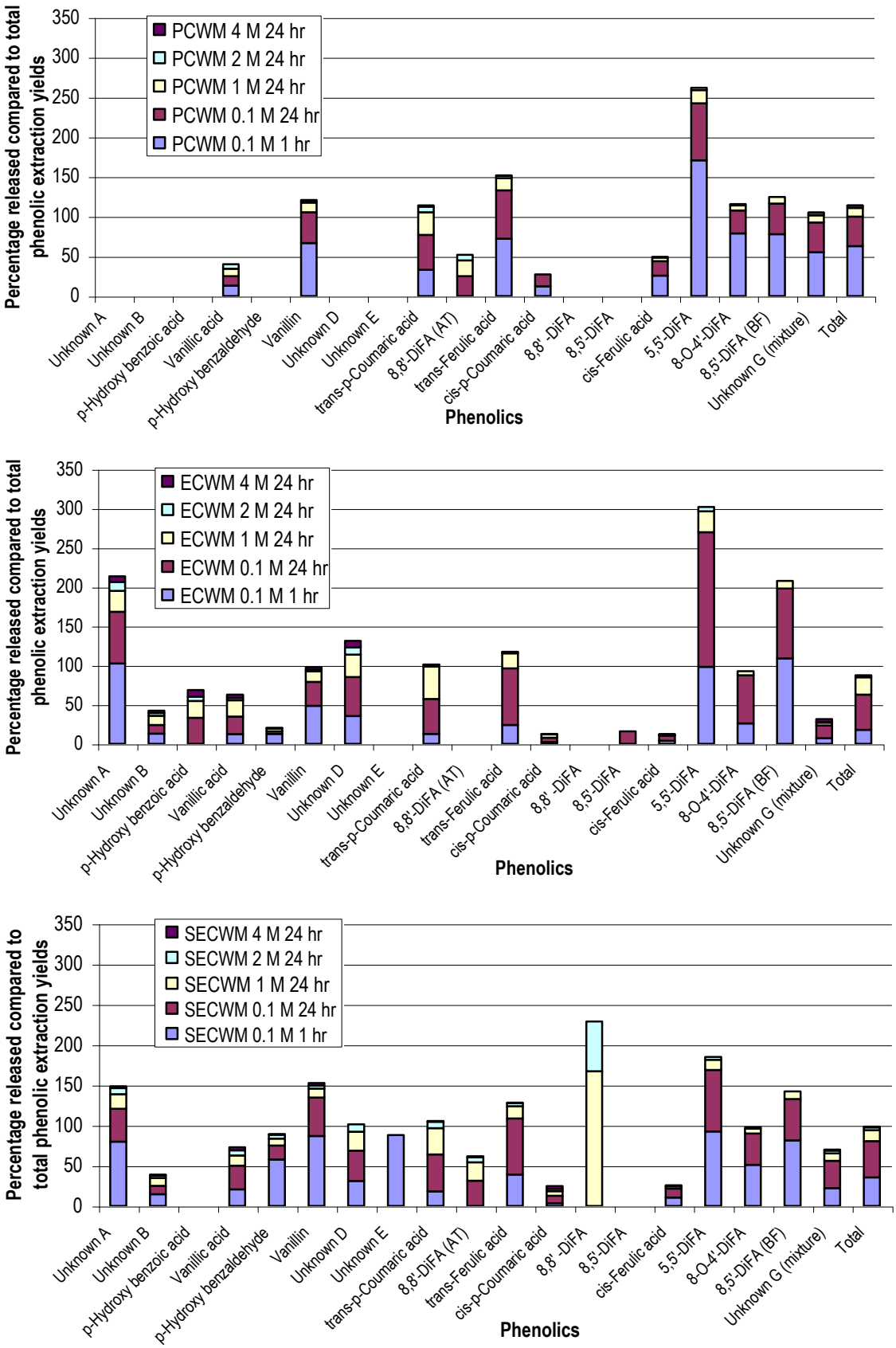

Figure 29: Percentage of phenolics released by sequential phenolic extraction compared to total phenolic extraction yields for parenchyma, epidermis and sub-epidermis. PCWM (top), ECWM (middle) and SECWM (bottom).

In ECWM, Unknown B, *p*-hydroxybenzaldehyde, *cis*-*p*-coumaric acid, 8,5'-DiFA, *cis*-ferulic acid and Unknown G were not extracted as well by the sequential phenolic extraction as by the total phenolic extraction, whereas more of Unknown A, 5,5'-DiFA and 8,5'-DiFA (BF) were extracted. In SECWM, Unknown B, 8,8'-DiFA (AT), *cis*-*p*-coumaric acid, 8,5'-DiFA and *cis*-ferulic acid were extracted more by the total phenolic extraction, whereas Unknown A, vanillin, 8,8'-DiFA and 5,5'-DiFA were extracted more by the sequential phenolic extraction.

The greater than 100% extraction of components by the sequential phenolic extraction may be due to the CWM being in alkali for a longer period of time in the sequential extraction, which may allow extraction of less accessible components. The less than 100% extraction of components by sequential phenolic extraction is most likely to be due to decomposition.

HPLC-MS analysis

Preliminary results from the HPLC-MS analysis are given for specific compounds in Figure 30. Assignments have been made on the basis of the quasimolecular ion masses, such as M+H, M+Na and characteristic fragmentation ions. An m/z=387 $(M+H)^+$ indicates a diferulic acid, an m/z=579 $(M+H)^+$ indicates a triferulic acid.

Two triferulic acids (TriFA) were identified at R_t=20.6 and 23.1 min. The first trimer was indicated by peaks at m/z=543 $(M-2H_2O+H)^+$, 561 $(M-H_2O+H)^+$, 387 $(DiFA+H)^+$ in positive ESI, and m/z=577 $(M-H)^-$ in negative ESI. The second trimer was indicated by peaks at m/z=543 $(M-2H_2O+H)^+$, 561 $(M-H_2O+H)^+$, 579 $(M+H)^+$, 593 $(M-H_2O+MeOH)^+$, 369 $(DiFA-H_2O)^+$, 193 $(FA-H)^+$, in positive ESI and m/z=577 $(M-H)^-$ in negative ESI. Accurate-mass HPLC-MS was carried out on more concentrated samples and the results are given in Section §8.4.

Retention time (min)	m/z	Identity
11.4	123 $(M+H)^+$	*p*-Hydroxybenzaldehyde
12.2	153 $(M+H)^+$	Vanillin
12.7	165 $(M+H)^+$, 147 $(M-H_2O+H)^+$, 206 $(M+ACN+H)^+$	*trans*-*p*-Coumaric acid
13.4	195 $(M+H)^+$, 177 $(M-H_2O+H)^+$, 236 $(M+ACN+H)^+$	*trans*-Ferulic acid
13.5	165 $(M+H)^+$	*cis*-*p*-Coumaric acid
14.5	195 $(M+H)^+$	*cis*-Ferulic acid
21.9	131 $(M-H_2O+H)^+$, 149 $(M+H)^+$, 190 $(M+ACN+H)^+$	*trans*-Cinnamic acid
14.4	387 $(M+H)^+$, 369 $(M-H_2O+H)^+$	8,5'-DiFA
20.0	369 $(M-H_2O+H)^+$, 387 $(M+H)^+$, 193 $(FA-H)^+$, 351 $(M-2H_2O+H)^+$	8-*O*-4'-DiFA
20.6	351 $(M-2H_2O+H)^+$, 387 $(M+H)^+$, 343, 325, 369 $(M-H_2O+H)^+$	8,5'-DiFA (BF)

Figure 30: Retention times and identifying ions for positive ESI analysis of 1 M NaOH, 24 hr alkali extractions.

Klason Lignin

The yield of lignin relative to dry weight of CWM was 2.4% for PCWM, 16.7% for ECWM and 13.4% for SECWM. This is to be expected as the small amount of vascular tissue would account for the low yield in the PCWM, and the greater amount of vascular tissue in the SECWM and secondary cell wall in the ECWM would account for their higher values. These results are quite similar to those of Chufa (*Cyperus esculentus*), another member of the *Cyperaceae*, where the Klason lignin for PCWM and ECWM was <2% and >20% respectively (Parker *et al.*, 2000). As will be described in Section §3.2.3, lignin was not observed under the microscope.

If ferulic acid is esterified/etherified to lignin, the presence of lignin in the epidermal and sub-epidermal tissues may have reduced the ability for alkali extraction to remove all the phenolics from the CWM (Lozovaya *et al.*, 1999; Sun *et al.*, 2001). Sun et al (2001) have put forward a method for removing the additional esterified phenolics from lignins solubilised during the alkali extraction. The amount of ferulic acid found to be esterified to lignin was significant in grasses (18-33%), and almost half (44-48%) of the *p*-coumaric acid was esterified to lignin, meaning the amounts described here of the two

major phenolics may be significantly higher, particularly in the epidermal tissues.

3.2.2 Carbohydrate composition

Neutral sugars

The sugar composition of the CWM is shown in Figures 31 and 32. The parenchyma, epidermis and sub-epidermis CWMs contained 820, 615 and 697 µg/mg of neutral sugars (anhydro-sugars) respectively. Most of the glucose is cellulosic, shown by the low level of glucose released by the 1 M H_2SO_4 hydrolysis (Figure 32).

By subtraction of the 1 M H_2SO_4 glucose value from the 72% (w/w) H_2SO_4 glucose value, the yield of cellulose from the parenchyma, epidermis and sub-epidermis CWM was 482, 274 and 357 µg/mg respectively (Figure 33).

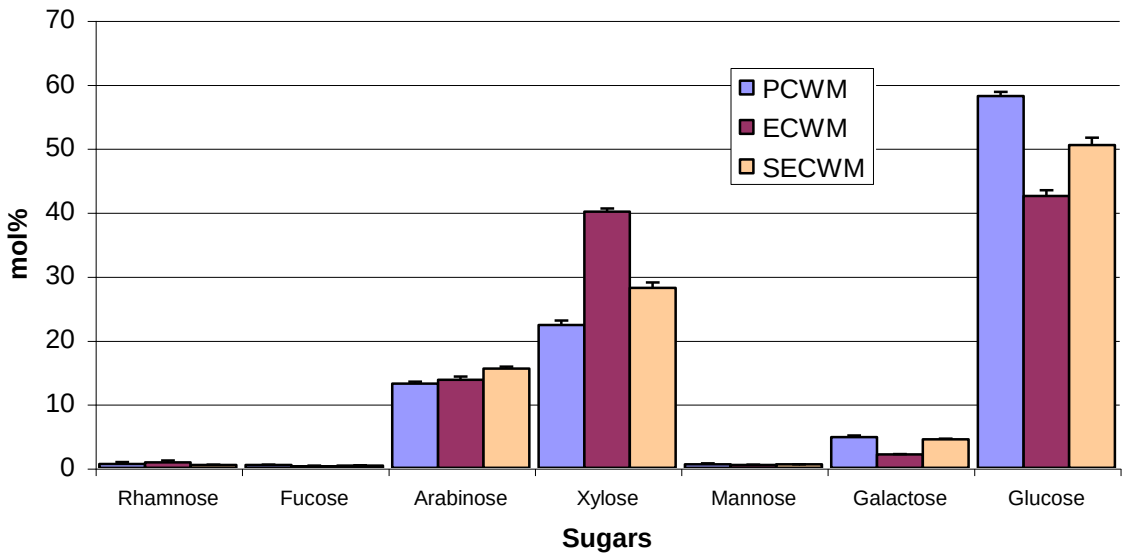

Figure 31: Results of 72% (w/w) H_2SO_4 hydrolysis of CWM (Batch 1) (errors are standard deviation of three determinations).

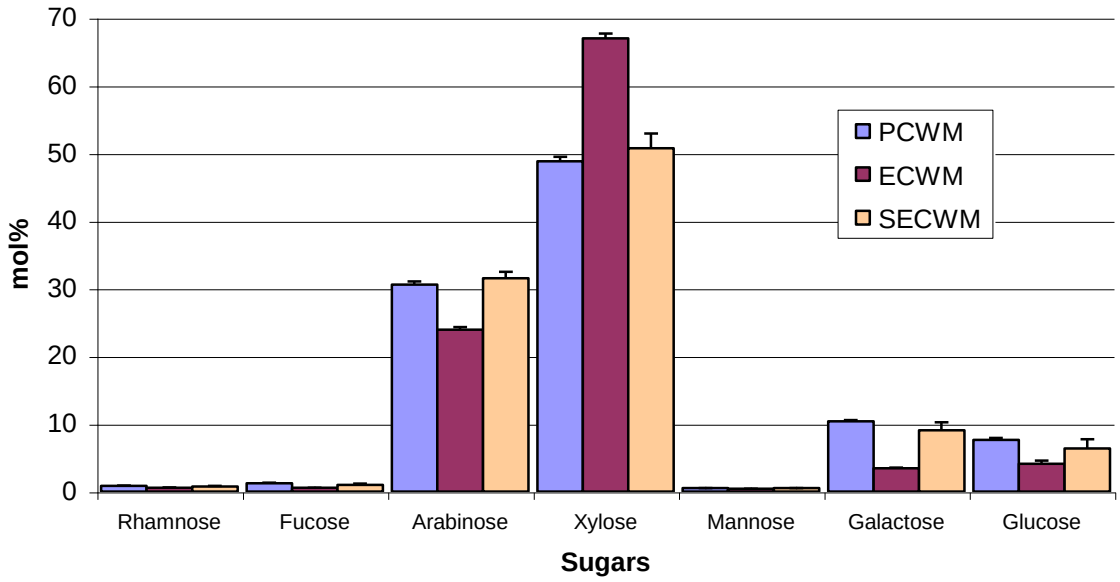

Figure 32: Results of 1 M H_2SO_4 hydrolysis of CWM (Batch 1) (errors are standard deviations of three determinations).

	µg carbohydrate / mg CWM								
	PCWM			ECWM			SECWM		
Sugar	72% (w/w) H_2SO_4	1 M H_2SO_4	Difference	72% (w/w) H_2SO_4	1 M H_2SO_4	Difference	72% (w/w) H_2SO_4	1 M H_2SO_4	Difference
Rhamnose	4.8	2.8	2.0	5.1	2.1	3.1	3.0	2.8	0.2
Fucose	3.5	4.1	-0.6	1.6	2.0	-0.3	2.6	3.7	-1.1
Arabinose	94.3	93.6	0.6	76.7	77.5	-0.8	96.0	104.7	-8.7
Xylose	159.9	149.3	10.5	223.2	216.8	6.4	174.2	169.1	5.1
Mannose	4.8	1.9	2.9	3.2	1.6	1.6	4.1	2.1	1.9
Galactose	42.3	39.1	3.2	14.4	13.7	0.8	34.0	37.2	-3.3
Glucose	510.6	28.8	481.8	290.8	16.4	274.4	383.5	26.2	357.2

Figure 33: Table showing the differences between the sugars hydrolysed by 72% (w/w) and 1 M H_2SO_4 in µg/mg.

The SECWM seems to have less cellulose than one might expect for a sample mostly made up of vascular tissues, which would usually have secondary cell walls, and therefore a higher cellulose content (McNeil *et al.*, 1984), but perhaps it is the parenchyma that is unusual. The parenchyma, epidermis and sub-epidermis CWM contained 320, 330 and 346 µg/mg of non-cellulosic

carbohydrate respectively. As can be seen in Figure 33, the composition of the carbohydrates varied significantly between the different tissues. The parenchyma had a larger proportion of glucose than the parenchyma or epidermis, but it also had less xylose. The epidermis had significantly more xylose than the other tissues, but less glucose and galactose. The sub-epidermis sample generally had intermediate amounts apart from arabinose, which was present in slightly greater amounts than in the other tissues. The low level of mannose in all three tissues implied that there were very few, if any, mannans, glucomannans or galactomannans in the CWC. Xylans, arabinans, arabinoxylans and xyloglucans were likely to be more abundant cell-wall polysaccharides.

The epidermis of the locule lining of pineapple, another sub-tropical monocot, contained a similar mol% of each sugar as the epidermis of CWC, whereas the parenchyma was fairly similar bar the proportion of glucose, which was significantly higher in CWC than in pineapple (Smith and Harris, 1995). The cell walls of chufa parenchyma have a broadly similar composition to PCWM, but the amount of arabinose is higher and the amount of glucose is lower in chufa. The cell walls of the chufa epidermis had a similar composition to those of ECWM, but the amounts of arabinose and glucose were lower in chufa (Parker *et al.*, 2000).

Uronic acids

The average amounts of uronic acid in parenchyma, epidermis and sub-epidermis were 124, 78 and 88 µg/mg of CWM respectively (raw data in Appendix E). The errors for the epidermis and sub-epidermis samples were quite large; this may have been due to the variation of particle size in these tissues. No distinction between galacturonic and glucuronic acids could be made using this method; therefore the uronic acid could have come from rhamnogalacturonan, homogalacturonan or glucuronoarabinoxylan.

The overall mol% of neutral sugars and uronic acids in the tissues are given in Figure 34, in which the results are also compared to those of a previous study (Parr *et al.*, 1996).

72% (w/w) H_2SO_4	Mol% CWM			
	PCWM	ECWM	SECWM	Parr *et al* PCWM
Rhamnose	0.59	0.81	0.44	0.30
Fucose	0.39	0.23	0.34	0.53
Arabinose	11.78	12.31	14.11	11.79
Xylose	19.74	35.43	25.28	27.51
Mannose	0.58	0.50	0.58	0.51
Galactose	4.22	1.85	3.99	4.81
Glucose	51.07	37.37	45.03	48.25
Uronic acids	11.62	11.49	10.24	6.31

Figure 34: Comparison of carbohydrate composition to reference values (uronic acids measured as GlcA equivalents).

Comparison of the data to previously published results for PCWM shows reasonable agreement with those of Parr *et al* (1996), apart from the xylose and uronic acid components, where xylose was lower and uronic acids higher than those previously reported.

Linkage analysis

The partially methylated alditol acetates (PMAAs) were identified by their mass spectra and their calculated relative retention times (to *myo*-inositol, 1,4-Glc or a phthalate contaminant). They were quantified using the peak areas obtained on the GC and the response factors of Sweet *et al* (1975). As the peaks sometimes co-eluted ((1→4)-linked Xyl, (1→2)-linked Xyl and terminal Gal (t-Gal) co-eluted and (1→3,4)-linked Xyl and (1→4)-linked Gal co-eluted) the proportion of each linkage was estimated from the mass spectrum. The results of methylation analysis can never be considered to be more than semi-quantitative for whole cell walls, as they tend not to be fully soluble in DMSO. The differences in susceptibility to hydrolysis of the different glycosidic bonds

means there is always a compromise to be achieved on reaction time (Fry, 1988).

		PCWM (Batch 1)			PCWM (Batch 2)	
		NaOH	Lithium dimsyl	Lithium dimsyl *	Lithium dimsyl	Lithium dimsyl *
SUGAR	LINKAGE	Mol%	Mol%	Mol%	Mol%	Mol%
Rha	(1-2)	0.51	0.00	0.00	0.00	0.00
Rha	(1-2,4)	0.45	0.00	0.00	0.00	0.00
Fuc	t-	0.00	0.41	0.00	0.00	0.00
Ara-f	t-	3.49	0.49	2.87	1.72	1.80
Ara-f	(1-3)	0.49	0.00	0.00	0.00	0.00
Ara-f	(1-5)	2.27	1.15	2.44	0.00	1.96
Xyl	t-	6.78	5.96	5.18	6.51	5.55
Xyl	(1-4)	2.75	3.34	3.22	2.63	1.90
Xyl	(1-2)	1.78	1.60	1.48	1.55	1.73
Xyl	(1-3,4)	2.04	3.78	5.32	2.09	0.95
Man	(1-4)	3.08	1.23	0.66	1.85	0.00
Gal	t-	2.73	1.51	1.90	1.51	3.98
Gal	(1-4)	0.68	1.01	0.69	0.63	0.37
Gal	(1-2)	0.00	0.35	0.00	0.00	0.00
Gal	(1-2,4)	0.70	0.00	0.00	0.00	0.00
Gal(A)	(1-4)	0.00	0.00	5.39	0.00	7.02
Gal(A)	(1-2,4)	0.00	0.00	0.75	0.00	0.00
Glc	t-	1.47	0.00	0.00	1.99	0.00
Glc	(1-4)	61.53	55.67	52.50	55.69	54.09
Glc	(1-4,6)	7.63	12.13	12.34	13.46	13.81
Glc	(1-3,4)	0.80	7.96	3.36	7.28	3.32
Glc	(1-3,4,6)	0.42	2.08	0.74	1.74	0.61
Glc	(1-2,4,6)	0.27	0.80	0.75	0.66	0.72
Glc	unmeth.	0.15	0.53	0.42	0.68	2.20
		100.00	100.00	100.00	100.00	100.00

* carboxyl reduction was carried out, t- indicates a terminal sugar residue, -f indicates a furanose ring structure, unmeth. indicates sugar was not methylated (Residues accounted for in interpretation, partially accounted for, not accounted for, accounted for by undermethylation.)

Figure 35: Methylation-analysis data for PCWM.

Figure 35 gives the methylation data for PCWM. The three sets of Batch 1 values should be comparable in terms of their initial composition, but as the analyses were made using three different methods, the following differences

indicate presumed differences in the reaction kinetics/thermodynamics and/or separation methods. For instance, the lithium dimsyl-catalysed samples showed no rhamnose present, less arabinose was detected and the glucose seemed to suffer more from undermethylation. Fucose and galactose were present, whereas with the NaOH-catalysed samples no fucose or galactose was detected. The use of Sep-Pak cartridges or dialysis may have affected the composition detected if the oligosaccharides that were removed during dialysis, but not Sep-Pak elution, were of a particular type. The tendency for uronic acids to undergo β-elimination was minimised by having one addition of methyl iodide, and that at as low a temperature as possible, but was probably not negated completely.

Comparing the two batches of PCWM, the PMAAs present in larger amounts, such as (1→4) and (1→4,6)-linked Glc, show reasonably close agreement, but some of the others do not. There is a systematic difference between the carboxyl-reduced samples and their non-reduced equivalents, the former allowing the detection of (1→4)-linked GalA (and in Batch 1, some (1→2,4)-linked GalA) along with more arabinose, but less mannose, galactose and highly linked glucose, indicating a lower incidence of undermethylation than with the lithium dimsyl method alone.

In both the non-reduced and reduced methods, Batch 1 had a higher total area than Batch 2, so these results are probably more reliable, as it appears more sample was injected on the column.

Taking into account the 72% (w/w) and 1 M H_2SO_4 results, which are probably more accurate than the methylation analysis results, an estimated 50 mol% of cell wall polysaccharide is cellulose, leaving 11.5 mol% of (1→4)-linked Glc in other polysaccharides.

Adding this remaining (1→4)-linked Glc (11.5 mol%) to t-Xyl (6.8 mol%) and (1→4,6)-linked Glc (7.6 mol%), t-Fuc (0.4 mol%), (1→2)-linked Gal (0.4 mol%) and (1→2)-linked Xyl (0.4 mol%) results in approximately 27 mol% of xyloglucan. By including at least one residue of each of the above types (plus

two t-Glc) the minimum degree of polymerisation of xyloglucan was estimated to be 77 (33:18:21:1:1:1:2). The percentage of branching points as inferred from the ratio of t-Xyl residues to total non-cellulosic (1→4)-linked and (1→4,6)-linked Glc residues is ~35%. The amount of xyloglucan is particularly high for a monocot, and would be considered quite high for a Type I wall (Fry, 1988). Using the system of O'Neill and York (O'Neill and York, 2003) the repeating units might be XXGG and XGGG, with some XFGG, which is more similar to other *Poales*, such as maize than anything else described. The other possibility is a mixture of XXGGG and XXFGG. Perhaps the high levels of xyloglucan in the cell wall could be due to it being used as storage carbohydrate, as it is in nasturtium seeds and tamarind (Waldron and Faulds, 2007).

Glucuronoxylans would usually be indicated by the (1→4)-linked Xyl, but the lack of glucuronic acid precludes this interpretation (Femenia *et al.*, 1999b); instead t-Ara, (1→4)-linked and (1→3,4)-linked Xyl indicate arabinoxylans (~7 mol%). By including at least one of each residue and two t-Xyl residues the degree of polymerisation of arabinoxylan was estimated to be 29 (8:11:8:2), which is probably lower than the reality. The percentage of branching points as inferred from the ratio of (1→3,4)-linked Xyl residues to (1→4)-linked and (1→3,4)-linked Xyl residues is ~43%

The proportions of GalA, Rha, Ara and Gal suggest two possible structural configurations. The first, assumes that the polysaccharide is RG I with significantly more GalA residues than Rha residues in the backbone, and long, predominantly Ara and Gal side chains. Alternatively, there may be sections of the polysaccharide that are predominantly homogalacturonan interspersed with sections of RG I. The sum of (1→2)-linked and (1→2,4)-linked Rha, (1→4)-linked GalA, (1→5)-linked Ara and (1→4)-linked Gal indicates ~9.3 mol% of RG I/HG. The degree of polymerisation of this polymer was estimated to be ~207 (11:10:119:50:15:2), indicating the complexity of the polymer. The percentage of branching points as inferred from the ratio of (1→2,4)-linked Rha residues to (1→2)-linked and (1→2,4)-linked Rha and (1→4)-linked GalA residues is ~7%, with approximately half of the rhamnose residues substituted.

Glucomannan is indicated by (1→4)-linked Man residues, and including sufficient (1→4)-linked Glc to give a 2:1 Man:Glc ratio indicates ~4.5 mol% is present. Glucomannan is the main hemicellulose polymer in the secondary wall, one type of glucomannan (Man:Glc is 1.6:1) is found in the corms of *Amorphophallus* species, as a carbohydrate reserve (Waldron and Faulds, 2007), and the same could be true for CWC.

A lack of (1→3)-linked Glc indicates there are no mixed linkage glucans or callose present, as would be expected for a non-Graminaceous monocot (McNeil *et al.*, 1984). A lack of (1→3)-linked Gal indicates there are no AG II polysaccharides present and therefore, as AG II is generally associated with arabinogalactan proteins, there are unlikely to be any AGPs in the cell walls (Waldron and Faulds, 2007). A lack of glucuronic acid rules out glucuronomannans.

In vivo acetylation of (1→4)-linked Glc at C3 may produce (1→3,4)-linked Glc residues under mild methylation conditions (Ryden and Selvendran, 1990). The (1→3,4)-linked Glc residues may also have been produced by undermethylation, thought to be responsible for the improbable (1→3,4,6)-linked, (1→2,4,6)-linked and (1→2,3,4,6)-linked Glc residues. Undermethylation is probably due to steric crowding within the cellulose microfibrils.

The presence of only (1→3,4) Xyl and not (1→2,4) Xyl branching points in the arabinoxylan implies it is more like those of the Gramineae (i.e. Oat spelt), but essentially the opposite of birchwood and larchwood xylans, which have only (1→2,4) Xyl branching points (Waldron and Faulds, 2007).

Onion has a significant proportion of xyloglucan in the cell wall, indicating it is more similar to dicotyledon parenchyma tissue than grass mesophyll (Redgewell and Selvendran, 1986); the same can now be said of CWC PCWM.

Methylation of the other tissues was also carried out. The SECWM underwent methylation with NaOH catalysis at the same time as the PCWM did; however

the lithium dimsyl experiments on ECWM and SECWM were carried out separately from the previous lithium dimsyl experiments on PCWM.

		SECWM			ECWM	
		NaOH	Lithium dimsyl	Lithium dimsyl *	Lithium dimsyl	Lithium dimsyl *
SUGAR	LINKAGE	Mol%	Mol%	Mol%	Mol%	Mol%
Rha	(1-2)	-	-	-	-	-
Fuc	t-	0.31	-	-	0.36	-
Ara-f	t-	4.42	6.88	0.76	4.57	5.72
Ara-f	(1-3)	-	0.00	0.71	0.82	8.62
Ara-f	(1-5)	2.36	1.85	2.47	1.19	4.56
Ara-p	t-	-	-	-	0.15	-
Xyl	t-	5.62	-	0.48	5.80	4.10
Xyl	(1-4)	7.88	43.54	5.18	18.48	32.94
Xyl	(1-3,4)	2.22	-	2.90	4.99	14.12
Xyl	(1-2,4)	-	5.11	0.68	0.95	2.11
Xyl	unmeth.	0.57	0.96	2.04	0.61	3.57
Man	t-	3.41	-	-	-	-
Man	(1-4)	-	1.50	-	1.37	-
Gal	t-	2.57	-	-	0.36	1.63
Gal	(1-6)	-	0.38	-	0.22	-
Gal	(1-4)	3.04	-	-	-	-
Gal	(1-4,6)	-	-	-	0.11	-
Gal	(1-3,6)	-	-	-	0.20	-
Gal	(1-2,4)	0.91	-	-	-	-
Gal	unmeth.	-	0.74	13.21	-	-
Glc	t-	1.51	1.11	-	0.59	-
Glc	(1-4)	55.67	29.37	2.12	49.60	14.11
Glc	(1-4,6)	6.67	3.12	0.53	6.89	3.22
Glc	(1-3,4)	1.00	0.91	-	-	-
Glc	(1-2,4)	-	0.99	-	1.10	-
Glc	(1-3,4,6)	0.76	0.33	-	0.80	-
Glc	(1-2,4,6)	0.50	0.50	-	0.41	-
Glc	unmeth.	0.50	2.70	68.92	0.43	-
Glc(A)	(1-4,6)					5.28
		100	100	100	100	100

* indicates samples were carboxyl reduced. t- indicates a terminal sugar residue. -f indicates a furanose ring. -p indicates a pyranose ring, unmeth. indicates sugar was not methylated

Figure 36: Methylation-analysis data for ECWM and SECWM.

The CWMs were cryo-milled to a fine powder and ethanol washed to remove the cell contents. Solubility in DMSO was an issue with these samples, resulting in extreme undermethylation, so only the SECWM NaOH treatment and the ECWM lithium dimsyl treatment will be discussed. The results are given in Figure 36.

An estimated 27 mol% of ECWM and 35 mol% of SECWM is cellulose, leaving 23 mol% and 20 mol% of (1→4)-linked Glc respectively for xyloglucan and glucomannan. The linkages represented imply the presence of xyloglucan, arabinoxylan, RG I and glucomannan. The proportion of xyloglucan seems to be reasonably consistent, but the proportion of arabinoxylan is higher in the ECWM, although the degree of branching seems to be conserved.

Carrot has the following polysaccharides, starting with the greatest, rhamnogalacturonan, cellulose (~25%), (1→4)-linked galactan, (1→5)-linked arabinan, (1→4)-linked xylan, (1→4)-linked mannan, and xyloglucan (Massiot *et al.*, 1988). As the main polysaccharide is rhamnogalacturonan, it is not particularly similar to CWC parenchyma. The cell walls of suspension cultured sycamore cells have 23% cellulose, 21% xyloglucan, 16% rhamnogalacturonan, 10% arabinan, 8% galactan, 2% arabinogalactan and 10% hydroxyproline-rich protein with 9% oligo-arabinosides attached to hydroxyproline (Talmadge *et al.*, 1973). The three main polysaccharides are the same as for CWC, but arabinoxylans are missing, which is probably an important component of CWC cell walls, so neither of these well studied systems is a good example to use for CWC.

Solubility of the CWMs may have been improved by using CWM stored as a frozen suspension rather than the dried material used in this instance (Redgewell and Selvendran, 1986). Preliminary methylations as described by Harris et al (Harris *et al.*, 1984) could also have been employed, but this would not have been suitable for the samples undergoing carboxyl reduction as uronic acid containing polysaccharides would be degraded by β-elimination.

The ratio of arabinose to xylose for arabinoxylans that bind to cellulose is 0.44 (22% branching), for arabinoxylans that do not bind to cellulose the ratio is 1.38 (65% branching, half of which are doubly branched) (McNeil *et al.*, 1975). The ratio of arabinose to xylose is 0.42 in CWC parenchyma. Highly substituted xylans are more likely to be flexible enough to support intramolecular formation of dimers (Hatfield 1999), but PCWM arabinoxylans have an intermediate degree of substitution, which may hinder the formation of dimers extracellularly, but not intraprotoplasmically.

3.2.3 Microscopy

CWC flesh has been shown previously to autofluoresce under alkali conditions (Brett and Waldron, 1996), but again these investigations did not include the skin. Figure 37a shows the morphology and natural pigmentation of the CWC epidermis. Figure 37b shows the yellow/green autofluorescence of the parenchyma cell walls at pH 9.6, the outer cortex cell walls are turquoise indicating the presence of ferulic acid, the vascular bundles that serve the buds and scales on the surface in the skin are blue indicating the presence of lignin.

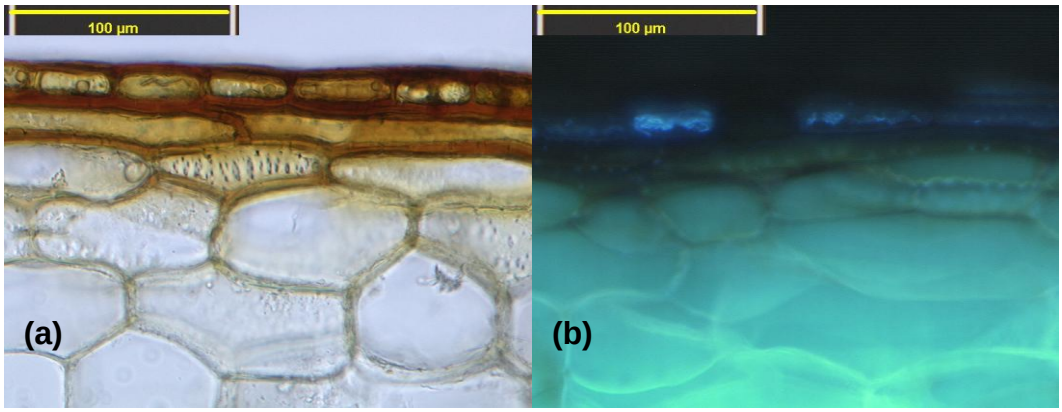

Figure 37: CWC sections illuminated by visible light (a); and UV light at pH 9.6 (b) (scale bar is 100 µm).

The autofluorescence seems to taper out towards the surface. This is unlikely to be due to a lack of phenolics, as the total and sequential extractions of phenolics showed the epidermis contained more than the parenchyma. This

lack of fluorescence could be due to a high concentration of pigment compounds stopping the incident light from reaching the phenolics, or by blocking the emission of fluoresced light.

3.2.4 Vortex-induced cell separation (VICS)

The results of the VICS tests are given in Figure 38. The degree of cell separation and the state of the surrounding liquor were observed.

	Room temperature 24 hr					
	Parenchyma		Whole epidermis		Outer epidermis	
	Liquor observations	VICS	Liquor observations	VICS	Liquor observations	VICS
Water	Colourless, cloudy	0.5	Red/orange *	1.0	Colourless, clear	1.0
0.5 M H_2SO_4	Colourless, cloudy	0.5	Colourless, clear	0.5	Colourless, clear	1.0
0.05 M TFA	Colourless, cloudy	1.5	Colourless, clear	0.5	Colourless, clear	0.5
1 M TFA	Colourless, cloudier	0.5	Colourless, cloudy	0.5	Colourless, clear	1.0
1 M NaOH	Pale yellow	0.5	Red/orange	0.0	Yellow	0.5
4 M NaOH	Pale yellow, gelled	2.0	Red/orange	0.0	Yellow/orange	0.5
	Room temperature 72 hr					
	Liquor observations	VICS	Liquor observations	VICS	Liquor observations	VICS
Water	Colourless, cloudy	0.5	Colourless, clear	0.5	Colourless, clear	0.5
0.5 M H_2SO_4	Colourless, cloudy	1.0	Colourless, clear	0.5	Colourless, clear	0.5
0.05 M TFA	Colourless, cloudy	1.5	Colourless, clear	0.5	Colourless, clear	0.5
1 M TFA	Colourless, cloudier	0.5	Colourless, cloudy	0.5	Colourless, clear	1.0
1 M NaOH	Pale yellow	1.5	Brown	2.0	Orange	0.5
4 M NaOH	Pale yellow	1.5	Red/brown	2.5	Orange	0.5
	100°C 3 hr					
	Liquor observations	VICS	Liquor observations	VICS	Liquor observations	VICS
Water	Colourless, cloudy	1.0	Pale brown, clear	0.0	Pale yellow	0.5
0.5 M H_2SO_4	Yellow, cloudy	4.5	Pale orange/brown	1.0	Very pale yellow	1.0
0.05 M TFA	Colourless, cloudy	1.5	Pale yellow	0.5	Pale yellow	1.0
1 M TFA	Yellow/green	4.5	Pale orange, cloudy	1.5	Pale yellow	1.5
1 M NaOH	Yellow/green	4.0	Dark brown	3.0	Orange	3.0
4 M NaOH	Yellow/green, gelled	4.0	Dark brown	2.5	Orange	2.5

* Possible contamination with NaOH

Figure 38: VICS scores and liquor observations for different storage conditions.

Parenchyma was generally more susceptible to VICS than the epidermal tissues, and was particularly susceptible to the 100°C treatments, four of which produced VICS scores indicating the tissues were severely disrupted, but not to the point of complete cell separation. The epidermal tissues gave almost identical results to each other under each condition (within 0.5 of each other), apart from prolonged exposure to concentrated alkali, in which whole epidermis seems to have fared slightly worse.

The gelling of the liquor in two of the three 4 M NaOH tubes containing parenchyma tissue can be explained by the presence of starch on the surface of the fresh material, as CWC flour is used to thicken soups in oriental cuisine. However, the involvement of cell wall phenolics may be indicated by it happening only in concentrated alkali.

The results presented here agree with those in a previous investigation (Parker and Waldron, 1995) for the concentrated hot acid treatments (0.5 M H_2SO_4 or 1 M TFA, 100 °C, 30 min) resulted in complete VICS, however the dilute acid treatment was not as effective in this instance as before. The previous experiments were done in triplicate, which probably reduced any errors attributable to natural variation, but a limited amount of fresh material was available.

3.3 Discussion

Due to the different demands placed on the three tissues of the CWC corms, differences in their cell wall compositions were studied.

3.3.1 Comparison of tissue types

The tissue types have been compared in terms of their overall composition, and their polysaccharide and phenolic composition.

Overall composition

The compositions of the tissues of CWC are given in Figure 39. The parenchyma cell wall is almost completely accounted for (within experimental error). The higher proportion of unidentified components in the epidermal and sub-epidermal CWM is probably due to it being less finely divided than the PCWM, reducing the ability of the various chemicals to act on the materials. There is also the possibility that there are significant amounts of protein and/or ash, but the difference is so large that it would seem unlikely.

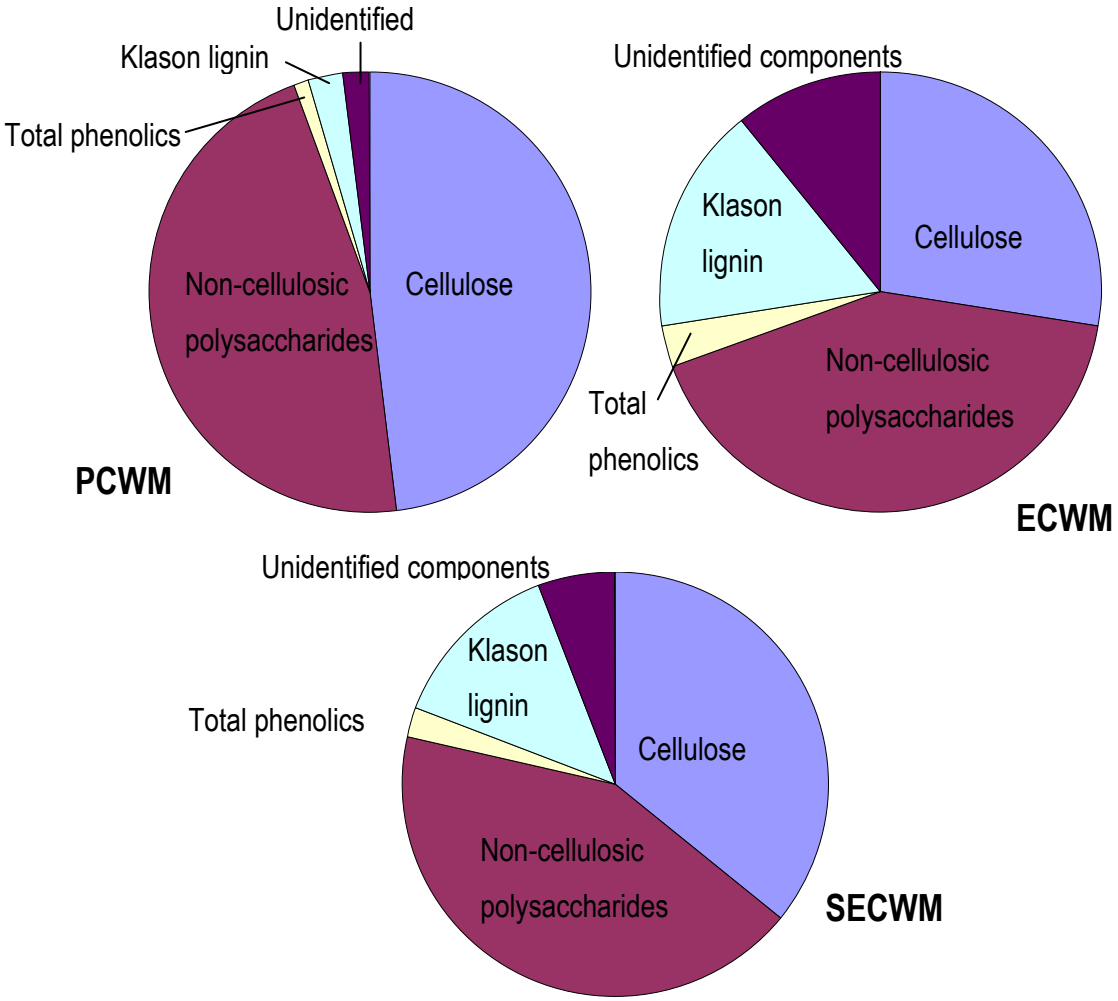

Figure 39: Comparison of the composition of the different tissues of CWC.

Brett and Waldron (1996) have presented some generalised cell-wall compositions for the primary walls of fruits and vegetables, cereal endosperm and cereal bran. PCWM is probably most similar to their fruit and vegetable

example in composition, although it does have more cellulose, less pectin and some lignin (protein was not quantified). ECWM and SECWM could not really be compared to the general examples because the lignin component indicates they are secondary cell walls

The variation in cellulose may indicate that in the secondary walls lignin is taking more of a structural role, meaning less cellulose is needed.

The non-cellulosic polysaccharides seem to be fairly consistent between the tissues, although there is a slight reduction in the more lignified tissues, which may indicate that the non-cellulosic polysaccharides are not removed when lignification occurs, but they are a smaller proportion because of the addition of lignin.

Polysaccharides

The hemicelluloses in CWC parenchyma were thought to be predominantly arabinoxylans, but this investigation has shown that xyloglucan predominates, with some arabinoxylan and a small amount of glucomannan. The pectin component is rhamnogalacturonan I, probably with some homogalacturonan domains distributed throughout the chain. Rhamnogalacturonan II is found in most cell walls, making it likely that it is present in small amounts in CWC cell wall, although it was not detected. The hemicelluloses in CWC epidermis and sub-epidermis are similar, although the proportion of arabinoxylan is increased in the ECWM, although there was more difficulty in the experimental analyses for these tissues, particularly ECWM. The cell walls of chufa have a broadly similar composition: for the parenchyma, chufa has higher amounts of arabinose and lower amounts of glucose, whereas for the epidermis, chufa has lower amounts of arabinose and glucose (Parker *et al.*, 2000).

Phenolics

As CWC epidermis has such high levels of phenolics, *p*-coumaric acid in particular, there may be an important physiological role for them in this tissue.

This seems to agree with the theory of Wende *et al* (2000) that phenolics might protect cells against damage by pathogens and/or soil abrasion. The increased levels of *p*-coumaric acid in the epidermis tissues in tandem with the higher lignin content agrees with the idea that *p*-coumaric acid is often associated with lignin. Ferulic acid, in monomeric and dimeric form, is associated with the poorly lignified parenchyma tissue. The dimers are probably involved in interpolymeric cross-linking, probably of arabinoxylan and/or xyloglucan. The highest amount of dimers was found in the SECWM, as this is vascular tissue; perhaps more dimers are necessary to maintain cell adhesion in order to counteract the additional forces produced by osmotic pressure.

The presence of high amounts of ferulic acid (and other phenolics) may inhibit the growth of the fungus *Fusarium oxysporum* (Lattanzio *et al.*, 1994), one of the known pathogens of CWC.

3.3.2 Implications for CWC parenchyma-cell-wall structure

As previously observed with onions (Mankarios *et al.*, 1980), the cell walls of CWC are more similar to those of the dicotyledons than the Gramineae. The methylation data imply that arabinoxylan, which would have been expected to be the predominant hemicellulose, is actually not as prevalent as xyloglucan. The implications for the structure of the cell wall could be important (Figure 40), as this implies that there are essentially two layers of CWC cell wall, an inner layer that has a high degree of interaction between xyloglucan and cellulose, and an outer layer (including the middle lamella) that contains arabinoxylan and the phenolics attached as suggested previously.

Arabinoxylans are more abundant at the interface between cells and cell corners in wheat (Guillon *et al.*, 2004; Saulnier *et al.*, 2007), illustrating that different wall polysaccharides can be concentrated in defined domains of the cell wall (Roberts, 2001). As the phenolics have been shown to be concentrated at the cell corners in CWC (Parker and Waldron, 1995), it is likely that feruloylated arabinoxylans are concentrated at the cell corners of CWC.

The pectin appears to have a few long branches (not indicated in the diagram), which may allow it to form a three dimensional network that interlocks with the cellulose microfibrils, but does not actually connect to it directly. The linkages between pectin molecules, or between pectin and arabinoxylan, have not been investigated and are therefore not implied in the diagram.

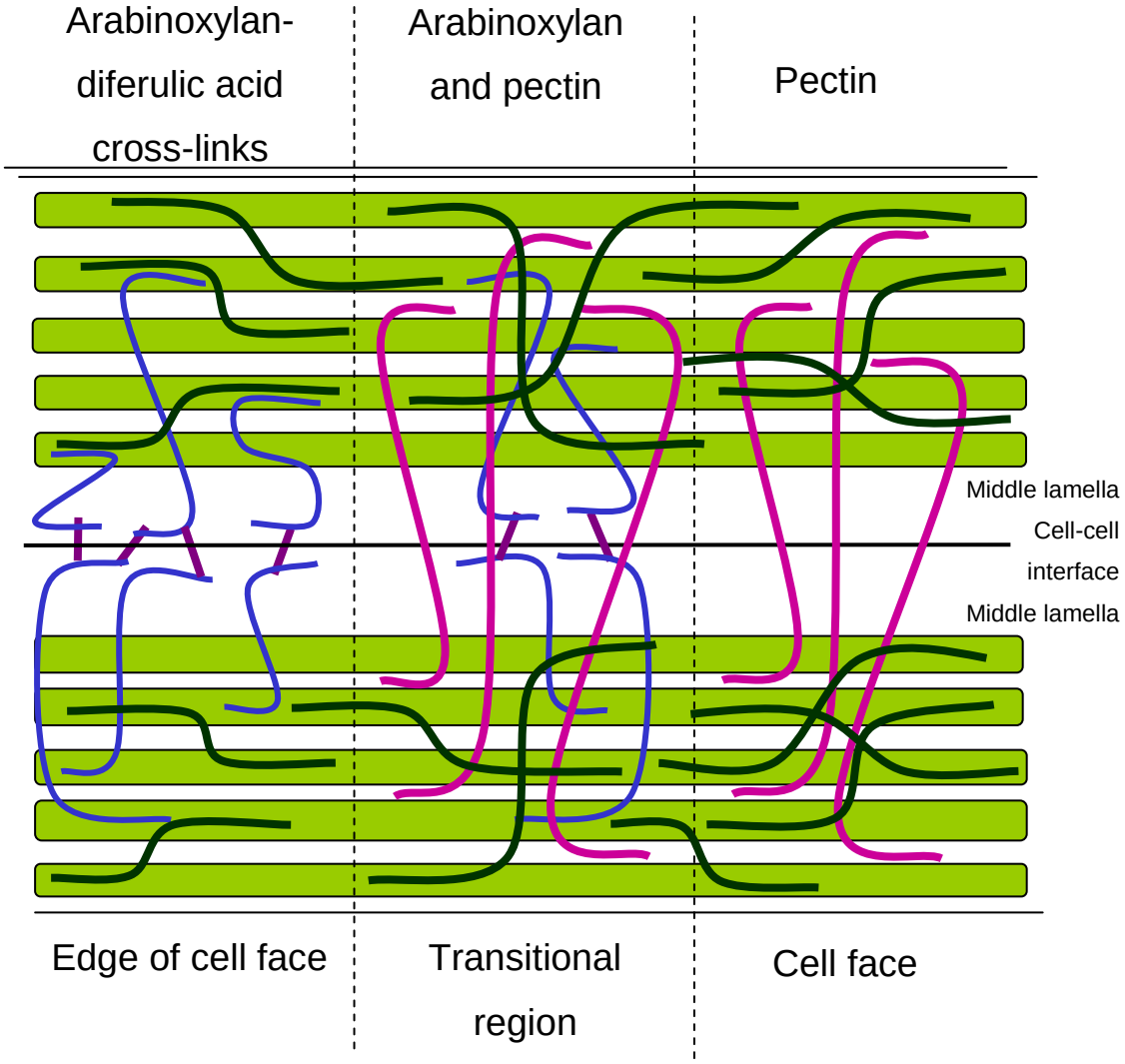

Figure 40: Cell-wall model of CWC parenchyma at the interface of two cells. XG is the major hemicellulose, the proportion of AX has been reduced. (Cellulose is green, XG is black, AX is blue, diferulic cross-links are purple, and pectin is pink)

Profiling data for the unidentified phenolics are given in Chapter 4, and the trimers extractable in sufficient quantities are more fully characterised in Chapter 8.

4 Profiling of Unidentified Phenolics:

The chromatographic profiles of the CWM phenolics are extremely complex and so in Chapter 3 only the identified phenolics were quantified. In this chapter the unidentified phenolics from CWM will be discussed.

Ralph et al (2000) have said that many plant cell wall components are still to be identified and this was found to be the case in Chinese water chestnut. As well as the well-documented phenolics described in Section §3.2.1, a number of unidentified compounds were discernible in the HPLC chromatograms. These compounds had UV spectra that were similar to the known phenolics. The total phenolic extraction produced seven unknowns (A-G), the first sequential phenolic extraction increased this number to eleven (H-K) and the second sequential phenolic extraction gave a total of 89 UV spectra (both known and unknown). Although these compounds are probably present in extremely small quantities, there is no way of knowing how important they are as part of the cell wall structure; after all, years ago, phenolics as a group were not regarded as being present in large enough quantities to make a difference to cell-wall properties, and so were not quantified as a matter of course, as they are now.

4.1 Attributes of unknown phenolics

Without extensive experimentation these phenolics cannot be identified, but their properties can be catalogued in order to make subsequent assignment easier, which should allow one to go back to the data once the required identification work is carried out. For each unidentified compound four attributes were recorded:

- Retention time
- Relative retention time
- UV maxima and minima
- Spectrum shape group

4.1.1 Retention time

In general, as retention time increases, the molecules get larger, meaning that hydroxybenzoic acids and aldehydes are followed by hydroxycinnamic acids, then by dehydrodimers, then presumably by dehydrotrimers etc (although there is considerable overlap).

4.1.2 Relative retention time (RRT)

Relative retention time is the retention time of a peak relative to that of an internal standard, which can aid identification because it should be reproducible between runs, assuming the same solvent gradient and column are used.

4.1.3 UV maxima and minima

The UV chromatogram is produced at just one wavelength (280 nm), but the DAD detects and records the spectrum from 200 to 360 nm. Examining the spectrum of a compound can allow measurement of the wavelengths at which the absorption is at a maximum or minimum. These wavelengths can be compared to literature values and to each other to indicate their degree of conjugation, for example the absorption maxima of benzene, benzoic acid and cinnamic acid in water are 203.5, 230 and 273 nm respectively, showing the absorption maxima increasing as conjugation increases.

4.1.4 Spectrum shape group

The shape of the spectrum may give some indication of similarities in the molecular structure to known components. The known molecules have been split into eight groups in terms of their general spectra; the unknowns will then be assigned to the closest group. The representative spectra shapes are

shown in Figure 41, and examples of how the spectra shape groupings are applied to known phenolics are given in Figure 42.

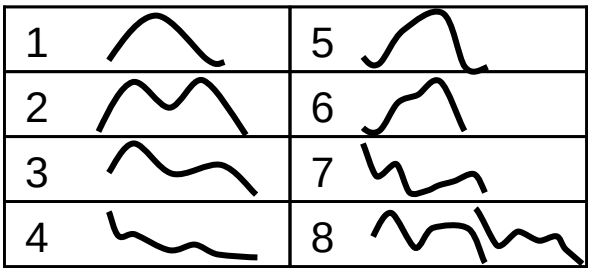

Figure 41: Representative spectra shapes.

Compound	RT (min)	RRT	Spectrum shape group	Max (nm)	Min (nm)
Protocatechuic acid	7.7	0.30	3	260/294	236/281
p-OH benzoic acid	11.3	0.44	1	255	225
p-OH phenyl acetic acid	11.7	0.46	4	221/276	251
Vanillic acid	12.3	0.48	3	261/291	236/281
p-OH benzaldehyde	14.1	0.55	1	285	240
Vanillin	15.3	0.59	2	279/310	250/296
trans-*p*-Coumaric acid	16.1	0.63	5	225/310	249
8,8'-DiFA (AT)			7	246/335	273
trans-Ferulic acid	16.9	0.66	6	236/324	262
cis-*p*-Coumaric acid			1	300	257
8,5'-DiFA			5	324	266
cis-Ferulic acid	18.1	0.70	5	314	261
5,5'-DiFA			5	246/325	273
8-*O*-4'-DiFA			6	235/327	260
8,5'-DiFA (BF)			5	324	265
trans-Cinnamic acid	25.7	1.00	1	214/277	233

Figure 42: Example of attributes of known phenolics (RRT relative to* trans*-cinnamic acid in standard mixture).

Compound	Spectrum shape group	Max (nm)	Min (nm)	Reference
8-*O*-4'/8,5'-TriFA	5	217/235/317	210/224/260	(Bunzel *et al.*, 2005)
5,5'/8-*O*-4'(H_2O)-TriFA	6	317	265	(Bunzel *et al.*, 2005)
8-*O*-4'/8,5'-TriFA	5	217/240/319	210/225/267	(Bunzel *et al.*, 2003a)
8-*O*-4'/8-*O*-4'-TriFA	6	320	260	(Funk *et al.*, 2005)
8,8'(AT)/8-*O*-4'-TriFA	6	240/325	265	(Funk *et al.*, 2005)

Figure 43: Attributes of known triferulic acids.

Some UV spectra have been produced for trimers of ferulic acid (Bunzel *et al.*, 2003a; Bunzel *et al.*, 2005; Funk *et al.*, 2005) and their attributes are given in Figure 43 Their spectra shapes have similarities to those of *trans*-ferulic acid and *cis*-ferulic acid.

4.2 Unknown phenolics from total phenolic extraction

In the total phenolic extraction samples seven unknown phenolics were detected at R_t = 6.9, 9.4, 13.9, 14.5, 14.7, 16.3 and 25.5 min; these were defined by their spectra, as shown in Figure 44, and Unknown Phenolic F was subsequently identified as 8,8'-DiFA (and included in the quantifications in Chapter 3).

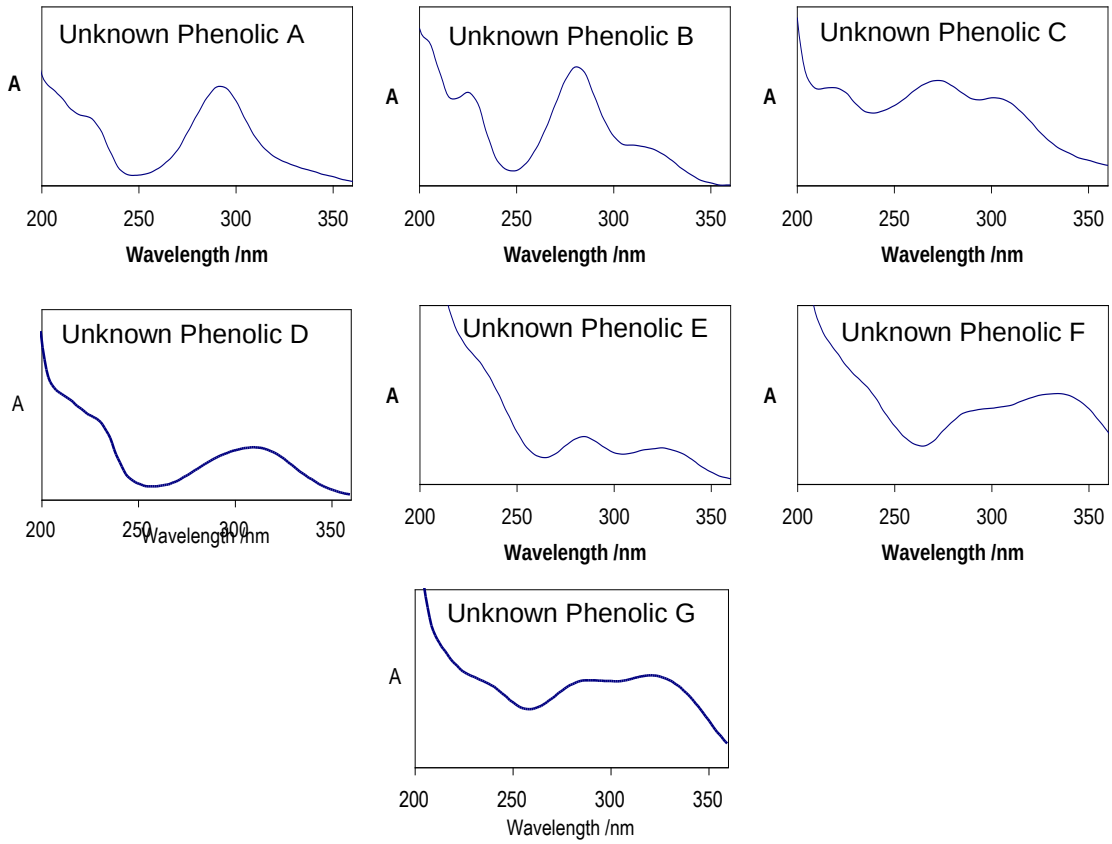

Figure 44: Absorbance spectra for Unknown Phenolics A-G.

The attributes of Unknown Phenolics A-G are tabulated in Figure 45. Unknown Phenolics B and G do not easily fit into one particular category. Unknown Phenolic G may be a triferulic acid, as it elutes quite late in the run and has a spectrum not that dissimilar to the diferulates.

Compound	RT (min)	RRT	Spectrum shape group	Max (nm)	Min (nm)
Unknown Phenolic A	6.9	0.28	1	292	248
Unknown Phenolic B	9.4	0.38	1 or 3	226/281/311	218/249/307
Unknown Phenolic C	13.9	0.56	3	218/273/302	211/239/295
Unknown Phenolic D	14.5	0.58	1	311	258
Unknown Phenolic E	14.7	0.59	2	284/325	265/305
Unknown Phenolic F (8,8'-DiFA)	16.3	0.65	6	333	265
Unknown Phenolic G	25.5	1.02	2 or 6	290/321	259/304

Figure 45: Attributes of Unknown Phenolics A-G from total phenolic extraction.

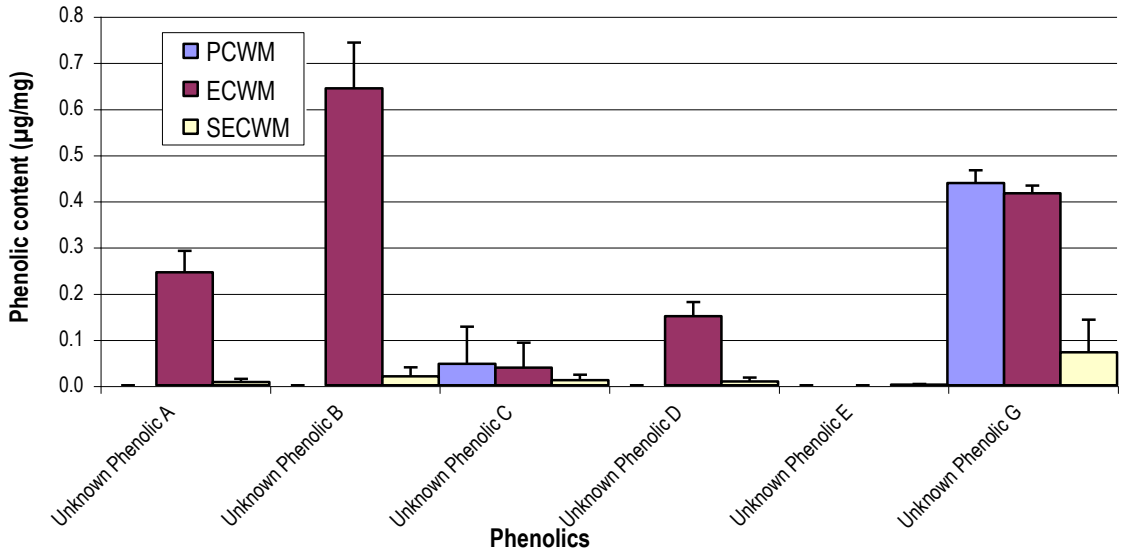

Figure 46: Relative abundance of unknown phenolics released by total phenolic extraction from PCWM, ECWM and SECWM (errors are standard deviations of three determinations).

An indication of their relative abundance is given in Figure 46. The calculations used an assumed molecular weight of 150 for Unknown Phenolics A-E, and a response factor of 0.33 for all the unknown phenolics. For Unknown Phenolic G

the assumed molecular weight was 386.36, as it was likely that it had a higher molecular weight. The ECWM contains significantly more of these unknown phenolics, as it did with the known phenolics, indicating that all phenolics may have an important role to play in the epidermis.

4.3 Unknown phenolics from sequential phenolic extraction

The first sequential phenolic extraction procedure extracted a greater number of unknown phenolics than the total phenolic extraction, probably due to the greater amount of starting material used (and possibly the greater volume of NaOH solution). As with the total phenolic extraction, an indication of their relative abundance is given in Figure 47.

It appears that there are essentially two groups of unknown phenolics: Unknown Phenolics E, H, I and K, that are apparently totally removed in the least aggressive alkali treatment; and Unknown Phenolics A, B, D and G, that seem to have significant resistance to alkali. The attributes of the new Unknown Phenolics H-K are tabulated in Figure 48.

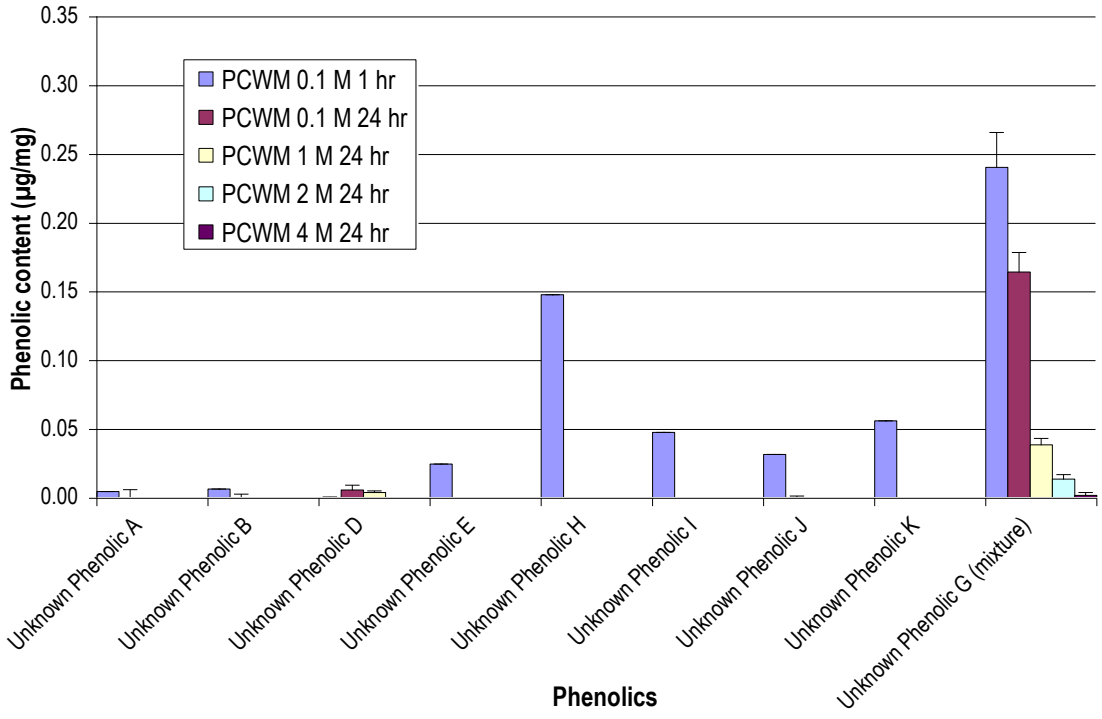

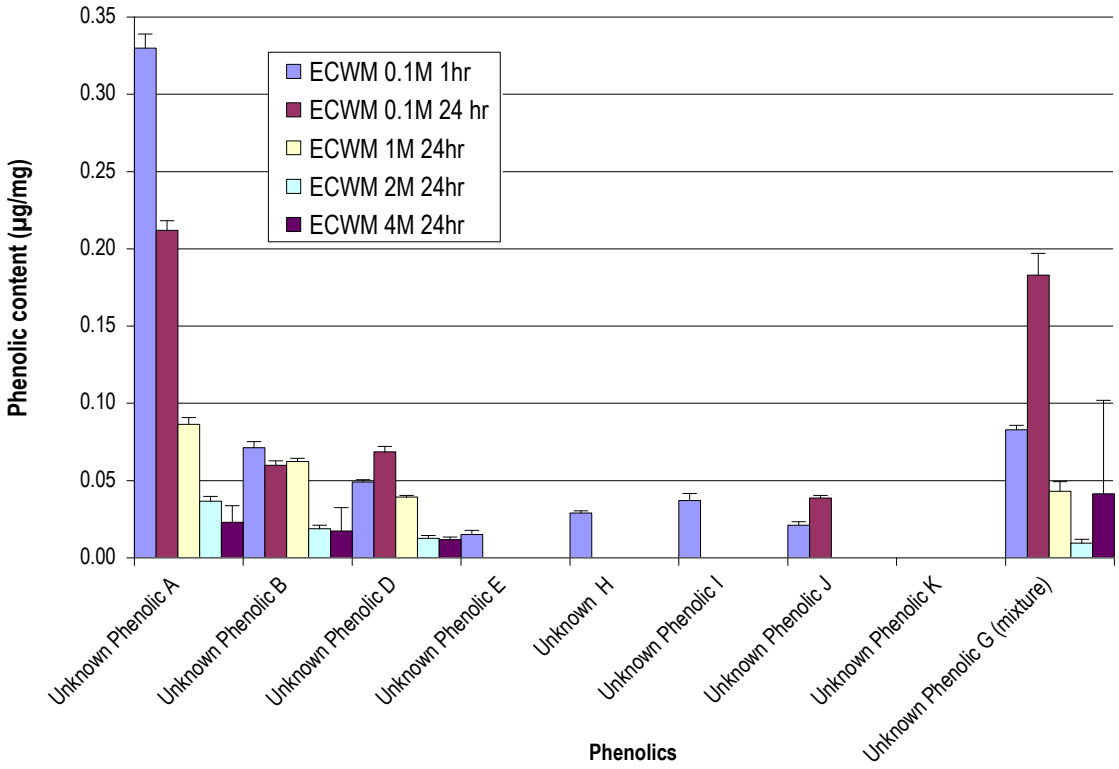

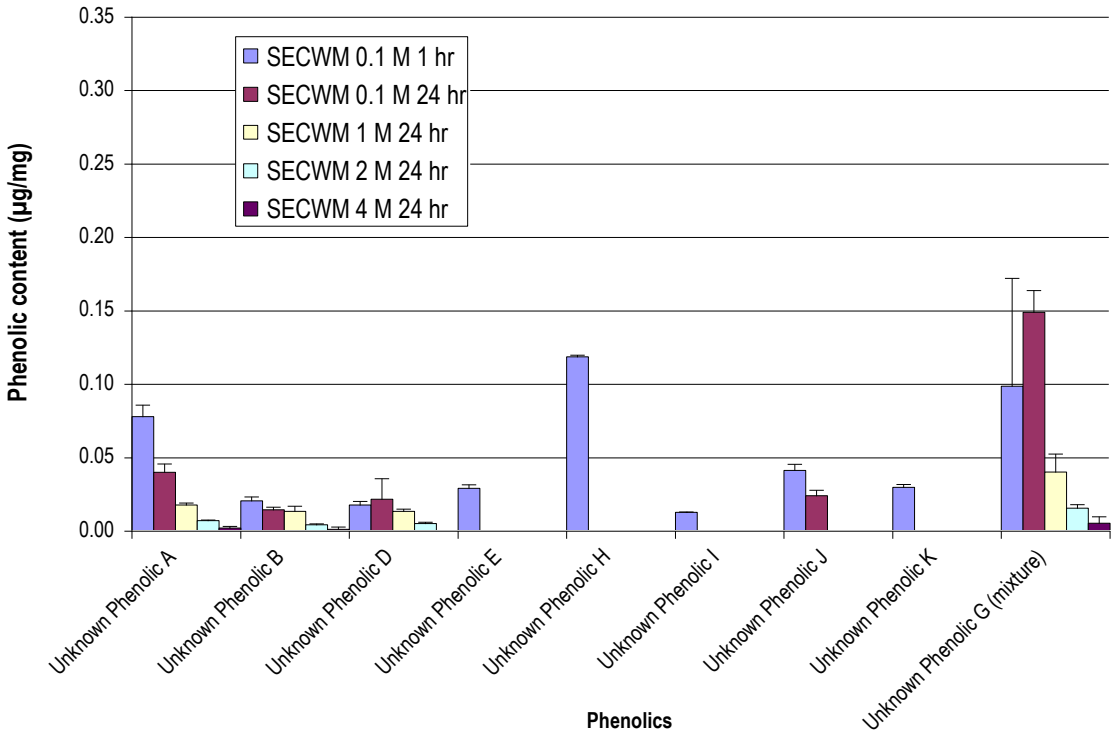

Figure 47: Relative abundance of unknown phenolics released by sequential phenolic extraction (PCWM (previous page), ECWM (top) and SECWM (bottom), errors are standard deviations of three determinations).

Compound	RT (min)	RRT	Spectrum shape group	Max (nm)	Min (nm)
Unknown Phenolic H	14.7	0.63	8	270	233/301
Unknown Phenolic I	15.6	0.66	8	262	287
Unknown Phenolic J	16.4	0.70	8	254/310	285/320
Unknown Phenolic K	17.7	0.75	8	260/297	285/315

Figure 48: Attributes of Unknown Phenolics H-K.

In the sequential phenolic extraction, Unknown Phenolic G was indicated to be a mixture rather than a pure compound; one of these compounds was indicated to be a triferulic acid by LC-MS, see Section § 3.2.1.

4.4 Unknown phenolics from further sequential phenolic extraction

A final experiment which included 0.1 M 1 hr (triplicate data analysis), 0.1 M 24 hr, 1 M 24 hr, 2 M 24 hr, 4 M 24 hr, 4 M 24 hr (total) and 4 M 4 days (total) extractions yielded 89 phenolics, 75 of which were unknown phenolics. In order to give them unique identifiers the labelling of all the phenolics was changed to a numbering system (Appendix F). Twelve of the phenolics appeared in eight or nine of the data analyses; some were known phenolics, such as *p*-coumaric acid or *trans*-ferulic acid and some were Unknown Phenolics (3, 6, 48 and 52). These unknown phenolics had areas greater than 1% of that for *trans*-ferulic acid in the chromatogram for the 4 M 24 hr total phenolic extraction, indicating they may be significant. Interestingly, Unknown Phenolics 19 and 46 had spectra similar to 8,8'-DiFA (AT), suggesting there may be other phenolics that share its unusual molecular structure. Unknown Phenolics 43 and 88 had unusual spectra that were included in Spectra Group 8.

4.5 Summary

A thorough survey of CWC parenchyma cell wall phenolics has been carried out and sufficient information recorded about each compound to enable identification, and possibly quantification, in the future. Selected samples were analysed by LC-MS and the results are given in Chapter 8.

5 Characterisation of Cell-Wall Polymers in Parenchyma of Chinese Water Chestnut:

The sequential extraction of cell-wall polymers should help to test the hypothesis about the cell wall structure of CWC, by giving fractions of polysaccharides that can be analysed to determine if their structure agrees with that suggested.

The traditional sequential extraction involves the following steps (Redgewell and Selvendran, 1986; Selvendran and O'Neill, 1987):

- 2 M Imidazole, pH 7, 20°C – Imidazole removes very weakly bound pectic polysaccharides held in the wall by Ca^{2+} only.
- 50 mM CDTA (cyclohexane-*trans*-1,2-diamine-N,N,N',N'-tetraacetate, Na^{+} salt), pH 6, 20°C – CDTA is a chelating agent which is thought to solubilise pectic polysaccharides held in place by Ca^{2+} ions.
- 50 mM Na_2CO_3, 1°C and 20°C – Na_2CO_3 removes pectic polysaccharides by hydrolysis of weak ester cross-links. Pectic polysaccharides are prone to β-elimination reactions at higher temperatures, so low temperatures are used first. $NaBH_4$ is used to prevent step-wise peeling of sugar units from the reducing terminus of polysaccharides, by reducing the reducing carbonyl group to an alcohol.
- KOH, 20°C – Increasing concentrations of alkali are used in sequence, usually 0.5 M, 1 M and 4 M. The 0.5 M KOH extracts any remaining pectin. 1 M KOH extracts different hemicelluloses, such as arabinoxylans. 4 M KOH extracts xyloglucans, and combining 4 M KOH with 3-4% boric acid extracts glucomannans.

5.1 Methods

Previous sequential extractions of PCWM indicated that only a small proportion of the sugars present were extracted before the 0.5 M KOH stage (Ng and

Waldron, 2004); therefore, although CDTA and Na_2CO_3 extractions were carried out, only the KOH fractions were dialysed, quantified and analysed further (Figure 49). The KOH fractions and the final residue had their sugar and phenolic content measured and linkage analysis carried out. Batch 2 PCWM was used for the experiments in this chapter.

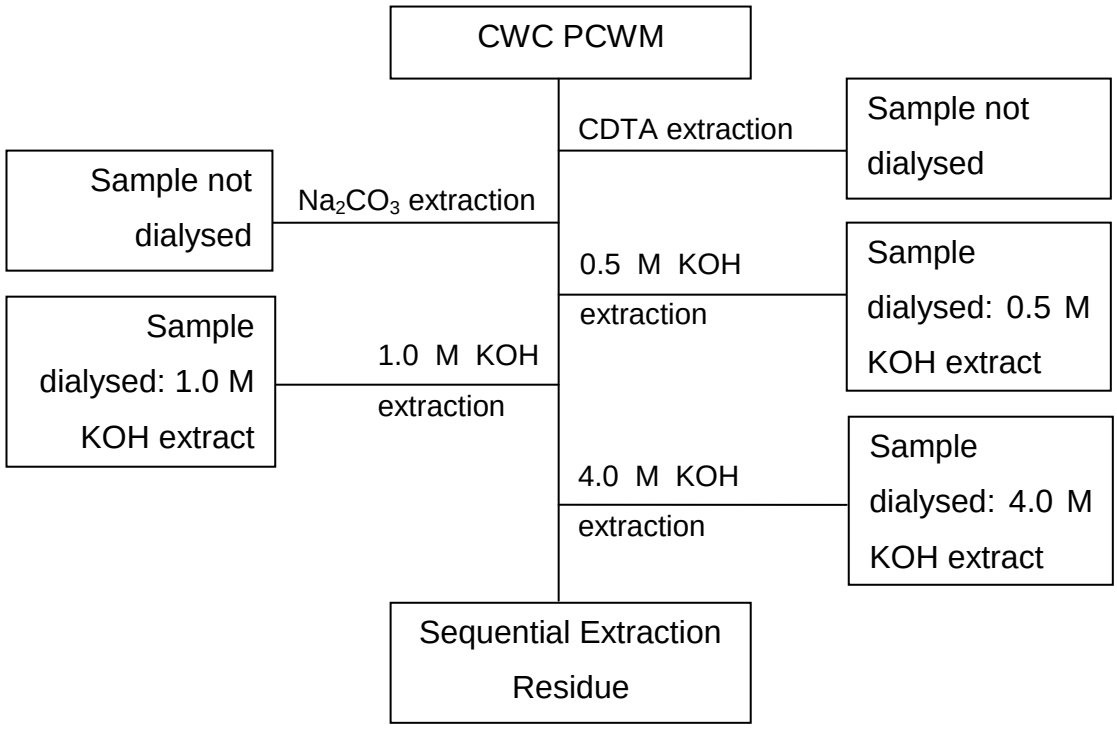

Figure 49: Sequential extraction procedure.

5.1.1 Analysis of extracts and residue

The residue and three KOH extracts were analysed for neutral sugars, uronic acids and phenolics as usual (~0.5 mg). They were also analysed by LC-MS (~5 mg of extracts, ~50 mg of residue) in an attempt to produce samples for LC-SPE and subsequent NMR analysis as described in Chapter 9. The extracts were also dissolved in 50:50 (v:v) MeOH:water and injected directly onto the LC-MS.

5.2 Results

The yields for the KOH extracts and residue are given in Figure 50. It appears that the CDTA and Na_2CO_3 treatments extracted ~20% of the cell wall material, assuming experimental error is minimal.

	Weight (g)	Yield %
PCWM	2.001	
0.5 M KOH	0.051	2.5
1.0 M KOH	0.056	2.8
4.0 M KOH	0.297	14.8
Residue	1.174	58.7
Total	1.578	78.9

Figure 50: Yields for KOH extracts and residue from sequential extraction.

The 4.0 M KOH treatment extracted significantly more than 0.5 or 1.0 M KOH, presumably because a considerable proportion of PCWM is xyloglucan and this is not usually extracted until the 4 M KOH stage, as strong alkali is required to swell the cellulose microfibrils and release the xyloglucan.

5.2.1 Carbohydrate composition

The carbohydrate compositions of the sequential-extraction extracts and residue are given in Figure 51.

This initial interpretation assumes that arabinose comes from arabinoxylan or arabinan side chains of rhamnogalacturonan I; xylose comes from arabinoxylans and xyloglucan; glucose comes from xyloglucan; and galactose and uronics come from rhamnogalacturonan I.

Arabinoxylan and pectin are removed in all the extractions, and it is difficult to determine the exact proportions from the simple sugars analysis. Some

xyloglucan is present in all the extracts; ~5.5, 5 and 30 mol% of the total polysaccharide extracted is removed by 0.5, 1.0 and 4.0 M KOH, respectively. This is what would be expected if the xyloglucan is trapped within the cellulose microfibrils. In the residue there is still some xyloglucan and pectin, and maybe a little arabinoxylan, associated with the cellulose microfibrils. The methylation analysis should help determine which polysaccharides are extracted at which alkali concentration.

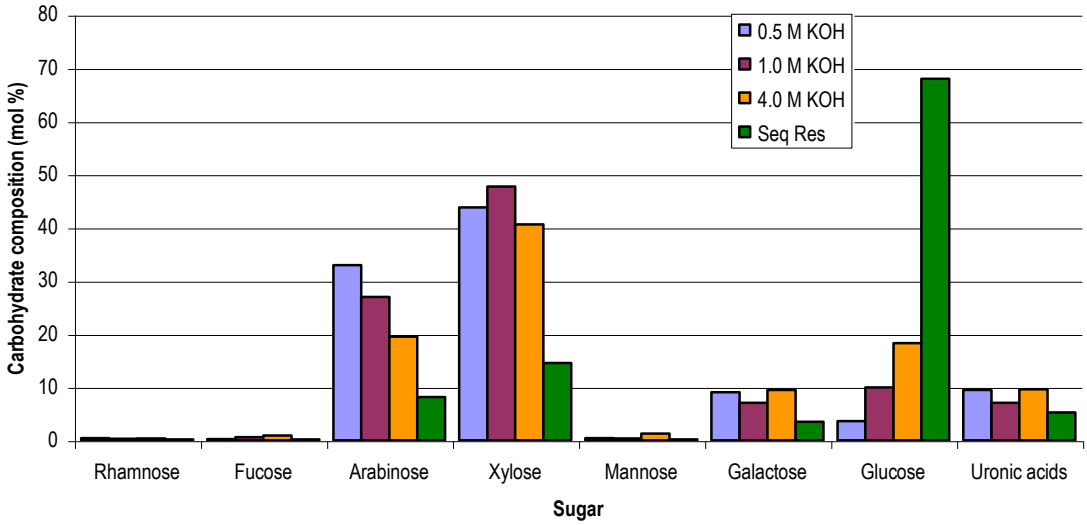

Figure 51: Carbohydrate composition of extracts and residue from sequential extraction.

5.2.2 Linkage analysis

Methylation analysis was carried out using the lithium dimsyl catalyst, with carboxyl reduction, on 3.5-4.5 mg samples of the extracts and residue; the results of which are given in Figure 52. Unfortunately the total mol% values for each sugar do not compare favourably with the sugars analysis and the proportion of apparently unmethylated sugars is excessive. The sugars were probably unmethylated because of the inability of the reagents to access the polysaccharides. This may have been caused by aggregation of the polysaccharide chains when they were freeze-dried. Because of the high proportion of unmetylated sugars stoichiometry has not been taken into account in the interpretation of the results.

		0.5 M KOH extract		1.0 M KOH extract		4.0 M KOH extract		Residue	
SUGAR	LINKAGE	Li dimsyl	Li dimsyl*	Li dimsyl	Li dimsyl*	Li dimsyl	Li dimsyl*	Li dimsyl	Li dimsyl*
Rha	(1-2)						0.32		
Fuc	t-	0.19				1.22	1.04		
Ara-f	t-	24.03	24.73		3.65	18.88	6.82	1.68	1.18
Ara-f	(1-3)	4.85	5.14		2.94	4.30	3.49		
Ara-f	(1-2)	1.07	1.34				0.43		
Ara-f	(1-5)	2.58	2.53		3.75	2.84	0.46		
Ara-p	t-	0.08				0.18			
Ara-p	(1-3,4)	0.63				0.42	1.29		
Ara-p	Unmeth.	3.56			6.00				
Xyl	t-	4.12	4.46		2.19	15.30	7.31	0.91	
Xyl	(1-4)	22.56	29.42	6.97	12.99	2.17	18.13	1.96	
Xyl	(1-2)				0.00		3.95		
Xyl	(1-3,4)	26.78	5.85		7.93	23.90	27.25	1.86	2.35
Xyl	(1-2,4)	3.65	4.79		1.40				
Xyl	Unmeth.		4.17		1.07	1.98	2.90		
Man	(1-4)		0.53			4.56	3.01		
Gal	t-	2.36	1.16		0.51	5.05	1.10	1.34	
Gal	(1-2)		1.17		0.45		3.61		0.33
Gal	(1-3)	0.11	0.35						
Gal	(1-6)		0.60				0.21		
Gal	(1-2,3)	0.19							
Gal	(1-4,6)	0.17				0.45			
Gal	(1-3,6)	0.93	0.98						
Gal	(1-3,4,6)	0.15							
Gal	Unmeth.		0.55	7.23	7.26			9.97	32.65
Gal(A)	(1-6)						0.13		
Gal(A)	(1-3,4,6)						0.64		
Glc	t-					0.34			
Glc	(1-4)	0.49			1.04	6.59	4.59	2.04	
Glc	(1-4,6)	0.78	1.60		1.86	10.41	5.88		
Glc	(1-3,4)	0.18				0.48	0.32		
Glc	(1-2,4)	0.11				0.46	1.08		
Glc	(1-3,4,6)	0.11					0.64		
Glc	(1-2,4,6)	0.07				0.47	0.47		
Glc	(1-2,3,6)	0.02							
Glc	Unmeth.	0.23		85.81	41.02		1.46	80.25	63.49

Figure 52: Linkage analysis of sequential-extraction extracts and residue.

		0.5 M KOH		1.0 M KOH		4.0 M KOH		Residue	
SUGAR	LINKAGE	Li dimsyl	Li dimsyl*	Li dimsyl	Li dimsyl*	Li dimsyl	Li dimsyl*	Li dimsyl	Li dimsyl*
Glc(A)	(1-6)		6.54		2.01				
Glc(A)	(1-4,6)		1.79		3.94		3.00		
Glc(A)	(1-2,4,6)		2.30				0.47		

* carboxyl reduction was carried out, t- indicates a terminal sugar residue, -f and –p indicate furanose or pyranose ring structures where both were detected, unmeth. indicates sugar was not methylated

Figure 52b: Linkage analysis of sequential-extraction extracts and residue (continued).

0.5 M KOH extract

Terminal arabinose and (1→4), (1→3,4) and (1→2,4)-linked xylose indicates the majority of the polysaccharide released are arabinoxylans. Terminal xylose, (1→4) and (1→4,6)-linked glucose indicates a very small proportion of xyloglucan was released. The uronic acids released were identified as (1→4), (1→4,6) and (1→2,4,6)-linked glucuronic acid; this does not agree with the linkage analysis for the PCWM, where the uronic acid present was identified as (1→4)-linked galacturonic acid. The difference may be due to difficulties in interpreting the GC-MS results. Some arabinan-containing pectin was probably present in this extract.

1.0 M KOH extract

Both the analyses for the 1.0 M KOH extracts have high levels of unmethylated sugars, which affect the mol% values for the other sugar residues. Terminal arabinose, (1→4) and (1→3,4)-linked xylose indicates that again the majority of the extracted polysaccharides are arabinoxylans. Terminal xylose, and (1→4) and (1→4,6)-linked glucose indicate that a small amount of xyloglucan was also released. Pectin is indicated to be in this extract by (1→5)-linked arabinose.

4.0 M KOH extract

Terminal arabinose, (1→4) and (1→3,4)-linked xylose indicates that again the majority of the extracted polysaccharides are arabinoxylans, although they are more branched than those of the previous extracts. Terminal xylose, and (1→4)

and (1→4,6)-linked glucose indicate that a significant amount of xyloglucan was released; the (1→2)-linked galactose may also derive from xyloglucan. Glucomannan is also released in this fraction, indicated by the (1→4)-linked mannose residues. Pectin is indicated to be in this extract by (1→5)-linked arabinose.

Residue

Terminal arabinose and (1→3,4)-linked xylose indicate that there were still small amounts of arabinoxylans present. Terminal xylose may indicate that a small amount of xyloglucan was also present. The undermethylation of cellulose was acute in the residue, presumably because the microfibrils had no matrix polysaccharides holding them apart and preventing hydrogen bonding.

5.2.3 Phenolic composition

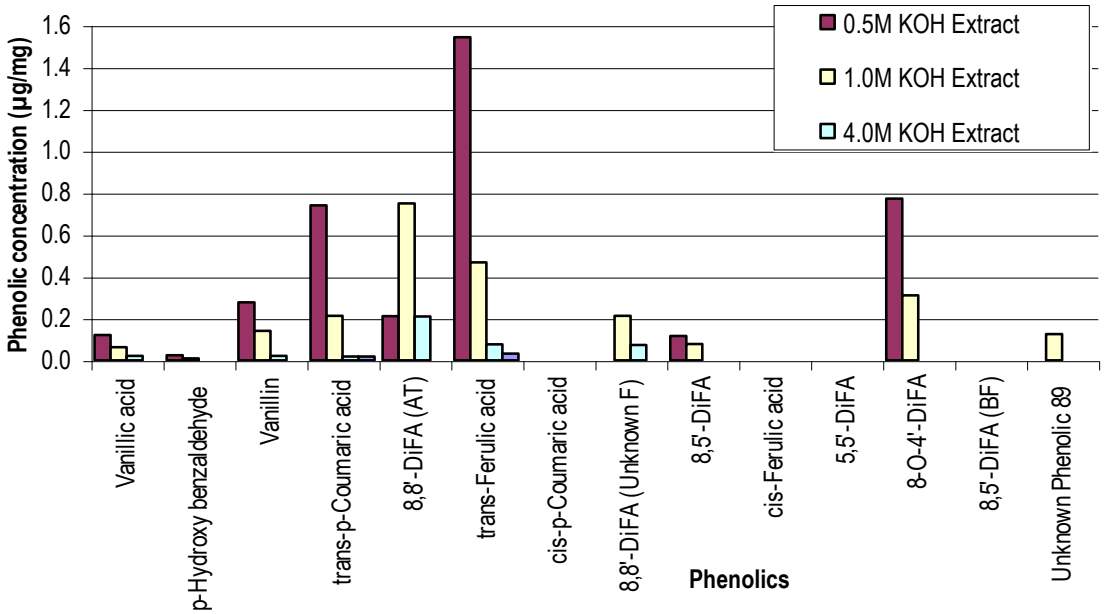

Figure 53: Phenolics in sequential extracts and residue from sequential extraction.

The 0.5 M KOH released the greatest amount of phenolics of the three extractions, including significant amounts of 8-*O*-4'-DiFA (Figure 53). The 1.0 M

KOH released a greater amount of 8,8'-DiFA (AT), 8,8'-DiFA and Unknown Phenolic 89 than the 0.5 M KOH extraction, with 8,8'-DiFA (AT) being the most prevalent; this may be due to these phenolics having more stable ester bonds to their respective polysaccharides, or because they are partially protected by the polysaccharides removed by previous extractions.

The 4.0 M KOH extract contained relatively small amounts of phenolics, but 8,8'-DiFA (AT) was present in the greatest amounts, suggesting that its linkages to polysaccharides are more resistant to alkali than those of the other phenolics. The sequential extraction residue released *trans*-ferulic and *trans*-*p*-coumaric acid only. It would seem that the residue, which should have been fully extracted by the previous treatments, yields more phenolics when treated with 4 M NaOH, this has been observed previously in brewers' spent grain, wheat bran and asparagus, (Mandalari *et al.*, 2005; Rodríguez-Arcos *et al.*, 2004).

5.3 Discussion

At least 80% of the parenchyma cell wall is stable in CDTA and Na_2CO_3. The residue provides ~59% of the yield, which is quite close to the value of 48% for cellulose, but does indicate that some other polysaccharides are also present. The arabinoxylan that is present is preferentially extracted in the lower concentrations of KOH, whereas xyloglucan is removed at higher concentrations.

These results agree with the hypothesis that xyloglucans do not just hydrogen-bond to the surface of the microfibrils, but are trapped within them, and can only be released by swelling of the microfibrils in concentrated alkali (Baba *et al.*, 1994). The arabinoxylans that are extracted by 4.0 M KOH are held in the wall by a mechanism that is not disrupted until the 4.0 M KOH extraction; the mechanism could be the physical entanglement with xyloglucan, or alkali-stable covalent cross-links to xyloglucan. It appears that not only the 8,8'-DiFA (AT), but also the 8,8'-DiFA could have a role in this mechanism, as these were the only dimers removed by the 4.0 M KOH. Perhaps they form a few key linkages

that make the difference between the polysaccharides being soluble or insoluble. The linkages across the middle lamella, which are probably the 8,8'-DiFA (AT), are responsible for cell adhesion, but may break in 1.0 M KOH due to being more exposed.

The methylation analysis should be repeated; preferably on samples that have not been freeze-dried, to reduce undermethylation due to aggregation. It may be better to use the NaOH method, which seems to be more reliable.

6 Development and Evaluation of Biochemical Methods of Cell-Wall Disassembly:

Pectins in the cell walls of the dicotyledonous *Amaranthaceae* species, such as sugar beet (Clausen *et al.*, 2004; Colquhoun *et al.*, 1994; Rombouts and Thibault, 1986), spinach (Fry, 1982; Ishii and Tobita, 1993) and quinoa (Renard *et al.*, 1999), have been found to be feruloylated at *O*-2 and/or *O*-5 of Ara residues in the arabinan chains, or *O*-6 of Gal residues in the galactan chains, in the side chains of homogalacturonan and rhamnogalacturonan (Micard *et al.*, 1997b; Ralet *et al.*, 2005). Heteroxylans in the cell walls of monocotyledonous species such as wheat (Saulnier *et al.*, 2007; Smith and Hartley, 1983), barley (Gubler *et al.*, 1985) and pineapple (Smith and Harris, 2001) are feruloylated at *O*-5 of Ara residues or GlcA residues. Feruloylated xyloglucan (*O*-4 of xylose feruloylated) has been found in bamboo shoots by Ishii et al (1990). Ishii (1997) reviewed all the phenolic polysaccharides that had been produced up to that date. Since then a number of feruloylated (but not *p*-coumaroylated) polysaccharides have been discovered.

The ability of ferulic acid dimers to cross-link polysaccharides was first proved by Ishii (1991) who isolated and characterized a 5,5'-DiFA esterified to two arabinoxylan trisaccharides. Ferulic acid dimers that are connected to oligosaccharides at both ends have been isolated from maize bran, specifically Ara-5,5'-DiFA-Ara, Xyl-Ara-5,5'-DiFA-Ara and Ara-8-*O*-4'-DiFA-Ara, using mild acid hydrolysis (Allerdings *et al.*, 2005; Saulnier *et al.*, 1999) and from sugar beet, specifically Ara-Ara-8-*O*-4'-DiFA-Ara-Ara, using enzyme digestion (Levigne *et al.*, 2004b). Even a small number of these dimers, forming extracellularly, could significantly affect the mechanical properties of the cell walls by increasing the M_w of the polysaccharides significantly and creating a three dimensional network (Saulnier *et al.*, 2007).

In order to expand our understanding of CWC cell wall structure, fragments of polysaccharide, esterified with ferulic acid and its dimers, need to be produced. Of particular interest is the 8,8'-DiFA (AT), due to its proposed role in cell

adhesion (Parker, 2000). The preferred method to achieve this is enzyme digestion, as with foreknowledge of the activities present in the formulations, there is some degree of control as to which linkages are broken. This chapter details the preliminary work for the enzyme digestion method.

6.1 Enzyme preparations

Three enzyme preparations were tested: *T. viride* xylanase – a pure xylanase; Ultraflo (*Humicola insolens*) - a mixture of β-glucanase and xylanase, with small amounts of cellulase, pentosanase, arabinanase, feruloyl esterase and hemicellulase activity; Driselase (*Basidiomycetes*) – a mixture of laminarinase, xylanase and cellulase (from Sigma-Aldrich data sheet), with no feruloyl esterase activity.

6.2 Methods

Fry (1982) noted that Driselase contained phenolic contaminants, so the Driselase powder was partially purified as described by him, with a few slight modifications. 1 g of Driselase powder was dissolved in 10 ml of sodium acetate buffer (50 mM pH 5.0) at 4°C for 2 hr. The resulting suspension was centrifuged at 13,000 rpm, 4°C for 15 min to remove solid material. The supernatant was collected and combined, and the pellet resuspended in buffer twice followed by centrifugation as above to ensure that all of the enzyme was transferred. The volume of supernatant was measured and sufficient $(NH_4)_2SO_4$ added to give a 75% saturated solution, before mixing at 4°C for 2 hr. The suspension was centrifuged as above and the supernatant discarded. The pellet was resuspended in 75% saturated $(NH_4)_2SO_4$ twice and centrifuged as above. The resulting pellet was dissolved in 28 ml of water, and then 2.5 ml aliquots eluted on pre-prepared PD-10 columns using 3.5 ml of water. The solution had 3.016 g of glycerol added per ml of solution before freezing at -20°C. All Driselase used in the experiments described in this chapter was purified in this way.

Enzyme preparations were added (33.5 µl of *T. viride* xylanase, 450 µl of Ultraflo and 2 ml of Driselase) to ~50 mg of PCWM (Batch 2) and 100 ml of 0.02% (w/v) NaN_3, incubated and agitated at 37°C for 48 hr, with a second addition of enzyme after 24 hr. The enzymes were denatured by boiling. The residue was separated from the liquor by filtration (0.45 µm cellulose acetate) and both the residue and supernatant were freeze-dried. They were then treated as shown in Figure 54.

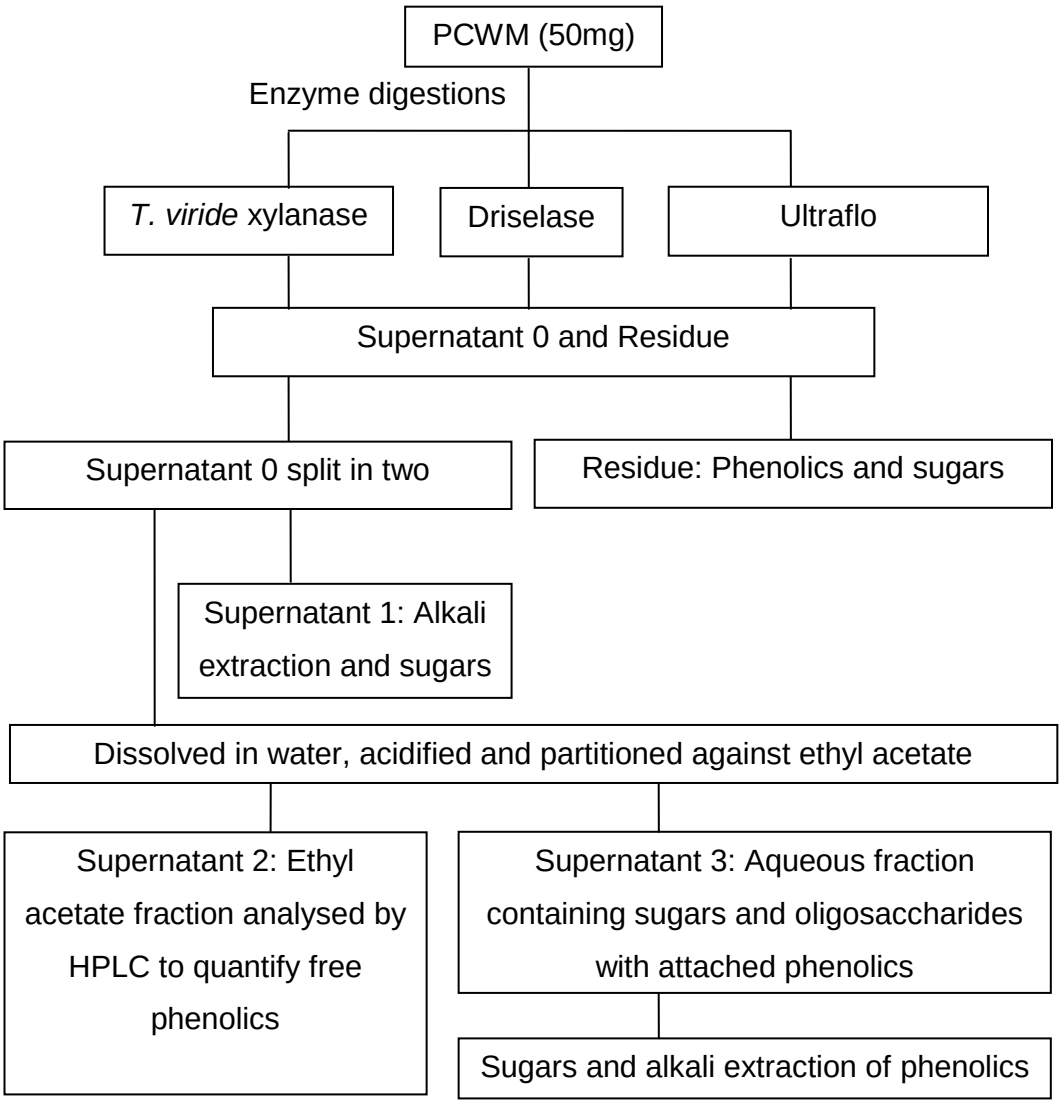

Figure 54: Experimental scheme for enzyme digestions.

6.3 Yields

The yields of residue and Supernatant 0 are given in Figure 55. Ultraflo and Driselase solubilised between 85-95% of the PCWM, whereas *T. viride* xylanase only solubilised ~6%. The weight of enzyme added was not known, so the weight of residue plus the weight of supernatant was higher than the original weight of PCWM.

	PCWM (mg)	Residue (mg)	Supernatant 0 (mg)	Total recovered (mg)
***T. viride* 1**	49.6	46.5	32.2	78.7
***T. viride* 2**	49.4	46.1	31.3	77.4
Ultraflo 1	49.0	3.3	488.0	491.3
Ultraflo 2	50.7	5.9	416.0	421.9
Driselase 1	50.4	7.5	219.5	227.0
Driselase 2	49.8	5.7	226.6	232.3

Figure 55: Yields from preliminary enzyme digestion.

6.4 Analysis of residues and supernatants

6.4.1 Sugar composition

The sugar composition of the residue was measured using the 72% (w/w)-H_2SO_4 hydrolysis method and for Supernatants 1 and 3 using the 1 M-hydrolysis method outlined in Section §2.7. Uronic acids were not measured. The results given in Figure 56 show that, consistent with the low degree of solubilisation achieved by *T. viride* xylanase, the composition of the residue barely changed. Driselase reduced the amount of glucose significantly, and that of arabinose, xylose and galactose slightly. Ultraflo significantly reduced all the major cell wall sugars. The results for Supernatant 1 (Figure 57) are inconsistent with expectations, in that the results indicate that Ultraflo released more glucose than was present in the first place; and also,

examination of the chromatograms indicated the presence of an unidentified sugar not usually seen in CWC.

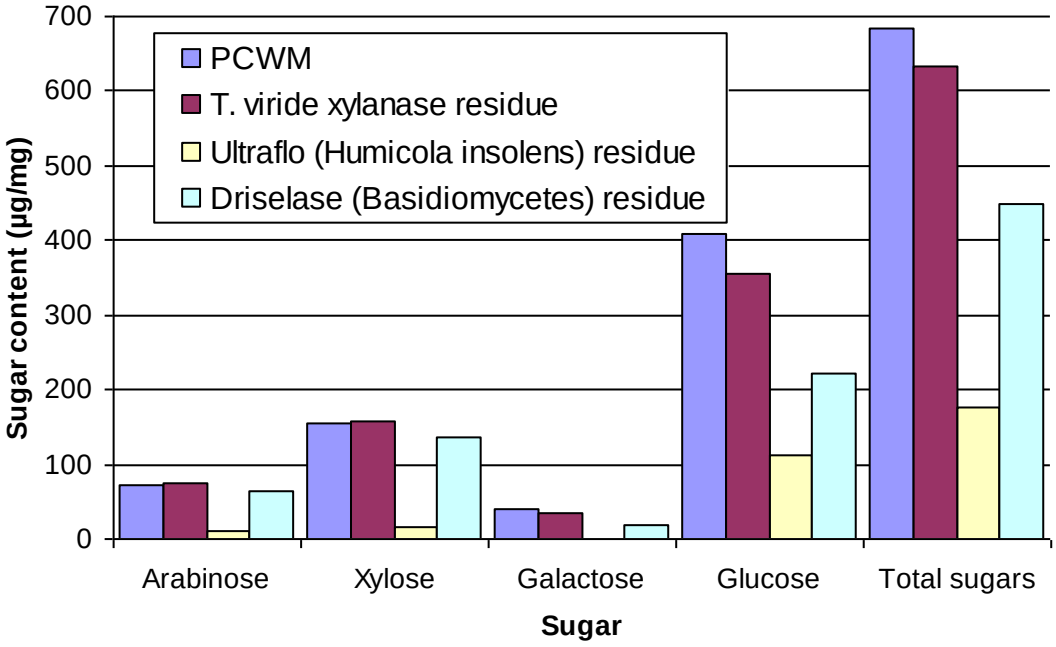

Figure 56: Average sugar composition of residues after enzyme digestion, compared to PCWM.

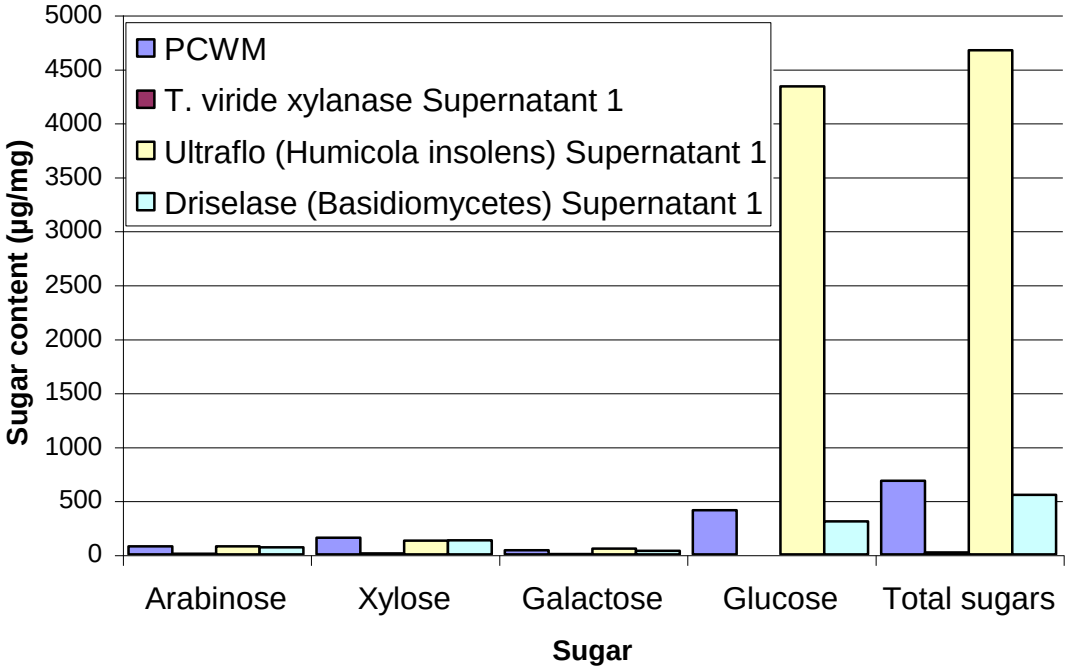

Figure 57: Average sugar composition of Supernatant 1 from each enzyme digestion (per mg of PCWM digested), compared to PCWM.

The unexpected discovery that there was more sugar than was originally present in the PCWM indicates there are sugars in the Ultraflo enzyme preparation, and as this may be true to some extent for all three enzymes, the residue data are probably more reliable. The results for Supernatant 3 (not shown) were essentially the same as those for Supernatant 1, except that the small amount of rhamnose that was present in the *T. viride* Supernatant 1 was not present in *T. viride* Supernatant 3.

6.4.2 Phenolic composition

The phenolic composition was measured for the residue and for all four supernatants. The residue and Supernatant 1 had phenolics measured as outlined in Section §2.3. Supernatant 0 was run on the HPLC unprocessed, in the hope of finding a spectrum similar to that of the 8,8'-DiFA (AT), which would indicate a possible DiFA-polysaccharide fragment. No such peak was found, but as 8,8'-DiFA (AT) is present only in small amounts anyway, it may still have been present, but undetectable. Other peaks were detected, although not identified, and Ultraflo released the greater number and amount of these (Figure 58), indicating, perhaps, the release of fragments attached to other phenolics, or possible contamination.

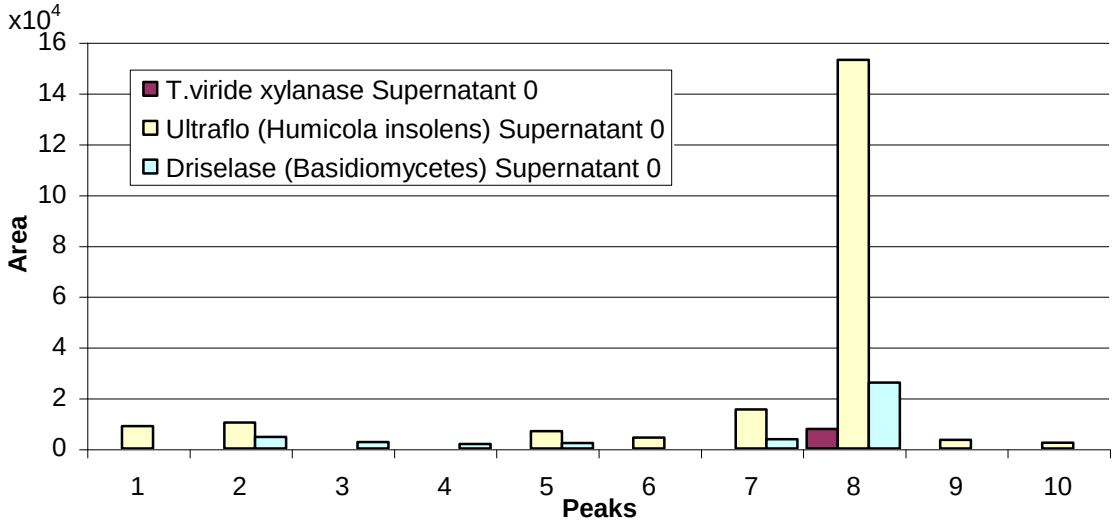

Figure 58: Supernatant 0 HPLC results (all peaks unidentified).

Supernatant 2 was the ethyl acetate fraction from the partitioning step and contained any free phenolics; it was dried down and redissolved in MeOH:water (50:50 v:v). Supernatant 3 was analysed by the usual "total phenolics" method, but the volume of supernatant was measured and the concentration of the NaOH solution doubled, so that when equal volumes of the two were combined a final concentration of 4 M NaOH was achieved. Supernatant 3 contained phenolics still bound to oligosaccharides.

The original PCWM contained 11.6 µg/mg of phenolics; in the residue this was reduced by Driselase to 9.9 µg/mg and Ultraflo to 1.7 µg/mg, but increased by *T. viride* xylanase to 14.4 µg/mg (Figure 59).

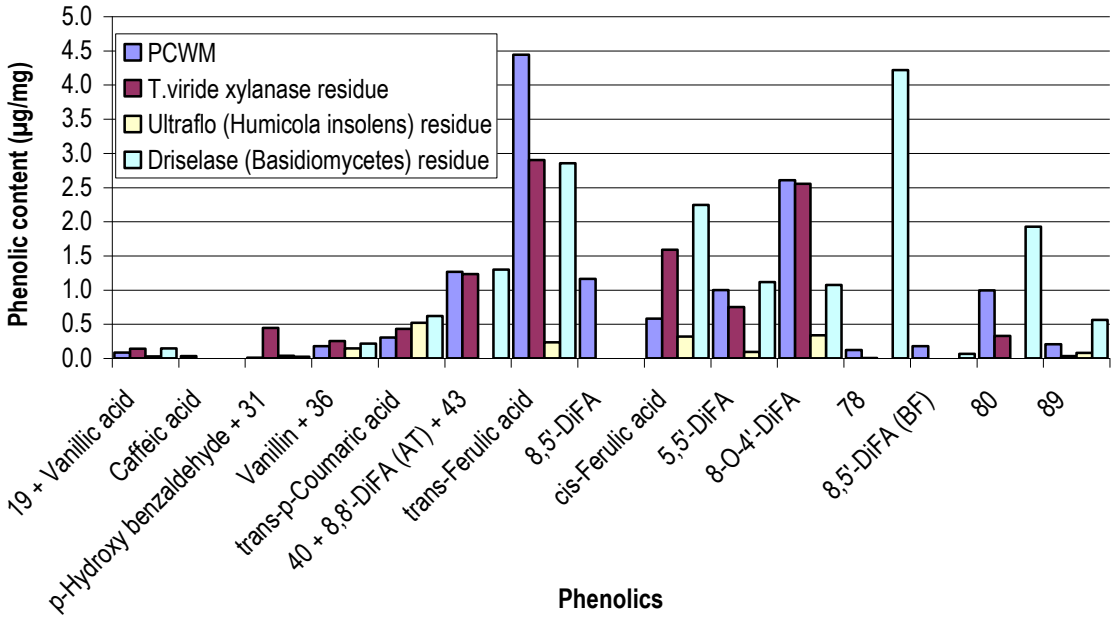

Figure 59: Comparison of phenolics in undigested PCWM and enzyme digest residues (values are averages from two digestions).

The numbers in the x-axis labels of Figure 59 refer to unknown phenolics as listed in Appendix F. The *T. viride* residue had higher amounts of *p*-hydroxybenzaldehyde and *cis*-ferulic acid than the original material, indicating there could be some contamination, or that the xylanase made them more accessible to NaOH; however the increase in *cis*-ferulic acid is similar in size to the decrease in *trans*-ferulic acid and may indicate isomerisation. The

Driselase residue had a number of peaks that were higher than the original material, particularly *cis*-ferulic acid and peaks 78, 80 and 89, indicating there could be some contamination. The *T. viride* xylanase and Driselase do not appear to have removed the 8,8'-DiFA (AT) which was one of the main targets of this investigation, indicating they may not be the best choice for the digestion.

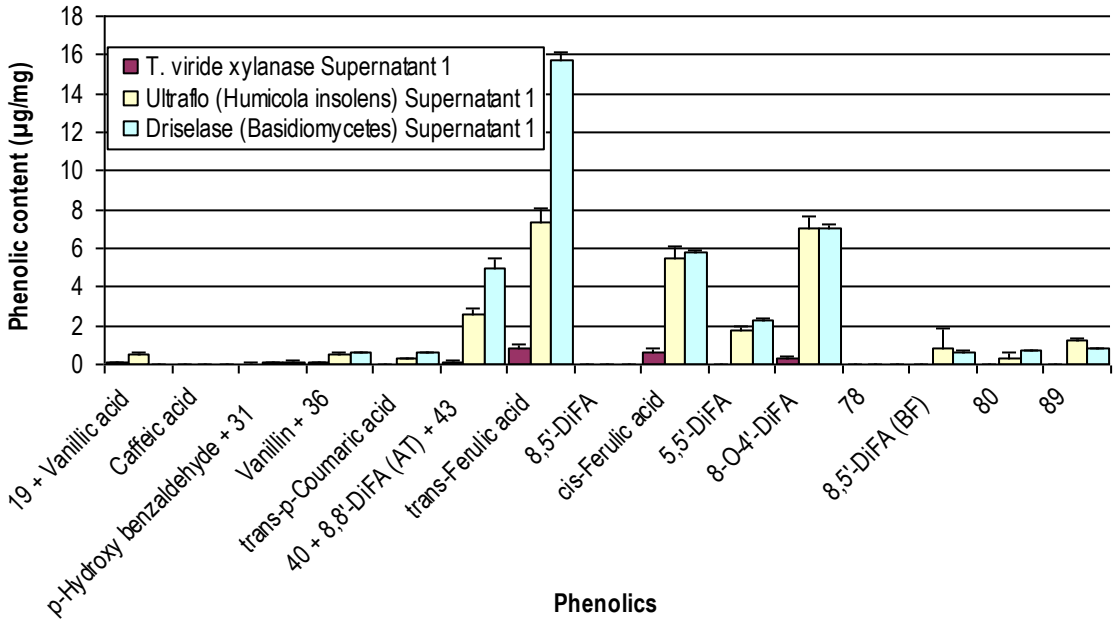

Figure 60: Phenolics in enzyme digest Supernatant 1 (alkali extracted) (errors are standard deviations of two replicates from two digestions).

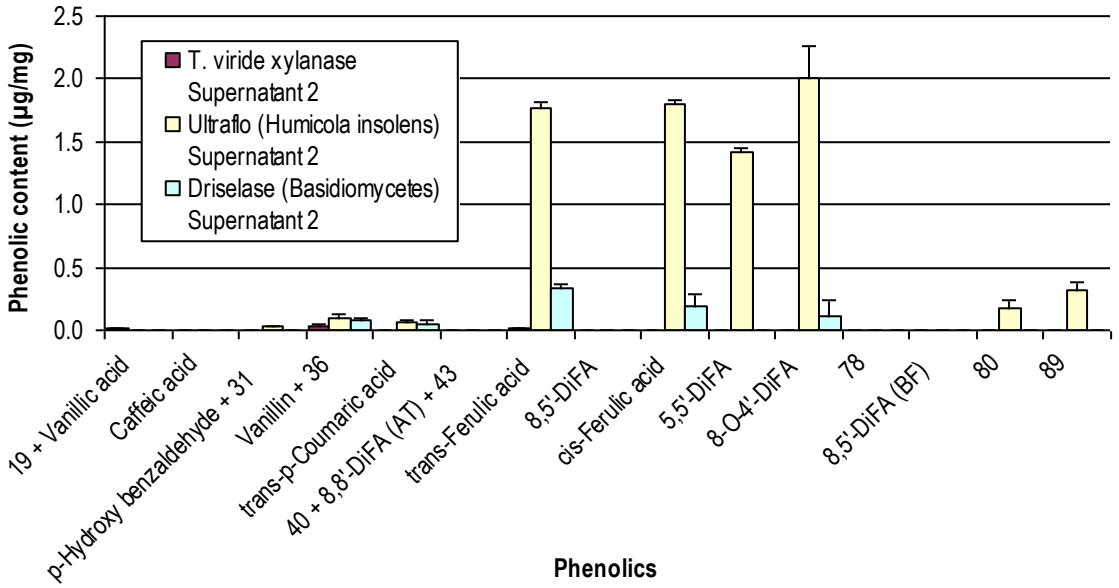

Figure 61: Phenolics in enzyme digest Supernatant 2 (free phenolics) (errors are standard deviations of two replicates from two digestions).

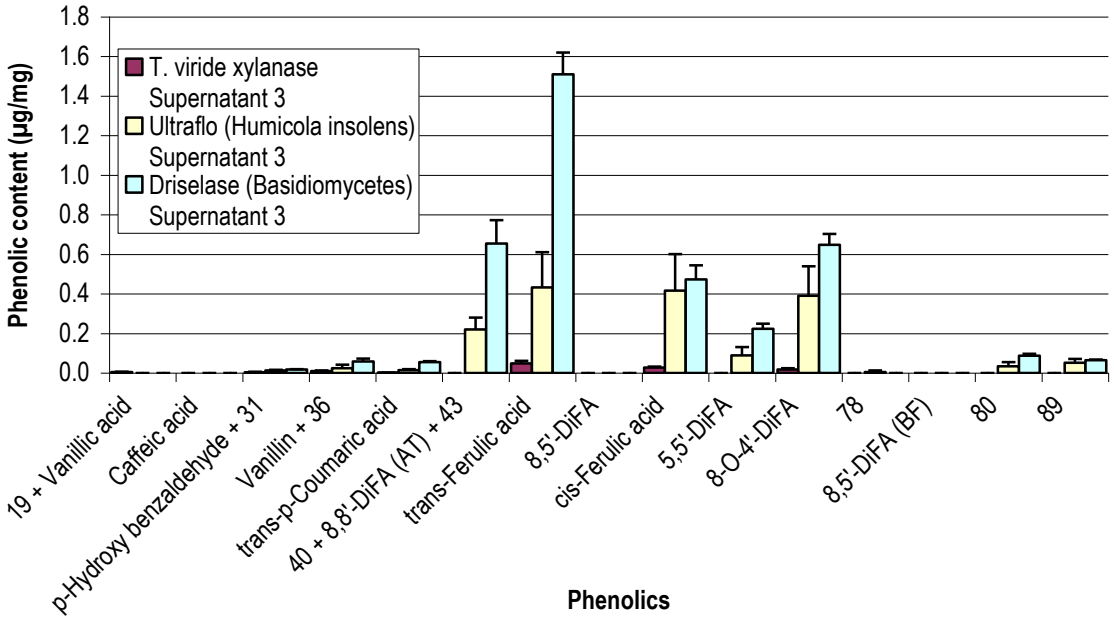

Figure 62: Phenolics in enzyme digest Supernatant 3 (alkali extracted after free phenolics removed) (errors are standard deviations of two replicates from two digestions).

The results for Supernatants 1, 2 and 3 are shown in Figures 60-62 and are discussed together for each enzyme treatment. As with Figure 59, the numbers in the x-axis labels of Figures 60-62 refer to unknown phenolics as listed in Appendix F

T. viride *xylanase*

The only phenolic that was present at a lower level in the residue than in the PCWM and that also appeared in the supernatants was *trans*-ferulic acid; it appears to have been attached to the small amounts of polysaccharide released, as there was very little in Supernatant 2, which should have contained any free phenolics.

Ultraflo

Most of the phenolics were present at a lower level in the residue than in the PCWM and these also appeared in the supernatants, particularly 8,8'-DiFA (AT), *trans*-ferulic acid, *cis*-ferulic acid, 5,5'-DiFA and 8-*O*-4'-DiFA. The data

from Supernatants 1 and 3, and the sugars analysis imply that most of these phenolics were still attached to arabinoxylan or xyloglucan. The 8,8'-DiFA (AT) was the only phenolic to be released that was not also released in the free form (Supernatant 2). As Ultraflo contains feruloyl esterase activity it is not surprising that it released the greatest quantity of free phenolics of the three enzymes.

Driselase

As the total amounts of 8,8'-DiFA (AT), *trans*-ferulic acid, *cis*-ferulic acid, 5,5'-DiFA and 8-*O*-4'-DiFA were higher than what was in the PCWM originally, it is reasonable to assume there was some contamination from the enzyme preparation. The only phenolics that were present at a lower level in the residue than in the PCWM and that also appeared in the supernatants were *trans*-ferulic acid and 8-*O*-4'-DiFA, both of which appear as both free and bound phenolics. However, as there is no known feruloyl esterase activity in Driselase, the free phenolics are probably from contaminants in the preparation. As the 8,8'-DiFA (AT) was only released by alkali extraction of the supernatants and the values are extremely high relative to the PCWM, it may be that Driselase contains 8,8'-DiFA (AT) esterified to oligosaccharides. Wende and Fry (1997) have shown previously that even when purified as described, Driselase contains some ferulic acid, possibly esterified to sugar residues; therefore the enzyme preparation will need further purification if it is to be used in the future.

6.5 Releasable phenolics from Ultraflo and purified Driselase

Ultraflo and purified Driselase were analysed for phenolic content to determine if they were the source of the additional phenolics detected in the digestions (Figure 63).

The phenolics results for Driselase indicated a range of phenolics were present, some of which were present in relatively high quantities, and included four diferulic acids. The phenolics results for Ultraflo indicated that, with respect to

phenolics, the preparation was free from appreciable contamination, excluding a little vanillic and *p*-coumaric acid, making it suitable for phenolic-based analyses.

	Ultraflo		Driselase	
Phenolics	Average (µg/ml)	S.D.	Average (µg/ml)	S.D.
Phenylacetic acid	0.00	0.00	1.73	0.36
Vanillic acid	0.64	0.07	0.88	0.04
p-Hydroxybenzaldehyde	0.00	0.00	1.23	0.19
Vanillin	0.00	0.00	1.37	0.08
trans-*p*-Coumaric acid	0.74	0.08	1.47	0.15
8,8'-DiFA (AT)	0.00	0.00	7.07	0.67
trans-Ferulic acid	0.00	0.00	26.29	0.51
8,5'-DiFA	0.00	0.00	2.91	0.41
cis-Ferulic acid	0.00	0.00	0.76	0.12
5,5'-DiFA	0.00	0.00	3.70	1.14
8-*O*-4'-DiFA	0.00	0.00	2.44	0.04
Total	1.38	0.11	46.41	3.01

Figure 63: Phenolics extracted from Ultraflo and purified Driselase by 4 M NaOH.

6.6 Releasable sugars from Ultraflo and purified Driselase

	Ultraflo		Driselase	
Sugars	Average (µg/ml)	S.D.	Average (µg/ml)	S.D.
Rhamnose	58	1	43	17
Fucose	38	8	18	6
Arabinose	490	1	138	42
Xylose	142	2	139	41
Mannose	3099	95	415	141
Galactose	901	10	36	18
Glucose	96604	883	452	623
Total	101332		1241	

Figure 64: Sugars extracted from Ultraflo and purified Driselase by 72% (w/w) H_2SO_4.

Ultraflo and purified Driselase were analysed for sugar content to determine if they were the source of the additional sugars detected in the digestions (Figure 64). The sugars results for Driselase were inconsistent, but on average there were ~1250 µg/ml, particularly glucose and mannose (~400 µg/ml each). The sugars results for Ultraflo were high (~100 mg/ml), and resulted in the GC chromatogram showing overloaded peaks.

As expected from the digestion results glucose was present in the greatest amounts. At least some of the sugars could be covalently attached to the enzymes, so the figures above are maximum values. However, it would indicate that neither of these enzyme preparations is suitable for the current investigation; even so a number of researchers have used Driselase to produce phenolic-oligosaccharides in the past (Bunzel *et al.*, 2002; Levigne *et al.*, 2004a; Ralet *et al.*, 1994b). The manufacturer's data sheet (Sigma-Aldrich) for Driselase states that approximately 15% of the raw powder is protein. This shows that there are significant amounts of other components, which presumably include sugars and phenolics. Studies that have used Driselase, without purification, may have been affected by the phenolic contamination shown here and quantified by Wende and Fry (1997) as 39.6 nmol saponifiable ferulate in 2.5 mg purified Driselase. Figure 65 lists a selection of references that have used Driselase (or a component thereof) to break down plant cell-wall polysaccharides, whole CWM or alcohol-insolubule residue (AIR). For each one the type and amount of substrate is given, as is the type of purification of Driselase used, and whether enzyme-only controls were included. The types of purification method used have been encoded in Figures 65 and 65b as follows:

- NS – No method specified
- Supernatant – Raw Driselase powder dissolved in water or buffer, then centrifuged, and the resulting supernatant used
- Fry – The partial purification method described by Fry (1982) or similar
- Specific – More specific methods designed to isolate a particular enzyme activity

Reference	Substrate	Purification Method	Resulting Driselase	Reaction vol.	Total Substrate	Total Driselase in reaction	Controls
(McCleary, 1979)	Legume galactomannans	Specific	Purified *β*-D-Mannanase	22 ml	0.1 g	2 ml, 0.4 µkat	N
(Fry, 1982)	Spinach CWM	Fry	Purified powder	-	20 mg	0.60%	Y
(Fry, 1983)	Spinach CWM	Fry	Purified powder	-	20 mg	0.60%	N
(Hoebler and Brillouet, 1984)	Larchwood xylan	Specific	Purified xylanase	1.2 ml	6 mg	5-200 µl	N
(Ishii and Hiroi, 1990)	Bamboo shoot CWM	Fry	60 mg/ml solution	1 L	20 g	180 mg	N
(Borneman *et al.*, 1990)	Bermuda grass CWM	Fry	9.2 mg protein /ml solution	102 ml	5 g	18.4 mg protein	N
(Ishii and Tobita, 1993)	Spinach leaf CWM	Fry	60 mg/ml solution	1 L	20 g	180 mg	N
(Ralet *et al.*, 1994b)	Sugar beet pulp AIR	Supernatant	10 mg protein /ml solution	10 ml	100 mg	10 mg protein	N
(Ralet *et al.*, 1994b)	Sugar beet pulp AIR	Supernatant	1 g protein /L solution	1 L	10 g	1 g protein	N
(Colquhoun *et al.*, 1994)	Sugar beet pulp AIR	Supernatant	1 g protein /L solution	1 L	10 g	1 g protein	N
(Ralet *et al.*, 1994a)	Sugar beet pulp AIR	Supernatant	1 mg/ml solution	1 L	10 g	1 g*	N
(Ralet *et al.*, 1994a)	Wheat bran	Supernatant	1 mg/ml solution	1 L	10 g	1 g*	N
(Wende and Fry, 1997)	Fescue AIR	Fry	Purified powder	10 ml	200 mg	50 mg	Y
(Smith and Harris, 2001)	Pineapple	Fry	11.9 mg protein /ml solution	1 ml	10 mg	0.238 mg	Y
(Bunzel *et al.*, 2002)	Wild rice IDF	NS	Raw powder	900 ml	10 g	1 g	N
(Gardner *et al.*, 2002)	Arabidopsis AIR	Fry	0.5% solution	-	10 mg	1.25 µg	N
(Clausen *et al.*, 2004)	Wheat/Sugar beet	Supernatant	1 g protein /L solution	-	10 g	1 g protein	N
(Levigne *et al.*, 2004a)	Sugar beet CWM	NS	Raw powder	1 L	10 g	1 g	N
(Encina and Fry, 2005)	Maize AIR	Fry	Purified powder	1 ml*	20 mg*	1%	N
(Ralet *et al.*, 2005)	Sugar beet CWM	Supernatant	Supernatant from 67.8 mg/ml	-	<10 g*	9.5 ml	N

Figure 65: Table of selected enzyme-digestion conditions for other researchers.

Reference	Substrate	Purification Method	Resulting Driselase	Reaction vol.	Total Substrate	Total Driselase in reaction	Controls
(Ardiansyah *et al.*, 2006)	Rice bran	NS	Raw powder	500 ml	<500 g	0.1 mg	N
(Nergard *et al.*, 2006)	Polysaccharide samples	Specific	Purified exo-*β*-D-(1-3)-galactanase	5 ml	5 mg	5 µg, 0.007 U	N
(Tsumuraya *et al.*, 2006)	Acacia gum	Specific	Purified exo-*β*-D-(1-3)-galactanase	12 ml	57 mg	1.8 U	N

* Not explicit in text, NS – None specified, Supernatant – Driselase dissolved in water or buffer, then centrifuged, and the resulting supernatant used, Fry – The partial purification method of Fry (1982), Specific – More specific methods designed to isolate a particular enzyme activity, CWM – Cell Wall Material, AIR – Alcohol Insoluble Residue, IDF – Insoluble Dietary Fibre

Figure 65b: Table of selected enzyme-digestion conditions for other researchers (continued).

The experiments where a specific enzyme activity has been extracted from Driselase should be free of phenolic and sugar contaminants. In contrast, those using raw Driselase are likely to have introduced significant contaminants into their reaction, as 85% of the added material was not protein (manufacturer's data sheet). However, without analysing Driselase powder it is difficult to know how problematic the contamination would be. Dissolving raw Driselase powder in water or buffer and centrifuging the resulting suspension yields a brown supernatant from which only the insoluble contaminants have been removed. The experiments using this method of purification will still have some contamination, although less than if raw powder was used. For those using the Fry method of purification the ratio of Driselase to substrate is probably more important. For instance, an estimated 2% of the phenolics would originate from Driselase if 4 ml of purified enzyme was used with 1 g of substrate; however this figure is based on CWC, so it could be much higher in other plants. In any case, enzyme-only controls appear to be highly recommended when using Driselase to produce fragments of feruloylated cell-wall polysaccharides; only then can the fragments created be said to have originated from the plant material.

6.7 Discussion

Driselase would have been the enzyme preparation of choice, due to its high degree of solubilisation of the material and lack of FAE activity, but as it was contaminated with the very phenolics that were of most interest, it was deemed unsuitable. Ultraflo was also unsuitable due to the apparent contamination from sugars and its ability to release esterified phenolics. As the *T. viride* xylanase was poor at solubilising the material there was no choice but to resort to mild acid hydrolysis, as described in Chapter 7.

For those wishing to use Driselase for future studies a possible method for avoiding the phenolic contamination problem would be to purify out the individual activities and recombine them to give a clean preparation with known activity. The isolation of an exo-β-(1→3)-D-galactanase and an exo-cellulase (Kanda *et al.*, 1978; Tsumuraya *et al.*, 2006) from Driselase has already been achieved.

7 Development, Evaluation and Exploitation of Chemical Methods of Cell-Wall Disassembly:

The aim of these experiments was to elucidate the nature of the phenolic-polysaccharide associations, particularly those which cross-link polysaccharide chains. This included determining which phenolics are esterified to polysaccharides, and whether they cross-link polysaccharide chains, particularly the 8,8'-DiFA (AT) that is thought to be so important for cell adhesion in CWC (Parker, 2000).

As enzyme digestion was not suitable for this, due to the contamination of the enzyme preparations with sugars and phenolics (see Chapter 6), a chemical method was chosen, even though chemical methods are less specific. The method chosen to produce the phenolic-polysaccharide fragments from CWC PCWM was mild acid hydrolysis with 0.05 M TFA, which has been used to produce phenolic-polysaccharide fragments in the past (Allerdings *et al.*, 2005; Allerdings *et al.*, 2006; Funk *et al.*, 2005; Saulnier *et al.*, 1999).

7.1 Methods

As multiple hydrolyses were carried out and numerous sub-fractions were produced, a flow diagram has been produced as a guide to the various treatments (Figure 66).

Fragments were produced by mild acid hydrolysis of ~1 g PCWM (Batch 2) using 100 ml of 0.05 M TFA at 100°C for 3 hr. These conditions were chosen by refering to kinetic experiments done by Saulnier *et al* (1995) that showed that a 3 hr hydrolysis gave the best balance between hydrolysing the sugars and leaving the phenolics esterified to sugars. The mixture was cooled and filtered through a 0.45 µm PTFE membrane filter under vacuum (the filter was moistened with ethanol first). The residue was washed with 2 x 100 ml of water, combining the washings with the original filtrate, and then frozen. The TFA was

removed from the hydrolysate by repeated evaporation in a rotary evaporator at 45-47°C with extra water. The TFA was considered to have been removed when the hydrolysate pH was stable at 4 and no vinegar smell was detected. A film accumulated on the inside of the round-bottomed flask, but it could not be removed with water, so some loss must have occurred.

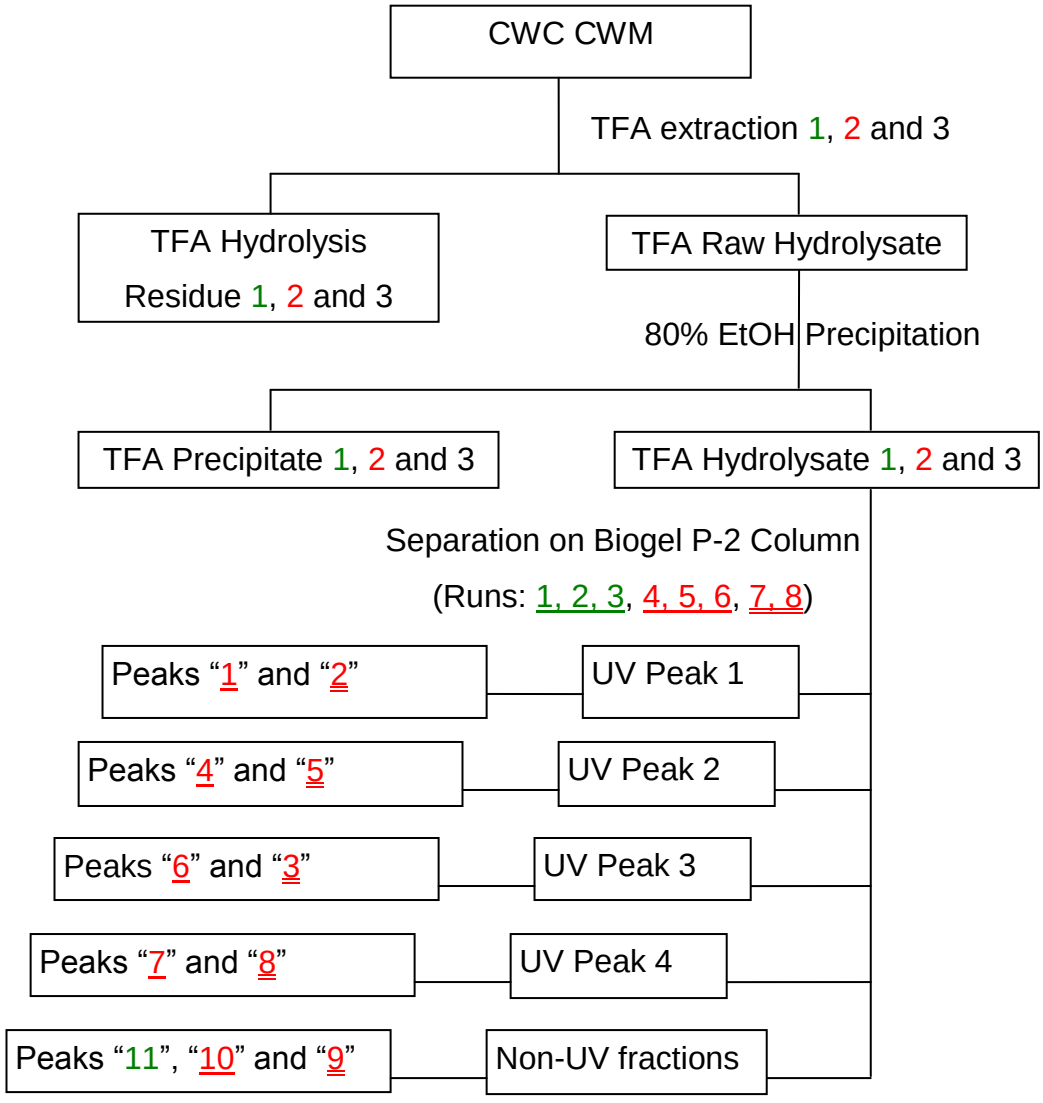

Colour coding indicates the original hydrolysis
Underlines indicate which Biogel P-2 runs were combined (eg Peaks "1", "4", "6", "7" and "10" come from runs 4-6).

Figure 66: TFA-hydrolysis fraction guide.

7.1.1 Ethanol precipitation

The volume of hydrolysate was measured and sufficient absolute ethanol added to produce a final concentration of 80% ethanol. The solution was stirred at 4°C for 25 hr, to remove the larger polysaccharides by precipitation (Fry, 1988). The suspension was filtered through a 0.45 µm PTFE membrane filter under vacuum and washed with 50 ml of 80% ethanol. The residue was frozen and freeze-dried on the membrane filter to reduce losses. The filtrate was rotary evaporated at 41°C until the volume had reduced to a few millilitres. A small portion of the filtrate was removed and freeze-dried for use in the analyses, the remainder was frozen.

7.1.2 Characterisation of residues and supernatants

Figure 67 gives the yields of residue, hydrolysate/supernatant and precipitate for the TFA hydrolyses. It appears the yields improved with practice.

	Hydrolysis 1	Hydrolysis 2	Hydrolysis 3
Starting material (g)	1.004	1.019	1.837
Residue (g)	0.563	0.566	1.090
Hydrolysate (g)	0.263[a]	0.043[b]	0.101[b]
Ethanol precipitate (g)	0.080	0.314	0.611
Yield (%)	82.3	90.6	98.1

[a] before ethanol precipitation, [b] after ethanol precipitation

Figure 67: Yields of residue, hydrolysate and ethanol precipitate from TFA hydrolyses.

Sugars

The residue (~4 mg), supernatant (~1 mg) and precipitate (~3.5 mg) from Hydrolysis 1 were analysed for sugars using the 1 M H_2SO_4 method described in Section §2.7.

The residue had a high proportion of xylans and xyloglucan, with perhaps some galactans also remaining (Figure 68). The supernatant had mostly arabinoxylan and some galactan (probably removed from RG I). The precipitate had pectin (RG I), some xyloglucan and a high proportion of xylans.

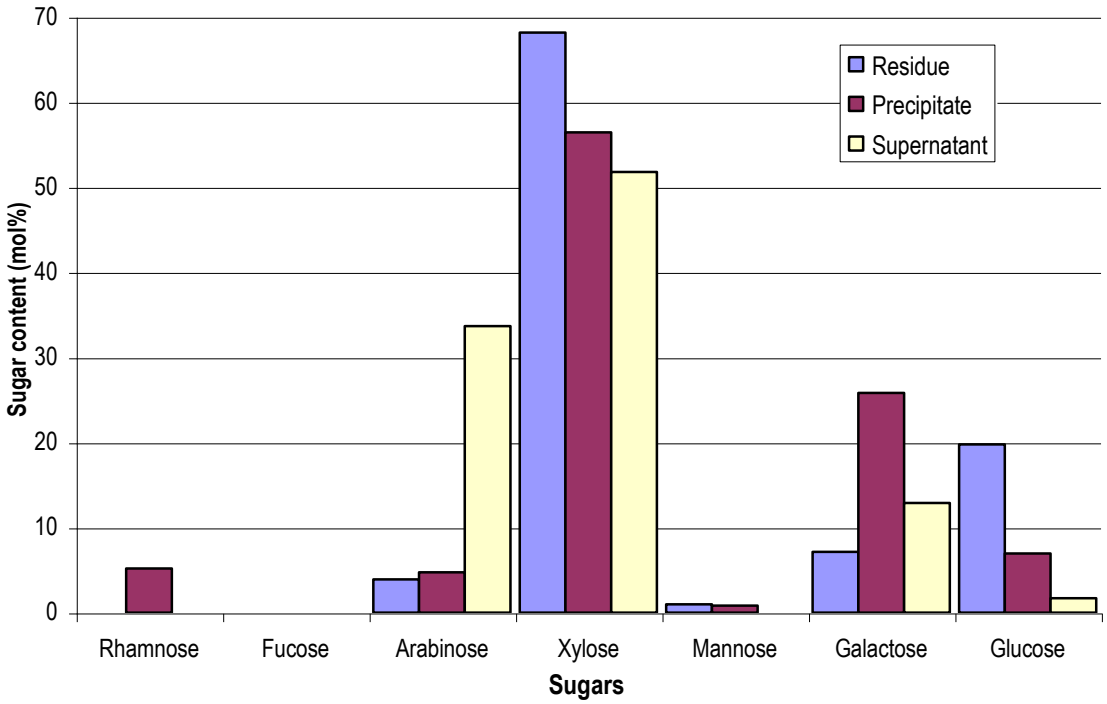

Figure 68: 1 M H_2SO_4 sugars results for the residue, supernatant and ethanol precipitate from TFA Hydrolysis 1 (values are averages from two determinations).

The residue (~0.5 mg), supernatant (~1 mg) and precipitate (~3.5 mg) from Hydrolyses 2 and 3 were analysed for sugars using the 72% (w/w) H_2SO_4 method from Section §2.7. The residues had a higher proportion of cellulose than the starting material, but there were also some xyloglucans and probably a small amount of pectin (Figure 69). The precipitates contained pectin (RG I) and xylans, with a little xyloglucan.

The supernatant contained mostly arabinoxylan and some galactan (probably removed from RG I). It appears that the arabinose sidechains were hydrolysed from arabinoxylan, releasing the xylans from the wall; the long xylan chains were then precipitated by ethanol along with the pectin. The polysaccharides

remaining in solution were short oligosaccharides of arabinoxylan and galactan, possibly esterified to ferulic acids.

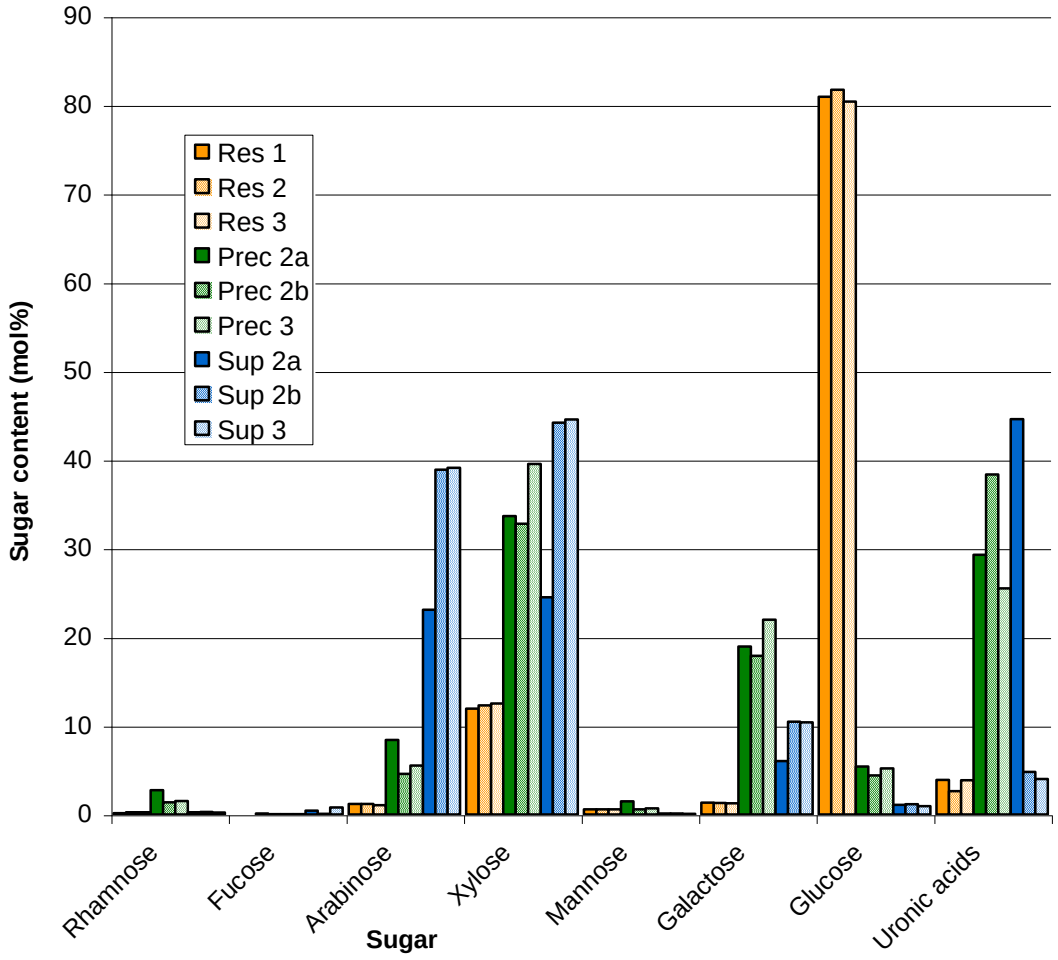

Figure 69: 72% (w/w) H_2SO_4 sugars results for the residue, supernatant and ethanol precipitate from TFA Hydrolyses 2 and 3 (uronic acids measured as GlcA equivalents).

Phenolics

The residue (~5 mg), supernatant (~1.5 mg) and precipitate (~4 mg) were analysed for phenolics using the total phenolic extraction method described in Section §2.3, but using 2 ml, not 1 ml, of 4 M NaOH. Ferulic acid was the predominant phenolic in the residue and supernatant from TFA Hydrolysis 1 (Figure 70) and in all three samples from TFA Hydrolyses 2 and 3 (Figure 71). In Precipitate 1 there were about equal amounts of *trans*-ferulic acid and 8-*O*-4'-DiFA. The 8,8'-DiFA (AT) was only detected in the residue of Hydrolysis 1,

probably due to using only a small sample of supernatant. The 8,8'-DiFA (AT) was present in all the samples from TFA Hydrolyses 2 and 3.

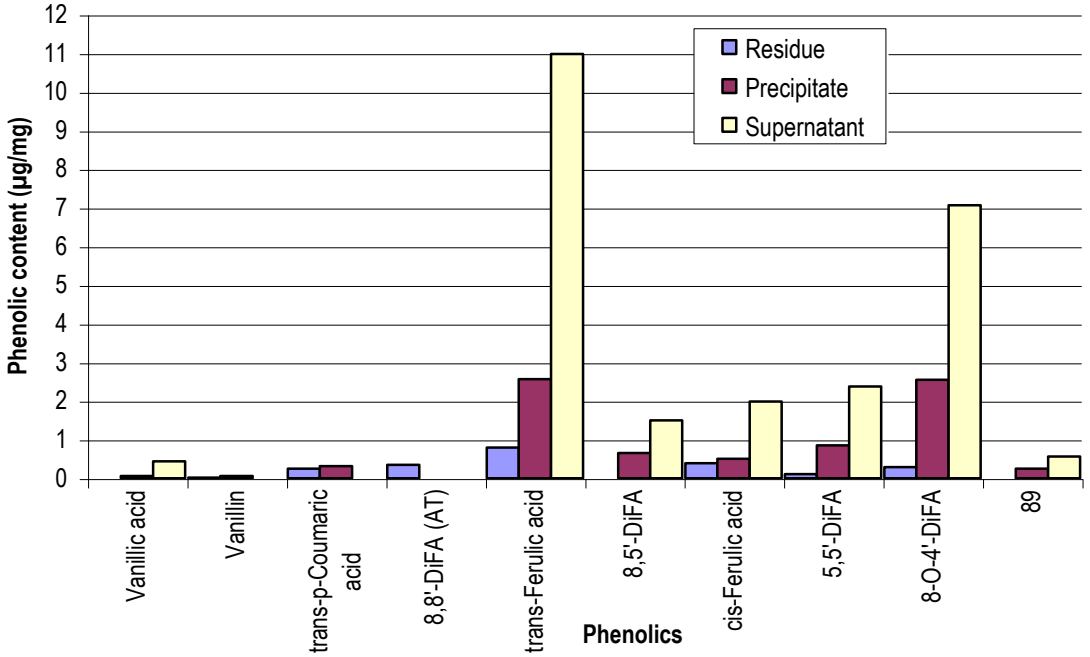

Figure 70: Phenolics in residue, precipitate and supernatant of TFA Hydrolysis 1 (values are averages of two (residue and supernatant) or three (precipitate) determinations).

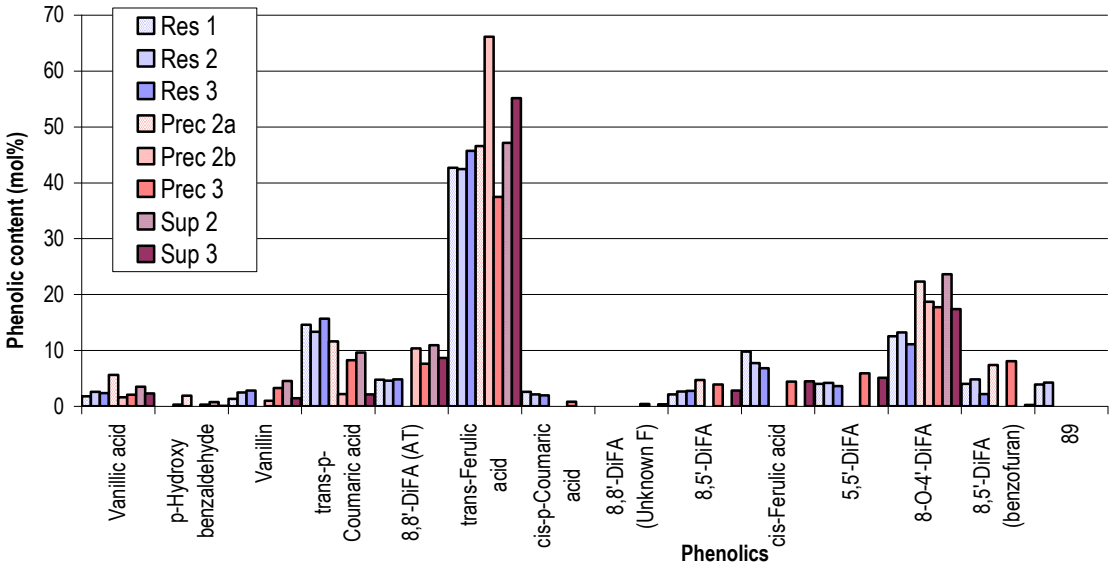

Figure 71: Phenolics in residue, precipitate and supernatants of TFA Hydrolyses 2 and 3.

The supernatants contained a complex mixture of known phenolics, so the separation on Biogel-P2 would hopefully be the stage at which the phenolic-polysaccharide fragments would begin to be purified.

7.1.3 Separation of supernatant components by column chromatography

The supernatant was defrosted and made up to 2 ml (Hydrolysis 1) or 5 ml (Hydrolysis 2) with deionised water, and applied to a column (2.6 cm x 90 cm) filled with Biogel P-2 in aliquots of 200 or 500 µl. Due to dead volumes in the syringe filters and sample loops, only 1.2 or 2.5 ml was actually injected onto the column. The significant increase in back pressure experienced when injecting the solution onto the column showed that at least some of the material was not in solution as the filter was getting blocked. Elution was with deionised water at 0.42 ml/min, monitoring was by UV detector at 280 nm (see Appendix G for original chromatograms). An automated fraction collector was used to collect a set number of fractions for a set time each (Figure 72). A total of eight runs were carried out, three from the first TFA hydrolysis, five from the second TFA hydrolysis and none from the third.

	Run 1	Run 2	Run 3	Run 4	Run 5	Run 6	Run 7	Run 8
Supernatant vol (ml)	0.2	0.5	0.5	0.5	0.5	0.5	0.5	0.5
Fraction vol (ml)	14.7	7.35	7.35	8.4	8.4	8.4	8.4	8.4
Fraction time (min)	35	17.5	17.5	20	20	20	20	20
No. of fractions	42	84	84	95	95	95	95	95
Total run time (min)	1470	1470	1470	1900	1900	1900	1900	1900
Total run time (hr)	24.5	24.5	24.5	31.7	31.7	31.7	31.7	31.7

Figure 72: Volumes of supernatant applied and fractions collected for Biogel P-2 runs.

7.2 Analysis of chromatography fractions to identify peaks and guide fraction recombination

Individual fractions did not contain enough phenolic-polysaccharide for the structural determination analyses, so the fractions were analysed to determine which fractions should be combined with each other.

7.2.1 UV absorption at 214, 280, 320 and 350 nm

Absorbances were measured using quartz cuvettes and a spectrophotometer fitted with a cell changer. Initially every fraction was analysed, in later runs only the fractions collected during a peak, as indicated by the FPLC UV detector, were analysed. After each set of samples the cuvettes were rinsed with distilled water and 100% ethanol and left to dry.

7.2.2 Phenol-H_2SO_4 total sugars assay

This method was scaled down from the original put forward by Dubois *et al* (1956) for use on a microplate scale. In acid-washed culture tubes, 80 µl of sample/glucose standard was combined with 2 µl of 80% (w/v) phenol solution and 200 µl of 96% (w/v) H_2SO_4. To ensure the reaction went to completion, the samples were vortexed and heated at 100°C for 10 min, and then cooled in an ice bath (Masuko *et al.*, 2005). The absorbance of 200 µl of the resulting solutions was measured at 490 nm using a Molecular Devices microplate reader (Sunnyvale, California). This method is not quantitative when a mixture of sugars is being analysed due to the variation in colour response between different sugars.

7.2.3 Folin-Ciocalteu total phenolic assay

In 1.5 ml microtubes, 625 µl of sample/ferulic acid standard was combined with 625 µl of Folin-Ciocalteu reagent (diluted to 1.0 N acid from supplied 2.0 N acid solution; Sigma-Aldrich, Dorset, UK). The samples were incubated at room temperature for 3 min, 125 µl of saturated Na_2CO_3 solution was added, and then the samples were incubated at room temperature for 1 hr. The microtubes were centrifuged (Heraeus Biofuge Fresco; Thermo Scientific, Waltham. Massachusetts) at 13000 rpm for 5 min to sediment any precipitate, and then the absorbance of 200 µl of supernatant was measured at 750 nm, using a microplate reader. This method measures the reducing capacity of a sample and is therefore not specific for phenol groups; it is less suitable for complex samples (Huang *et al.*, 2005), particularly those containing protein, as the procedure was developed from a protein assay (Singleton *et al.*, 1998). However, in these samples, it is unlikely that there are significant amounts of interfering compounds.

7.2.4 Results for Run 1

Measurements of total sugars, total phenolics and absorbance at 280 nm were compared for all fractions of Run 1 (Figure 73). Some of the sugar peaks were not coincident with a phenolic peak, implying that the phenolics were only attached to certain oligosaccharides.

Fractions (7-9, 21 and 23-26) were selected for 1 M H_2SO_4 sugars analysis; the results showed that only arabinose, xylose and galactose were present (Figure 74). Fraction 9 appeared to contain no sugar whatsoever. Of the fractions that did contain sugars, Fractions 7, 8 and 21 contained only xylose, Fraction 23 contained xylose and galactose, Fraction 26 contained arabinose and xylose and Fractions 24 and 25 contained all three sugars.

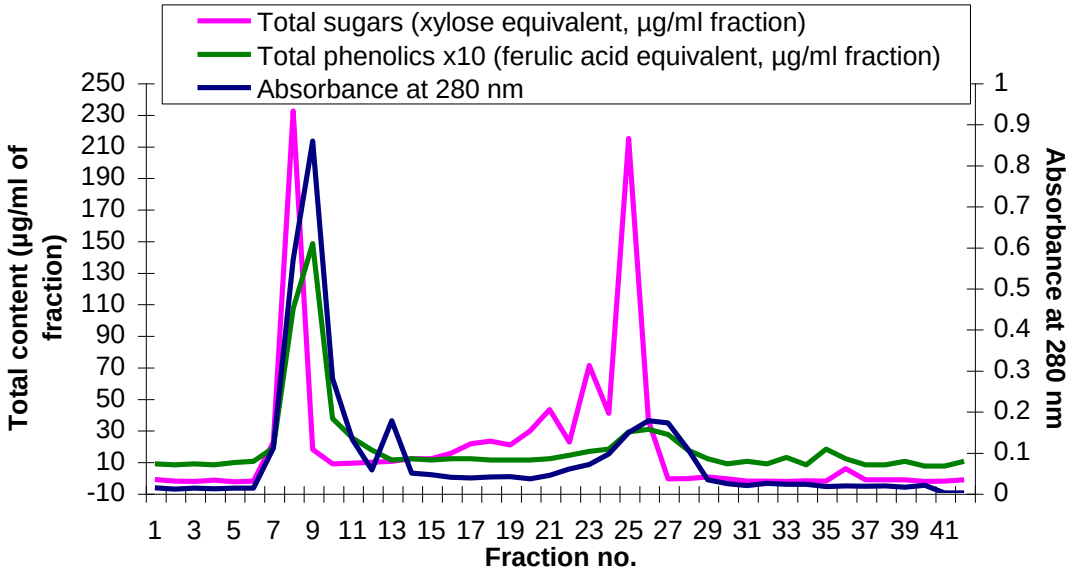

Figure 73: Comparison of total phenolics, total sugars and absorbance data for Run 1 (total phenolics as ferulic acid equivalents x10, total sugars as xylose equivalents).

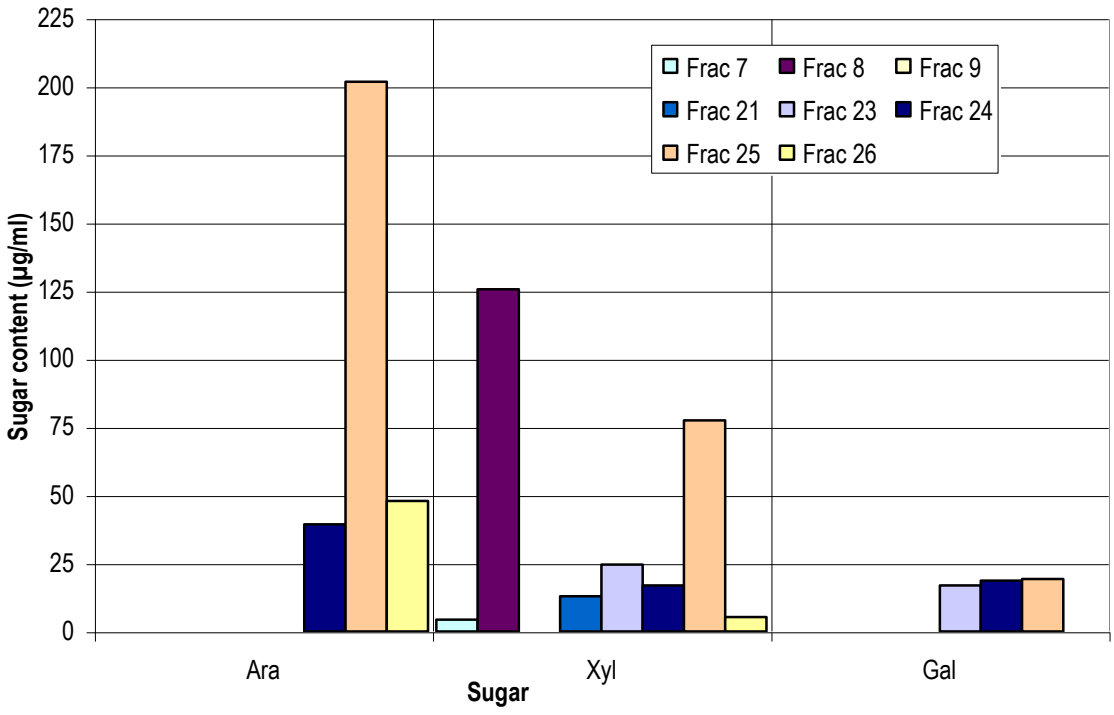

Figure 74: 1 M H_2SO_4 sugars results for selected fractions from Run 1 (values are averages from two determinations).

Selected Fractions (8-10, 14, 25-27, 33 and 35) had phenolics analysis carried out; the results showed that *p*-hydroxybenzaldehyde was the predominant phenolic detected; however the errors for *p*-hydroxybenzaldehyde were very large, implying that it came from an external source (Figure 75). *Cis* and *trans*-ferulic acid were found in Fractions 8, 9, 14, 25 and 26. Diferulic acids were found in Fractions 8 and 9. Vanillin was found in Fractions 9, 10 and 27.

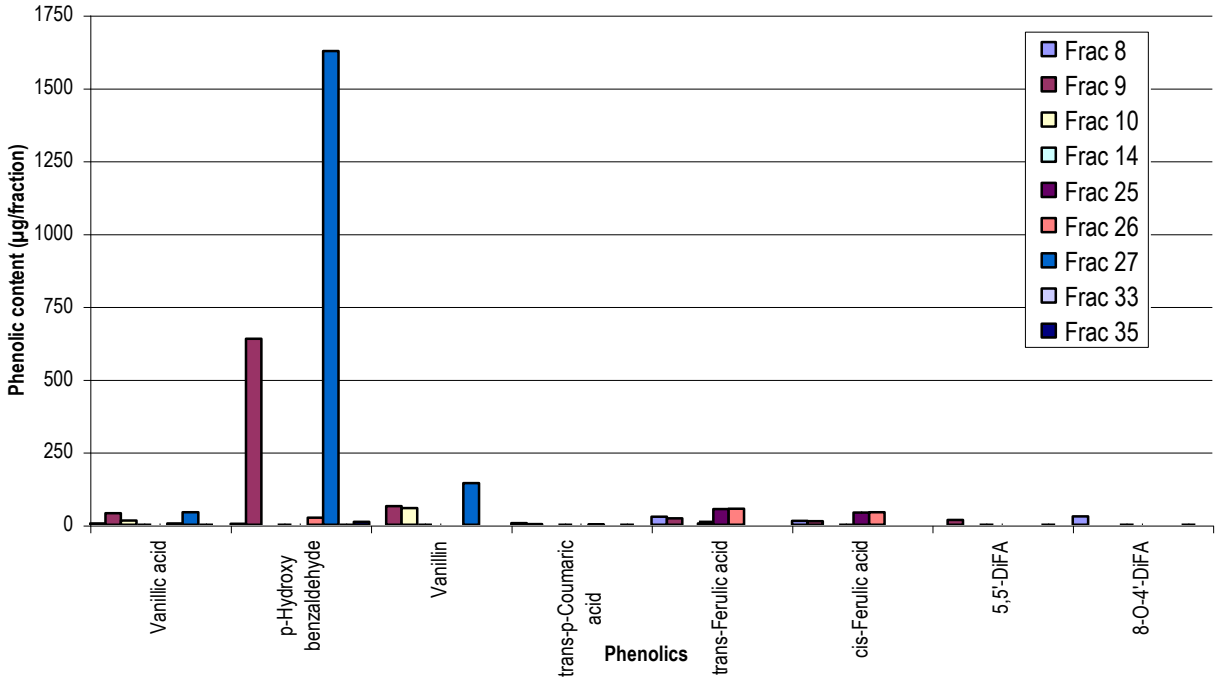

Figure 75: Phenolics results for selected fractions from Run 1 (values are averages of two determinations).

The phenolics and sugars results were not consistent, so were of little help when trying to decide which fractions to combine, so the absorbance measurements were used.

7.2.5 Results of absorbance measurements

The graphs of the absorbance at 320 nm for the fractions from Runs 4-6 are shown in Figure 76. The graphs of the absorbances at 214, 280 and 350 nm were very similar graphs to that for 320 nm.

The fractions with an absorbance above 0.025 (UV Peak 1), 0.110 (UV Peak 2), 0.044 (UV Peak 3) and 0.030 A (UV Peak 4) at 320 nm were combined into two sets of four “Peaks”, one set from Runs 4-6 and one set from Runs 7 and 8 (for full details of which fractions were combined see the colour-coded spreadsheet in Appendix H).

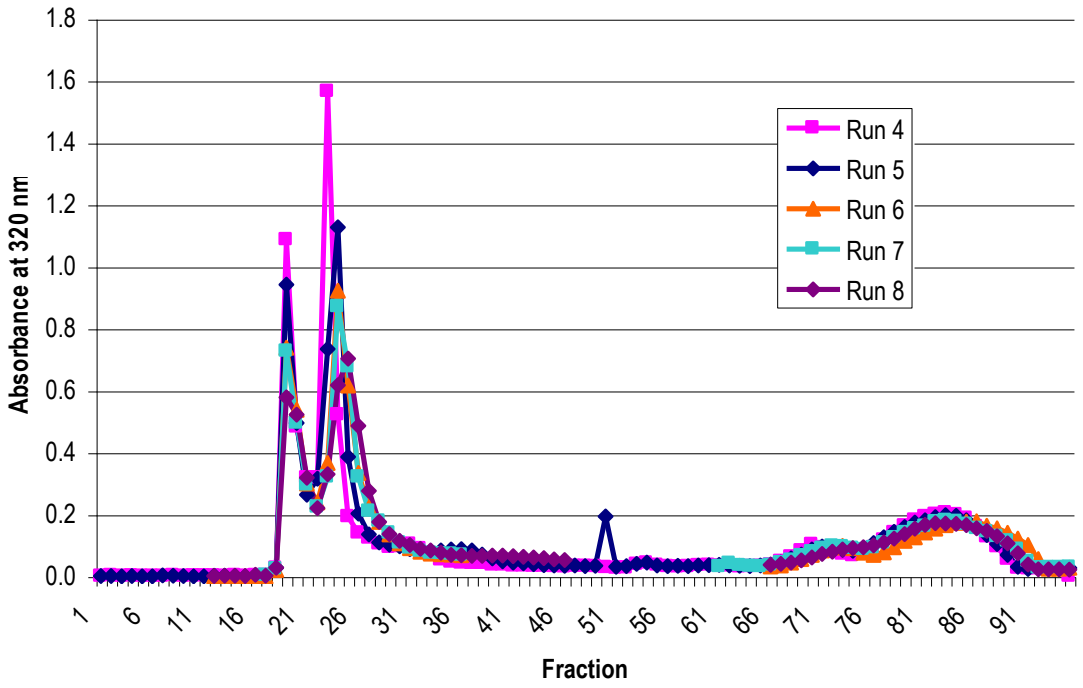

Figure 76: Absorbance of Biogel P-2 fractions at 320 nm (Runs 4-8).

These combined fractions will be referred to as Peaks 1-8 and the fractions that were not UV-fluorescent are Peaks 9-11 (the numbering of these peaks is not intuitive; please refer to Figure 66 for details). All Peaks were concentrated under vacuum and then freeze-dried. The freeze-dried samples were removed and weighed (Set b), but a relatively large amount adhered to the round-bottomed flasks they had been freeze-dried in, so the flasks were rinsed with small volumes of water, transferred to small vials and then freeze-dried again (Set a). The yields were greatest for the non-UV Peaks 9-11. Peaks 1 and 2 gave the next greatest yield, followed by Peaks 4 and 5.

7.3 Characterisation of peaks

Analysis of some of the peaks was hampered by the sticky texture and small amount of sample. Because the samples were sticky they had to be weighed directly into culture tubes, meaning the balance did not register the small masses accurately; this necessitated the use of mol% rather than µg/mg for the reporting of the results. The peaks were analysed for phenolic and sugar content, and by methylation analysis, but the standard methods were scaled down due to sample size.

7.3.1 Thin-layer chromatography

Thin-layer chromatography (TLC) was carried out on 20 x 20 cm aluminium-backed silica-gel (60 F_{254}) plates using chloroform:acetic acid (99.8%):water (6:7:1 v:v:v) as eluent and Marshal's reagent as developer (Figure 77). Marshal's reagent was produced by boiling 200 ml EtOH, 20 ml conc. H_2SO_4 and 1.8 g N-(1-naphthyl)ethylenediamine dihydrochloride together; the resulting solution was mixed carefully and stored in a dark place (Bounias, 1980).

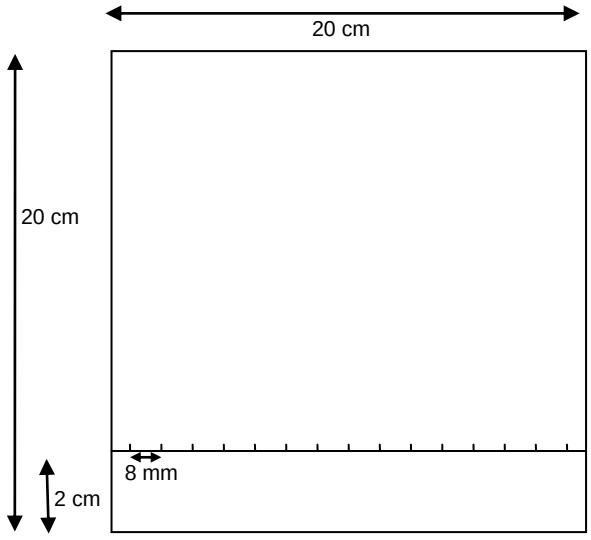

Figure 77: Diagram of TLC-plate layout.

The standards used were: Glc, Man, Ara and GalA or GlcA (10 mM) and a mixture of xylose, xylobiose, xylotriose, xylotetraose and xylopentose (40 mM) combined in the ratio (5:4:3:2:1) to give a final concentration of 8 mM. The plates were eluted for 2 x 6 hr and then allowed to dry before developer was applied in one smooth movement. The plate was allowed to drip dry for a few minutes before developing the colour in an oven at 95-105°C for 5-10 min. The plate was removed at the point at which there was some colour distinction between the hexoses and pentoses. Developed plates were then scanned in colour at 600 dpi. The freshness of the developer made a significant difference to the quality of the resulting TLC; the developer had been freshly made in Figure 78 resulting in stronger colours and clearer spots than if old developer was used (not shown). When fresh developer was used there were obvious differences in colour between the uronic acids (orange/brown), hexoses (pink/purple) and pentoses (blue/purple).

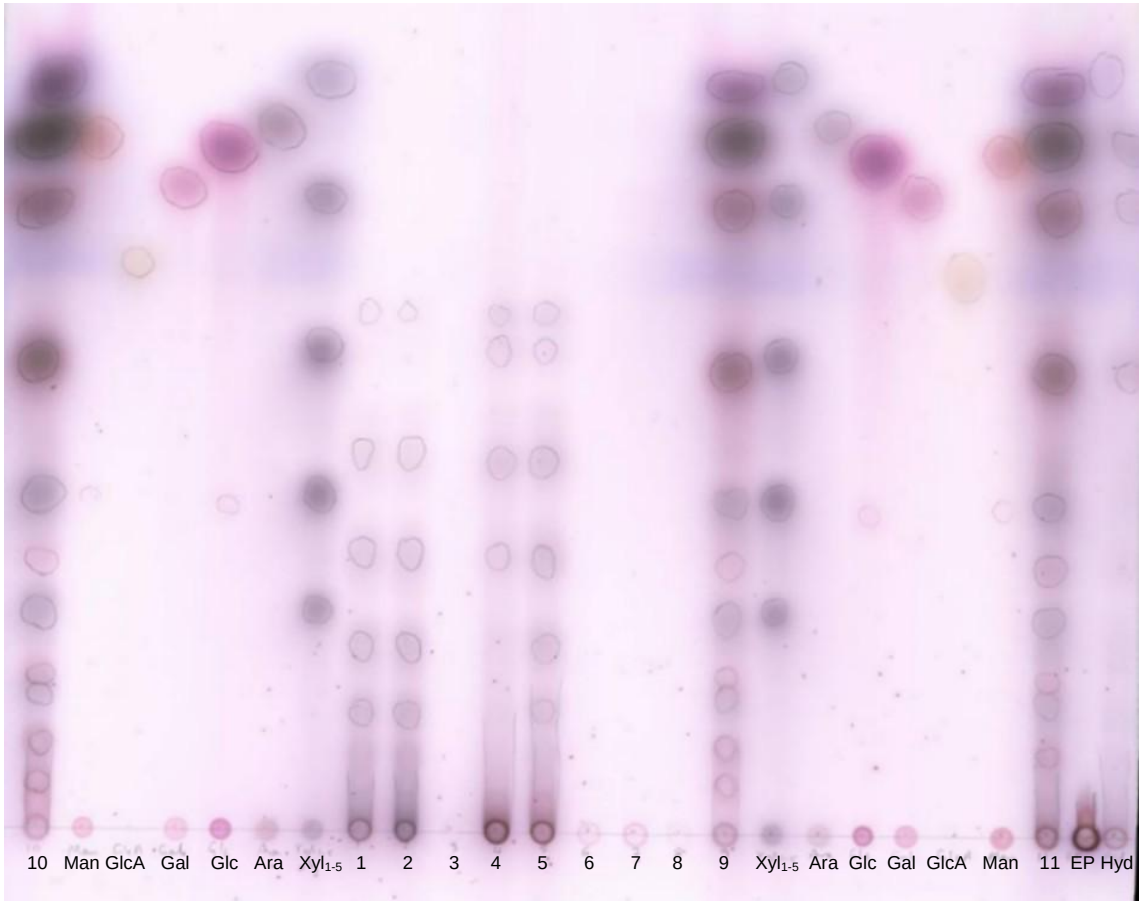

Figure 78: TLC plate showing standards, combined peaks and residues from the second TFA hydrolysis, with perceived spots marked in pencil.

Peaks 1, 2, 4 and 5 appeared to contain relatively high-molecular-weight polysaccharides, which judging from the colours of the spots, were probably predominantly pentoses. Peaks 3, 6, 7 and 8 gave no detectable spots, but they had very low yields generally. Peaks 9, 10 and 11 appeared to have high concentrations of sugars and a number of different sugar residues; as these were the combined non-UV fractions, there were obviously a lot of oligosaccharides that did not have a phenolic attached to them.

7.3.2 Carbohydrate composition and linkage analysis of peaks

The sugar composition (72% (w/w) H_2SO_4) of the peaks was analysed, and the results are given in Figure 79. The data are organised so that the two peak samples that came from the same UV peak across Runs 4 to 8 are adjacent to each other. The sugars of Peaks 1 and 2 were essentially xylose, with a little arabinose. The sugars for Peaks 4 and 5 were a mixture of xylose, arabinose, galactose and glucose. The sugars for Peaks 3 and 6 were a mixture of arabinose, glucose, xylose, galactose and rhamnose. The sugars for Peaks 7 and 8 were mainly arabinose and glucose, with some galactose, xylose and rhamnose. The sugars for Peaks 9, 10 and 11 were arabinose, xylose and galactose.

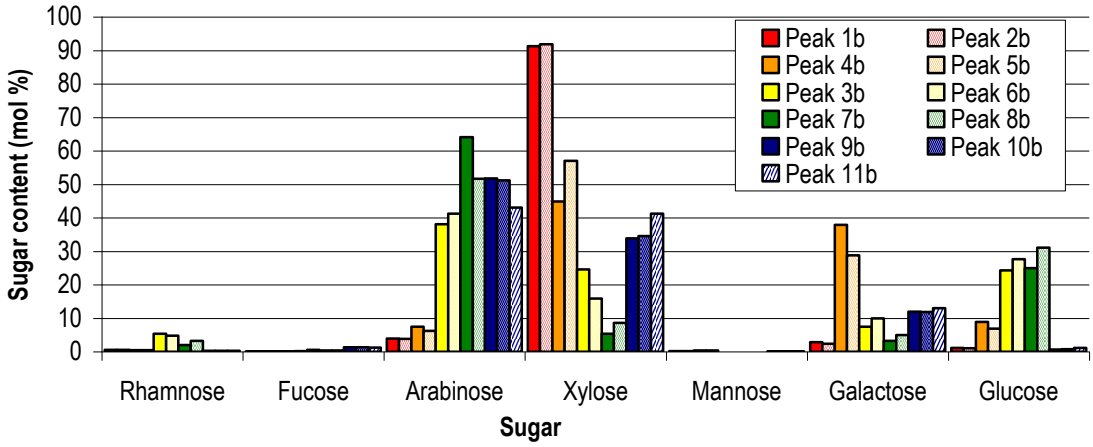

Figure 79: Sugars results for Peaks 1-11 (Set b – larger of the two samples retrieved for each peak, see §7.2.5 for explanation).

Methylation analysis of the peaks was done using the lithium dimsyl method with carboxyl reduction and the results are presented in Figures 80 and 81.

Peak 2 contained xylans, but it also contained some galacturonic acid, even though the majority of the pectins were precipitated in 80% ethanol. Peaks 4 and 5 consisted of xylan, galactan and xyloglucan and possibly some arabinan. Peaks 3 and 6 consisted of arabinoxylan, xyloglucan and possibly some arabinan. Peaks 7 and 8 contained (arabino)xylans and possibly some xyloglucan.

		Peak 4	Peak 4*	Peak 6	Peak 6*	Peak 7	Peak 7*
SUGAR	LINKAGE	Mol%	Mol%	Mol%	Mol%	Mol%	Mol%
Fuc	t-					0.2	
Ara-f	t-					5.9	
Ara-f	(1-3)					0.8	
Ara-f	(1-5)		5.9			1.0	
Ara-p	unmeth.				11.7	0.4	
Xyl	t-	9.7	4.0			3.2	
Xyl	(1-4)	44.0	35.6	18.6	13.0	7.2	58.7
Xyl	(1-3,4)					58.4	
Xyl	(1-2,4)					0.4	
Xyl	unmeth.				24.8	0.5	
Man	(1-4)					0.3	
Gal	t-	4.1			0.4	0.1	8.9
Gal	(1-6)		2.5				
Gal	(1-4)	25.3	27.4				
Gal	(1-4,6)	8.4	7.0				
Gal	(1-3,6)					0.1	
Gal	unmeth.		3.7			1.9	
Glc	(1-4)	4.2	5.4	49.9		1.1	
Glc	(1-4,6)	4.3				2.3	
Glc	unmeth.		8.5	31.5	50.2	16.2	32.5

* carboxyl reduction was carried out, t- indicates a terminal sugar residue, -f indicates a furanose ring structure, -p indicates a pyranose ring structure, unmeth. indicates sugar was not methylated

Figure 80: Methylation-analysis data for Peaks 4, 6 and 7.

Although arabinose is present in all the samples according to the sugars analysis, it does not appear to be present to the same extent in the methylation analysis. As ferulic acid is usually esterified to arabinose, perhaps it is interfering with the methylation reaction (Ishii, 1997).

		Peak 2	Peak 2*	Peak 5	Peak 5*	Peak 3	Peak 3*	Peak 8	Peak 8*
SUGAR	LINKAGE	Mol%	Mol%	Mol%	Mol%	Mol%	Mol%	Mol%	Mol%
Fuc	t-					0.5			
Ara-f	t-	0.9				11.1			
Ara-f	(1-3)					1.5			
Ara-f	(1-5)	0.9		1.2	1.2	4.2			
Ara-p	unmeth.					0.9			
Xyl	t-	12.3	3.8	3.6	5.5	6.4		12.6	
Xyl	(1-4)	76.3	55.4	51.0	42.3	16.9	5.4	62.7	18.2
Xyl	(1-3)	0.6			1.3				
Xyl	(1-3,4)	3.7	7.4			11.8		2.0	
Xyl	(1-2,4)	2.8	6.5		1.4			0.9	
Xyl	unmeth.	1.1	5.5		3.3	0.9			
Man	(1-4)					0.8			
Gal	t-			1.7	1.4	0.4			1.4
Gal	(1-6)	0.3		1.8	0.9				
Gal	(1-4)			22.9	25.7	0.2		1.4	
Gal	(1-2)		3.6			0.2			
Gal	(1-4,6)			7.6	6.1	0.5			
Gal	unmeth.				3.4	3.6	15.9		
GalA	(1-4)		11.4						
GalA	(1-4,6)		2.4						
Glc	(1-4)	0.3		3.6	2.0	2.1			
Glc	(1-4,6)	0.4	1.4	5.1	3.6	4.4			
Glc	(1-2,4)			0.2					
Glc	unmeth.	0.6	2.6	1.3	2.0	33.8	78.7	20.5	80.4

* carboxyl reduction was carried out, t- indicates a terminal sugar residue, -f indicates a furanose ring structure, -p indicates a pyranose ring structure, unmeth. indicates sugar was not methylated

Figure 81: Methylation-analysis data for Peaks 2, 5, 3 and 8.

7.3.3 Phenolic composition

Comparing the phenolic acid data for equivalent peaks, the data are generally consistent (Figure 82). Occasionally, the phenolics present in lower concentrations were not detected in both equivalent peaks; this may have been due to the small sample size. *trans*-Ferulic acid was always present and 8,8'-DiFA (AT) and 8-*O*-4' DiFA were also detected in most of the peaks.

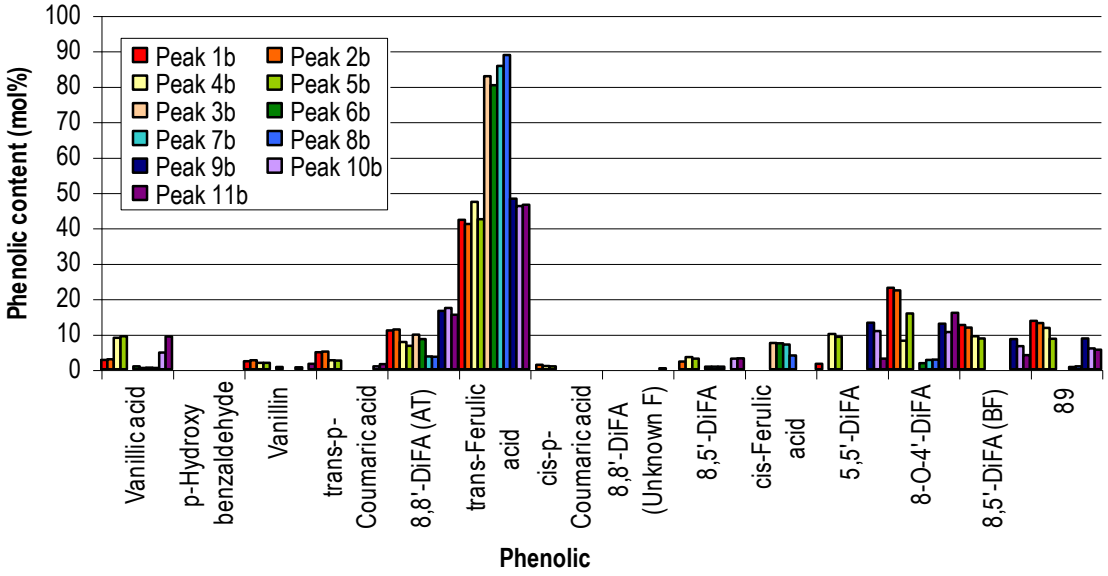

Figure 82: Phenolics in Peaks 1-11 (Set b – larger of the two samples retrieved for each peak, see §7.2.5 for explanation).

Peaks 1 and 2 probably have ferulic acid, 8-*O*-4'-DiFA, 8,5'-DiFA (BF) and 8,8'-DiFA (AT) esterified via single arabinose residues to xylan oligosaccharides. Peaks 4 and 5 may have ferulic acid, dimers and possibly vanillic acid esterified to oligosaccharides of xylan, galactan and xyloglucan via arabinose. Peaks 3 and 6 contained ferulic acid and 8,8'-DiFA (AT), possibly esterified to oligosaccharides of arabinoxylan, xyloglucan and arabinan. Peaks 7 and 8 contained ferulic acid and 8,8'-DiFA (AT), possibly esterified to oligosaccharides of arabinoxylan.

7.4 LC-MS to detect phenolic-polysaccharide linkages

All of the fraction samples and a sample of TFA Hydrolysate 3 were dissolved in methanol:water (50:50 v:v) and run directly on the HPLC-MS (MicroToF). Residue 3 (~50 mg) and Precipitate 3 (~76 mg) were extracted in 10 and 15.2 ml of 4 M NaOH respectively, using a scaled-up version of the usual total phenolic extraction method from Section §2.3. Accurate-mass analysis was carried out on the MicroToF LC-MS as described in Section §8.3.2. It was hoped that purified samples of phenolic-oligosaccharides would be produced for NMR analysis; however there were problems with collection of the components after HPLC separation and these are described in Section §8.3.3.

7.4.1 Alkali extract of TFA/80%-ethanol precipitate

The chromatogram for the TFA/80%-ethanol precipitate showed an apparent plethora of ferulic acid trimers, when the m/z=579 ions were extracted (Figure 83). On careful inspection, using the accurate masses, not all of them were triferulic acids.

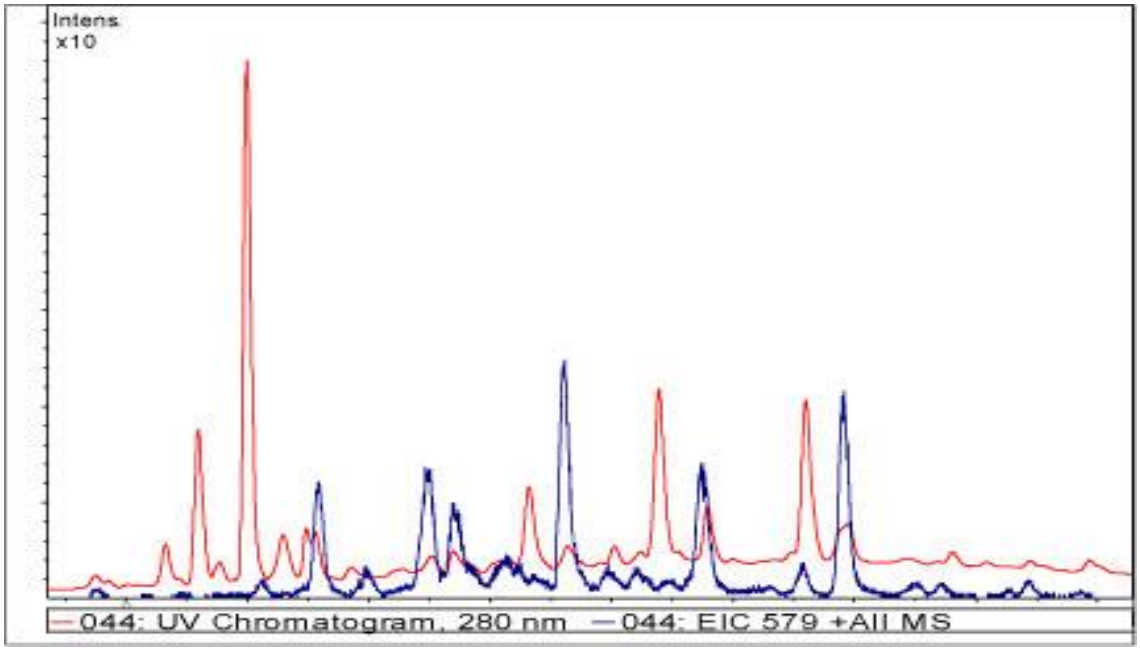

Figure 83: Total-ion and extracted-ion (m/z=579) chromatograms for TFA/80%-ethanol Precipitate 3, showing the large number of possible triferulic acids.

The TFA precipitate had a particularly clear 8,8'-DiFA (AT) spectrum (Figure 100, §8.4.4) because the *trans*-*p*-coumaric acid was not solubilised to the same degree as the ferulic acids. At least one tetramer and three trimers of ferulic acid were identified; their spectra are given in Section §8.4.4. One of the trimers elutes with 8,5'-DiFA and *cis*-ferulic acid, and so care should be taken, when assessing chromatograms, that the UV spectrum of a peak at the right relative retention time is the correct one.

7.4.2 TFA Hydrolysate 3

Figure 84 gives mass-spectrometric data for ferulic acid-arabinobiose and ferulic acid-galactobiose, to which the MS data from the hydrolysate and peaks were compared. The TIC and UV chromatograms of TFA-Hydrolysate 3 are shown in Figure 85. Assuming the pentoses indicated are all arabinose, three ferulic acid-arabinose fragments, one ferulic acid-arabinobiose fragment and six diferulic acid-arabinose fragments were detected in the hydrolysate (Figure 86). Interestingly there is no sign of any *p*-coumaric acid-pentose or DiFA-hexose fragments.

Compound	Characteristic Ions	Molecular weight	Molecular formula	Reference
FA-Ara-Ara	481 (M+Na)+ 459 (M+H)+, 497 (M+K)+, 309 (M-pentose)+, 177 (M-2 x pentose)+	458.1424	$C_{20}H_{26}O_{12}$	(Ishii and Tobita, 1993)
FA-Gal-Gal	541 (M+Na)+, 519 (M+H)+, 557 (M+K)+, 339 (M-hexose)+, 177 (M-2 x hexose)+	518.1636	$C_{22}H_{30}O_{14}$	(Ishii and Tobita, 1993)

Figure 84: MS data for some ferulic acid-polysaccharide fragments.

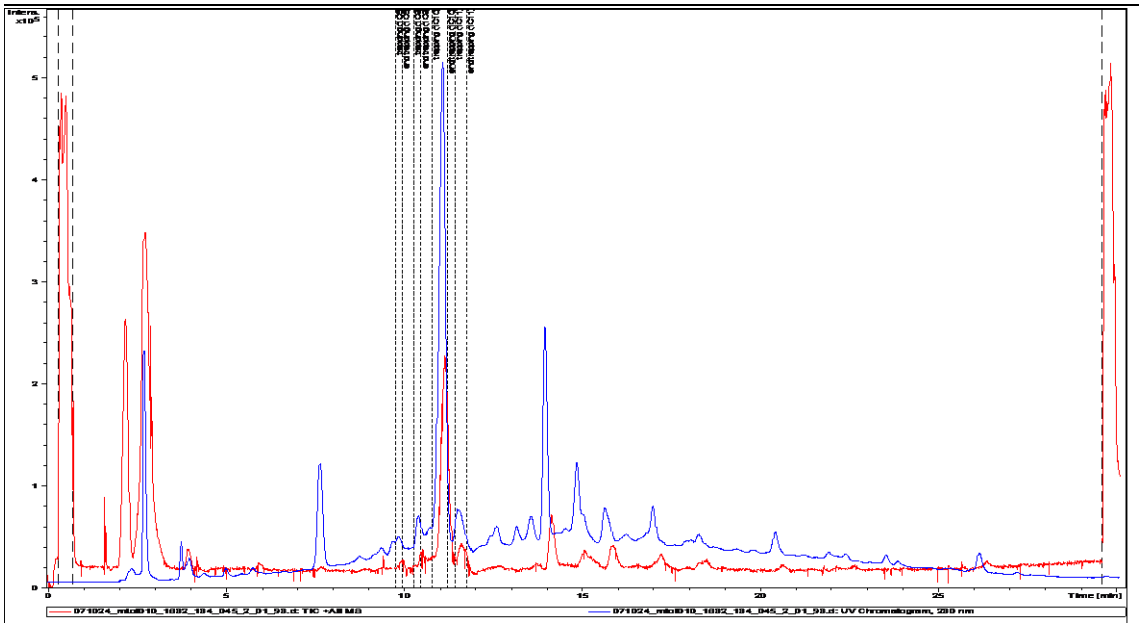

Figure 85: Total-ion and UV chromatograms for TFA-Hydrolysate 3.

Compound	Retention time	Masses	Molecular formula	Molecular weight
Ferulic acid-Ara	8.955	177, 309	$C_{15}H_{18}O_8$	326.1002
Ferulic acid-Ara-Ara	10.571	177, 309, 327, 441, 459, 481	$C_{20}H_{26}O_{12}$	458.1424
Ferulic acid-Ara	11.251	309, 177, 327, 349	$C_{15}H_{18}O_8$	326.1002
Ferulic acid-Ara	11.681	309, 177, 353	$C_{15}H_{18}O_8$	326.1002
DiFA-Ara	17.199	501, 541, 519	$C_{25}H_{26}O_{12}$	518.1424
DiFA-Ara	18.109	391, 501, 519, 369, 177	$C_{25}H_{26}O_{12}$	518.1424
DiFA-Ara	18.311	309, 177, 327, 441, 459, 481	$C_{25}H_{26}O_{12}$	518.1424
DiFA-Ara	18.461	385, 403, 519, 501, 541, 177	$C_{25}H_{26}O_{12}$	518.1424
DiFA-Ara	18.986	501, 519, 309	$C_{25}H_{26}O_{12}$	518.1424
DiFA-Ara	19.517	301, 501, 519	$C_{25}H_{26}O_{12}$	518.1424

Figure 86: The diferulic acid-arabinose fragments detected in TFA-Hydrolysate 3.

7.4.3 Alkali extract of TFA Residue 3

The total-ion and UV chromatograms for the TFA-Residue-3 alkali extract are given in Figure 87; the extracted-ion (m/z=579) chromatogram (Figure 88) showed a possible six triferulic acids. Analysis of the accurate mass ions

confirmed peaks for *trans*-ferulic acid, *trans-p*-coumaric acid, 8,8'-DiFA (AT), 8-*O*-4'-DiFA and one TriFA.

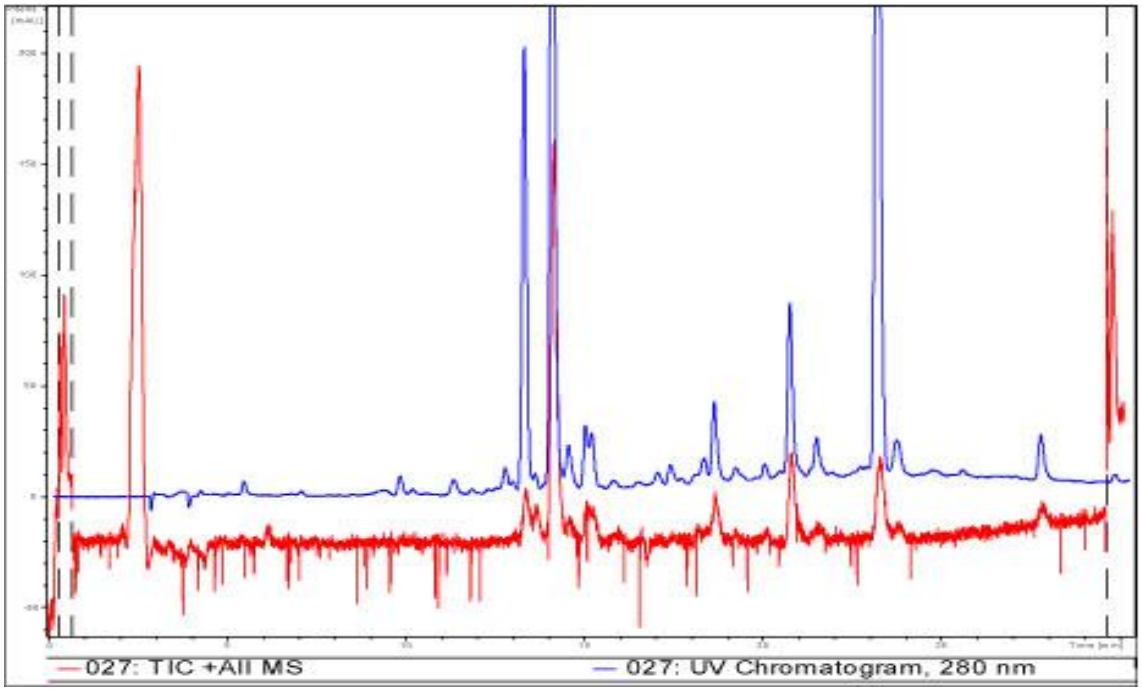

Figure 87: Total-ion and UV chromatograms for TFA-Residue-3 alkali extract.

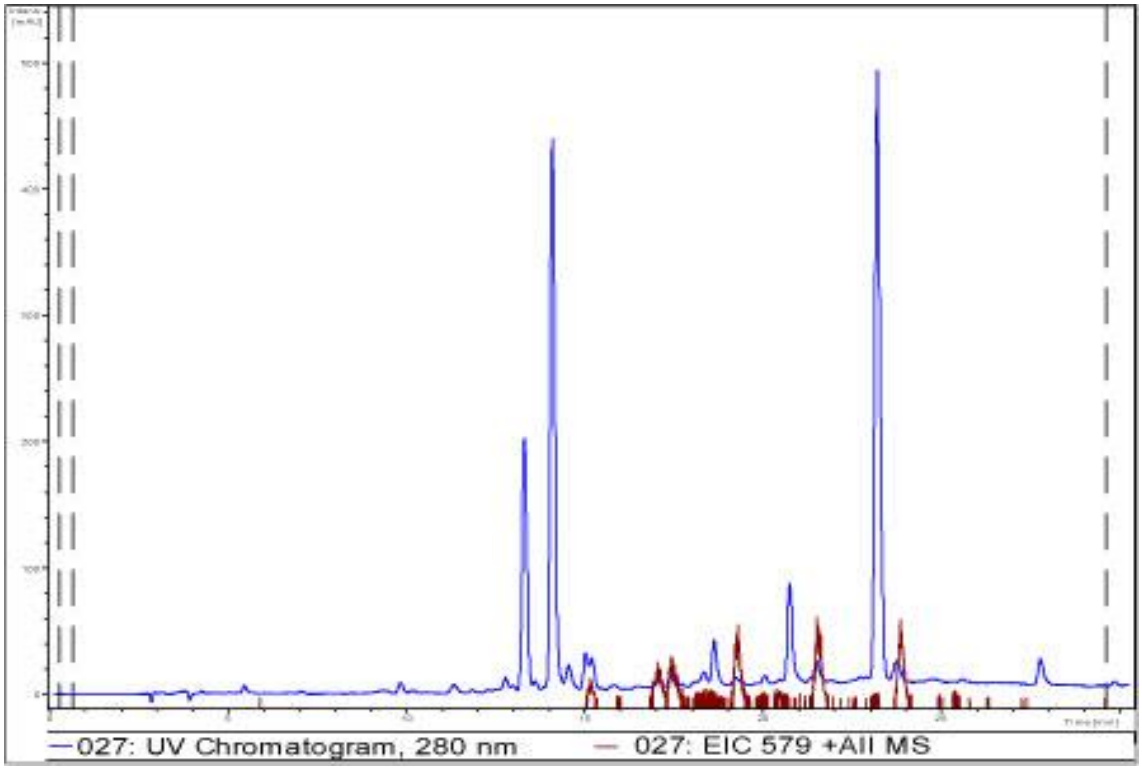

Figure 88: UV and extracted-ion (m/z=579) chromatograms for TFA-Residue-3 alkali extract.

7.4.4 Biogel P-2 chromatography peaks

Ferulic acids esterified to oligosaccharides were identified using the same fragmentation ions as those presented in Figure 86. Where pentoses were indicated by the fragmentation patterns, it has been assumed that they are arabinose. Of the Biogel P-2 peaks, Peaks 1, 2, 4 and 5 did not contain any detectable ferulic acid esterified to polysaccharides. Peaks 3, 6, 7 and 8 did contain ferulic acids: Peak 3 contained two ferulic acid-arabinobiose fragments (M_w = 458.1); Peak 6 contained two ferulic acid-arabinobiose fragments (M_w = 458.1) and a ferulic acid-arabinose fragment (M_w = 326.1); Peak 7 contained four ferulic acid-arabinose fragments (M_w = 326.1) and Peak 8 contained two ferulic acid-arabinobiose fragments (M_w = 458.1) and three ferulic acid-arabinose fragments (M_w = 326.1).

7.5 Discussion

The results of the vortex-induced cell separation (VICS) in 0.05 M TFA, as described in Section §3.2.4, indicated that the conditions used here for the digestion were not sufficient to produce significant cell separation. This may indicate that a more concentrated solution would have been more effective at producing the phenolic-polysaccharide fragments of interest. Looking at the VICS data, changing the length and temperature of the digestion may not make any difference; so changing the concentration of TFA is the next logical step. In future this could be tested by carrying out further VICS experiments. A two-step TFA hydrolysis of CWM, using 0.05 M TFA initially and 0.1 M TFA on the 0.05 M TFA hydrolysate, as described by Ralet *et al* (2005) could be employed, as there was a significant amount of polysaccharide precipitated by ethanol, indicating that not all the sugar was in the ideal size range for separation. A 0.1 M TFA hydrolysis could also be used on the ethanol precipitate and/or the residue.

The mass-spectrometric data indicated that there were a range of ferulic acid-polysaccharide linkages detected in the hydrolysate and Peaks 3, 6, 7 and 8. There were also six diferulic acid-arabinose fragments detected in the hydrolysate, but not the peaks.

Bunzel *et al* (2008) have recently shown that the 8,8'-DiFA (AT) is esterified to arabinose (Figure 89). They extracted 4.1 mg from 80 g of insoluble maize-bran fibre, so the amounts used in these experiments were therefore one or two orders of magnitude too small for this linkage to be identified.

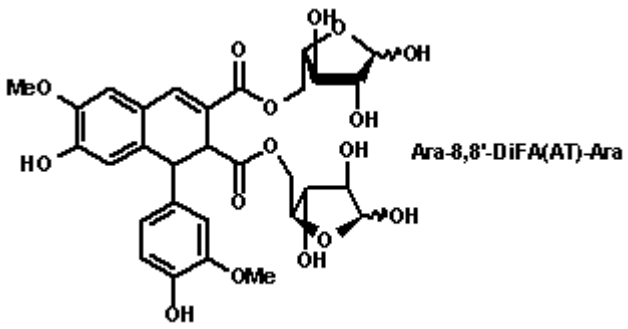

Figure 89: Structure of Ara-8,8'-DiFA (AT)-Ara as extracted from maize bran by Bunzel* et al *(2008).

8 MS and NMR of Selected Components of Chinese Water Chestnut Cell Walls:

The aim of the work in this chapter was to get the structural information via accurate mass spectrometry and NMR to determine the phenolic-polysaccharide linkages present in CWC cell walls and also to find and identify any higher oligomers of ferulic acid that may be present. In particular, the 8,8'-DiFA (AT) esterified to polysaccharide was sought in order to prove that CWC contained this linkage, lending support to the hypothesis that it plays a key part in the thermal stability of CWC mechanical properties (Parker *et al.*, 2003). Finding higher oligomers of ferulic acid in CWC would show that they are not restricted to maize or even the *Poaceae*. Assuming trimers were found by MS, it was hoped that their molecular structures could be elucidated by NMR.

8.1 Solid-phase-extraction theory

Solid-phase extraction of peaks resulting from liquid chromatography of a complex mixture is a relatively new technique that has allowed Exarchou *et al* to analyse in detail the secondary metabolites of oregano (Exarchou *et al.*, 2003). The main advantages of this method are:

The elution solvent can be different from the NMR solvent as the elution solvent is evaporated off before addition of the NMR solvent, reducing the volume of deuterated solvents required and allowing the most suitable solvents to be used for both stages.

Samples are concentrated as the volume of solvent required to elute the sample from the cartridge is often less than was used to apply it; the concentration can be further increased by using the same cartridges on multiple runs of the same sample, giving a substantial increase in sensitivity.

Although this is a new technique there has been a rapid take-up of the technology for studying crude alcohol extracts from plants (Christophoridou *et*

al., 2007; Exarchou *et al.*, 2003; Wang *et al.*, 2003). This appears to be the first study that has focused on cell-wall components.

8.2 Nuclear magnetic resonance (NMR) theory

Nuclear Magnetic Resonance (NMR) uses the magnetic properties of particular nuclei to give structural information about the molecule in question. Some nuclei have a nuclear spin (I) and the presence of a spin makes these nuclei behave like tiny bar magnets. Nuclei with an odd mass number have nuclear spins that are multiples of ½. In an applied magnetic field the nuclear magnets can align themselves in 2I + 1 ways. Both ^{1}H and ^{13}C have spins of ½; they can therefore only have two alignments, one aligned with the applied field (low energy) and one opposed to it (high energy). When a radio-frequency signal is applied to the system at the natural frequency at which they turn in the magnetic field, some of the nuclei are promoted from the low-energy state to the high-energy state. The frequencies are dependent on the size of the magnetic field, so for greater resolution powerful superconducting magnets cooled with liquid helium are used, allowing the higher operational frequencies (200-750 MHz) found in modern machines. Fourier-transform (FT)-style data acquisition gives a good signal to noise ratio from one pulse and is therefore quicker than the traditional continuous-wave (CW) method. Using the FT method allows the results from multiple pulses to be added together, further improving the signal to noise ratio; this is particularly useful for ^{13}C experiments. It is necessary to use solvents that do not contain ^{1}H; D_2O, CCl_4, and $CDCl_3$ are commonly used, and the choice is generally determined by the solubility of the target compound.

There are three main pieces of data for each NMR peak:
The area under the peak (integration) gives an indication of how many atoms are in that particular environment; this is particularly useful for proton spectra. The chemical shift (δ) is a field-independent measure of this phenomenon defined by the difference between the peak frequency and the frequency of the internal standard, TMS (tetramethylsilane), in Hz, divided by the operating frequency in MHz. It is expressed as fractions of the applied field in parts per

million (ppm). Chemical shift is plotted from right to left with the maximum values being 10 (for ^{1}H) and 200 (for ^{13}C). Minute differences in the magnetic environment of each nucleus, due to variations in electron density, slightly affect the frequency at which the nucleus comes into resonance, so each chemically distinct atom will give a separate peak in the spectrum. Nuclei in a high-electron-density region experience a field that is slightly weaker than those in a low-electron-density region, so bonding to an electronegative atom would shift the peak to the left, as it would withdraw electrons. The presence of π bonds and benzene rings can also significantly affect the chemical shift. A proton has two possible spin states, so a ^{13}C atom bonded to a proton will experience two slightly different magnetic fields. There is a very small energy difference between these two states, so they are essentially equally likely; this gives rise to a doublet peak as the two states have slightly different resonance frequencies. The separation between the two peaks is called the coupling constant, J; when there is only one bond between the carbon and hydrogen, it is properly labelled as $^{1}J_{CH}$. If there were two protons, they would both split the peak twice, giving four peaks, but as the coupling constant is the same, two of the peaks overlap to give the central peak, which has double the intensity of the other two. Three protons would give four peaks with the intensity ratio 1:3:3:1. Similarly, four protons would give five peaks with the intensity ratio 1:4:6:4:1. Proton-decoupled ^{13}C spectra have this effect cancelled by irradiating the sample with a strong signal covering the frequencies normally used for measuring proton spectra. The coupling constant can provide useful structural information in proton spectra, as the size of the coupling constant can give an indication of how the protons are linked to each other.

8.3 Methods

8.3.1 Scale-up of phenolic extraction of CWM

To get a good result from the NMR experiments approximately 1 mg of the pure compound is required. From previous experiments it was clear that a large

amount of CWM would need to be extracted in order to get the required amount.

PCWM (1.91 g, Batch 2), ECWM (1.54 g, Batch 1) and SECWM (1.89 g, Batch 1) were measured into 1 L conical flasks and mixed with degassed 4 M NaOH to give a final concentration of 5 mg CWM per ml of solution (this is the same as the initial total phenolic extraction). They were wrapped in foil and extracted for 24 hr. Solutions were filtered through GFC and 200 µl of *trans*-cinnamic acid was added, before the solutions were acidified with concentrated HCl. The acidified solutions were then extracted against 3 x 200 ml ethyl acetate. The ethyl acetate fractions were evaporated under vacuum at 40°C in a rotary evaporator and redissolved in 1.5 ml (ECWM) or 1 ml (PCWM and SECWM) MeOH:water (50:50 v:v).

8.3.2 LC-MS experiments

Reverse-phase HPLC combined with UV and ESI MS was carried out on the scaled-up alkali extracts of CWM. This was done in collaboration with Mark Philo. The HPLC system (Agilent Binary HP1100) was connected via a Bruker NMR-MS interface to an Agilent G1315B DAD detector, a Bruker Daltonics MicroToF and a Prospekt 2 solid-phase-extraction interface and dispenser. The HPLC column and method were the same as that used in the phenolic extractions. After the HPLC separation the outflow was split 1:20 (MS:UV) to avoid overloading the MS. The MS parameters are listed in Appendix I. Hystar 3.2, Hystar Postprocessing and AMDIS software were used to analyse the data. Internal calibration was provided by sodium formate at the beginning and end of each run. Both positive and negative ionisations were tested initially, but positive ionisation gave better results, so all the samples were tested in positive mode.

8.3.3 NMR experiments

Peaks of interest were identified from the MS and UV data of the samples. The samples containing interesting peaks were run again and the real-time UV and total-ion chromatograms were used to select peaks for collection manually (Figure 90). The peaks were collected on Hysphere GP 10-12 µm cartridges. The Hysphere GP cartridges were chosen for this experiment as they contain a good generic sorbent, which also has good elution efficiency (Bert Ooms *et al.*, 2000). After the cartridges were dried with dry N_2, they were eluted using 140 µl of deuterated acetonitrile (99.8%d, Cambridge Isotope Laboratories), transferred to 1.5 ml microtubes and frozen in a dry nitrogen atmosphere at –20°C to reduce contamination with protons until the NMR was available.

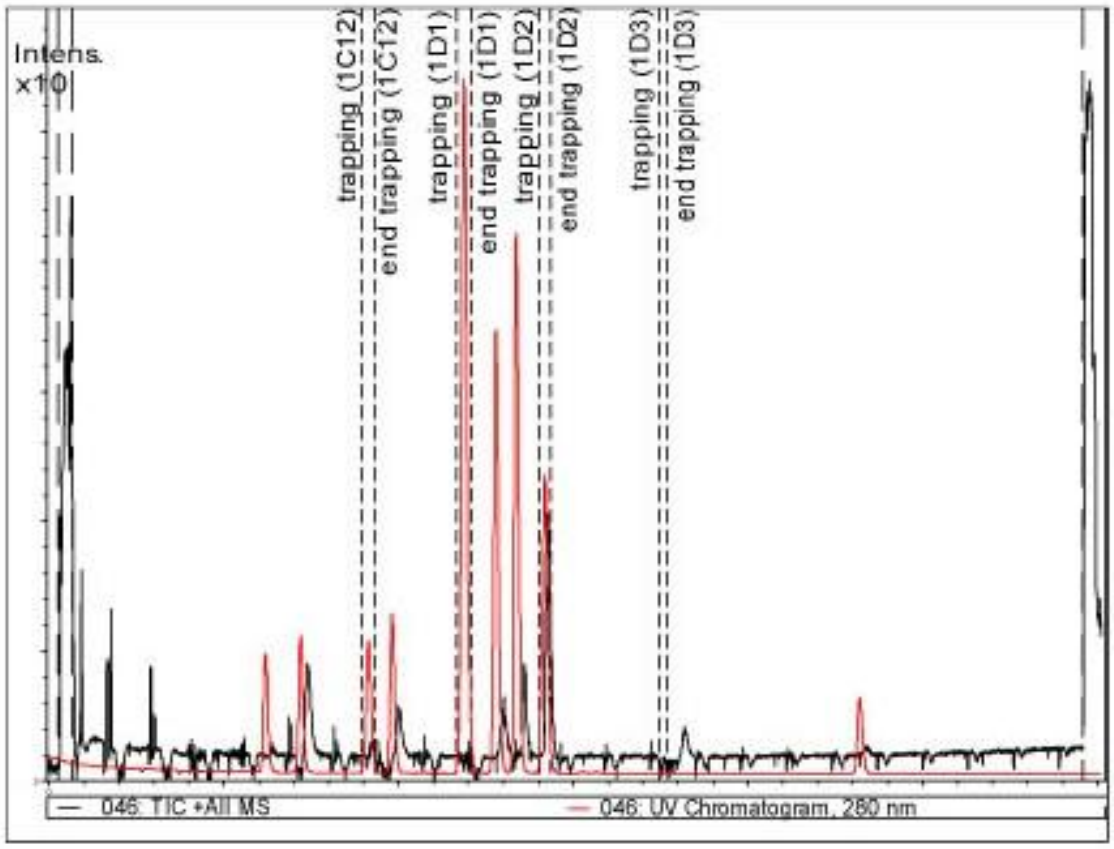

Figure 90: Example chromatogram showing manual peak collection of three peaks (1C12, 1D1, 1D2) and one blank (1D3).

Ian Colquhoun and Laetitia Shintu carried out the NMR experiments on a Bruker Avance NMR spectrometer, operating at 600.13 MHz for ^{1}H and equipped with a cryoprobe. Samples were transferred to 2 mm o.d. NMR tubes (Bruker MATCH system) and proton NMR was used to assess the viability of the collected samples for the full suite of NMR experiments (see Appendix J for details). Unfortunately it appears that none of the collected samples was present in sufficient quantity to get an unambiguous NMR spectrum. Figure 91 has the spectrum for a blank sample, taken from an apparently empty section of a standard run, and for a putatively identified ferulic acid-arabinose fragment. The spectra are very similar to each other, implying that there was some contamination from somewhere. As the cartridges had not been used previously, the contamination cannot come from them, so the likeliest answer is that the compounds were adsorbing to the tubing used in the transfer processes.

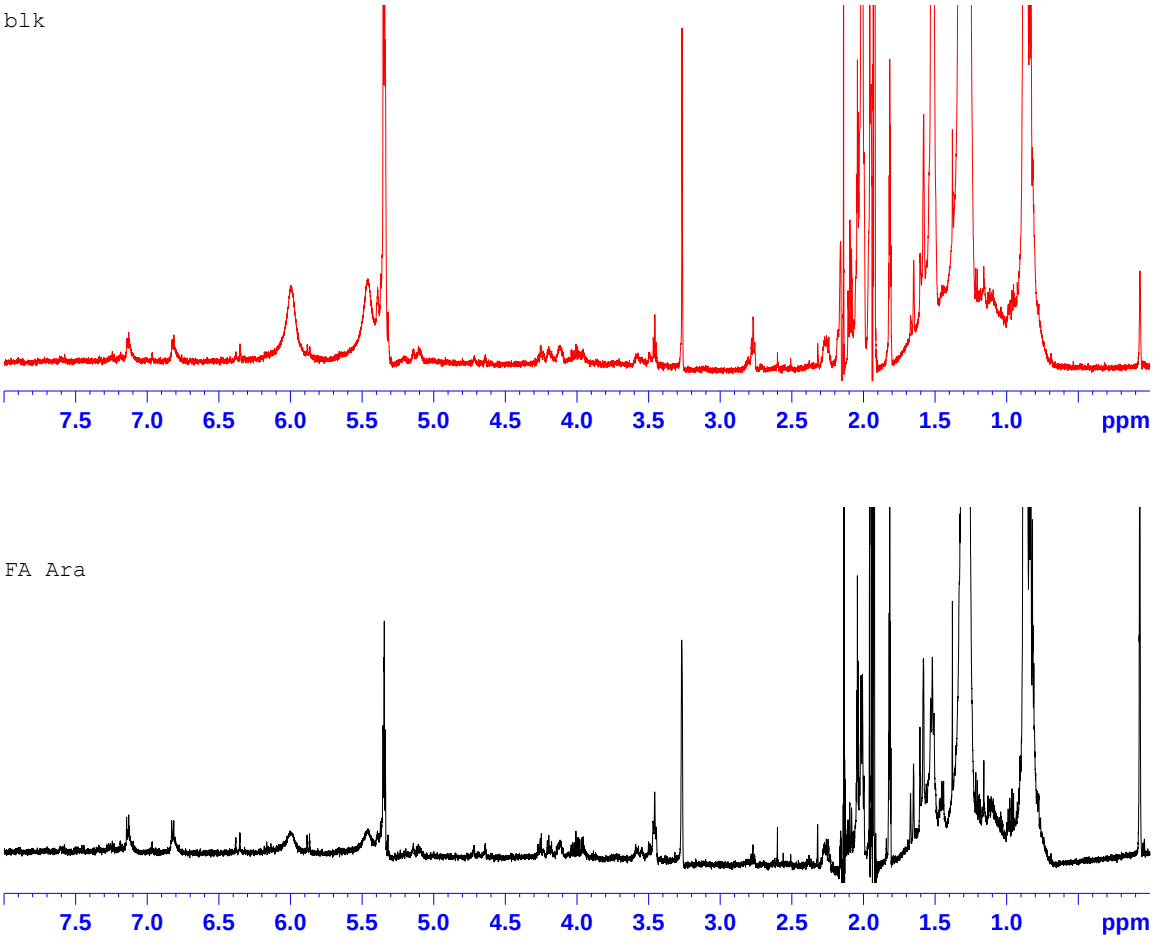

Figure 91: NMR spectra of blank and putatively-identified FA-Ara.

In addition it appears that not as much sample as possible was eluted onto the cartridges due to a timing error. The image of the UV peak appearing on the screen was used to determine when to start and stop collecting peaks; however, there is a delay-time built into the system to account for the transit time from the detector to the SPE unit. This time was set incorrectly and so some of the peak was not collected.

8.4 Molecules indicated by MS

For each sample, extracted-ion chromatograms were produced for the predicted fragment ions 165, 177, 195, 369, 387 and 579. Internal calibration (HPC calibration) was carried out using the sodium formate internal calibrant at either end of the chromatogram to correct the accurate molecular mass values (Figure 92).

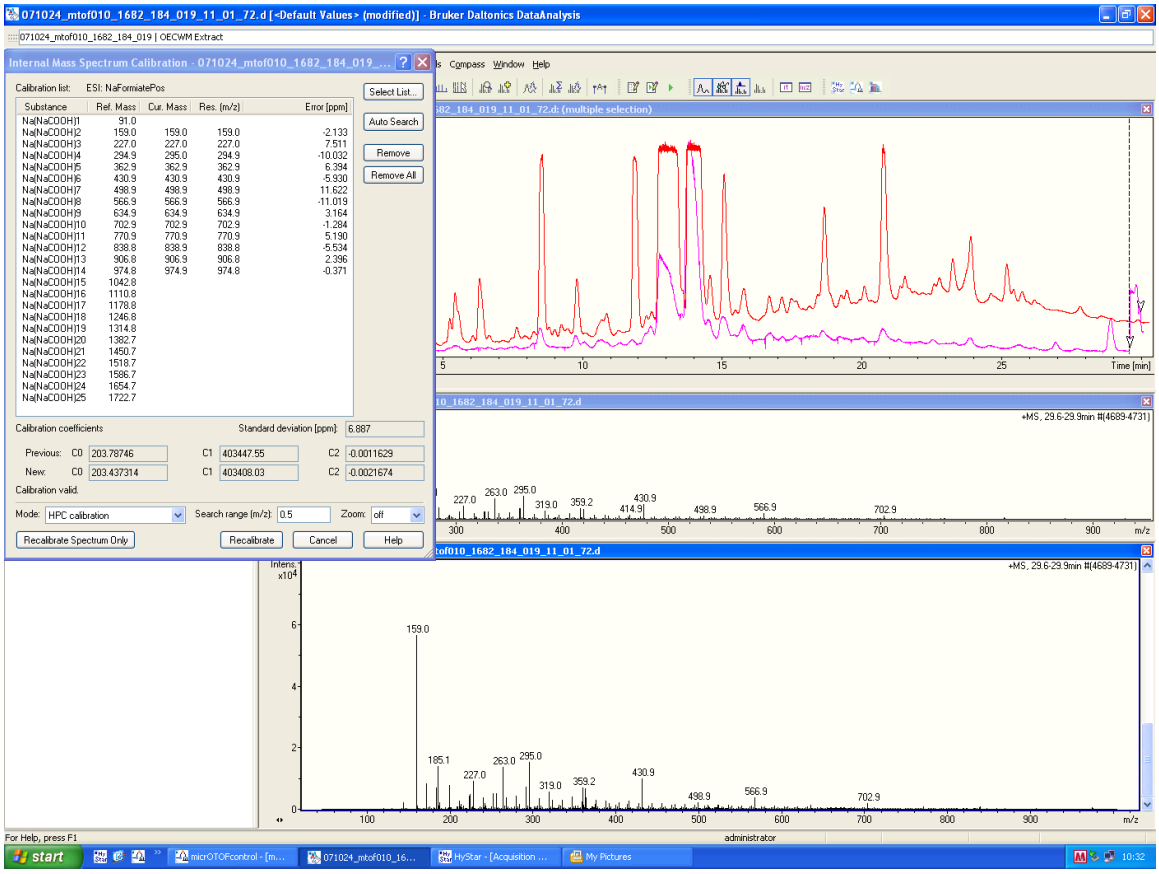

Figure 92: Example of HPC calibration using sodium formate as calibrant.

Selected peaks were averaged and background subtracted, and the accurate molecular masses indicated compared to theoretical values generated from the likely formulae. Figure 93 shows a typical analysis for ferulic acid. The program automatically includes carbon, hydrogen, nitrogen and oxygen in its predictions; nitrogen was excluded as the compounds of interest do not contain nitrogen; sodium was included, so that any quasimolecular $M+Na^+$ ions were detected. A 15 mDa error was generally used to limit the formulae produced, but for some of the samples the calibration was unsuccessful due to a software error, in which case it was increased to 30 mDa.

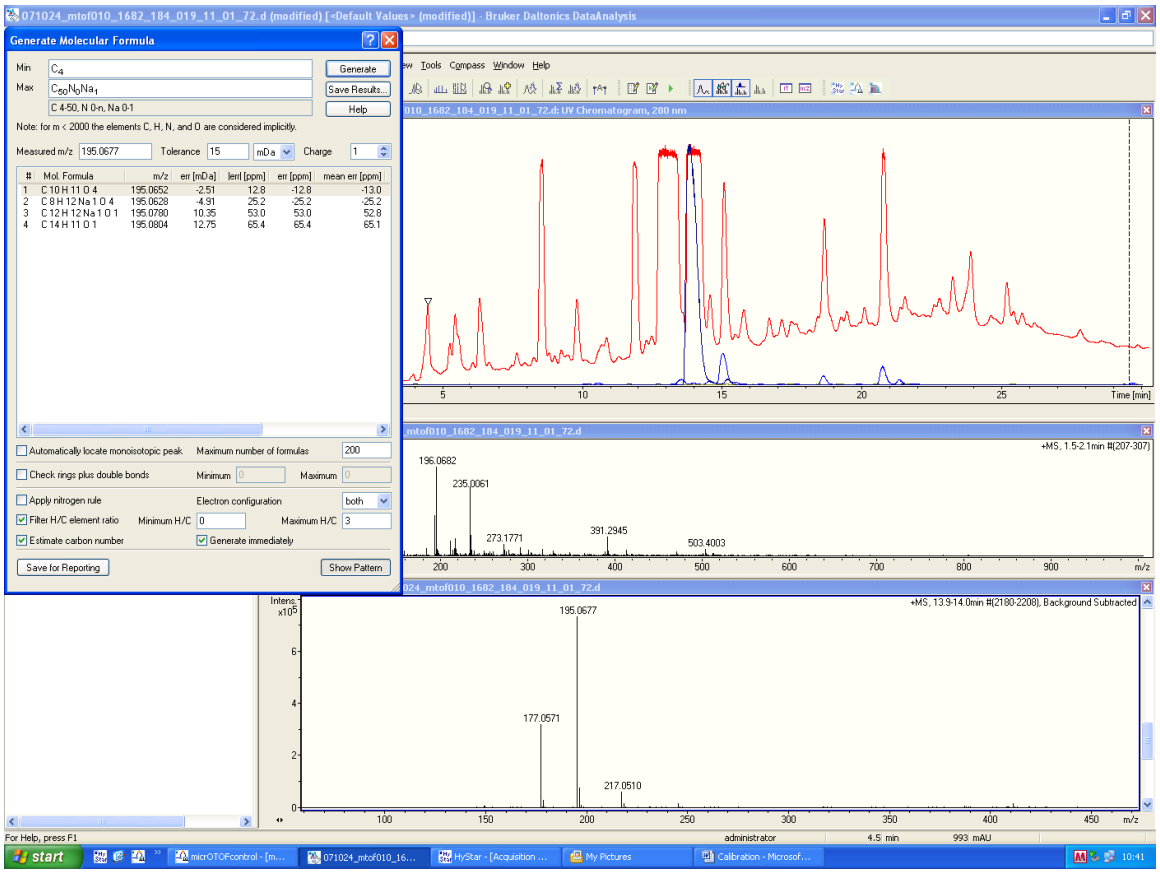

Figure 93: Example of generated molecular formulae for ferulic acid.

8.4.1 PCWM alkali extract

Although the UV chromatogram for the PCWM extract seemed reasonably similar to those recorded previously, the TIC chromatogram seemed very

messy and only a few recognisable peaks were found (Figure 94). Therefore many of the spectra for the dimers and trimers of ferulic acid that follow are taken from the ECWM-, SECWM- and TFA-precipitate alkali-extract chromatograms. The compounds that were detected and identified are listed in Figure 95. Notably none of the dimers was identified; this was a problem with the sample, as a repeat of the run produced the same result.

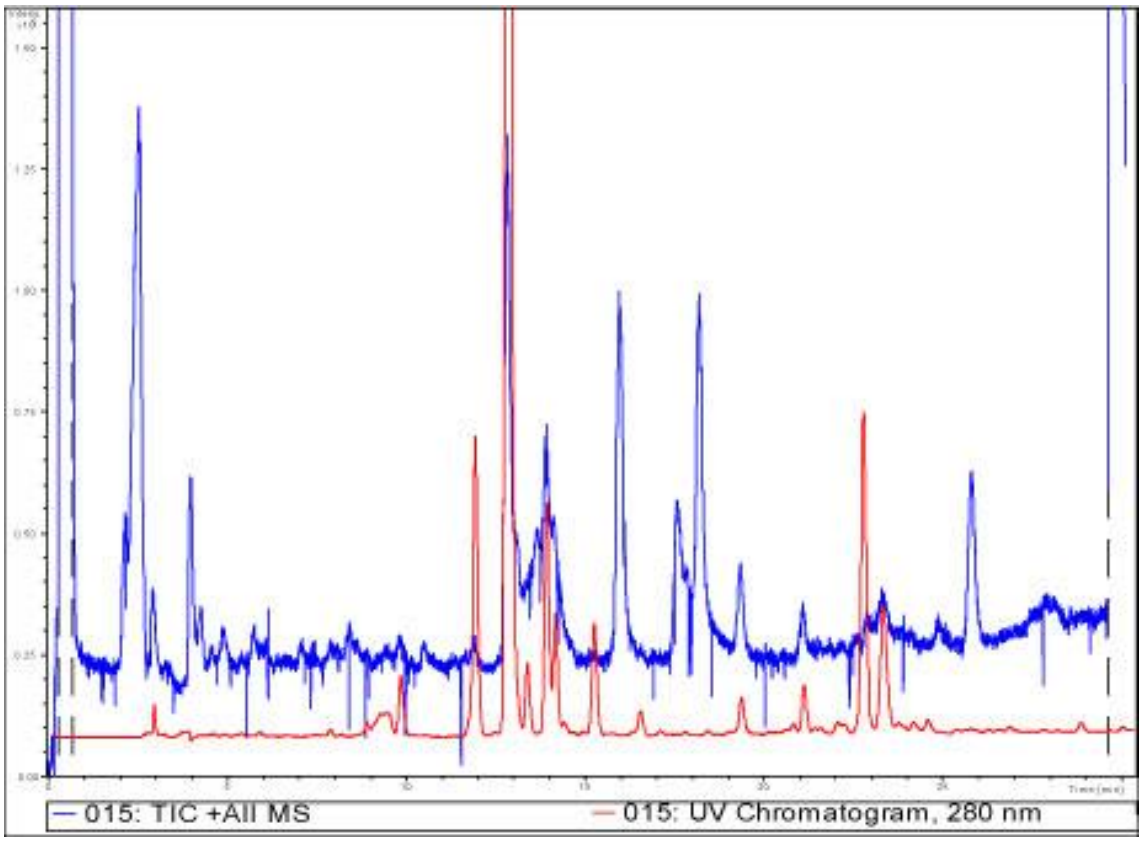

Figure 94: Total-ion and UV chromatograms of PCWM alkali extract.

Retention time (min)	Characteristic ions	Identity	Molecular formula	Molecular weight
9.6	169.0442 $(M+H)^+$	Vanillic acid	$C_8H_8O_4$	168.0423
12.6	153.0501 $(M+H)^+$	Vanillin	$C_8H_8O_3$	152.0473
13.1	165.0509 $(M+H)^+$	*trans-p*-Coumaric acid	$C_9H_8O_3$	164.0473
13.9	177.0464 $(M-H_2O+H)^+$, 195.0532 $(M+H)^+$	*trans*-Ferulic acid	$C_{10}H_{10}O_4$	194.0579

Figure 95: Compounds detected by accurate-mass MS in PCWM.

8.4.2 SECWM alkali extract

Figure 96 shows the UV and TIC chromatograms for the SECWM alkali extract. As well as the six usual dimers, two possible trimers and a tetramer were detected in the SECWM (Figure 97).

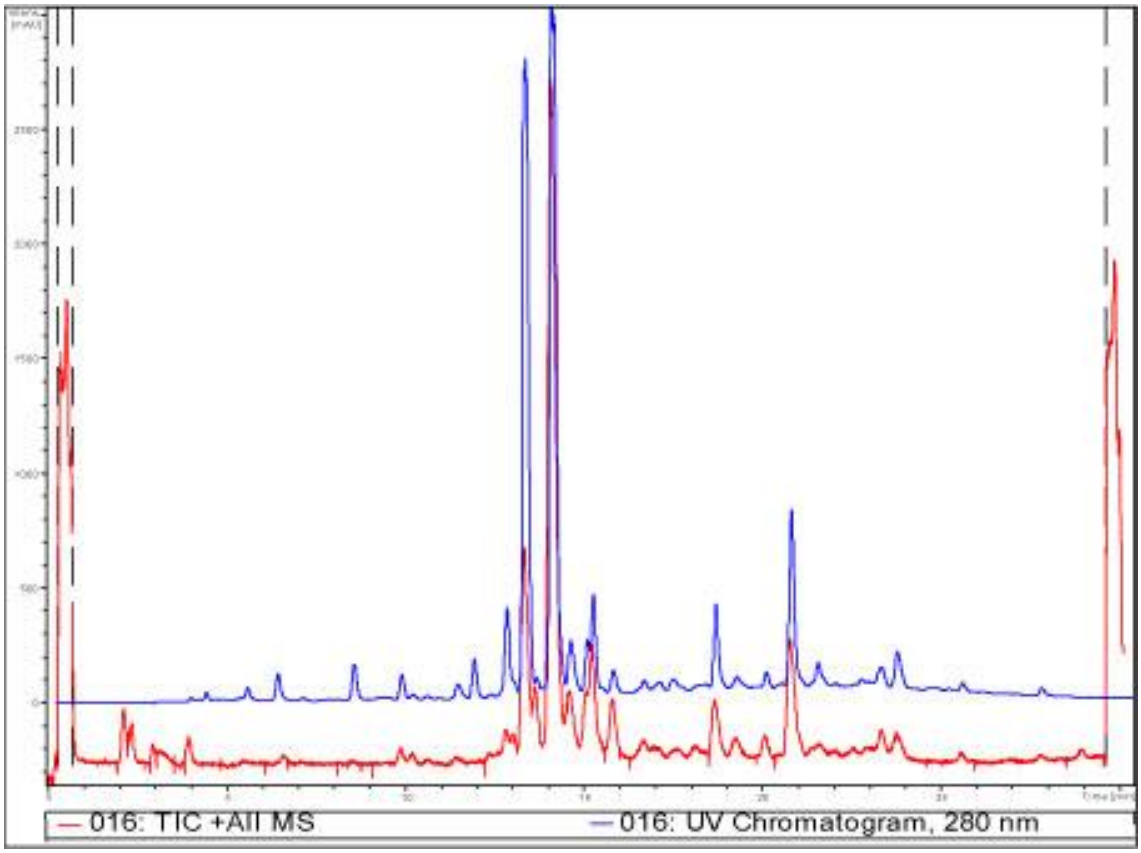

Figure 96: Total-ion and UV chromatograms for SECWM alkali extract.

Retention time (min)	Characteristic ions	Identity	Molecular formula	Molecular weight
9.7	169.0405 $(M+H)^+$	Vanillic acid	$C_8H_8O_4$	168.0423
12.6	153.0512 $(M+H)^+$	Vanillin	$C_8H_8O_3$	152.0473
13.1	165.0515 $(M+H)^+$, 147.0405 $(M-H_2O+H)^+$, 187.0270 $(M+Na)^+$	*trans-p*-Coumaric acid	$C_9H_8O_3$	164.0473
13.5	341.0976, 369.0938 $(M-H_2O+H)^+$, 387.1136 $(M+H)^+$, 409.0879 $(M+Na)^+$, 773.2012 $(Mx2-H)^+$	8,8'-DiFA (AT)	$C_{20}H_{18}O_8$	386.1002

Figure 97: Compounds detected by accurate-mass MS in SECWM.

Retention time (min)	Characteristic ions	Identity	Molecular formula	Molecular weight
13.9	195.0532 $(M+H)^+$, 177.0470 $(M-H_2O+H)^+$, 217.0340 $(M+Na)^+$	*trans*-Ferulic acid	$C_{10}H_{10}O_4$	194.0579
14.4	387.1042 $(M+H)^+$, 195.0541 $(FA+H)^+$, 177.0476 $(FA-H_2O+H)^+$, 369.0927 $(M-H_2O+H)^+$	8,8'-DiFA	$C_{20}H_{18}O_8$	386.1002
15.0	387.1035 $(M+H)^+$, 369.0927 $(M-H_2O+H)^+$, 409.0875 $(M+Na)^+$, 773.2011 $(Mx2-H)^+$	8,5'-DiFA	$C_{20}H_{18}O_8$	386.1002
15.0	195.0532 $(M+H)^+$, 177.0470 $(M-H_2O+H)^+$, 217.0336 $(M+Na)^+$	*cis*-Ferulic acid	$C_{10}H_{10}O_4$	194.0579
15.1	579 $(M+H)^+$, 601 $(M+Na)^+$	Trimer?	$C_{30}H_{26}O_{12}$	578.1424
17.5	561.1351 $(M-H_2O+H)^+$, 579.1432 $(M+H)^+$, 387.1010 $(DiFA+H)^+$	Trimer?	$C_{30}H_{26}O_{12}$	578.1424
18.4	387.1035 $(M+H)^+$, 369.0920 $(M-H_2O+H)^+$, 773.2002 $(Mx2-H)^+$, 409.0871 $(M+Na)^+$	5,5'-DiFA	$C_{20}H_{18}O_8$	386.1002
20.6	387.1042 $(M+H)^+$, 369.0933 $(M-H_2O+H)^+$, 193.0389 $(FA-H)^+$, 409.0876 $(M+Na)^+$, 773.2021 $(Mx2-H)^+$	8-*O*-4'-DiFA	$C_{20}H_{18}O_8$	386.1002
21.3	561.1325 $(M-H_2O+H)^+$, 579.1295 $(M+H)^+$, 387.1062 $(M+H)^+$, 369.0822 $(M-H_2O+H)^+$, 601.1163 $(M+Na)^+$, 409.1001 $(M+Na)^+$	8,5'-DiFA (BF) + Trimer?	$C_{20}H_{18}O_8$ $C_{30}H_{26}O_{12}$	386.1002 578.1424
23.761	771.1951 $(M+H)^+$, 595.1751 $(C_{31}H_{31}O_{12})^+$, 367.0766 $(DiFA-H)^+$	Tetramer?	$C_{40}H_{34}O_{16}$	770.1847

Figure 97b: Compounds detected by accurate-mass MS in SECWM (continued).

8.4.3 ECWM alkali extract

The column was somewhat overloaded by the ECWM sample. The overloading was identified by the poor peak shape in the UV chromatogram shown in Figure 98.

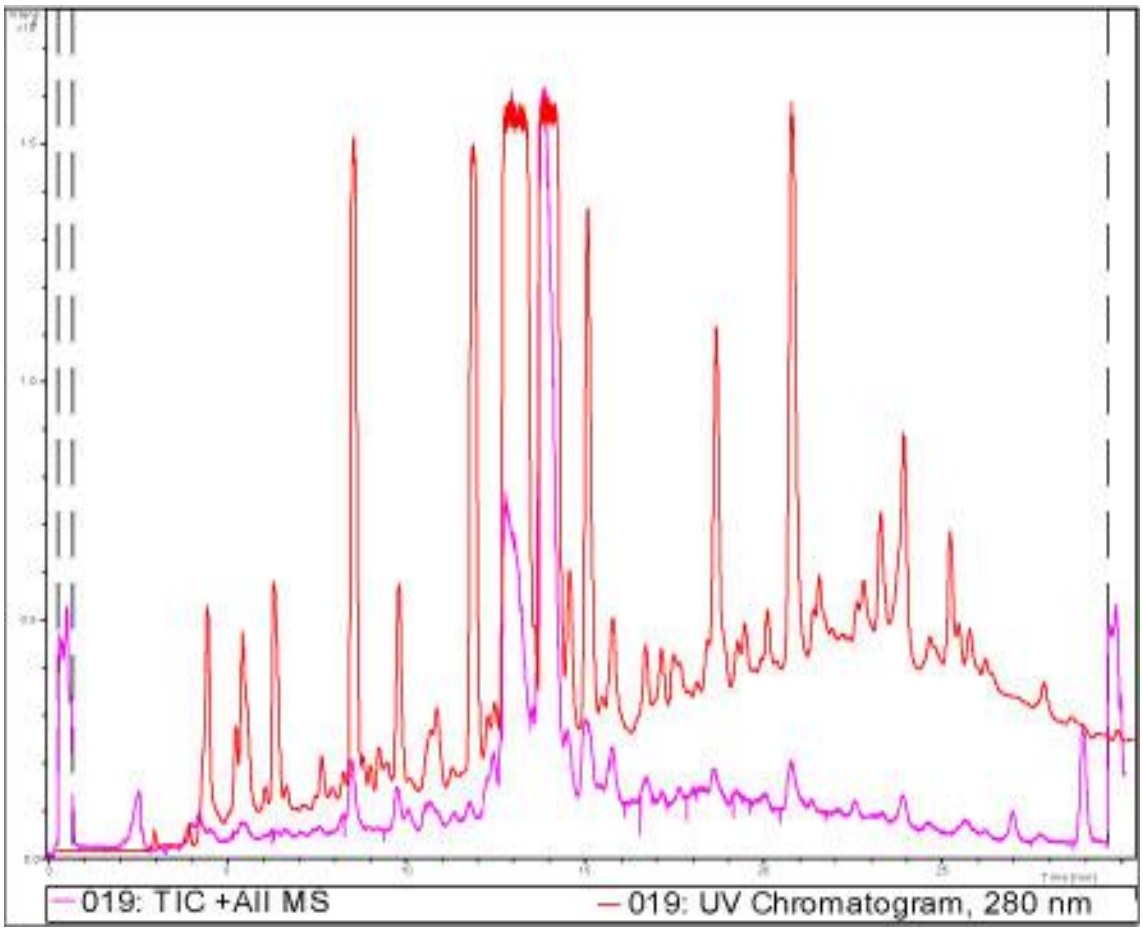

Figure 98: Total-ion and UV chromatograms for ECWM alkali extract.

A number of phenolics were detected and these are listed in Figure 99 with their identifying ions; these included four trimers and some unidentified dimers.

Retention time /min	Characteristic ions	Identity	Molecular formula	Molecular weight
9.793	169	Vanillic acid	$C_8H_8O_4$	168.0423
12.850	165, 147	*trans*-p-Coumaric acid	$C_9H_8O_3$	164.0473
13.823	177, 195	*trans*-Ferulic acid	$C_{10}H_{10}O_4$	194.0579
13.518	341, 369, 387, 409, 773	8,8'-DiFA (AT)	$C_{20}H_{18}O_8$	386.1002
14.548	369, 401, 387, 341	8,8'-DiFA	$C_{20}H_{18}O_8$	386.1002
14.997	387, 369, 773	8,5'-DiFA	$C_{20}H_{18}O_8$	386.1002
15.185	177, 195	*cis*-Ferulic acid	$C_{10}H_{10}O_4$	194.0579
15.435	387, 341, 401, 369, 419	DiFA ?	$C_{20}H_{18}O_8$	386.1002
17.039	579, 561, 595, 543	Trimer?	$C_{30}H_{26}O_{12}$	578.1424
17.627	369, 341, 387, 401	5,5'-DiFA	$C_{20}H_{18}O_8$	386.1002
17.419	561, 579, 595, 611	Trimer?	$C_{30}H_{26}O_{12}$	578.1424
17.489	495, 579, 561, 595, 543	Trimer?	$C_{30}H_{26}O_{12}$	578.1424
18.601	387, 369, 773	8-O-4 Dimer	$C_{20}H_{18}O_8$	386.1002
19.175	373, 341, 419, 579, 613, 595, 385, 401	Trimer?	$C_{30}H_{26}O_{12}$	578.1424
20.420	387, 369, 479, 773	DiFA ?	$C_{20}H_{18}O_8$	386.1002
21.289	387, 403, 369	DiFA ?	$C_{20}H_{18}O_8$	386.1002

Figure 99: Compounds detected by accurate-mass MS in ECWM.

8.4.4 Phenolic dimers and trimers

Some of the dimers have a signal at m/z=773, due to gas-phase dimer formation inside the MS. A true tetramer would have an m/z of 771 due to it losing two protons during the oxidative coupling process.

8,8'-DiFA (AT)

The mass spectrum of 8,8'-DiFA (AT) ($C_{20}H_{18}O_8$ M_w 386.36) is shown in Figure 100. The identification ions for 8,8'-DiFA (AT) are shown below.

- 341.0986 indicates a formula of $C_{19}H_{17}O_6$, M-CH_2O_2+H^+ ion (ppm error 9.1)
- 369.0954 indicates a formula of $C_{20}H_{17}O_7$, M+H-H_2O^+ ion (ppm error 9.5)
- 387.1060 indicates a formula of $C_{20}H_{19}O_8$, M+H^+ ion (ppm error 4.1)

- 409.0868 indicates a formula of $C_{20}H_{18}O_8Na$, $M+Na^+$ ion (ppm error 9.6)
- 773.1993 indicates a formula of $C_{40}H_{37}O_{16}$, $2M+H^+$ ion (ppm error 10.7)

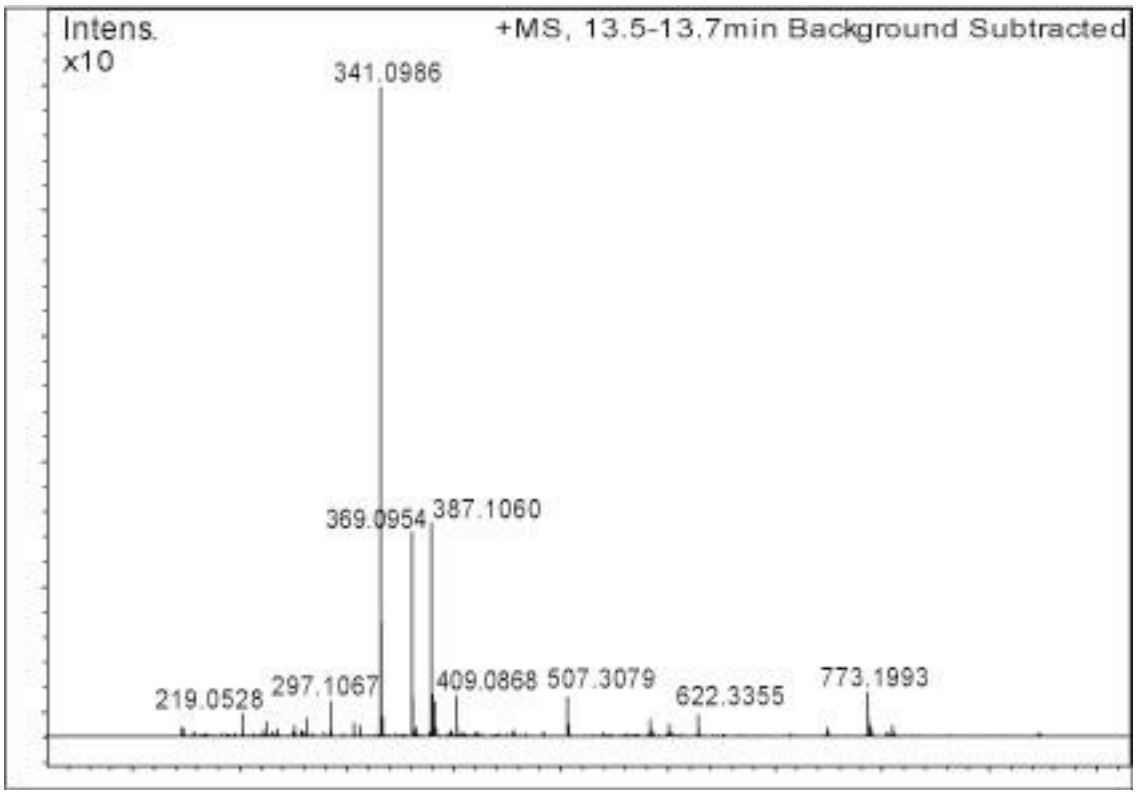

Figure 100: Mass spectrum of 8,8'-DiFA (AT) extracted from TFA/80%-ethanol Precipitate 3.

These data, together with the UV spectrum (not shown) confirmed the presence of 8,8'-DiFA (AT). This spectrum shows the signal for the gas-phase dimer formed inside the MS.

5,5'-DiFA

The mass spectrum of 5,5'-DiFA ($C_{20}H_{18}O_8$ M_w 386.36) is shown in Figure 101. The identification ions for 5,5'-DiFA are shown below.

- 369.0939 indicates a formula of $C_{20}H_{17}O_7$, $M+H-H_2O^+$ ion (ppm error 7.9)
- 387.1055 indicates a formula of $C_{20}H_{19}O_8$, $M+H^+$ ion (ppm error 4.7)
- 409.0866 indicates a formula of $C_{20}H_{18}O_8Na$, $M+Na^+$ ion (ppm error 0.0)
- 773.1920 indicates a formula of $C_{40}H_{37}O_{16}$, $2M+H^+$ ion (ppm error 17.3)

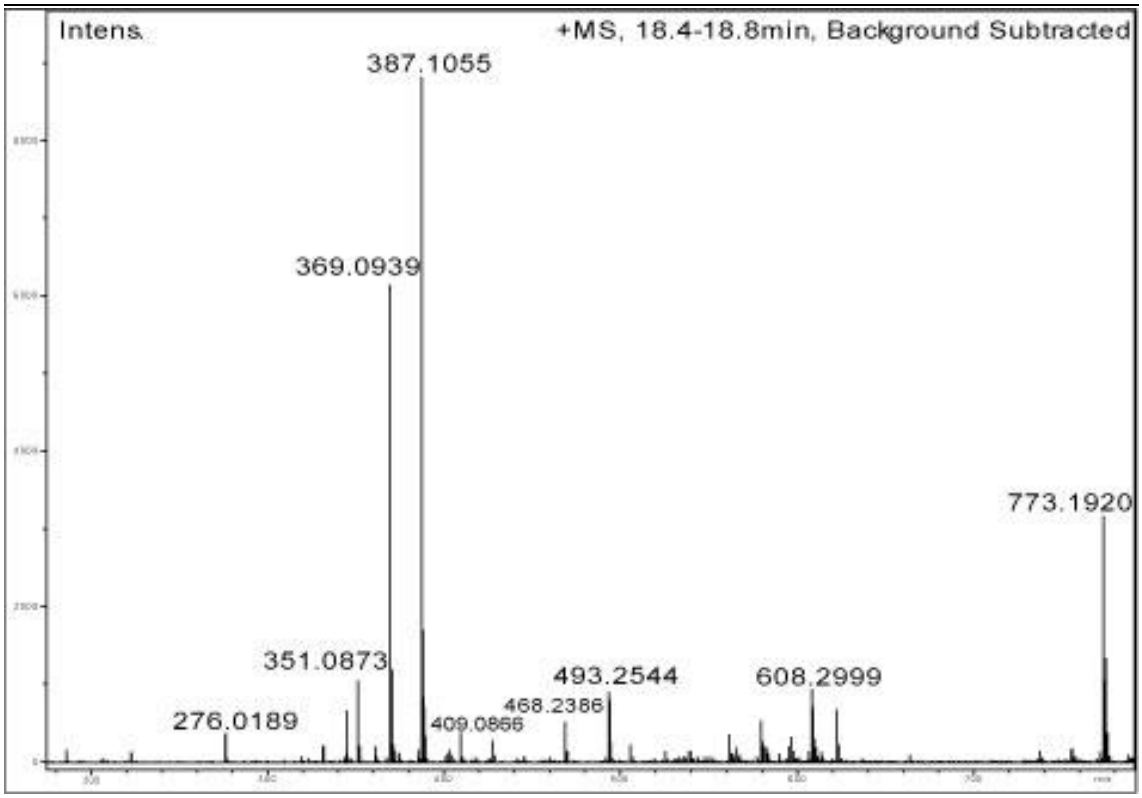

Figure 101: Mass spectrum of 5,5'-DiFA extracted from TFA/80%-ethanol Precipitate 3.

8-O-4'-DiFA

Figure 102 shows the mass spectrum of 8-*O*-4'-DiFA ($C_{20}H_{18}O_8$ M_w 386.36). The identification ions for 8-*O*-4'-DiFA are shown below.

- 193.0364 indicates a formula of $C_{10}H_9O_4$ (ppm error 66.1)
- 387.1761 indicates a formula of $C_{20}H_{19}O_8$, $M+H^+$ ion (ppm error 6.9)
- 369.0949 indicates a formula of $C_{20}H_{17}O_7$, $M+H-H_2O^+$ ion (ppm error 8.3)
- 409.0863 indicates a formula of $C_{20}H_{18}O_8Na$, $M+Na^+$ ion (ppm error 0)
- 773.1986 indicates a formula of $C_{40}H_{37}O_{16}$, $2M+H^+$ ion (ppm error 13.7)

These data and the UV spectrum (not shown) confirm the presence of 8-*O*-4'-DiFA. The m/z=193 ion is strongly indicative of the 8-O-4 dimer as shown in Figure 103. The gas-phase dimer (m/z=773) is formed inside the MS.

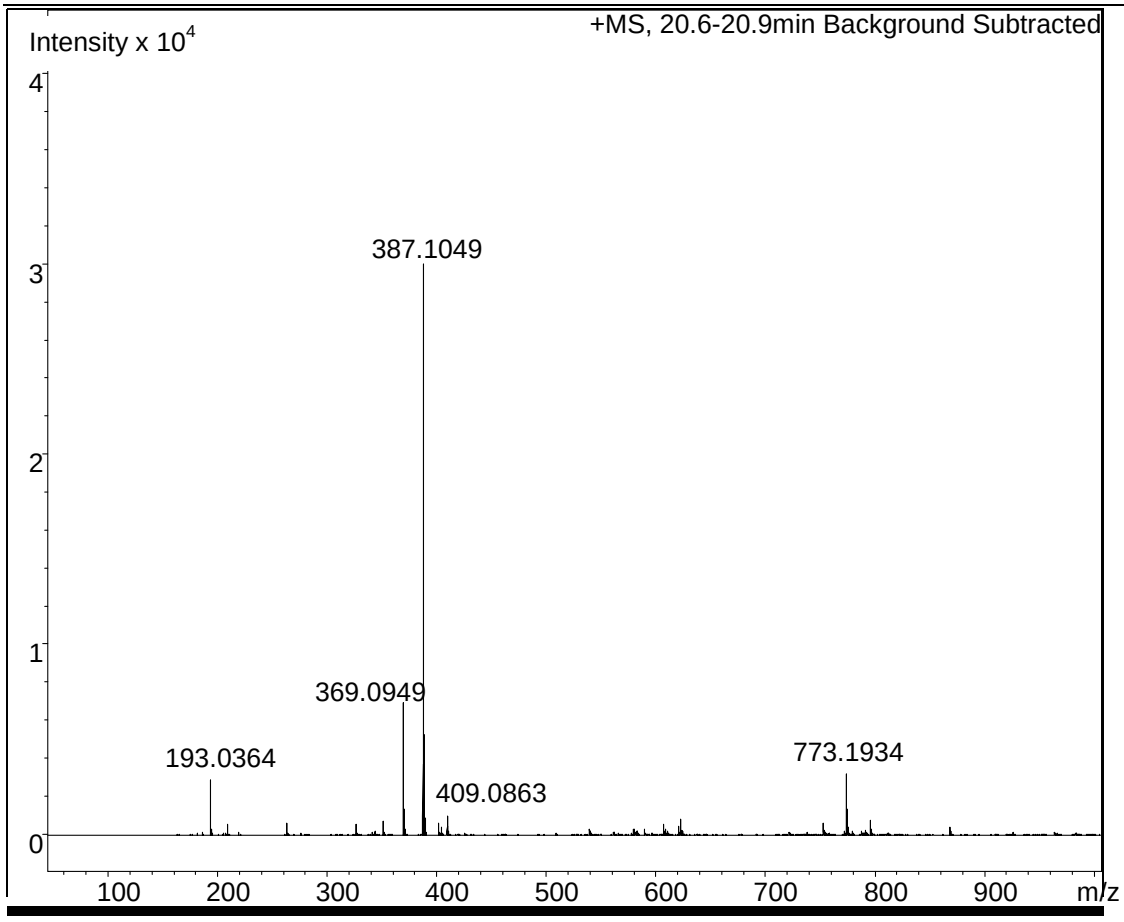

Figure 102: Mass spectrum of 8-O-4'-DiFA extracted from TFA/80%-ethanol Precipitate 3.

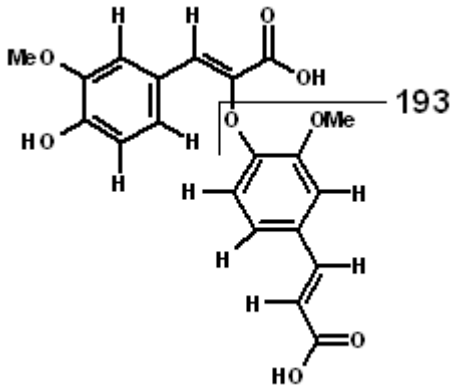

Figure 103: Splitting of 8-O-4'-DiFA to give m/z=193.

The MS data from Section §3.2.1 indicated the presence of trimers in CWC CWM; this was confirmed in the SECWM total phenolic extract by LC-MS.

Triferulic and tetraferulic acids

To identify the triferulic and tetraferulic acids, the masses of the ions produced were compared to those from previously reported trimers and tetramers (Figure 104).

Compound	Characteristic ions	Molecular weight	Molecular formula	Reference
8,5'/5,5'-TriFA	601 $(M+Na)^+$, 617 $(M+K)^+$	578.1424	$C_{30}H_{26}O_{12}$	(Bunzel *et al.*, 2006)
8,8'(THF)/5,5'-TriFA	619 $(M+Na)^+$, 635 $(M+K)^+$	595.1452	$C_{30}H_{27}O_{13}$	(Bunzel *et al.*, 2006)
8-*O*-4'/5,5'/8-*O*-4'-TetraFA	793 $(M+Na)^+$, 809 $(M+K)^+$	770.1847	$C_{40}H_{34}O_{16}$	(Bunzel *et al.*, 2006)
8-*O*-4/5,5/8,5 TetraFA	793 $(M+Na)^+$, 809 $(M+K)^+$	770.1847	$C_{40}H_{34}O_{16}$	(Bunzel *et al.*, 2006)

Figure 104: Masses for triferulic and tetraferulic acids already discovered.

The spectra of a triferulic and three tetraferulic acids are given in Figures 105-108. The $M+H^+$ ions should have accurate masses of 579.1503 ($C_{30}H_{27}O_{12}$) and 771.1925 ($C_{40}H_{35}O_{16}$).

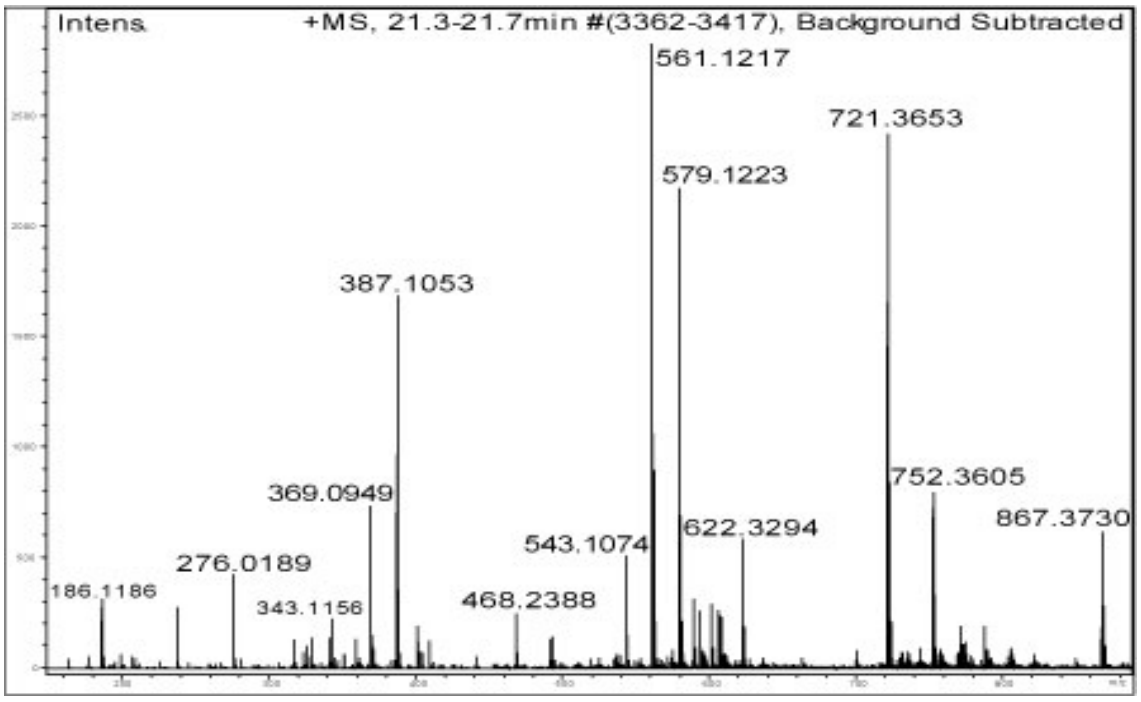

Figure 105: Accurate-mass spectrum of a triferulic acid from TFA/80%-ethanol Precipitate 3.

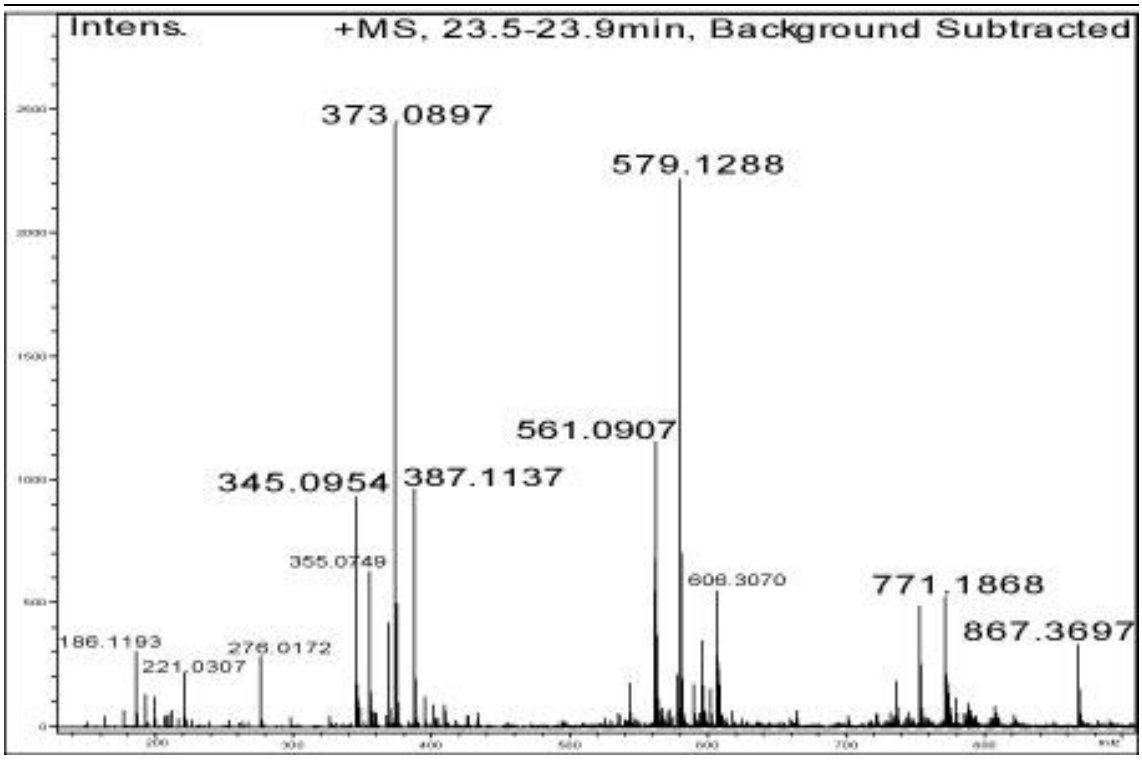

Figure 106: Accurate-mass spectrum of a tetraferulic acid found in TFA/80%-ethanol Precipitate 3.

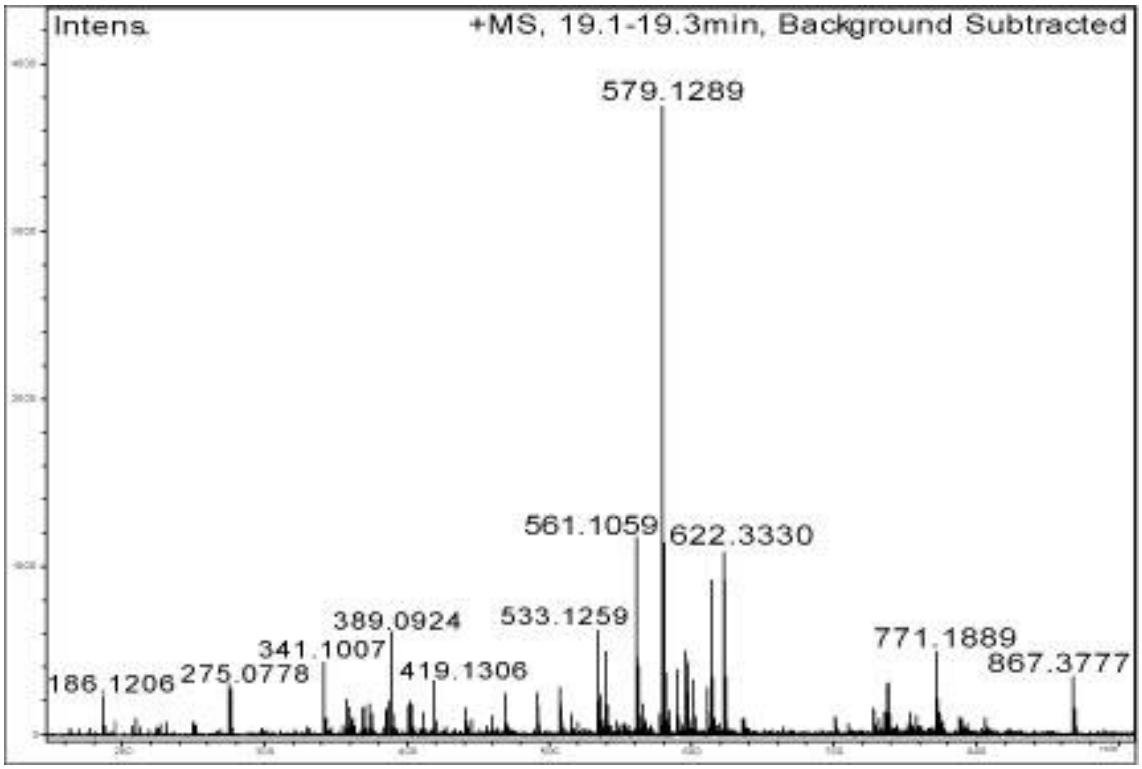

Figure 107: Accurate-mass spectrum of a tetraferulic acid found in TFA/80%-ethanol Precipitate 3.

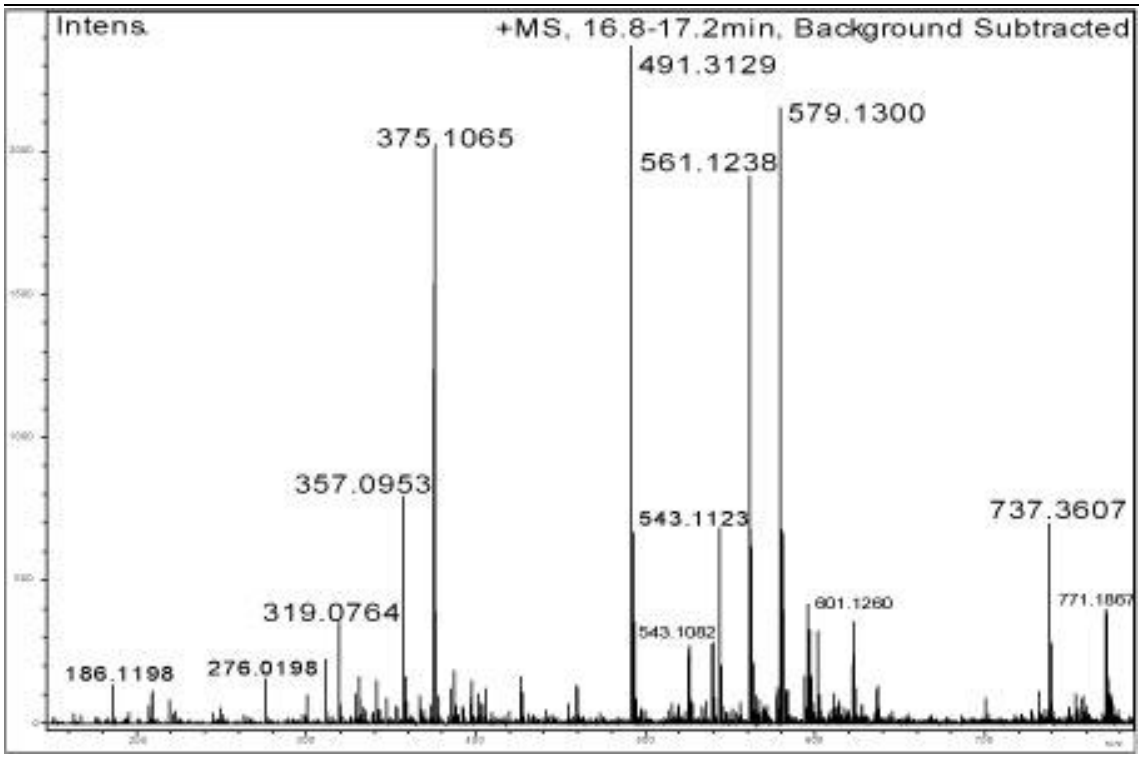

Figure 108: Accurate-mass spectrum of a tetraferulic acid found in TFA/80%-ethanol Precipitate 3.

8.4.5 Phenolic-polysaccharide linkages

The phenolic-polysaccharide linkages found in the TFA hydrolysate and Biogel P-2 peaks are described in detail in Sections §7.4.2 and §7.4.4. Assuming the pentoses indicated by the MS data are all arabinose, three ferulic acid-arabinose fragments (M_w = 326.1), one ferulic acid-arabinobiose fragment (M_w = 458.1) and six diferulic acid-arabinose fragments (M_w = 518.1) were detected in the hydrolysate (Figure 86, Section §7.4.2). Interestingly there was no sign of any *p*-coumaric acid-pentose or DiFA-hexose fragments. The earlier eluting peaks did not contain any detectable ferulic acid esterified to polysaccharides, however, Peaks 3, 6, 7 and 8 did contain ferulic acids: Peak 3 contained two ferulic acid-arabinobiose fragments; Peak 6 contained two ferulic acid-arabinobiose fragments and a ferulic acid-arabinose fragment; Peak 7 contained four ferulic acid-arabinose fragments and Peak 8 contained two ferulic acid-arabinobiose fragments and three ferulic acid-arabinose fragments.

Ferulic acid attached to two pentoses was found in the hydrolysate and Peaks 3, 6 and 8. Ferulic acid attached to one pentose was found in the hydrolysate and Peaks 6, 7 and 8. More than one ferulic acid-arabinose peak appeared in some samples implying that more than one point of attachment to the pentose is present. The same could be said for the ferulic acid-arabinobiose. Six diferulic acid-arabinose fragments were detected in the hydrolysate; presumably this indicates differences in the parent diferulic acid and also the attachment point to arabinose.

8.5 Discussion

LC-SPE is a new technique at IFR and these samples were the first to be analysed by the technique here. Unfortunately due to time constraints the samples were run without sufficient prior testing of the system, which led to only a small proportion of the available compound being captured on the cartridge, making the subsequent NMR insufficiently clear in virtually all of the samples tested. Optimisation of the following components of the SPE method should give considerably better results:

- Peak collection delay time – the right delay time will ensure that the majority of the peak is collected
- SPE cartridges – although the Hysphere GP cartridges appear to be suitable, it is possible that there are cartridges that are more suitable
- Multiple trapping – cartridges could be used to collect the same peak from multiple HPLC runs to increase the concentration of compound on the cartridge
- Elution solvent – acetonitrile may not be the best solvent for the elution; perhaps water or a mixture of deuterated water and methanol/ethanol would be more appropriate as that is the solvent mixture used to dissolve phenolic standards
- Transfer tubing adsorption – the tubing could be rinsed more thoroughly between transfers, or better solvents may reduce the adsorption problem; alternatively a different tubing material may be necessary

- Direct transfer to NMR tubes – these samples were not directly transferred to the NMR tubes as the tubes were not available at the time of transfer, this should reduce any transfer losses to a minimum

Accurate-mass spectra combined with the UV spectra for the 8-*O*-4'-DiFA, 5,5'-DiFA and 8,8'-DiFA (AT) has shown that these dimers are present in the plant cell walls. The analysis has also identified trimers and tetramers of ferulic acid in CWC cell walls. Ferulic acid-arabinose and ferulic acid-arabinobiose fragments have been confirmed in the hydrolysate and Biogel P-2 peaks; as were six diferulic acid-arabinose fragments in the hydrolysate. This confirms that ferulic and diferulic acids are esterified to the polysaccharides of CWC cell walls, but they could not be identified due to problems with the solid-phase extraction procedure. Diferulic acid linkages between polysaccharides were not implied by these results as no diferulic acid-arabinobiose was detected.

9 General Discussion:

The investigation aimed to support the following hypotheses:

- The compositions of the cell walls of three different tissues of CWC are different, reflecting their roles in the plant's physiology.
- Phenolics cross-link polysaccharides in the cell walls of CWC. It was hoped that the structure of any phenolic-polysaccharide fragments produced could be elucidated. If one was found to contain 8,8'-DiFA (AT) it would add weight to the theory that the 8,8'-DiFA (AT) forms the linkage responsible for the thermal stability of CWC mechanical properties.
- Higher oligomers of ferulic acid are present in a plant that is not a member of the *Poaceae.*

The general conclusions for these hypotheses are stated below:

9.1 Cell walls in different tissues of CWC

The data presented in Chapter 3 showed that there were significant differences between the cell walls of the three different tissues studied (Figure 39, §3.3.1). The decrease in cellulose in the secondary cell wall indicates lignin is taking more of a structural role. The non-cellulosic polysaccharides seem to be fairly consistent between the tissues. The hemicelluloses in CWC parenchyma were thought to be predominantly arabinoxylans, but in fact it is xyloglucan, with some arabinoxylan and a small amount of glucomannan. The pectin component is rhamnogalacturonan I. The hemicelluloses in CWC epidermis and sub-epidermis are similar, although the proportion of arabinoxylan is increased in the ECWM.

CWC epidermis had the highest levels of phenolics, *p*-coumaric acid in particular; presumably it has an important physiological role protecting cells against damage by pathogens and/or soil abrasion. The dimers are probably

involved in interpolymeric cross-linking, probably of arabinoxylan and/or xyloglucan. The highest amount of dimers was found in the SECWM; as this is vascular tissue, perhaps more dimers are necessary to maintain cell adhesion in order to counteract the additional forces produced by osmotic pressure. The presence of high amounts of ferulic acid (and other phenolics) may inhibit the growth of the fungus *Fusarium oxysporum* (Lattanzio *et al.*, 1994), one of the known pathogens of CWC. From this information a new model for the structure of CWC cell walls was put forward (Figure 40, §3.3.2)

9.2 Characterisation of unknown phenolics

A large number of unknown phenolics are present in the cell walls of CWC; although a thorough survey had not been planned initially, it was thought worth while in case novel components were identified and therefore could perhaps be quantified in the same investigation. Although sufficient information was not available to assign structures to the unknowns, sufficient information was recorded about each so that should they be identified in the future, retrospective quantification would be possible. The data are discussed in depth in Chapter 4 and tabulated in Appendix F.

9.3 Cell wall cross-links

The development and evaluation of biochemical and chemical methods for producing phenolic-polysaccharide fragments is presented in Chapters 6 and 7.

Contamination of Driselase with the phenolics and sugars that were under investigation prevented its use for producing phenolic-polysaccharide fragments; so 0.05 M TFA was used instead. The mass-spectrometric data indicated that there were a range of ferulic acid-polysaccharide linkages detected in the hydrolysate and in Peaks 3, 6, 7 and 8. There were also six diferulic acid-arabinose fragments detected in the hydrolysate. Without the help of NMR identification no conclusions could be made about the exact linkages

between (di)ferulic acids and the polysaccharides of CWC cell walls. No *p*-coumaric acid-arabinose fragments or ferulic acid-hexose fragments were detected.

Bunzel et al (2008) have isolated Ara-8,8'-DiFA (AT)-Ara in maize bran insoluble fibre, proving that it does cross-link polysaccharides. This discovery lends weight to the argument that 8,8'-DiFA (AT) is instrumental in the maintenance of cell-cell adhesion put forward by Parker *et al* (2003). The amounts of CWM used in these experiments were one or two orders of magnitude too small for this linkage to be identified, and this is reflected in the fact that no compounds with masses that matched diferulic acid-arabinobiose were detected.

9.4 Higher oligomers of ferulic acid

The mass spectrometry results given in Chapter 8 indicate that trimers and tetramers of ferulic acid are present in CWC cell walls, although which particular ones has not been identified. Theoretically there should be at least 19 possible structures (Ralph *et al.*, 2004), and only five have been identified to date (Bunzel *et al.*, 2005; Bunzel *et al.*, 2006; Funk *et al.*, 2005). As adding each successive ferulic acid molecule adds to the number of possible structures available, there may be huge numbers of ferulic acid oligomers present in plant cell walls.

9.5 Limitations

Production of cell-wall material necessitates the breaking of some bonds and therefore reduces the amount of information available from this material. The material extracted from the CWM may not give a true picture of the whole, as some components may be extracted more easily than others during the process.

The lack of data available on variety, country of origin, growing and storage conditions for the CWC, it having been bought from retail outlets, negates the comparison of different batches of CWM. The major exporters are China, Thailand and Taiwan, and these are therefore the likely countries of origin, but growing conditions within these countries could vary widely. It would be expected that variety, growing and storage conditions could have a significant effect on the cell-wall composition (Lempereur *et al.*, 1997). The best way to get around this issue would be to obtain CWC direct from growers in China, or to obtain different varieties, distinguish them genetically, and then grow them under controlled conditions.

9.6 Future work

There are a number of experiments that need to be done to continue towards the aim of determining which molecules and/or linkages are responsible for the crisp texture of Chinese water chestnuts.

9.6.1 Improved TFA hydrolysis methodology

A sequential TFA hydrolysis using increasing concentrations, perhaps 0.01 M, 0.025 M, 0.05M and 0.1 M TFA could be used to produce a less complex mixture of FA-oligosaccharide fragments at each stage, allowing easier separation and purification. This would also give some indication of which linkages are most chemically stable when phenolic linkages are involved.

9.6.2 Degradation of cell wall by purified CWC-specific enzymes

As *Fusarium oxysporum* (together with *Geotrichium*, *Cerastomella paradoxa Trichoderma viride*, *Uromyces* sp., *Cylindrosporium eleocharidis*) (Brecht, 2004) is one of the few listed pathogens for CWC, purified enzymes derived from its cultures could be characterised with regard to their activities. These could then

be used in two ways: i) to determine which linkages are key to cell-cell adhesion in CWC by using particular enzyme treatments to produce significant textural changes in the whole tissue, ii) individually, synergistically and sequentially to degrade CWC cell walls, to produce phenolic-polysaccharides for further study.

Alternatively, the existing enzyme preparations could be purified to allow enzymic degradation without contamination of the resulting supernatants.

9.6.3 Improved LC-SPE methodology

Improvement of the LC-SPE methodology, primarily by ensuring the timing of the peak collection has been optimised, and that the solid-phase cartridge and elution solvent are the most favourable should ensure that the investigations of the previous sections could be put to the best possible use. Also, the utilisation of the multiple-trapping facility should allow sufficient sample for good-quality NMR analysis.

9.6.4 Stability of phenolic-polysaccharide linkages in alkali

Alkali extraction of phenolics from CWC may be time-dependent, and a full course of time-course experiments will help to optimise the method for extracting phenolics and may clarify which diferulic acids are stable in dilute alkali regardless of time; allowing better agreement between the loss of particular phenolics and reduction in cell adhesion.

9.6.5 Investigations of CWC leaf-cell walls

Little is known about CWC leaf cell walls, although the leaves of CWC are used in some cultures for weaving into mats. In fact there are two ecotypes found in Fiji that show a difference in the toughness of their leaves, one has “soft” leaves suitable for weaving mats, whilst the other has “hard” leaves which are

unsuitable (Klok *et al.*, 2002). The difference between these leaves is presumably on account of the presence of complete septa in place of the usually-incomplete septa, due to some genetic abnormality. As there has been very limited genetic analysis carried out on CWC generally, identifying the abnormality could present a major challenge. Microscopy pictures of CWC leaves are in Appendix K.

9.6.6 Completion of CWC cell-wall models

To produce a complete picture of CWC parenchyma cell walls, the protein content and composition should be studied, as this would give the required information to determine the presence of extensin. Analysis of the proteins present would also aid understanding of which other proteins/enzymes are present in CWC cell walls and which therefore may be involved in polysaccharide formation, alteration and degradation.

Na_2CO_3 extraction removes methyl esters and phenolic esters, but not acetyl esters; therefore both methyl and phenolic esters may be involved in cell adhesion (Marry *et al.*, 2006). Therefore, the degree of *in vivo* methylation and acetylation of the cell-wall polysaccharides of CWC should be measured. An attempt was made to measure acetylation using a commercial testing kit during this study, but the results were inconsistent.

As listed in Section §1.3.1, a whole suite of antibodies is available to characterise cell walls, and some could be chosen to confirm the positions of the arabinoxylan, rhamnogalacturonan and xyloglucan in the cell walls. They could also be used to determine if AGP and extensin are present.

For the epidermis and sub-epidermis cell walls, in addition to the analyses listed above, an analysis of the lignin composition would also be required.

9.6.7 Alternative methods of polysaccharide analysis

Other methods for depolymerising polysaccharides exist; in particular one method from the chemical literature seems to be of interest (Wang *et al.*, 1998). It involves acetylating the polysaccharides and then selected conformations of β-D-aldosidic linkages present are oxidised by ozone to form esters. The polysaccharides are then cleaved by a nucleophile. The reaction is strongly controlled by stereoelectronic effects and so the reaction rates vary considerably with conformation, thus allowing specific linkages to be broken in a way similar to that achievable with enzymes. Although the reference mentioned uses purified samples of polysaccharide, there seems to be no reason why this could not be used on plant cell walls (or fractions thereof), bar their solubility in formamide, which is the suggested solvent for the initial acetylation. Depending on the susceptibility of phenolic esters to ozone this might lead to larger oligosaccharide chains linked by diferulic acid bridges being isolated.

9.6.8 Commercial uses for CWC cell-wall information

Fusarium oxysporum enzymes could also be used to break down CWC waste, such as the leaves (from harvesting) or epidermis (from canning), to produce a liquid preparation rich in phenolics and oligosaccharides, which may yield useful components suitable for further processing into high-value products.

Combined harvesting of leaves and corms could produce additional streams of income for farming communities. However harvesting the leaves would probably affect the degree to which harvestable corms were produced, as corms are usually harvested once the leaves have died back; therefore, using the leaves for weaving and eating the corms may be mutually exclusive activities.

The unexpected gelling of a few of the solutions during the VICS experiment could be usefully investigated, as food-based gels have many uses in the food and pharmaceutical industries. If they do contain relatively high levels of

phenolics, however, they could be unpalatable and so unsuitable for food applications, but this does not preclude other applications.

10 Appendices:

A Solution preparation

0.5% SDS solution:
10 g of sodium dodecyl sulfate (Sigma) and 1.142 g of sodium metabisulfate (Sigma) made up to 2 L with deionised water, mixed very slowly to prevent foaming.

1.5% SDS solution:
30 g of sodium dodecyl sulfate (Sigma) and 1.903 g of sodium metabisulfate (Sigma) made up to 2 L with deionised water, mixed very slowly to prevent foaming.

KI/I_2:
1.5 g of iodine and 0.5 g of potassium iodide made up to 50 ml with deionised water.

Sulfuric acid reagent (25 mM $Na_2B_4O_7.10H_2O$ in 96% H_2SO_4):
2.385 g $Na_2B_4O_7.10H_2O$ made up to 250 ml with 96% H_2SO_4 (takes at least 1 hr to dissolve).

50 mM CDTA:
0.48 g of $Na_2S_2O_5$ and 9.1 g of CDTA (Na^+ salt, Sigma) dissolved in 400 ml deionised water (to give final concentrations of 5 and 50 mM respectively). NaOH solution (2 M) was added dropwise, bringing the pH back up to 7. As the pH increased the CDTA dissolved. The solution was then made up to 500 ml with deionised water.

B HPLC parameters

Instrument conditions

Simple phenolics

Instrument control method

Instrument: Perkin Elmer HPLC-DAD consisting of Quaternary LC Pump Model 200Q/410 with LC-235 Diode Array Detector and ISS-200 Autosampler

Channel parameters

Data will be collected from channel A

Delay time:	0.00 min
Run time:	30.00 min
Sampling rate:	2.4414pts/s

	Channel A	Channel B
Signal source	LC235C	LC235C

Autosampler method

Injection source:	Autosampler		
Injection volume:	40 µl	Flush volume:	1000 µl
Loop size:	150 µl	Flush speed:	Medium
Fixed mode:	Off	Flush cycles:	2
Excess volume:	5 µl	Air cushion:	5 µl
Sample syringe size:	250 µl	Sample speed:	Medium
Needle level:	5%		
Inject delay time:	0.00 min		

Detector parameters

Step	Time	A (nm)	B (nm)	BWA (nm)	BWB (nm)
1	30.00	280	325	5	5

Min wavelength:	210 nm	Spectral threshold:	Normal
Spectral acquisition mode:	Time	Sampling period:	1.6 s
Start time:	0.1 min	End time:	30.00 min
Lamp off at end of run:	No		

Pump parameters

Step	Time	Flow	A	B	40-40-20	10% Acetonitrile	Curve
0	0.5	1.00	0.0	0.0	10.0	90.0	0.0
1	25.0	1.00	0.0	0.0	75.0	25.0	1.0
2	5.0	1.00	0.0	0.0	100.0	0.0	1.0
3	10.0	1.00	0.0	0.0	10.0	90.0	-3.0
4	2.0	1.00	0.0	0.0	10.0	90.0	0.0

Ready time:	60.0 min	Standby time:	15.0 min
Standby flow:	0.1 ml/min	Solvent saver:	No
Saver Equ. time:	0.0 min	Shutdown:	No
Min pressure:	200 PSI	Max pressure:	3500 PSI

Timed events

There are no timed events in this method

Real-time plot parameters

Pages	Offset (mV)	Scale (mV)	
Channel A	1	-30.000	250.000

Processing parameters

Bunch factor:	5 points
Noise threshold:	24 µV
Area threshold:	122.00 µV

Peak separation criteria

Width ratio:	0.200
Valley-to-peak ratio:	0.010

Exponential skim criteria

Peak height ratio:	5.000
Adjusted height ratio:	4.000
Valley height ratio:	3.000

Baseline timed events

No baseline timed events

C GC parameters – sugars analysis

Instrument conditions

Instrument:	Perkin Elmer Autosystem XL
Column:	RESTEK Rtx-225
Column length:	30 m x 320 µm internal diameter
Carrier gas:	Helium
Flow rate:	2 ml/min
Split ratio:	1:1
Temperature:	Gradient
Injector temperature:	250°C
Notes:	Split ratio set to 60:1 at 2 minutes, and back to 10:1 at 10 minutes

Channel parameters

Data will be collected from channel A	
Channel A signal source:	DetA
Analogue output:	INT
Attenuation:	-6
Offset:	5.0 mV
Delay time:	0.00 min
Run time:	78.00 min
Sampling rate:	12.5 pts/s

Autosampler method

Injection volume:	1.0 µl	Sample washes:	2
Injection speed:	NORM	Sample pumps:	6
Viscosity delay:	0	Pre-sequence washes:	0
Waste vial:	1	Solvent A washes:	6

Carrier's parameters

Carrier A control:	PFlow – He
Column A length:	30.00m
Column A diameter:	320 µm
Vacuum compensation:	OFF
Split control mode:	Ratio
Set point:	0.0:1
Initial setpoint:	2.0 ml/min
Initial hold:	999 min

Valve configuration and settings

Valve 1:	SPLIT ON
Valves 2-6:	NONE

Detector parameters

Detector A:	FID	Detector B:	NONE
Range:	1		
Time constant:	200		
Autozero:	ON		
Ref gas flow:	250.0 ml/m		
MKUp gas flow	25.0 ml/m		

Heated zones

Injector A:	PSSI	Injector B:	NONE
Initial set point:	250°C	Injector B setpoint:	OFF
Initial hold:	999.00 min		
Detector A:	250°C		
Detector B:	0°C		
Auxiliary (NONE):	0°C		

Oven program

Cryogenics:	OFF		
Initial temperature:	140°C	Maximum temperature:	350°C
Initial hold:	5.00 min	Equilibration time:	2.0 min
Ramp 1:	2.5°C/min to 210°C, hold for 45 min		
Total run time:	78.00 min		

Timed events

SPL1:	set to 60 at 1.00 min
SPL1:	set to 10 at 10.00 min

Real-time plot parameters

Channel A – Pages:	1	Offset:	0.000 mV	Scale:	1000.000 mV

D GC parameters – PMAA analysis

Instrument conditions

Instrument:	Perkin Elmer Autosystem XL
Column:	RESTEK Rtx-225
Column length:	30m x 320 µm internal diameter
Carrier gas:	Helium
Flow rate:	2 ml/min
Split ratio:	1:1
Temperature:	Gradient
Injector temperature:	200°C
Notes:	Split ratio set to 60:1 at 1 minute, and back to 10:1 at 10 minutes

Channel parameters

Data will be collected from channel A	
Channel A signal source:	DetA
Analogue output:	INT
Attenuation:	-6
Offset:	5.0 mV
Delay time:	0.00 min
Run time:	83.89 min
Sampling rate:	12.5 pts/s

Autosampler method

Injection volume:	1.0 µl	Sample washes:	2
Injection speed:	NORM	Sample pumps:	6
Viscosity delay:	0	Pre-sequence washes:	0
Waste vial:	1	Solvent A washes:	6

Carrier's parameters

Carrier A control:	PFlow – He
Column A length:	30.00m
Column A diameter:	320 µm
Vacuum compensation:	OFF
Split control mode:	Ratio
Set point:	0.0:1
Initial setpoint:	2.0 ml/min
Initial hold:	999 min

Valve configuration and settings

Valve 1:	SPLIT ON
Valves 2-6:	NONE

Detector parameters

Detector A:	FID	Detector B:	NONE
Range:	1		
Time constant:	200		
Autozero:	ON		
Ref gas flow:	250.0 ml/m		
MKUp gas flow	25.0 ml/m		

Heated zones

Injector A:	PSSI	Injector B:	NONE
Initial set point:	200°C	Injector B setpoint:	OFF
Initial hold:	999.00 min		
Detector A:	250°C		
Detector B:	0°C		
Auxiliary (NONE):	0°C		

Oven program

Cryogenics:	OFF		
Initial temperature:	55°C	Maximum temperature:	350°C
Initial hold:	5.00 min	Equilibration time:	2.0 min
Ramp 1:	45.0°C/min to 140°C, hold for 2.0 min		
Ramp 2:	2.0°C/min to 210°C, hold for 40.0 min		
Total run time:	78.00 min		

Timed events

SPL1:	set to 60 at 1.00 min
SPL1:	set to 10 at 10.00 min

Real time plot parameters

Channel A – Pages:	1	Offset:	0.000 mV	Scale:	1000.000 mV

MS parameters

Type	EI
Source temp	200 deg
Quad temp	106 deg
Ion Pol	POS
MassGain	-156
MassOffs	-10
Emission	34.6
EleEnergy	69.9
AmuGain	1739
AmuOffs	136
Filament	1
Wid219	-0.016
DC Pol	NEG
Repeller	16.55

IonFocus	90.2
HED	ON
EntLens	1.0
EntOffs	18.57
EMVolts	1800

E Uronic acid raw data

Below is the table for the uronic acid standards and the resulting calibration curves.

Dilution	Stock conc. (mg/ml)	Concentration (mg/0.2ml aliquot)	Standards Plate 1					Real absorbance
			1	2	3	Mean	Control	
0	0.0000	0.0000	0.037	0.038	0.038	0.038	0.038	0.000
5	1.0052	0.0010	0.054	0.052	0.054	0.053	0.048	0.005
15	1.0052	0.0030	0.081	0.095	0.078	0.085	0.046	0.039
25	1.0052	0.0050	0.094	0.124	0.115	0.111	0.042	0.069
35	1.0052	0.0070	0.130	0.125	0.116	0.124	0.047	0.077
Dilution	Stock conc. (mg/ml)	Concentration (mg/0.2ml aliquot)	Standards Plate 2					Real absorbance
			1	2	3	Mean	Control	
0	0.0000	0.0000	0.037	0.038	0.038	0.038	0.039	-0.001
5	1.0052	0.0010	0.057	0.050	0.056	0.054	0.046	0.008
15	1.0052	0.0030	0.079	0.096	0.076	0.084	0.049	0.035
25	1.0052	0.0050	0.091	0.127	0.118	0.112	0.047	0.065
35	1.0052	0.0070	0.114	0.125	0.118	0.119	0.052	0.067

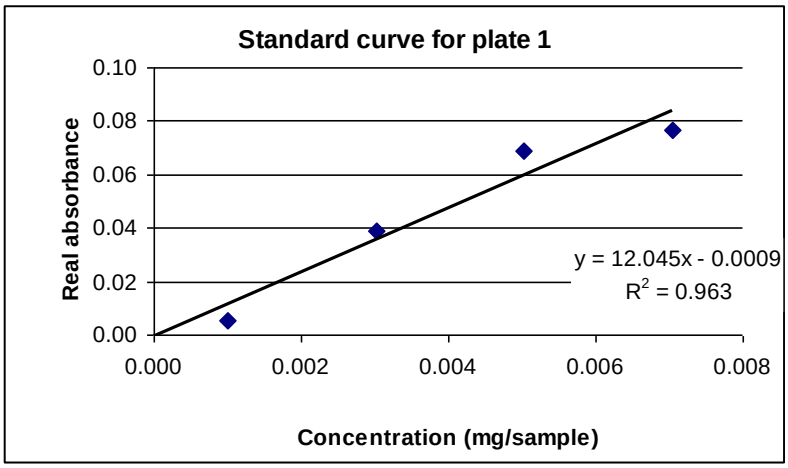

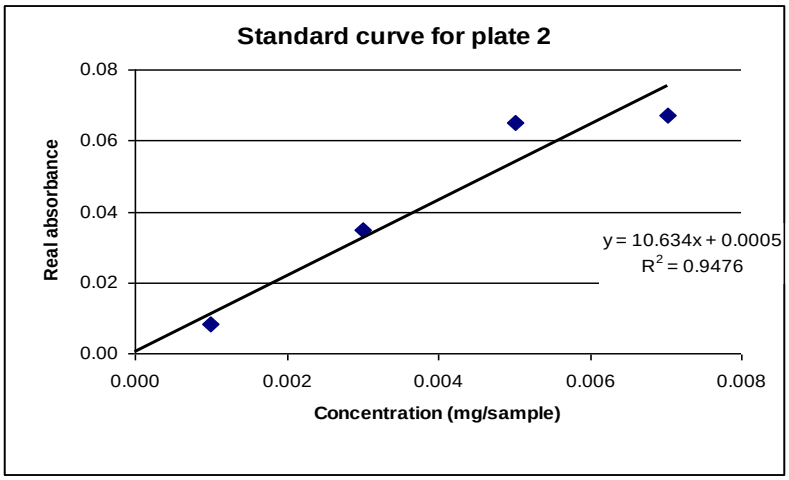

Below are the tables containing the raw data for the uronic acid values given in Section §3.2.2. The values given in the main text take into account the fact that water is released when the uronic acids are part of a polysaccharide chain.

Sample	Sample (mg)	Concentration (mg/0.2ml aliquot)	Samples Plate 1					Real absorbance
			1	2	3	Mean	Control	
F1	2.0	0.0333	0.132	0.133	0.134	0.133	0.078	0.055
F2	3.9	0.0650	0.230	0.249	0.239	0.239	0.134	0.105
F3	3.8	0.0633	0.227	0.214	0.197	0.213	0.111	0.102
S1	2.4	0.0400	0.128	0.199	0.101	0.143	0.074	0.069
S2	2.4	0.0400	0.102	0.131	0.109	0.114	0.074	0.040
S3	3.7	0.0617	0.152	0.135	0.167	0.151	0.087	0.064
M1	2.6	0.0433	0.166	0.147	0.142	0.152	0.097	0.055
M2	4.0	0.0667	0.200	0.207	0.210	0.206	0.141	0.065
M3	3.5	0.0583	0.157	0.177	0.198	0.177	0.115	0.062

Sample	Calculated uronics (mg/0.2ml aliquot)	Uronics (µg/mg)	Average (µg/mg)
F1	0.0046	**139.2**	**136.5**
F2	0.0088	**135.7**	
F3	0.0085	**134.5**	
S1	0.0034	**85.9**	**86.2**
S2	0.0034	**84.9**	
S3	0.0054	**87.8**	
M1	0.0044	**102.0**	**97.4**
M2	0.0060	**90.5**	
M3	0.0058	**99.7**	

F Peak list for Unknown Phenolics

Spectrum no.	Peak identity	Std		4 M 24 hr Total phenolic extraction			Average RRT	Peak shape	Wavelength (nm)	
		RT	RRT	RT	Area	Area relative to tFA			Max	Min
2			0.00	5.78	24108.34	0.37	0.23	5	216/287	242
3			0.00	6.06	149870.92	2.27	0.24	2	283/309	251/298
4			0.00	6.52	14408.19	0.22	0.27	4	226/278	255
5			0.00	7.02	10876.07	0.17	0.28	1	261	224
6			0.00	7.23	16873.39	0.26	0.29	1	265	225
7	Protocatechuic acid	7.6936	0.30	nd	nd	0.00	nd	3	260/294	236/281
8			0.00	nd	nd	0.00	0.31	1	284	253
9			0.00	8.20	12186.25	0.18	0.33	1	270	230
10			0.00	8.43	34431.14	0.52	0.34	6	223/325	264
11			0.00	8.95	8038.81	0.12	0.36	3	229/279/305	246/300
12			0.00	nd	nd	0.00	0.38	1	251	210
13	Std unknown 1 (Chlorogenic)	9.9054	0.38	nd	nd	0.00	nd	6	239/327	230/265
14			0.00	9.88	10438.47	0.16	0.39	4	280	262
15			0.00	10.23	2353.85	0.04	0.41	4	283	258
16			0.00	nd	nd	0.00	0.42	1	255	210/227
17			0.00	10.94	5224.81	0.08	0.44	1	225/295	260
18	*p*-Hydroxybenzoic acid	11.3254	0.44	nd	nd	0.00	nd	1	255	225
19			0.00	11.52	67172.03	1.02	0.46	7	322	260
20	*p*-Hydroxy phenyl acetic acid	11.7418	0.46	nd	nd	0.00	nd	4	221/276	251
21			0.00	11.95	25227.03	0.38	0.48	2or6	325	267
22	left shoulder of vanillic acid	12.0627	0.47	nd	nd	0.00	nd	1	314	266
23	Vanillic acid	12.2948	0.48	11.35	67172.03	1.02	0.47	3	261/291	236/281
24			0.00	11.76	19387.99	0.29	0.48	4	233/280	268
25			0.00	nd	nd	0.00	0.48	1	240/285	215/274
26	Std unknown 2 (Caffeic)	12.4723	0.48	12.34	20085.75	0.30	0.49	6	239/325	263
27	Std unknown 3	13.6123	0.53	nd	nd	0.00	nd	1	311	260
28			0.00	12.66	7812.40	0.12	0.51	3	285/319	260/305
29			0.00	12.82	4471.91	0.07	0.53	4	225/280	254
30	*p*-Hydroxybenzaldehyde (+?)	14.1380	0.55	13.16	27535.49	0.42	0.54	1	285	240

Spectrum no.	Peak identity	Std		4 M 24 hr Total phenolic extraction			Average RRT	Peak shape	Wavelength (nm)	
		RT	RRT	RT	Area	Area relative to tFA			Max	Min
31			0.00	13.32	18401.83	0.28	0.53	6or7	291/330	271/300
32			0.00	nd	nd	0.00	0.54	5	325	270
33			0.00	13.92	243338.28	3.69	0.56	4	220/277	248
34			0.00	nd	nd	0.00	0.57	2	298/318	266/308
35	Vanillin	15.2849	0.59	14.21	379186.13	5.75	0.58	2	279/310	250/296
36			0.00	14.38	nd	0.00	0.58	1	275	241
37			0.00	14.52	46123.64	0.70	0.59	5	310	260
38			0.00	14.74	761569.35	11.55	0.59	4	282	259
39	*trans*-*p*-Coumaric acid	16.1109	0.63	14.90	761569.35	11.55	0.61	5	225/310	249
40			0.00	15.20	225228.75	3.42	0.61	2 or 6	285/322	264/304
42	8,8'-DiFA (AT)		0.00	15.28	225228.75	3.42	0.62	7	246/335	273
43			0.00	15.39	225228.75	3.42	0.62	8	280/308	265/293
44	*trans*-Ferulic acid	16.9206	0.66	15.70	6591080.75	100.00	0.64	6	236/324	262
45	*cis*-*p*-Coumaric acid		0.00	nd	nd	0.00	0.65	1	300	257
46			0.00	nd	nd	0.00	0.67	7	330	270
47			0.00	16.13	153950.01	2.34	0.65	6	323	264
48			0.00	16.35	126014.50	1.91	0.67	3	277-284	254-261
49			0.00	16.58	937493.59	14.22	0.68	5	324	266
50	*cis*-Ferulic acid	18.0633	0.70	16.77	819789.21	12.44	0.69	5	314	261
51			0.00	17.11	88631.17	1.34	0.69	4	280	260
52			0.00	17.34	84369.19	1.28	0.71	3	286/325	256-265/310
53			0.00	17.96	27223.32	0.41	0.72	6	254/317	274
54			0.00	18.10	69768.56	1.06	0.74	3	233/287/320	256/310
55			0.00	nd	nd	0.00	0.74	5	322	275
56			0.00	18.40	186680.32	2.83	0.73	3	285/323	262/316
57			0.00	nd	nd	0.00	0.75	3	277/319	246/306
58			0.00	nd	nd	0.00	0.75	6	323	270
59			0.00	18.70	295328.53	4.48	0.75	5	320	273
60			0.00	18.83	724990.03	11.00	0.76	5	237/320	266

Spectrum no.	Peak identity	Std		4 M 24 hr Total phenolic extraction			Average	Peak	Wavelength (nm)	
		RT	RRT	RT	Area	Area relative to tFA	RRT	shape	Max	Min
61			0.00	nd	nd	0.00	0.77	5	240/321	271
62			0.00	18.94	72490.03	1.10	0.77	2	290/320	263/304
63			0.00	19.11	45359.11	0.69	0.76	2	285/316	265
64			0.00	19.27	64135.48	0.97	0.77	6	320	265
65			0.00	19.45	145018.23	2.20	0.77	5	319	266
66			0.00	nd	139324.42	2.11	0.80	2	286	261
67			0.00	19.59	nd	0.00	0.79	3	265/301	287
68	5,5'-DiFA		0.00	19.82	932284.23	14.14	0.80	5	246/325	273
69	5,5' right shoulder		0.00	nd	nd	0.00	0.82	6	322	266
70	5,5' a		0.00	nd	nd	0.00	0.84	6	321	265
71	5,5' b		0.00	20.31	304981.80	4.63	0.82	6	326	268
72			0.00	nd	nd	0.00	0.82	4	281	266
73			0.00	20.53	304981.80	4.63	0.82	2	290/320	264/302
74			0.00	20.83	24876.54	0.38	0.83	2	290/318	271/304
75			0.00	21.16	211801.38	3.21	0.85	5	316	270
76			0.00	21.62	76606.88	1.16	0.87	5	322	262
77	8-*O*-4'-DiFA		0.00	22.10	1563691.94	23.72	0.89	6	235/327	260
78	8-*O*-4' a		0.00	22.38	74347.21	1.13	0.90	5	321	270
79	8,5'-DiFA (BF)		0.00	22.85	88827.24	1.35	0.92	5	324	265
80	8,5' BF b		0.00	23.10	519915.50	7.89	0.93	5	325	267
81			0.00	nd	nd	0.00	0.95	6	323	270
82			0.00	23.64	nd	0.00	0.95	6	322	264
83			0.00	nd	nd	0.00	0.96	6	326	262
84			0.00	nd	nd	0.00	0.98	1	282	263
85			0.00	nd	nd	0.00	0.99	5	224/323	270
86	*trans*-Cinnamic acid	25.74	1.00	25.06	3865158.52	58.64	1.00	1	214/277	233
87			0.00	25.19	374414.95	5.68	1.00	5	234/309	259
88			0.00	25.63	272496.45	4.13	1.02	8	283	266
89			0.00	25.85	310012.81	4.70	1.03	2or6	290/325	263/305
90	Std unknown 4	26.8902	1.04	nd	nd	0.00	nd	4	227/278	217/256
91			0.00	nd	nd	0.00	1.04	2	287/321	267/308

G Biogel P-2 original chromatograms

The original UV chromatograms produced during the Biogel P-2 chromatography.

Run 1	
Chart speed	5 mm/min
Flow rate	0.42 ml/min
Fraction time	35 min
Time constant	10 s
Absorbance Units	2
Chart speed decreased from 5 mm/min to 0.5 mm/min during run	

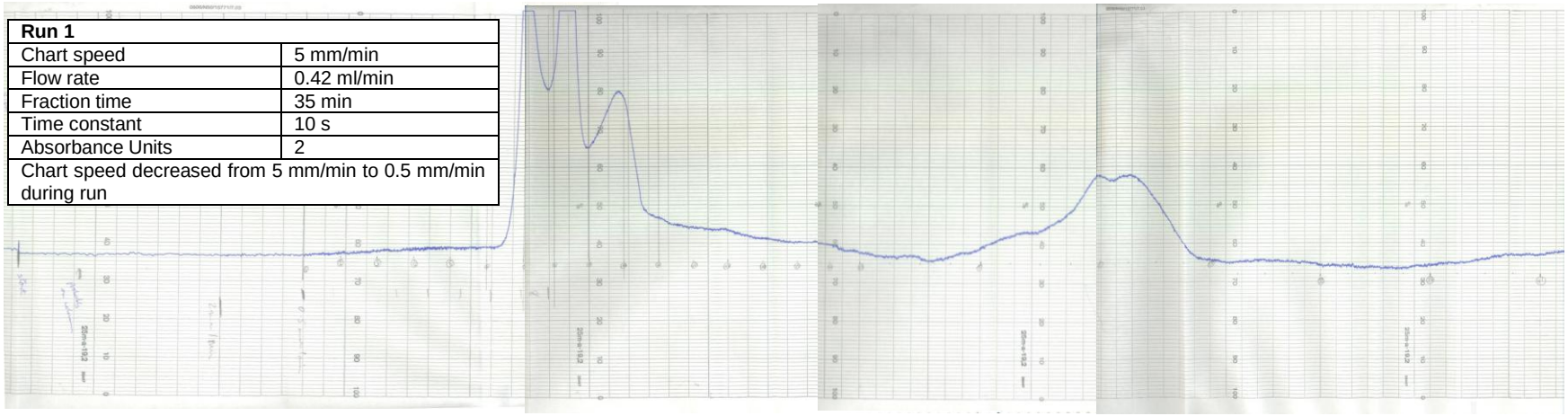

Run 2	
Chart speed	0.5 mm/min
Flow rate	0.42 ml/min
Fraction time	35 min
Time constant	10 s
Absorbance Units	2
UV detector broke down during run	

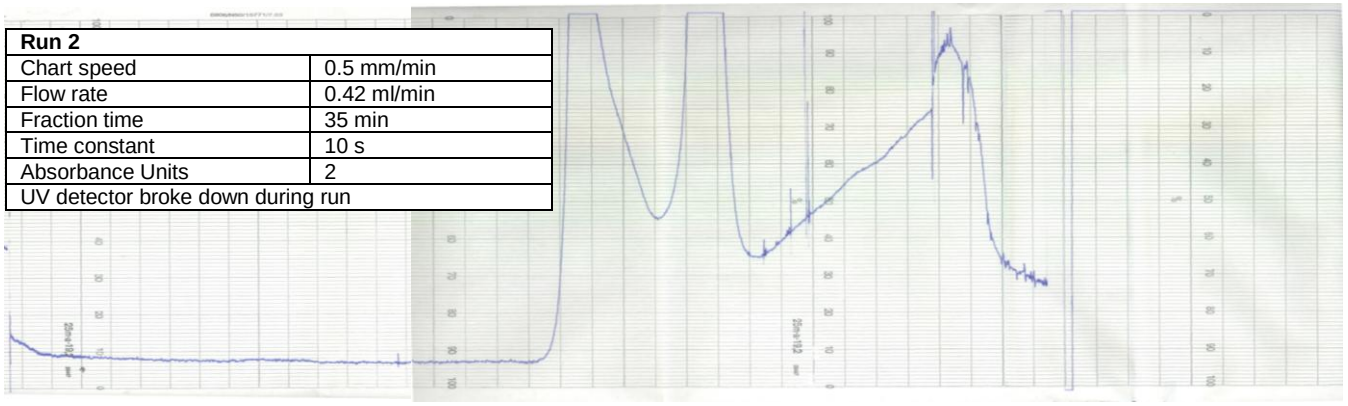

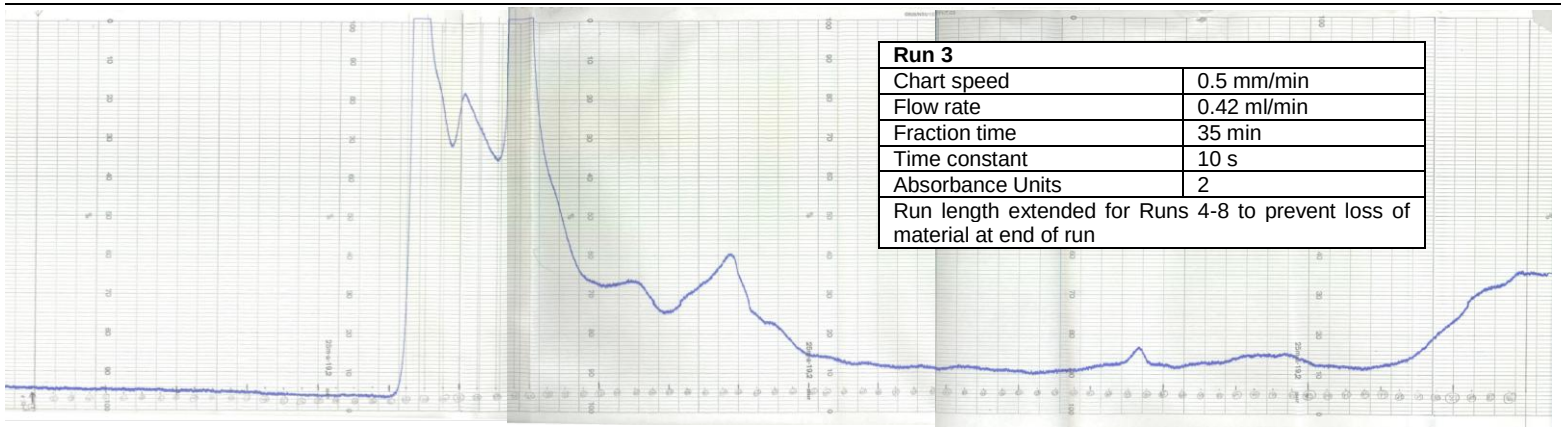

Run 3	
Chart speed	0.5 mm/min
Flow rate	0.42 ml/min
Fraction time	35 min
Time constant	10 s
Absorbance Units	2
Run length extended for Runs 4-8 to prevent loss of material at end of run	

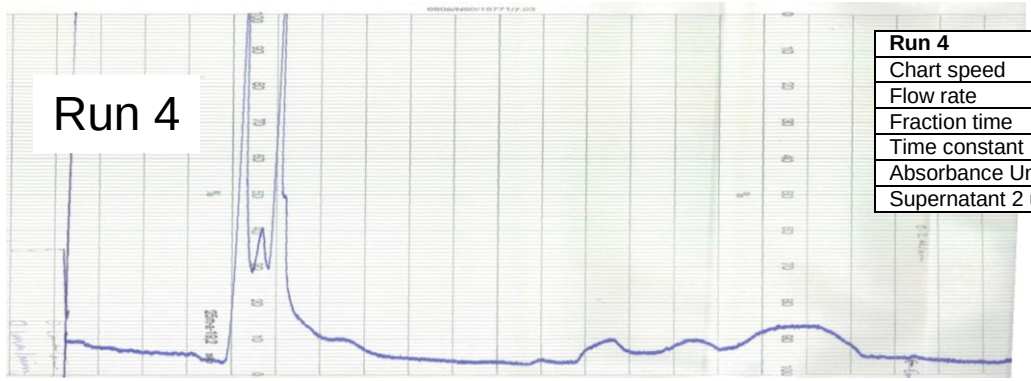

Run 4	
Chart speed	0.1 mm/min
Flow rate	0.42 ml/min
Fraction time	35 min
Time constant	10 s
Absorbance Units	2
Supernatant 2 used	

Run 5

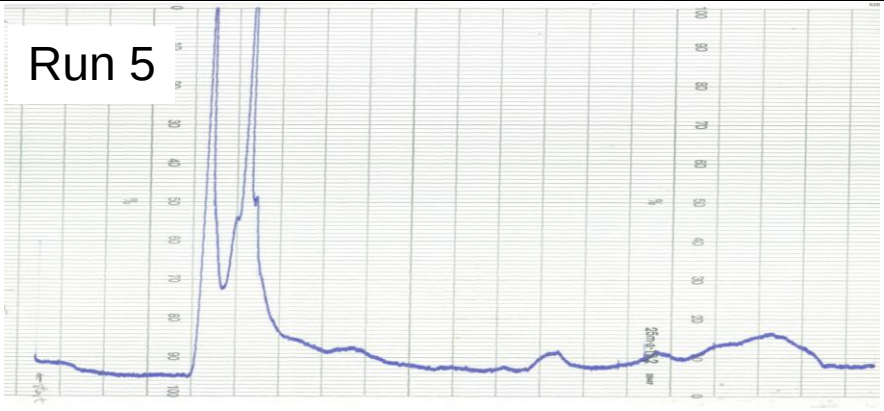

Run 5	
Chart speed	0.1 mm/min
Flow rate	0.42 ml/min
Fraction time	35 min
Time constant	10 s
Absorbance Units	2

Run 6

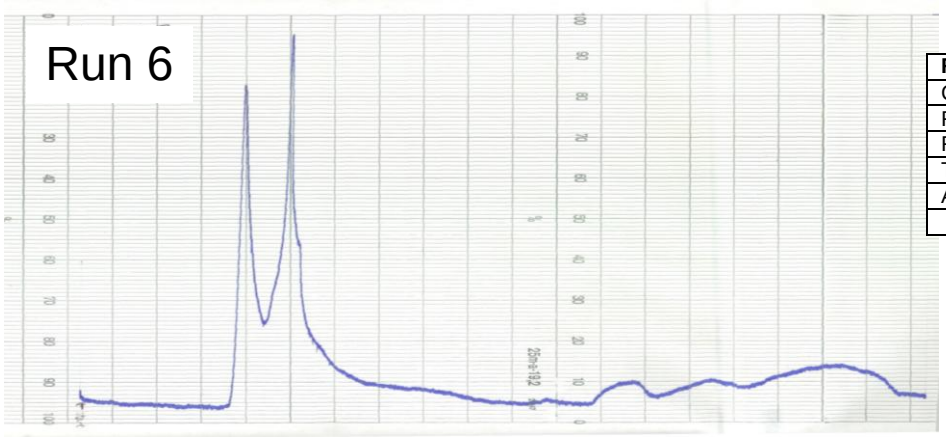

Run 6	
Chart speed	0.1 mm/min
Flow rate	0.42 ml/min
Fraction time	35 min
Time constant	10 s
Absorbance Units	2

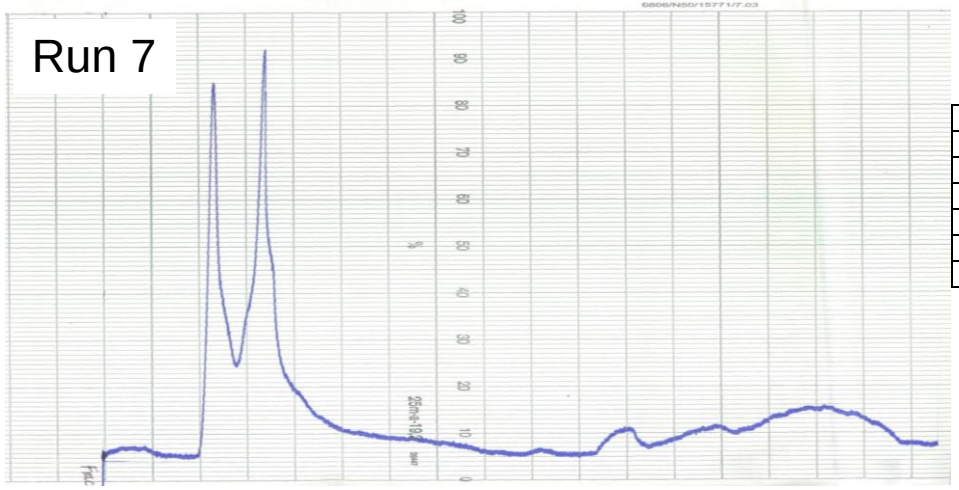

Run 7	
Chart speed	0.1 mm/min
Flow rate	0.42 ml/min
Fraction time	35 min
Time constant	10 s
Absorbance Units	2

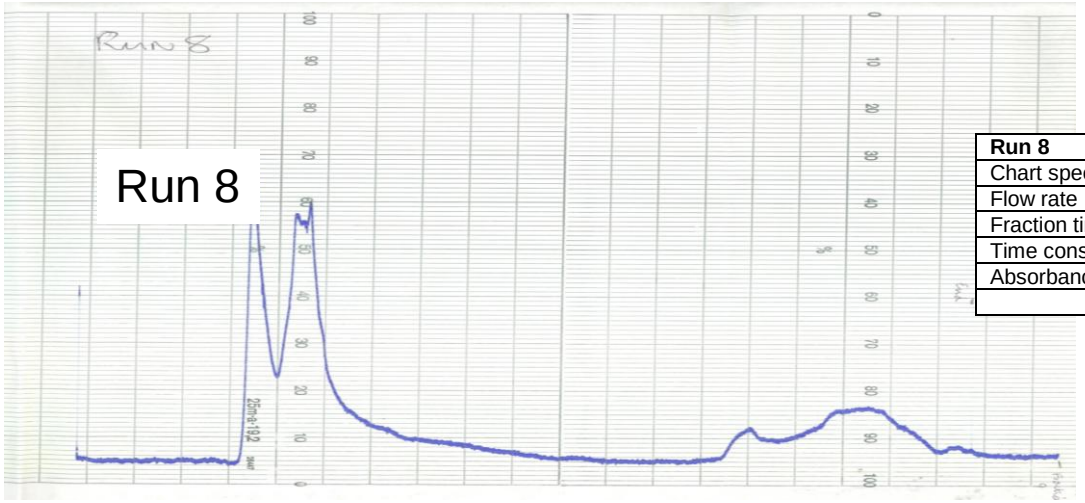

Run 8	
Chart speed	0.1 mm/min
Flow rate	0.42 ml/min
Fraction time	35 min
Time constant	10 s
Absorbance Units	2

The chromatograms for Runs 4-8 were more consistent than those for Runs 1-3 because very little time elapsed between the first and last runs (26 days), whereas for Runs 1-3 sigificant amounts of time elapsed between the first and last runs (79 days).

H Combining fractions from Biogel P-2

Biogel P-2 Run 4 numbered universal	Run 4 fraction	Run 5 fraction	Run 6 fraction		Run 7 numbered universal	Run 7 fraction	Run 8 fraction	
1	1	1	1		1	1	1	Peak 1
2	2	2	2		2	2	2	Peak 2
3	3	3	3		3	3	3	Peak 3
4	4	4	4		4	4	4	Peak 4
5	5	5	5		5	5	5	Peak 5
6	6	6	6		6	6	6	Peak 6
7	7	7	7		7	7	7	Peak 7
8	8	8	8		8	8	8	Peak 8
9	9	9	9		9	9	9	Peak 9
10	10	10	10		10	10	10	Peak 10
11	11	11	11		11	11	11	
12	12	12	12		12	12	12	
13	13	13	13		13	13	13	
14	14	14	14		14	14	14	
15	15	15	15		15	15	15	
16	16	16	16		16	16	16	
17	17	17	17		17	17	17	
18	18	18	18		18	18	18	
19	19	19	19		19	19	19	
20	20	20	20		20	20	20	
21	21	21	21, 22		21	21	21	
22	22	22	23		22	22	22	
23	23	23	24		23	23	23	
24	24	24	25		24	24	24	
25	25	25	26		25	25	25	
26	26	26	27		26	26	26	
27	27	27	28, 29		27	27	27	
28	28	28	-		28	28	28	
29	29	29	-		29	29	29	
30	30	30	30		30	30	30	
31	31	31	31		31	31	31	
32	32	32	32		32	32	32	
33	33	33	33		33	33	33	
34	34	34	34		34	34	34	
35	35	35	35		35	35	35	
36	36	36	36		36	36	36	
37	37	37	37		37	37	37	
38	38	38	38		38	38	38	
39	39	39	39		39	39	39	
40	40	40	40		40	40	40	
41	41	41	41		41	41	41	
42	42	42	42		42	42	42	
43	43	43	43		43	43	43	
44	44	44	44		44	44	44	
45	45	45	45		45	45	45	
46	46	46	46		46	46	46	
47	47	47	47		47	47	47	

Biogel P-2 Run 4 numbered universal	Run 4 fraction	Run 5 fraction	Run 6 fraction		Run 7 numbered universal	Run 7 fraction	Run 8 fraction	
48	48	48	48		48	48	48	Peak 1
49	49	49	49		49	49	49	Peak 2
50	50	50	50		50	50	50	Peak 3
51	51	51	51		51	51	51	Peak 4
52	52	52	52		52	52	52	Peak 5
53	53	53	53		53	53	53	Peak 6
54	54	54	54		54	54	54	Peak 7
55	55	55	55		55	55	55	Peak 8
56	56	56	56		56	56	56	Peak 9
57	57	57	57		57	57	57	Peak 10
58	58	58	58		58	58	58	
59	59	59	59		59	59	59	
60	60	60	60		60	60	60	
61	61	61	61		61	61	61	
62	62	62	62		62	62	62	
63	63	63	63		63	63	63	
64	64	64	64		64	64	64	
65	65	65	65		65	65	65	
66	66	66	66, 67		66	66	66	
67	67	67	68, 69		67	67	67	
68	68	68	70		68	68	68	
69	69	69	71		69	69	69	
70	70	70	72		70	70	70	
71	71	71	73		71	71	71	
72	72	72	74		72	72	72	
73	73	73	75		73	73	73	
74	74	74	76		74	74	74	
75	75	75	77		75	75	75	
76	76	76	78		76	76	76	
77	77	77	79		77	77	77	
78	78	78	80		78	78	78	
79	79	79	81		79	79	79	
80	80	80	82		80	80	80	
81	81	81	83		81	81	81	
82	82	82	84		82	82	82	
83	83	83	85		83	83	83	
84	84	84	86		84	84	84	
85	85	85	87		85	85	85	
86	86	86	88		86	86	86	
87	87	87	89		87	87	87	
88	88	88	90		88	88	88	
89	89	89	91		89	89	89	
90	90	90	92		90	90	90	
91	91	91	93		91	91	91	
92	92	92	94		92	92	92	
93	93	93	95		93	93	93	
94	94	94	-		94	94	94	
95	95	95	-		95	95	95	

I MicroToF parameters

Source:		
End plate offset	-500 V	128 nA
Capillary	4200 V	6 nA
Nebulizer	1.0 Bar	1.0 Bar
Dry gas	7.0 l/min	7.0 l/min
Dry temp	180°C	
Transfer:		
Capillary exit	100.0 V	
Skimmer	33.3 V	
Hexapole 1	21.5 V	
Skimmer 2	24.0 V	
Hexapole 2	23.0 V	
Hexapole RF	120.0 Vpp	
Detector	1000 V	
Lens 1 extraction	20.8 V	
Lens 1 transfer	52.0 µs	
Lens 1 pre puls storage	5.8 µs	
Mass range	50 to 1000 m/z	

J NMR parameters

PULPROG = lc1pnf2	Bruker pulse program with double solvent suppression (H_2O + CH_3CN)
TD = 32768	Number of data points
NS = 4000	Number of scans
SWH (Hz) = 12019.23	Spectral width
AQ (s) = 1.3632404	Acquisition time
D1 = 2.00000000	Delay time
P1 (µs) = 7.50	90 ° pulse width

K Microscopy of CWC leaves

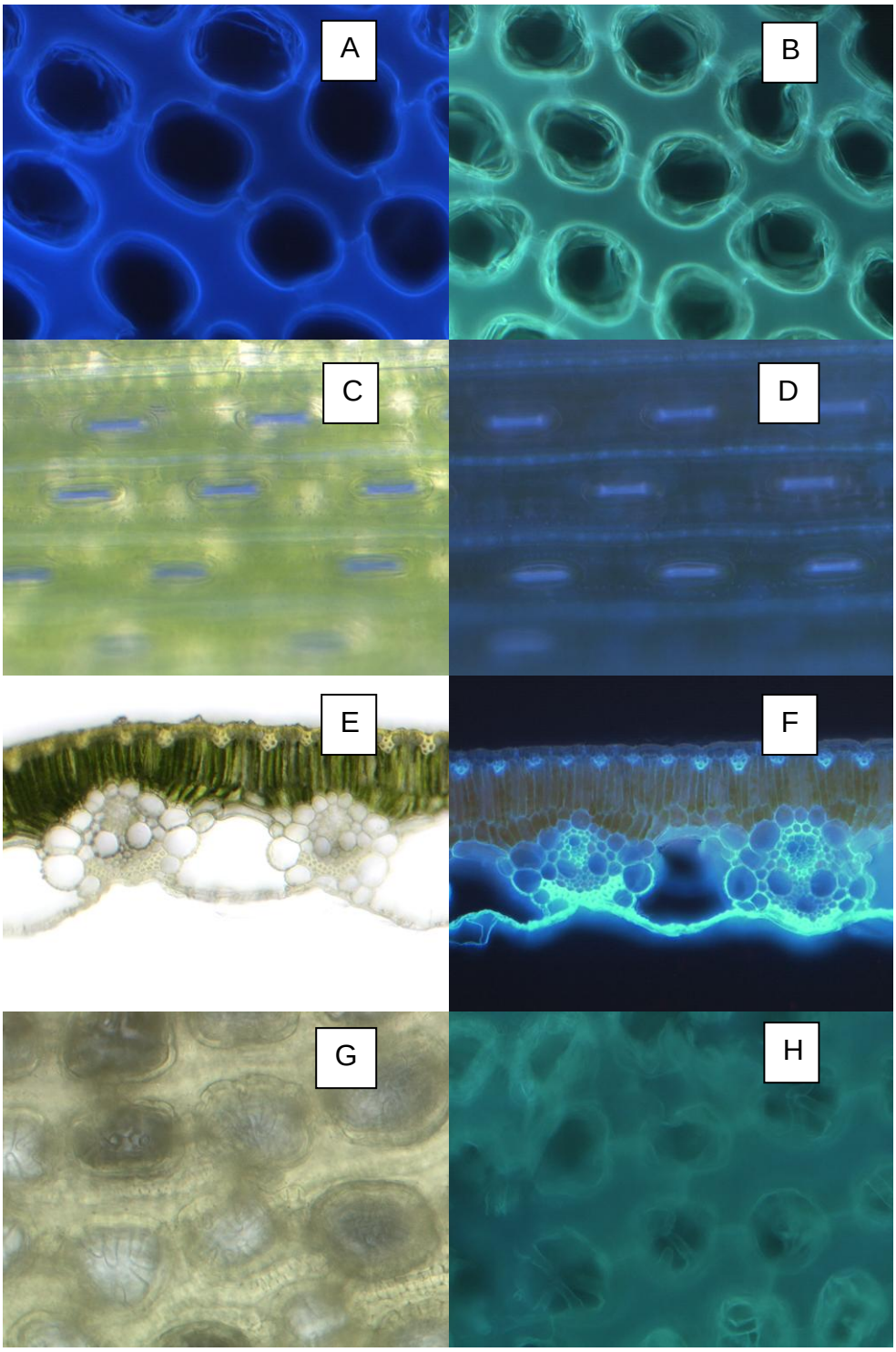

Figure 109: Micrographs of Chinese water chestnut leaf-cell walls: a, leaf septum, UV light, dark field; b, leaf septum in alkali, UV light, dark field; c, leaf epidermis, UV light, bright field; d, leaf epidermis, UV light, dark field; e, transverse section of leaf in alkali, bright field; f, transverse section of leaf, UV light, dark field; g, thickened leaf septum in alkali, bright field; h, thickened leaf septum in alkali, UV light, dark field.

11 Glossary:

2-DOG: 2-Deoxyglucose

4-*O*-5'-DiFA: 4-*O*-5' diferulic acid

5,5'-DiFA: 5,5' diferulic acid

8,5'-DiFA: 8,5' diferulic acid

8,5'-DiFA (BF): 8,5' diferulic acid (benzofuran form)

8,5'-DiFA (DC): 8,5' diferulic acid (decarboxylated form)

8,8'-DiFA: 8,8' diferulic acid

8,8'-DiFA (AT): 8,5' diferulic acid (aryltetralin form)

8,8'-DiFA (THF): 8,8' diferulic acid (tetrahydrofuran form)

8-*O*-4'-DiFA: 8-*O*-4' diferulic acid

ACN: Acetonitrile

Ara: Arabinose

CWC: Chinese water chestnut (*Eleocharis dulcis*)

CWM: Cell wall material

DiFA: Diferulic acid

ECWM: Epidermis cell wall material

EtOH: Ethanol

FAE: Feruloyl esterase

Fuc: Fucose

Gal: Galactose

GalA: Galacturonic acid

GC: Gas chromatography

Glc: Glucose

GlcA: Glucuronic acid

HPLC: High performance liquid chromatography

IDF: Insoluble dietary fibre

LC-MS: Liquid chromatography – mass spectrometry

Man: Mannose

MeOH: Methanol

MWCO: Molecular weight cut off

NMR: Nuclear magnetic resonance

PCWM: Parenchyma cell wall material

PDA: pH dependent autofluorescence

PGA: Polygalcturonan

PPCO: Polypropylene copolymer

Rha: Rhamnose

SECWM: Secondary epidermis cell wall material

t-: Terminal sugar residue

TetraFA: Tetraferulic acid

TriFA: Triferulic acid

Xyl: Xylose

12 References:

Abdel-Aal, E-S M, Hucl, P, Sosulski, F W, Graf, R, Gillot, C, and Pietrzak, L. (2001) Screening spring wheat for midge resistance in relation to ferulic acid content. J Agr Food Chem 49:3559-3566.

Albersheim, P and Anderson, A J. (1971) Host-pathogen interactions. 3. Proteins from plant cell walls inhibit polygalacturonases secreted by plant pathogens. P Natl Acad Sci USA 68:1815-1819.

Allerdings, E, Ralph, J, Schatz, P F, Gniechwitz, D, Steinhart, H, and Bunzel, M. (2005) Isolation and structural identification of diarabinosyl 8-O-4-dehydrodiferulate from maize bran insoluble fibre. Phytochemistry 66:113-124.

Allerdings, E, Ralph, J, Steinhart, H, and Bunzel, M. (2006) Isolation and structural identification of complex feruloylated heteroxylan side-chains from maize bran. Phytochemistry 67:1276-1286.

Andreasen, M F, Kroon, P A, Williamson, G, and Garcia-Conesa, M-T. (2001a) Esterase activity able to hydrolyze dietary antioxidant hydroxycinnamates is distributed along the intestine of mammals. J Agr Food Chem 49:5679-5684.

Andreasen, M F, Kroon, P A, Williamson, G, and Garcia-Conesa, M-T. (2001b) Intestinal release and uptake of phenolic antioxidant diferulic acids. Free Radical Bio Med 31:304-314.

Ardiansyah, Shirakawa, H, Koseki, T, Ohinata, K, Hashizume, K, and Komai, M. (2006) Rice bran fractions improve blood pressure, lipid profile, and glucose metabolism in stroke-prone spontaneously hypertensive rats. J Agr Food Chem 54:1914-1920.

Baba, K, Sone, Y, Misaki, A, and Hayashi, T. (1994) Localization of xyloglucan in the macromolecular complex composed of xyloglucan and cellulose in pea stems. Plant Cell Physiol 35:439-444.

Bidlack, J, Malone, M, and Benson, R. (1992) Molecular structure and component integration of secondary cell walls in plants. Proc Okla Acad Sci 72:51-56.

Blakeney, A B and Stone, B A. (1985) Methylation of carbohydrates with lithium methylsulphinyl carbanion. Carbohyd Res 140:319-324.

Bonnin, E, Dolo, E, Le Goff, A, and Thibault, J-F. (2002) Characterisation of pectin subunits released by an optimised combination of enzymes. Carbohyd Res 337:1687-1696.

Borneman, W S, Hartley, R D, Himmelsbach, D S, and Ljungdahl, L G. (1990) Assay for *trans*-para-coumaroyl esterase using a specific substrate from plant-cell walls. Anal Biochem 190:129-133.

Bounias, M. (1980) *N*-(1-Naphthyl) ethylene diamine dihydrochloride as a new reagent for nanomole quantification of sugars on thin-layer plates by a mathematical calibration process. Anal Biochem 106:291-295.

Brecht, J K. (2004) Waterchestnut in Agriculture handbook number 66: The commercial storage of fruits, vegetables, and florist and nursery stocks. Gross, K C, Wang, C Y, and Saltveit, M (Eds.) USDA, http://www.ba.ars.usda.gov/hb66/141waterchestnut.pdf

Brett, C T and Waldron, K W. (1996) Physiology and biochemistry of plant cell walls. Chapman & Hall, London, UK. ISBN 0412580608

Bunzel, M, Ralph, J, Marita, J M, and Steinhart, H. (2000) Identification of 4-O-5'-coupled diferulic acid from insoluble cereal fiber. J Agr Food Chem 48:3166-3169.

Bunzel, M, Allerdings, E, Sinwell, V, Ralph, J, and Steinhart, H. (2002) Cell wall hydroxycinnamates in wild rice (*Zizania aquatica* L.) insoluble dietary fibre. Eur Food Res Technol 214:482-488.

Bunzel, M, Ralph, J, Funk, C, and Steinhart, H. (2003a) Isolation and identification of a ferulic acid dehydrotrimer from saponified maize bran insoluble fiber. Eur Food Res Technol 217:128-133.

Bunzel, M, Ralph, J, Kim, H, Lu, F, Ralph, S A, Marita, J M, Hatfield, R D, and Steinhart, H. (2003b) Sinapate dehydrodimers and sinapate-ferulate heterodimers in cereal dietary fiber. J Agr Food Chem 51:1427-1434.

Bunzel, M, Ralph, J, and Steinhart, H. (2004) Phenolic compounds as cross-links of plant derived polysaccharides. Czech J Food Sci 22:64-67.

Bunzel, M, Ralph, J, Funk, C, and Steinhart, H. (2005) Structural elucidation of new ferulic acid-containing phenolic dimers and trimers isolated from maize bran. Tetrahedron Lett 46:5845-5850.

Bunzel, M, Ralph, J, Brüning, P, and Steinhart, H. (2006) Structural identification of dehydrotriferulic and dehydrotetraferulic acids isolated from insoluble maize fiber. J Agr Food Chem 54:6409-6418.

Bunzel, M, Allerdings, E, Ralph, J, and Steinhart, H. (2008) Cross-linking of arabinoxylans via 8-8-coupled diferulates as demonstrated by isolation and identification of diarabinosyl 8-8(cyclic)-dehydrodiferulate from maize bran. J Cereal Sci 47:29-40.

Burk, D H and Ye, Z-H. (2002) Alteration of oriented deposition of cellulose microfibrils by mutation of a katanin-like microtubule-severing protein. The Plant Cell 14:2145-2160.

Carnachan, S M and Harris, P J. (2000) Ferulic acid is bound to the primary cell walls of all gymnosperm families. Biochem Syst Ecol 28:865-879.

Carpita, N C and Gibeaut, D M. (1993) Structural models of primary-cell walls in flowering plants - consistency of molecular-structure with the physical-properties of the walls during growth. Plant Journal 3:1-30.

Carpita, N C, Defernez, M, Findlay, K, Wells, B, Shoue, D A, Catchpole, G, Wilson, R H, and McCann, M C. (2001) Cell wall architecture of the elongating maize coleoptile. Plant Physiol 127:551-565.

Chesson, A, Provan, G J, Russell, W R, Scobbie, L, Richardson, A J, and Stewart, C. (1999) Hydroxycinnamic acids in the digestive tract of livestock and humans. J Sci Food Agr 79:373-378.

Choudhury, R, Srai, S K, Debnam, E, and Rice-Evans, C A. (1999) Urinary excretion of hydroxycinnamates and flavonoids after oral and intravenous administration. Free Radical Bio Med 27:278-286.

Christophoridou, S, Dais, P, Tseng, L-H, and Spraul, M. (2007) Separation and identification of phenolic compounds in olive oil by coupling high-performance liquid chromatography with postcolumn solid-phase extraction to nuclear magnetic resonance spectroscopy (LC-SPE-NMR). J Agr Food Chem 53:4667-4679.

Clausen, M H, Willats, W G T, and Knox, J P. (2003) Synthetic methyl hexagalacturonate hapten inhibitors of antihomogalacturonan monoclonal antibodies LM7, JIM5 and JIM7. Carbohyd Res 338:1797-1800.

Clausen, M H, Ralet, M C, Willats, W G T, McCartney, L, Marcus, S E, Thibault, J-F, and Knox, J P. (2004) A monoclonal antibody to feruloylated-(1→4)-beta-D-galactan. Planta 219:1036-1041.

Cline, K and Albersheim, P. (1981) Host-pathogen interactions. 17. Hydrolysis of biologically-active fungal glucans by enzymes isolated from soybean cells. Plant Physiol 68:221-228.

Coimbra, M A, Rigby, N M, Selvendran, R R, and Waldron, K W. (1995) Investigation of the occurrence of xylan-xyloglucan complexes in the cell walls of olive pulp (*Olea europaea*). Carbohyd Polym 27:277-284.

Colquhoun, I J, Ralet, M C, Thibault, J-F, Faulds, C B, and Williamson, G. (1994) Structure identification of feruloylated oligosaccharides from sugar-beet pulp by NMR spectroscopy. Carbohyd Res 263:243-256.

Cosgrove, D J. (1999) Enzymes and other agents that enhance cell wall extensibility. Ann Rev Plant Physiol Plant Mol Biol 50:391-417.

Cosgrove, D J. (2001) Wall structure and wall loosening. A look backwards and forwards. Plant Physiol 125:131-134.

Cosgrove, D J. (2005) Growth of the plant cell wall. Nature Reviews 6:850-860.

Crepin, V F, Faulds, C B, and Connerton, I F. (2004) Functional classification of the microbial feruloyl esterases. Appl Microbiol Biot 63: 647–652

Darvill, A G, McNeil, M, and Albersheim, P. (1978) Structure of plant cell walls. VIII. A new pectic polysaccharide. Plant Physiol 62:418-422.

Darvill, A, McNeil, M, Albersheim, P, and Delmer, D. (1980) The plant cell in the primary cell walls of flowering plants. In The Biochemistry of Plants: A comprehensive treatise, Volume 1. Academic Press, New York, USA. ISBN 0126754047

Deobald, L A and Crawford, D L. (1987) Activities of cellulase and other extracellular enzymes during lignin solubilization by *Streptomyces viridosporus*. Appl Microbiol Biot 26:158-163.

Dubois, M, Gilles, K A, Hamilton, J K, Rebers, P A, and Smith, F. (1956) Colorimetric method for determination of sugars and related substances. Anal Chem 28:350-356.

El Modafar, C and El Boustani, E. (2001) Cell wall-bound phenolic acid and lignin contents in date palm as related to its resistance to *Fusarium oxysporum*. Biol Plantarum 44:125-130.

Emons, A M C and Mulder, B M. (2000) How the deposition of cellulose microfibrils builds cell wall architecture. Trends Plant Sci 5:35-40.

Encina, A and Fry, S C. (2005) Oxidative coupling of a feruloyl-arabinoxylan trisaccharide (FAXX) in the walls of living maize cells requires endogenous hydrogen peroxide and is controlled by a low-M_r apoplastic inhibitor. Planta 223:77-89.

Exarchou, V, Godejohann, M, van Beek, T A, Gerothanassis, I P, and Vervoort, J. (2003) LC-UV-Solid-Phase-Extraction-NMR-MS combined with a cryogenic flow probe and its application to the identification of compounds present in Greek oregano. Anal Chem 75:6288-6294.

Faulds, C B and Williamson, G. (1995) Release of ferulic acid from wheat bran by a ferulic acid esterase (FAE-III) from *Aspergillus niger*. Appl Microbiol Biot 43:1082-1087.

Faulds, C B and Williamson, G. (1999) The role of hydroxycinnamates in the plant cell wall. J Sci Food Agr 79:393-395.

Femenia, A, Rigby, N M, Selvendran, R R, and Waldron, K W. (1999a) Investigation of the occurrence of pectic-xylan-xyloglucan complexes in the cell walls of cauliflower stem tissues. Carbohyd Polym 39:151-164.

Femenia, A, Waldron, K W, Robertson, J A, and Selvendran, R R. (1999b) Compositional and structural modification of the cell wall of cauliflower (*Brassica oleracea* L var botrytis) during tissue development and plant maturation. Carbohyd Polym 39:101-108.

Ferguson, L R, Fong Lim, I, Pearson, A E, Ralph, J, and Harris, P J. (2003) Bacterial antimutagenesis by hydroxycinnamic acids from plant cell walls. Mutat Res 542:49-58.

Fry, S C. (1979) Phenolic components of the primary cell wall and their possible role in the hormonal regulation of growth. Planta 146:343-351.

Fry, S C. (1982) Phenolic components of the primary cell wall. Biochem J 203:493-504.

Fry, S C. (1983) Feruloylated pectins from the primary cell wall: their structure and possible functions. Planta 157:111-123.

Fry, S C. (1986) Cross-linking of matrix polymers in the growing cell walls of angiosperms. Ann Rev Plant Physio 37:165-186.

Fry, S C. (1987) Intracellular feruloylation of pectic polysaccharides. Planta 171:205-211.

Fry, S C. (1988) The Growing Plant Cell Wall: Chemical and metabolic analysis. Longman Scientific & Technical, Harlow, UK. ISBN 0582018978

Fry, S C. (2003) Primary cell wall metabolism: tracking the careers of wall polymers in living plant cells. New Phytol 161:641-675.

Fry, S C, Willis, S C, and Paterson, A E J. (2000) Intraprotoplasmic and wall-localised formation of arabinoxylan-bound diferulates and larger ferulate coupling-products in maize cell-suspension cultures. Planta 211:679-692.

Funk, C, Ralph, J, Steinhart, H, and Bunzel, M. (2005) Isolation and structural characterisation of 8-*O*-4/8-*O*-4- and 8-8/8-*O*-4-coupled dehydrotriferulic acids from maize bran. Phytochemistry 66:363-371.

Funk, C, Braune, A, Grabber, J H, Steinhart, H, and Bunzel, M. (2007) Moderate ferulate and diferulate levels do not impede maize cell wall degradation by human intestinal microbiota. J Agr Food Chem 55:2418-2423.

Garcia-Conesa, M-T, Plumb, G W, Waldron, K W, Ralph, J, and Williamson, G. (1997) Ferulic acid dehydrodimers from wheat bran: isolation, purification and antioxidant properties of 8-O-4-diferulic acid. Redox Rep 3:319-323.

Gardner, K H and Blackwell, J. (1974) Structure of native cellulose. Biopolymers 13:1975-2001.

Gardner, S L, Burrell, M M, and Fry, S C. (2002) Screening of *Arabidopsis thaliana* stems for variation in cell wall polysaccharides. Phytochemistry 60:241-254.

Geissman, T and Neukom, H. (1971) Vernetzung von Phenolcarbonsäure-estern von Polysacchariden durch oxydative phenolische Kupplung. Helv Chim Acta 54:1108-1112.

Grabber, J H, Hatfield, R D, and Ralph, J. (1996) Altering lignin-composition, structure and cross-linking: Potential impact on cell wall degradation. Abstr Pap Am Chem S 211:54.

Grabber, J H, Ralph, J, and Hatfield, R D. (2000) Cross-linking of maize walls by ferulate dimerization and incorporation into lignin. J Agr Food Chem 48:6106-6113.

Gubler, F, Ashford, A E, Bacic, A, Blakeney, A B, and Stone, B A. (1985) Release of ferulic acid esters from barley aleurone. II. Characterization of the feruloyl compounds released in response to GA3. Aust J Plant Physiol 12:307-317.

Guillon, F, Tranquet, O, Quillien, L, Utille, J P, Juan Ordaz Ortiz, J, and Saulnier, L. (2004) Generation of polyclonal and monoclonal antibodies against arabinoxylans and their use for immunocytochemical location of arabinoxylans in cell walls of endosperm wheat. J Cereal Sci 40:167-182.

Gunawardena, A H L A, Greenwood, J S, and Dengler, N G. (2007) Cell wall degradation and modification during programmed cell death in lace plant, *Aponogeton madagascariensis* (*Aponogetonaceae*). Am J Bot 94:1116-1128.

Hanley, A B, Russell, W R, and Chesson, A. (1993) Formation of substituted truxillic and truxinic acids in plant cell walls-a rationale. Phytochemistry 33:957-960.

Harris, P J and Hartley, R D. (1980) Phenolic constituents of the cell walls of monocotyledons. Biochem Syst Ecol 8:153-160.

Harris, P J, Henry, R J, Blakeney, A B, and Stone, B A. (1984) An improved procedure for the methylation analysis of oligosaccharides and polysaccharides. Carbohyd Res 127:59-73.

Hartley, R D and Jones, E C. (1975) Effect of ultraviolet light on substituted cinnamic acids and the estimation of their *cis* and *trans* isomers by gas chromatography. J Chromatogr 107:213-218.

Hartley, R D and Jones, E C. (1976) Diferulic acid as a component of cell walls of *Lolium multiflorum*. Phytochemistry 15:1157-1160.

Hartley, R D and Morrison, W H. (1991) Monomeric and dimeric phenolic acids released from cell walls of grasses by sequential treatment with sodium hydroxide. J Sci Food Agr 55:365-375.

Hatfield, R D and Ralph, J. (1999) Modelling the feasibility of intramolecular dehydrodiferulate formation in grass walls. J Sci Food Agr 79:425-427.

Hoebler, C and Brillouet, J-M. (1984) Purification and properties of an endo-(1→4)-β-D-xylanase from *Irpex lacteus* (*Polyporus tulipiferae*). Carbohyd Res 128:141-155.

Huang, D, Ou, B, and Prior, R L. (2005) The chemistry behind antioxidant capacity essays. J Agr Food Chem 53:1841-1856.

Iiyama, K, Lam, T B T, and Stone, B A. (1990) Phenolic acid bridges between polysaccharides and lignin in wheat internodes. Phytochemistry 29:733-737.

Iiyama, K, Lam, T B T, and Stone, B A. (1994) Covalent cross-links in the cell wall. Plant Physiol 104:315-320.

Ishii, S. (1982) Enzymatic extraction and linkage analysis of pectic polysaccharides from onion. Phytochemistry 21:778-780.

Ishii, T. (1991) Isolation and characterization of a diferuloyl arabinoxylan hexasaccharide from bamboo shoot cell-walls. Carbohyd Res 219:15-22.

Ishii, T. (1997) Structure and functions of feruloylated polysaccharides. Plant Sci 127:111-127.

Ishii, T and Hiroi, T. (1990) Linkage of phenolic acids to cell-wall polysaccharides of bamboo shoot. Carbohyd Res 206:297-310.

Ishii, T and Tobita, T. (1993) Structural characterization of feruloyl oligosaccharides from spinach-leaf cell walls. Carbohyd Res 248:179-190.

Ishii, T, Hiroi, T, and Thomas, J R. (1990) Feruloylated xyloglucan and *p*-coumaroyl arabinoxylan oligosaccharides from bamboo shoot cell-walls. Phytochemistry 29:1999-2003.

Jamet, E, Canut, H, Boudart, G, and Pont-Lezica, R F. (2006) Cell wall proteins: a new insight through proteomics. Trends Plant Sci 11:33-39.

Jones, L, Seymour, G B, and Knox, J P. (1997) Localization of pectic galactan in tomato cell walls using a monoclonal antibody specific to (1→4)-beta-D-galactan. Plant Physiol 113:1405-1412.

Juge, N. (2006) Plant protein inhibitors of cell wall degrading enzymes. Trends Plant Sci 11:359-367.

Kahnt, G. (1967) *Trans-cis*-equilibrium of hydroxycinnamic acids during irradiation of aqueous solutions at different pH. Phytochemistry 6:755-758.

Kanda, T, Nakakubo, S, Wakabayashi, K, and Nisizawa, K. (1978) Purification and properties of an exo-cellulase of avicellulase type from a wood-rotting fungus, *Irpex lacteus* (*Polyporus tulipiferae*). J Biochem-Tokyo 84:1217-1226.

Keegstra, K, Talmadge, K W, Bauer, W D, and Albersheim, P. (1973) Structure of plant-cell walls. 3. Model of walls of suspension-cultured sycamore cells based on interconnections of macromolecular components. Plant Physiol 51:188-196.

Kern, S M, Bennett, R N, Needs, P W, Mellon, F A, Kroon, P A, and Garcia-Conesa, M-T. (2003) Characterization of metabolites of

hydroxycinnamates in the in vitro model of human small intestinal epithelium caco-2 cells. J Agr Food Chem 51:7884-7891.

Kerr, E M and Fry, S C. (2004) Extracellular cross-linking of xylan and xyloglucan in maize cell-suspension cultures: the role of oxidative phenolic coupling. Planta 219:73-83.

Kirby, A R, Gunning, A P, Waldron, K W, Morris, V J, and Ng, A. (1996) Visualization of plant cell walls by atomic force microscopy. Biophys J 70:1138-1143.

Klok, E J, Wilson, I W, Wilson, D, Chapman, S C, Ewing, R M, Somerville, S C, Peacock, W J, Dolferus, R, and Dennis, E S. (2002) Expression profile analysis of the low-oxygen response in Arabidopsis root cultures. The Plant Cell 14:2481-2494.

Knox, J P, Linstead, P J, Peart, J, Cooper, C, and Roberts, K. (1991) Developmentally regulated epitopes of cell-surface arabinogalactan proteins and their relation to root-tissue pattern-formation. Plant J 1:317-326.

Kremer, C, Pettolino, F, Bacic, A, and Drinnan, A. (2004) Distribution of cell wall components in *Sphagnum* hyaline cells and in liverwort and hornwort elators. Planta 219:1023-1035.

Kroon, P A, Faulds, C B, Ryden, P, Robertson, J A, and Williamson, G. (1997) Release of covalently bound ferulic acid from fiber in the human colon. J Agr Food Chem 45:661-667.

Lack, A J and Evans, D E. (2001) Plant Biology. BIOS Scientific Publishers Ltd, Oxford, UK. ISBN 1859961975

Lamport, D T A, Epstein, L. (1983) A new model for the primary-cell wall based on a concatenated extensin-cellulose network. In Current Topics in Plant Biochemistry and Physiology, Volume 2. Randall, D D, Blevins, D G, Larson, R L, Rapp, B J, (Eds). University of Missouri, Columbia, USA.

Lattanzio, V, De Cicco, V, Di Venere, D, Lima, G, and Salerno, M. (1994) Antifungal activity of phenolics against fungi commonly found encountered during storage. Ital J Food Sci 6:23-30.

Lempereur, I, Rouau, X, and Abecassis, J. (1997) Genetic and agronomic variation in arabinoxylan and ferulic acid contents of durum wheat (*Triticum durum* L.) grain and its milling fractions. J Cereal Sci 25:103-110.

Levigne, S, Thomas, M, Ralet, M C, Quéméner, B C, and Thibault, J-F. (2002) Determination of the degrees of methylation and acetylation of pectins using a C18 column and internal standards. Food Hydrocolloid 16:547-550.

Levigne, S, Ralet, M C, Quéméner, B C, Pollet, B, Lapierre, C, and Thibault, J-F. (2004a) Isolation from sugar beet cell walls of arabinan oligosaccharides esterified by two ferulic acid monomers. Plant Physiol 134:1173-1180.

Levigne, S, Ralet, M C, Quéméner, B C, and Thibault, J-F. (2004b) Isolation of diferulic bridges ester-linked to arabinan in sugar beet cell walls. Carbohyd Res 339:2315-2319.

Liu, R H. (2004) Potential synergy of phytochemicals in cancer prevention: mechanism of action. J Nutr 134:3479S-3485S.

Loh, J and Breene, W M. (1981) The thermal fracturability loss of edible plant-tissue - pattern and within-species variation. J Texture Stud 12:456-471.

Lozovaya, V V, Gorshkova, T A, Yablokova, E V, Rumyantseva, N I, Valieva, A, Ulanov, A, and Widholm, J M. (1999) Cold alkali can extract phenolic acids that are ether linked to cell wall components in dicotyledonous plants (buckwheat, soybean and flax). Phytochemistry 50:395-400.

MacAdam, J W and Grabber, J H. (2002) Relationship of growth cessation with the formation of diferulate cross-links and *p*-coumaroylated lignins in tall fescue leaf blades. Planta 215:785-793.

MacCormick, C A, Harris, J E, Gunning, A P, and Morris, V J. (1993) Characterization of a variant of the polysaccharide acetan produced by a mutant of *Acetobacter xylinum* strain CR1/4. J Appl Bacteriol 74:196-199.

Mandalari, G, Faulds, C B, Sancho, A I, Saija, A, Bisignano, G, LoCurto, R, and Waldron, K W. (2005) Fractionation and characterisation of arabinoxylans from brewers' spent grain and wheat bran. J Cereal Sci 42:205-212.

Mankarios, A T, Hall, M A, Jarvis, M C, Threlfall, D R, and Friend, J. (1980) Cell wall polysaccharides from onions. Phytochemistry 19:1731-1733.

Marry, M, Roberts, K, Jopson, S J, Huxham, I M, Jarvis, M C, Corsar, J, Robertson, E, and McCann, M C. (2006) Cell-cell adhesion in fresh sugar-beet root parenchyma requires both pectin esters and calcium cross-links. Physiol Plantarum 126:243-256.

Massiot, P, Rouau, X, and Thibault, J-F. (1988) Isolation and characterisation of the cell-wall fibres of carrot. Carbohyd Res 172:217-227.

Masuko, T, Minami, A, Iwasaki, N, Majima, T, Nishimura, S-I, and Lee, Y C. (2005) Carbohydrate analysis by a phenol-sulfuric acid method in microplate format. Anal Biochem 339:69-72.

May, C D. (1990) Industrial pectins: Sources, production and applications. Carbohyd Polym 12:79-99.

May, C D. (2000) Pectins. In Handbook of Hydrocolloids. Phillips, G O and Williams, P A (Eds.) Woodhead Publishing, Cambridge, UK. ISBN 1855735016

McCann, M C, Wells, B, and Roberts, K. (1990) Direct visualization of cross-links in the primary plant cell wall. J Cell Sci 96:323-334.

McCann, M C, Wells, B, and Roberts, K. (1992) Complexity in the spatial localization and length distribution of plant cell-wall matrix polysaccharides. J Microsc-Oxford 166:123-136.

McCartney, L and Knox, J P. (2002) Regulation of pectic polysaccharide domains in relation to cell development and cell properties in the pea testa. J Exp Bot 53:707-713.

McCartney, L, Marcus, S E, and Knox, J P. (2005) Monoclonal antibodies to plant cell wall xylans and arabinoxylans. J Histochem Cytochem 53:543-546.

McCleary, B V. (1979) Enzymic hydrolysis, fine structure, and gelling interaction of legume-seed D-galacto-D-mannans. Carbohyd Res 71:205-230.

McDougall, G J and Fry, S C. (1988) Inhibition of auxin-stimulated growth of pea stem segments by a specific nonasaccharide of xyloglucan. Planta 175:412-416.

McNeil, M, Albersheim, P, Taiz, L, and Jones, R L. (1975) The structure of plant cell walls. VII. Barley aleurone cells. Plant Physiol 55:64-68.

McNeil, M, Darvill, A G, Fry, S C, and Albersheim, P. (1984) Structure and function of the primary cell walls of plants. Anna Rev Biochem 53:625-663.

Mellon, F A. (2000) Introduction to principles and practice of mass spectrometry. In Mass Spectrometry of Natural Substances in Food. RSC, Cambridge, UK. ISBN 0845045716.

Merali, Z, Mayer, M J, Parker, M L, Michael, A J, and Smith, A C. (2007) Metabolic diversion of the phenylpropanoid pathway causes cell wall and morphological changes in transgenic tobacco stems. Planta 225:1165-1178

Micard, V, Grabber, J H, Ralph, J, Renard, C M G C, and Thibault, J-F. (1997a) Dehydrodiferulic acids from sugar-beet pulp. Phytochemistry 44:1365-1368.

Micard, V, Renard, C M G C, Colquhoun, I J, and Thibault, J-F. (1997b) End-products of enzymic saccharification of beet pulp, with a special attention to feruloylated oligosaccharides. Carbohyd Polym 32:283-292.

Midmore, D. (1997) Chinese waterchestnut. The New Rural Industries: A Handbook for Farmers and Investors. Available at: http://www.rirdc.gov.au/pub/handbook/chinwchst.html.

Mort, A J and Lamport, D T A. (1977) Anhydrous hydrogen-fluoride deglycosylates glycoproteins. Anal Biochem 82:289-309.

Mort, A J, Parker, S, and Kuo, M-S. (1983) Recovery of methylated saccharides from methylation reaction mixtures using Sep-Pak C_{18} cartridges. Anal Biochem 133:380-384.

Mudahar, G S and Jen, J J. (1991) Texture of raw and canned Jicama (*Pachyrhizus tuberosus*) and Chinese water chestnut (*Eleocharis dulcis*). J Food Sci 56:977-980.

Mueller-Harvey, I, Hartley, R D, Harris, P J, and Curzon, E H. (1986) Linkage of *p*-coumaroyl and feruloyl groups to cell-wall polysaccharides of barley straw. Carbohyd Res 148:71-85.

Myton, K E and Fry, S C. (1994) Intraprotoplasmic feruloylation of arabinoxylans in *Festuca arundinacea* cell cultures. Planta 193:326-330.

Nergard, C S, Kiyohara, H, Reynolds, J C, Thomas-Oates, J E, Matsumoto, T, Yamada, H, Patel, T, Petersen, D, Michaelsen, T E, Diallo, D, and Paulsen, B S. (2006) Structures and structure-activity relationships of three mitogenic and complement fixing pectic arabinogalactans from the malian antiulcer plants *Cochlospermum tinctorium* A. Rich and *Vernonia kotschyana* Sch. Bip. ex Walp. Biomacromolecules 7:71-79.

Ng, A, Parr, A J, Ingham, L M, Rigby, N M, and Waldron, K W. (1998) Cell wall chemistry of carrots (*Daucus carota* cv. Amstrong) during maturation and storage. J Agr Food Chem 46:2933-2939.

Ng, A and Waldron, K W. (2004) Personal communication.

Nunes, F M and Coimbra, M A. (2001) Chemical characterization of the high molecular weight material extracted with hot water from green and roasted arabica coffee. J Agr Food Chem 49:1773-1782.

O'Neill, M A and York, W S. (2003) The composition and structure of plant primary walls. In The Plant Cell Wall. Rose, J K C (Ed.) Blackwell, Oxford, UK. ISBN 084932811X

Obel, N, Porchia, A C, and Scheller, H V. (2003) Intracellular feruloylation of arabinoxylan in wheat: evidence for feruloyl-glucose as precursor. Planta 216:620-629.

Ogawa, K, Hayashi, T, and Okamura, K. (1990) Conformational analysis of xyloglucans. Int J Biol Macromol 12:218-222.

Ojinnaka, C, Jay, A J, Colquhoun, I J, Brownsey, G J, Morris, E R, and Morris, V J. (1996) Structure and conformation of acetan polysaccharide. Int J Biol Macromol 19:149-156.

Ooms, J A B, van Gils, G J M, Duinkerken, A R, and Halmingh, O. (2000) Development and validation of protocols for solid-phase extraction coupled to LC and LC-MS. American Laboratory News 32:52-57.

Ou, S and Kwok, K C. (2004) Ferulic acid: pharmaceutical functions, preparation and applications in food. J Sci Food Agr 84:1261-1269.

Oudgenoeg, G, Dirksen, E, Ingemann, S, Hilhorst, R, Gruppen, H, Boeriu, C G, Piersma, S R, van Berkel, W J H, Laane, C, and Voragen, A G J. (2002) Horseradish peroxidase-catalyzed oligomerization of ferulic acid on a template of tyrosine-containing tripeptide. J Biol Chem 24:21332-21340.

Parker, C C. (2000) The (bio)chemistry of cell adhesion in edible plant tissues: its role in texture. University of East Anglia, UK. PhD Thesis.

Parker, M L and Waldron, K W. (1995) Texture of Chinese water chestnut - involvement of cell-wall phenolics. J Sci Food Agr 68:337-346.

Parker, M L, Ng, A, Smith, A C, and Waldron, K W. (2000) Esterified phenolics of the cell walls of chufa (*Cyperus esculentus* L.) tubers and their role in texture. J Agr Food Chem 48:6284-6291.

Parker, C C, Parker, M L, Smith, A C, and Waldron, K W. (2001) Pectin distribution at the surface of potato parenchyma cells in relation to cell-cell adhesion. J Agr Food Chem 49:4364-4371.

Parker, C C, Parker, M L, Smith, A C, and Waldron, K W. (2003) Thermal stability of texture in Chinese water chestnut may be dependent on 8,8'-diferulic acid (aryltetralyn form). J Agr Food Chem 51:2034-2039.

Parr, A J, Waldron, K W, Ng, A, and Parker, M L. (1996) The wall-bound phenolics of Chinese water chestnut (*Eleocharis dulcis*). J Sci Food Agr 71:501-507.

Parr, A J, Ng, A, and Waldron, K W. (1997) Ester-linked phenolic components of carrot cell walls. J Agr Food Chem 45:2468-2471.

Pearce, G, Marchand, P A, Griswold, J, Lewis, N G, and Ryan, C A. (1998) Accumulation of feruloyltyramine and *p*-coumaroyltyramine in tomato leaves in response to wounding. Phytochemistry 47:659-664.

Phillipe, S, Tranquet, O, Utille, J-P, Saulnier, L, and Guillon, F. (2007) Investigation of ferulate deposition in endosperm cell walls of mature and developing wheat grains by using a polyclonal antibody. Planta 225:1287-1299.

Ralet, M C, Faulds, C B, Williamson, G, and Thibault, J-F. (1994a) Degradation of feruloylated oligosaccharides from sugar-beet pulp and wheat bran by ferulic acid esterases from *Aspergillus niger*. Carbohyd Res 263:257-269.

Ralet, M C, Thibault, J-F, Faulds, C B, and Williamson, G. (1994b) Isolation and purification of feruloylated oligosaccharides from cell-walls of sugar-beet pulp. Carbohyd Res 263:227-241.

Ralet, M C, André-Leroux, G, Quéméner, B C, and Thibault, J-F. (2005) Sugar beet (*Beta vulgaris*) pectins are covalently cross-linked through diferulic bridges in the cell wall. Phytochemistry 66:2800-2814.

Ralph, J, Helm, R F, and Quideau, S. (1992) Lignin-feruloyl ester cross-links in grasses. Part 2. Model compound syntheses. J Chem Soc Perk T 1 2971-2980.

Ralph, J, Quideau, S, Grabber, J H, and Hatfield, R D. (1994) Identification and synthesis of new ferulic acid dehydrodimers present in grass cell walls. J Chem Soc Perk T 1 3485-3498.

Ralph, J, Hatfield, R D, Grabber, J H, Jung, H, Quideau, S, and Helm, R F. (1996) Cell wall cross-linking in grasses: the importance of understanding plant chemistry and biochemistry. USDFRC 1996 Informational conference with dairy and forage industries. Available at: http://www.dfrc.wisc.edu:16080/Research_Summaries/ind_meet/dfrc1.pdf.

Ralph, J, Bunzel, M, Marita, J M, Hatfield, R D, Lu, F, Kim, H, Grabber, J H, Ralph, S A, Jiminez-Monteon, G, and Steinhart, H. (2000) Diferulates analysis: new diferulates and disinapates in insoluble cereal fibre. Polyphénols actualités 19:13-17.

Ralph, J, Bunzel, M, Marita, J M, Hatfield, R D, Lu, F, Kim, H, Schatz, P F, Grabber, J H, and Steinhart, H. (2004) Peroxidase-dependent cross-linking reactions of *p*-hydroxycinnamates in plant cell walls. Phytochemistry Reviews 3:79-96.

Redgewell, R J and Selvendran, R R. (1986) Structural features of cell-wall polysaccharides of onion *Allium cepa*. Carbohyd Res 157:183-199.

Renard, C M G C. (2005) Variability in cell wall preparations: quantification and comparison of common methods. Carbohyd Polym 60:515-522.

Renard, C M G C, Wende, G, and Booth, E J. (1999) Cell wall phenolics and polysaccharides in different tissues of quinoa (*Chenopodium quinoa* Willd). J Sci Food Agr 79:2029-2034.

Renger, A and Steinhart, H. (2000) Ferulic acid dehydrodimers as structural elements in cereal dietary fibre. Eur Food Res Technol 211:422-428.

Robbins, R J. (2003) Phenolic acids in foods: An overview of analytical methodology. J Agr Food Chem 51:2866-2887.

Roberts, K. (2001) How the cell wall acquired a cellular context. Plant Physiol 125:127-130.

Rodríguez-Arcos, R C, Smith, A C, and Waldron, K W. (2004) Ferulic acid crosslinks in asparagus cell walls in relation to texture. J Agr Food Chem 52:4740-4750.

Rombouts, F M and Thibault, J-F. (1986) Enzymic and chemical degradation and the fine structure of pectins from sugar-beet pulp. Carbohyd Res 154:189-203.

Rouau, X, Cheynier, V, Surget, A, Gloux, D, Barron, C, Meudec, E, Louis-Montero, J, and Criton, M. (2003) A dehydrotrimer of ferulic acid from maize bran. Phytochemistry 63:899-903.

Ryden, P and Selvendran, R R. (1990) Cell-wall polysaccharides and glycoproteins of parenchymatous tissues of runner bean (*Phaseolus coccineus*). Biochem J 269:393-402.

Samaj, J, Baluska, F, and Volkmann, D. (1998) Cell-specific expression of two arabinogalactan protein epitopes recognized by monoclonal antibodies JIM8 and JIM13 in maize roots. Protoplasma 204:1-12.

Saulnier, L, Vigouroux, J, and Thibault, J-F. (1995) Isolation and partial characterisation of feruloylated oligosaccharides from maize bran. Carbohyd Res 272:241-253.

Saulnier, L, Crépeau, M J, Lahaye, M, Thibault, J-F, Garcia-Conesa, M-T, Kroon, P A, and Williamson, G. (1999) Isolation and structural determination of two 5,5'-diferuloyl oligosaccharides indicate that maize heteroxylans are covalently cross-linked by oxidatively coupled ferulates. Carbohyd Res 320:82-92.

Saulnier, L, Sado, P-E, Branland, G, Charmet, G, and Guillon, F. (2007) Wheat arabinoxylans: Exploiting variation in amount and composition to develop enhanced varieties. J Cereal Sci 46:261-281.

Sawardeker, J S, Sloneker, J H, and Jeanes, A. (1965) Quantitative determination of monosaccharides as their alditol acetates by gas liquid chromatography. Anal Chem 37:1602-1604.

Seigler, D S. (1998) Plant secondary metabolism. Kluwer Academic Publishers, Dordrecht, The Netherlands. ISBN 0412019817

Selvendran, R R. (1991) Dietary fibre, chemistry and properties. In Encyclopedia of Human Biology. Yelles, M (Ed.) Academic Press, London, UK. ISBN 0122269802

Selvendran, R R and O'Neill, M A. (1987) Isolation and analysis of cell walls from plant material. In Methods of Biochemical Analysis. Glick, D (Ed.) John Wiley & Sons, Chichester, UK. ISBN 0471821950

Shahidi, F and Naczk, M. (2004) Phenolics in Food and Nutraceuticals. CRC Press LLC, Boca Raton, FL, USA. ISBN 1587161389

Sheffield Hallam University, Faculty of Health and Wellbeing Biosciences Division. (2004) Gas Chromatography. Available at: http://teaching.shu.ac.uk/hwb/chemistry/tutorials/chrom/gaschrm.htm

Singleton, V L, Othofer, R, and Lamuela-Raventós, R M. (1998) Analysis of total phenols and other oxidation substrates and antioxidants by means of Folin-Ciocalteu reagent. Method Enzymol 299:152-178.

Skoog, D A, West, D M, and Holler, F J. (1996) Fundamentals of Analytical Chemistry. Harcourt College Publishers, Orlando, FL, USA. ISBN 0030059380

Smallwood, M, Beven, A, Donovan, N, Neill, S J, Peart, J, Roberts, K, and Knox, J P. (1994) Localization of cell-wall proteins in relation to the developmental anatomy of the carrot root apex. Plant J 5:237-246.

Smallwood, M, Martin, H, and Knox, J P. (1995) An epitope of rice threonine-rich and hydroxyproline-rich glycoprotein is common to cell-wall and hydrophobic plasma-membrane glycoproteins. Planta 196:510-522.

Smallwood, M, Yates, E A, Willats, W G T, Martin, H, and Knox, J P. (1996) Immunochemical comparison of membrane-associated and secreted arabinogalactan-proteins in rice and carrot. Planta 198:452-459.

Smith, B G and Harris, P J. (1995) Polysaccharide composition of unlignified cell walls of pineapple [*Ananas comosus* (L.) Merr.] Fruit. Plant Physiol 107:1399-1409.

Smith, B G and Harris, P J. (2001) Ferulic acid is esterified to glucuronoarabinoxylans in pineapple cell walls. Phytochemistry 56:513-519.

Smith, M M and Hartley, R D. (1983) Occurrence and nature of ferulic acid substitution of cell-wall polysaccharides in graminaceous plants. Carbohyd Res 118:65-80.

Sridhar, R, Mohanty, S K, and Anjaneyulu, A. (1979) *In vivo* inactivation of rice tungro virus by ferulic acid. Phytopathol Z 94:279-281.

Stacey, N J, Roberts, K, and Knox, J P. (1990) Patterns of expression of the JIM4 arabinogalactan-protein epitope in cell-cultures and during somatic embryogenesis in *Daucus carota* L. Planta 180:285-292.

Steffan, W, Kovac, P, Albersheim, P, Darvill, A G, and Hahn, M G. (1995) Characterization of a monoclonal-antibody that recognizes an

arabinosylated (1→6)-Beta-D-galactan epitope in plant-complex carbohydrates. Carbohyd Res 275:295-307.

Stone, B A, Evans, N A, Bonig, I, and Clarke, A E. (1984) The application of Sirofluor, a chemically defined fluorochrome from aniline blue for the histochemical detection of callose. Protoplasma 122:191-195.

Sun, R-C, Sun, X-F, and Zhang, S-H. (2001) Quantitative determination of hydroxycinnamic acids in wheat, rice, rye and barley straws, maize stems, oil palm frond fiber, and fast-growing poplar wood. J Agr Food Chem 49:5122-5129.

Sweet, D P, Shapiro, R H, and Albersheim, P. (1975) Quantitative analysis by various g.l.c. response-factor theories for partially methylated and partially ethylated alditol acetates. Carbohyd Res 40:217-225.

Tahiri, M, Pellerin, P, Tressol, J C, Doco, T, Pepin, D, Rayssiguier, Y, and Coudray, C. (2000) The rhamnogalacturonan-II dimer decreases intestinal absorption and tissue accumulation of lead in rats. J Nutr 130:249-253.

Tahiri, M, Tressol, J C, Doco, T, Rayssiguier, Y, and Coudray, C. (2002) Chronic oral administration of rhamnogalacturonan-II dimer, a pectic polysaccharide, failed to accelerate body lead detoxification after chronic lead exposure in rats. Brit J Nutr 87:47-54.

Takeda, T, Furuta, Y, Awano, T, Mizuno, K, Mitsuishi, Y, and Hayashi, T. (2002) Suppression and acceleration of cell elongation by integration of xyloglucans in pea stem segments. Proc Natl Acad Sci USA 99:9055-9060.

Talbott, L D and Ray, P W. (1982) Molecular size and separability features of pea cell wall polysaccharides. Implication for models of primary wall structure. Plant Physiol 98:357-368.

Talmadge, K W, Keegstra, K, Bauer, W D, and Albersheim, P. (1973) The structure of plant cell walls: I. The macromolecular components of the

walls of suspension-cultured sycamore cells with a detailed analysis of the pectic polysaccharides. Plant Physiol 51:158-173.

Terpstra, A H M, Lapre, J A, de Vries, H T, and Beynen, A C. (2002) The hypocholesterolemic effect of lemon peels, lemon pectin, and the waste stream material of lemon peels in hybrid F1B hamsters. Eur J Nutr 41:19-26.

Theander, O and Westerlund, E A. (1986) Studies on dietary fiber. 3. Improved procedures for analysis of dietary fiber. J Agr Food Chem 34:330-336.

Thomas, M, Guillemin, F, Guillon, F, and Thibault, J-F. (2003) Pectins in the fruits of Japanese Quince (*Chaenomeles japonica*). Carbohyd Polym 53:361-372.

Thompson, J E and Fry, S C. (2000) Evidence for covalent linkage between xyloglucan and acidic pectins in suspension-cultured rose cells. Planta 211:275-286.

Topakas, E, Vafiadi, C, and Christakopoulos, P. (2007) Microbial production, characterization and applications of feruloyl esterases. Process Biochem 42:497-509.

Tsumuraya, Y, Mochizucki, N, Hashimoto, Y, and Kovác, P. (2006) Purification of an exo-β-(1→3)-D-galactanase of *Irpex lacteus* (*Polyporus tulipiferae*) and its action on arabinogalactan-proteins. J Biol Chem 265:7207-7215.

Valent, B S and Albersheim, P. (1974) The structure of plant cell walls. V. On the binding of gyloglucan to cellulose fibers. Plant Physiol 54:105-108.

Voragen, A G J, Pilnik, W, Thibault, J-F, Axelos, M A V, and Renard, C M G C. (1995) Pectins. In Food Polysaccharides and Their Applications. Stephen, A M (Ed.) Marcel Dekker, New York, USA. ISBN 0824793536

Waldron, K W and Faulds, C B. (2007) Cell wall polysaccharides: composition and structure. In Introduction to Glycoscience / Synthesis of Carbohydrates. Kamerling, J P, Boons, G-J, Lee, Y, Suzuki, A,

Taniguchi, N, and Voragen, A G J (Eds.) Elsevier, Oxford, UK. ISBN 9780444527462

Waldron, K W and Selvendran, R R. (1992) Cell-wall changes in immature asparagus stem tissue after excision. Phytochemistry 31:1931-1940.

Waldron, K W, Parr, A J, Ng, A, and Ralph, J. (1996) Cell wall esterified phenolic dimers: Identification and quantification by reverse phase high performance liquid chromatography and diode array detection. Phytochem Analysis 7:305-312.

Waldron, K W, Smith, A C, Parr, A J, Ng, A, and Parker, M L. (1997) New approaches to understanding and controlling cell separation in relation to fruit and vegetable texture. Trends Food Sci Tech 8:213-221.

Wang, Y, Hollingsworth, R I, and Kasper, D L. (1998) Ozonolysis for selectively depolymerizing polysaccharides containing β-D-aldosidic linkages. Proc Natl Acad Sci USA 95:6584-6589.

Wang, X, Kapoor, V, and Smythe, G A. (2003) Extraction and chromatography-mass spectrometric analysis of the active principles from selected Chinese herbs and other medicinal plants. Am J Chinese Med 31:927-944.

Ward, G, Hadar, Y, Bilkis, I, Konstantinovsky, L, and Dosoretz, C G. (2001) Initial steps of ferulic acid polymerization by lignin peroxidase. J Biol Chem 276:18734-18741.

Weber, B, Hoesch, L, and Rast, D M. (1995) Protocatechualdehyde and other phenols as cell-wall components of grapevine leaves. Phytochemistry 40:433-437.

Wende, G and Fry, S C. (1997) Digestion by fungal glycanases of arabinoxylans with different feruloylated side-chains. Phytochemistry 45:1123-1129.

Wende, G, Waldron, K W, Smith, A C, and Brett, C T. (1999) Developmental changes in cell-wall ferulate and dehydrodiferulates in sugar beet. Phytochemistry 52:819-827.

Wende, G, Waldron, K W, Smith, A C, and Brett, C T. (2000) Tissue-specific developmental changes in cell-wall ferulate and dehydrodiferulates in sugar beet. Phytochemistry 55:103-110.

Whitney, S E C, Brigham, J E, Darke, A H, Reid, J S G, and Gidley, M J. (1995) *In vitro* assembly of cellulose/xyloglucan networks - ultrastructural and molecular aspects. Plant J 8:491-504.

Willats, W G T, Marcus, S E, and Knox, J P. (1998) Generation of a monoclonal antibody specific to (1→5)-alpha-L-arabinan. Carbohyd Res 308:149-152.

Willats, W G T, Gilmartin, P M, Mikkelsen, J D, and Knox, J P. (1999) Cell wall antibodies without immunization: generation and use of de-esterified homogalacturonan block-specific antibodies from a naive phage display library. Plant J 18:57-65.

Willats, W G T, Limberg, G, Buchholt, H C, van Alebeek, G J, Benen, J, Christensen, T M I E, Visser, J, Voragen, A g J, Mikkelsen, J D, and Knox, J P. (2000) Analysis of pectin structure part 2 - Analysis of pectic epitopes recognised by hybridoma and phage display monoclonal antibodies using defined oligosaccharides, polysaccharides, and enzymatic degradation. Carbohyd Res 327:309-320.

Willats, W G T, McCartney, L, Steele-King, C G, Marcus, S E, Mort, A, Huisman, M, van Alebeek, G J W M, Schols, H A, Voragen, A G J, Le Goff, A, Bonnin, E, Thibault, J-F, and Knox, J P. (2004) A xylogalacturonan epitope is specifically associated with plant cell detachment. Planta 218:673-681.

Yates, E A, Valdor, J F, Haslam, S M, Morris, H R, Dell, A, Mackie, W, and Knox, J P. (1996) Characterization of carbohydrate structural features

recognized by anti-arabinogalactan-protein monoclonal antibodies. Glycobiology 6:131-139.

Yu, K W, Kiyohara, H, Matsumoto, T, Yang, H C, and Yamada, H. (2001) Characterization of pectic polysaccharides having intestinal immune system modulating activity from rhizomes of *Atractylodes lancea* DC. Carbohyd Polym 46:125-134.

Yui, T, Imada, K, Shibuya, N, and Ogawa, K. (1995) Conformation of an arabinoxylan isolated from the rice endosperm cell wall by X-ray diffraction and a conformational analysis. Biosci Biotechnol Biochem 59:965-968.